University of Alberta

Rapid Sizing of DNA and Analysis of Single Cells Using Capillary Electrophoresis

by

Woei G. Tan

A thesis submitted to the Faculty of Graduate Studies and Research in partial fulfillment of the requirements for the degree of Doctor of Philosophy

Department of Medical Microbiology and Immunology

Edmonton, Alberta

Fall 2000

National Library of Canada
Acquisitions and Bibliographic Services
395 Wellington Street
Ottawa ON K1A 0N4
Canada

Bibliothèque nationale du Canada
Acquisitions et services bibliographiques
395, rue Wellington
Ottawa ON K1A 0N4
Canada

Your file Votre référence

Our file Notre référence

The author has granted a non-exclusive licence allowing the National Library of Canada to reproduce, loan, distribute or sell copies of this thesis in microform, paper or electronic formats.

L'auteur a accordé une licence non exclusive permettant à la Bibliothèque nationale du Canada de reproduire, prêter, distribuer ou vendre des copies de cette thèse sous la forme de microfiche/film, de reproduction sur papier ou sur format électronique.

The author retains ownership of the copyright in this thesis. Neither the thesis nor substantial extracts from it may be printed or otherwise reproduced without the author's permission.

L'auteur conserve la propriété du droit d'auteur qui protège cette thèse. Ni la thèse ni des extraits substantiels de celle-ci ne doivent être imprimés ou autrement reproduits sans son autorisation.

0-612-59683-4

Canada

University of Alberta

Library Release Form

Name of Author: Woei Guang Tan

Title of Thesis: Rapid Sizing of DNA and Analysis of Single Cells Using Capillary Electrophoresis

Degree: Doctor of Philosophy

Year this Degree Granted: 2000

Permission is hereby granted to the University of Alberta Library to reproduce single copies of this thesis and to lend or sell such copies for private, scholarly or scientific research purposes only.

The author reserves all other publication and other rights in association with the copyright in the thesis, and except as herein before provided, neither the thesis nor any substantial portion thereof may be printed or otherwise reproduced in any material form whatever without the author's prior written permission.

June 1, 2000

1752 48 Street,
Edmonton, Alberta,
T6L 2X6

UNIVERSITY OF ALBERTA
FACULTY OF GRADUATE STUDIES AND RESEARCH

The undersigned certify that they have read, and recommend to the Faculty of Graduate Studies and Research for acceptance, a thesis entitled **Rapid Sizing of DNA and Analysis of Single Cells Using Capillary Electrophoresis** submitted by Woei G. Tan in partial fulfillment of the requirements for the degree of **Doctor of Philosophy**.

Dr. D. L. J. Tyrrell

Dr. N. J. Dovichi

Dr. M. M. Palcic

Dr. J. F. Elliott

Dr. X. C. Chris Le

Dr. S. A. Soper

April 28, 2000

Abstract

In chapter 1, an overview of Hepatitis B Virus (HBV) infection and non-radio-label based detection methods for HBV DNA are described. Also included in this chapter are introductions to laser-induced fluorescence, DNA separation in cellulose polymer solutions and single-cell analysis using CE.

In chapter 2, the use of hydroxyethyl cellulose (HEC) as a replaceable sieving polymer for DNA separation was described. Polymer concentration, separation efficiency, migration time, degradation of the sieving matrix were studied. A polymer concentration of 0.8% (w/v) was found to be suitable for the separation of a range of dye-labeled DNA fragments (229 to 903 bases) under denaturing conditions. HEC solution prepared in 0.1M TAPS buffer is stable for at least 6 months at 4 °C. This chapter also describes the construction of a CE instrument.

In chapter 3, a unique on-column labeling method for DNA fragments is described. In this technique, DNA fragments are labeled and detected simultaneously by interaction with oppositely migrating dye molecules during electrophoresis. Under this condition, significant amount of electrostatic interaction between the cationic dyes and the DNA fragments was demonstrated. This interaction could be preserved in the presence of excess dye in the system. The approach was able to resolve DNA fragments over a large size range (72bp to 23 kbp). The sensitivity of detection could be improved 4-fold by stacking dye molecules at the detector end of the capillary using a discontinuous buffering system.

Chapter 4 describes the detection of duck hepatitis B virus (DHBV) DNA using PCR and CE-LIF detection. A multi-primer system was used to demonstrate the reduction of DHBV DNA in serum and liver of infected ducklings upon antiviral

treatment. The use of this approach did not demonstrate truncation of viral DNA in response to short duration of treatment with (-)-β-L-2',3'-dideoxy-3'-thiacytidine. The same experiment indicated that 2-amino-6-methoxy purine 2' 3' dideoxyriboside is not able to completely inhibit viral DNA synthesis by blocking the 5' end of the viral DNA strand, suggesting that a longer duration of treatment is necessary to completely inhibit synthesis of viral DNA.

In chapter 5, quantitative competitive (QC) PCR were modified to address the accuracy of quantification and to facilitate eventual automation of this technique. The modified technique was used to investigate the efficiency of amplification during PCR, we showed that differences in amplification efficiency between a target and a competitor limit the accuracy of quantification using end point measurement. These differences fluctuated from cycle to cycle, and tended to give rise to high discrepancies in quantification at high cycle numbers. Sampling of PCR products from a range of cycles in which amplification efficiency is a constant would reduce these discrepancies.

In chapter 6, studies of enzyme activity using CE-LIF are reported. This chapter emphasizes the construction of a CE instrument that is capable of single-cell analysis. Using baker's yeast as a model, *in vivo* enzymatic hydrolysis of a fluorescence-labeled sugar substrate was studied. We showed that several hundred molecules of enzyme reaction products could be detected in a single yeast spheroplast. Confocal laser scanning microscopy confirmed the uptake and internalization of fluorescent substrate.

Chapter 7 addresses the potential use of CE-LIF for the detection, and quantification of DNA. Future development of CE for medical diagnosis using a multi-channel system for high throughput screening is suggested.

Preface

As we gain fundamental knowledge of the practical development of capillary electrophoresis (CE) nucleic acid separation, we are anticipating a growing application of this powerful analytical technique in molecular biology. DNA diagnoses of human diseases is an excellent example. It has important implications in the areas of genetic and medical research, clinical chemistry, and forensic science. For instance, probing the presence of specific viral DNA fragments by " sequence specific hybridization and amplification " presents the potential of CE for diagnosis of the stages of infection of an affected individual, prior, during, and post antiviral treatment. This is particularly beneficial for viral infections that don't already have effective treatment regimen. In the case of human Hepatitis B (HBV), no specific drug therapy is currently available to completely eliminate the infection, and hence therapy remains, as it has for the last two decades, symptomatic support. While the toll of these infections is gradually declining due to proper preventive measures such as the availability of new antiviral chemotherapy and liver transplantation, there are still a large number of people who were infected and who are dying every year. Hence an urgent need exists to speed the development of more potent therapeutic strategy in chronic HBV infection.

Treatment of HBV infection with various antiviral compounds has ranged from highly to partially effective. This ineffectiveness may result from the lack of potency of the compound itself, or a poorly designed drug administration regimen. The latter may include improper termination of treatment, as a result of inaccurate determination of a patient's status of infectivity at the end of treatment. Consequently, it is important

to establish highly sensitive, reliable, and economical detection methods to facilitate routine diagnosis and screening for HBV infection at hospital settings.

With the introduction of CE in the analysis of nucleic acids, a more robust and cost effective diagnostic screening becomes feasible due to a much shorter analysis time and reduction in labor required as well as more efficient data storage and retrieval. Compared to conventional separation techniques such as the slab gel system and high-performance liquid chromatography (HPLC), CE is superior in terms of speed and efficiency of separation, small sample volume requirement as well as the potential for automation. Capillary electrophoresis using cellulose derivatives is a rapid and convenient method of DNA separation. This-semi dilute, low viscosity polymer can be easily removed from capillary and be replenished. This type of cellulose matrix is a promising technique for the rapid and efficient separation of DNA restriction fragments up to 23 kilobase pairs in size.

For a given application, the choice of polymer has to be optimally determined. The strategy for selection may be somewhat arbitrary and not so critical in terms of the type of polymer or its chain length. However, an optimal polymer concentration in regards to separation efficiency, migration time, and resolution can be systematically determined. In addition to this, the choice of polymer concentration can also be influenced by the analyte and the condition subjected to separation, for example, single stranded versus double stranded DNA; 5' end labeled versus intercalating labeled DNA fragments; non-denaturing versus denaturing separation.

One unique characteristic of CE is the use of a small inner diameter capillary as a separation compartment. This creates a short viewing path length, which is a common

factor that limits the concentration sensitivity in CE analysis. As a result, even though the technique requires only nanoliter sampling volume, it is not a trace analysis technique, and relatively concentrated analyte solutions or pre-concentration methods are often required. In addition to this, effective sample clean up is usually required when a compound of analytical value (viral nucleic acids) is present in small quantity with high concentrations of undesirable compounds (e.g., host DNA, RNA and proteins). This occurs in samples obtained from serum and biopsy materials. These background contaminants can potentially affect sample injection, migration, separation efficiency and quantification. By carefully evaluating and controlling parameters crucial for development and validation of CE based assays, common problems associated with sensitivity of detection and reproducibility can be systematically investigated and reduced or eliminated.

The first commercial CE instrument emerged in 1988 and applications of CE in molecular diagnostics are still evolving. With the advent of the human genome projects, more genes linked to various diseases have been discovered. This also means that more effort will be invested into developing molecular technologies that can facilitate routine clinical diagnosis in a high throughput fashion. As well, there will be a growing need to improve on the currently labor intensive and cost ineffective ways to monitor stages of certain clinically significant infectious diseases. Determination of viral load will be the major emphasis in this area.

Acknowledgements

I express sincere appreciation for the efforts of all those who have supported the work reported in this thesis. In particular, I would like to thank my two supervisors, Dr. Tyrrell and Dr. Dovichi for providing me with tremendous amount of patience and guidance during my graduate years. I would also like to thank them for providing a research environment conducive for growing intellectually as well as professionally. I wish to acknowledge with thanks the significant contributions of the following people who have provided me with valuable guidance to my research work: Dr. M. Palcic, Dr. X. C. Le, Dr. E. Arriaga and Dr. C. Stathakis. I take pleasure in expressing my appreciation and thanks to the following colleagues for their collaboration: Dr. H. Ahmadzadeh, J. Fang, D. Richards, N. Li, and J. Huang. Proofreading of thesis was kindly provided by K. Schreiner and Dr. D. Tovell. I would like to thank my wife Louisa for her patience and support and providing me with so much encouragement. Last but not least, I would like to thank my parents for making it possible for me to study in Canada.

Table of Contents

Chap. 1. Introduction.....1

1.1 Hepatitis B Infection and advances in molecular diagnostics.....2

1.1.1 Overview of hepatitis B infection.....2

1.1.2 Replication strategy of HBV.....3

1.1.3 Treatment of chronic hepatitis B.....6

1.1.4 Detection of HBV DNA.....7

1.2 Non radio-labeled based detection of nucleic acids.....9

1.2.1 Laser-induced fluorescence detection.....9

1.2.2 Utility of laser-induced fluorescence in DNA analysis.....10

1.2.3 5' end labeling.....10

1.2.4 Intercalating dyes.....11

1.2.5 Random labeling.....12

1.3 DNA separation technology.....12

1.3.1 DNA separation using capillary electrophoresis.....12

1.3.2 Separation media.....14

1.3.3 Basic considerations for size-based separation.....15

1.3.4 DNA separation in cellulose polymer.....17

1.4 Single-cell analysis and CE-LIF.....18

1.4.1 General aspects and areas of applications.....18

1.4.2 Detection methods.....19

1.4.3 Future of single-cell analysis.....21

1.5 Bibliography.....21

Chap. 2. Hydroxyethyl Cellulose as a Replaceable Sieving Polymer for DNA Separation.....29

2.1 Introduction.....30

2.1.1 Theory of DNA separation.....30

2.1.2 Polymer solutions.....31

2.1.3 Hydroxyethyl Cellulose (HEC).....33

2.1.4 Polymer concentration.....35

2.2 Experimental.....36

2.2.1 CE apparatus.....36

2.2.2 Post-column detection.....37

2.2.3 Parameters for DNA separation.....37

2.2.4 Preparation of DHBV plasmid DNA.....39

2.2.5 Indirect fluorescence labeling of restriction fragments.....40

2.2.6 Influence of HEC concentration on DNA separation.....42

2.2.7 Stability of HEC under denaturing conditions.....43

2.3 Results and discussion.....44

2.3.1 Separation of DNA fragments using HEC polymer.....44

2.3.2 HEC concentration effect.....47

2.3.3 Behavior of separation: 5' end labeled vs. intercalating dye.....53

2.3.4 Influence of polymer concentration on theoretical plates.....53

2.3.5 Memory effect of HEC on capillary wall.....56

2.3.6 Stability of HEC.....58

2.3.7 Other cellulose polymers.....65

2.4 Conclusions.....67

2.5 Bibliography.....69

Chap. 3. On-Column Labeling of DNA Fragments and Detection by CE-LIF.....73

3.1 Introduction.....74

3.1.1 Labeling of DNA with nucleic acid stains.....74

3.1.2 Formation of DNA-dye complexes.....75

3.1.3 Parameters affecting complex stability.....76

3.2 Experimental.....77

3.2.1 Apparatus.....77

3.2.2 Parameters of CE separation.....78

3.2.3 Post-column detection.....78

3.2.4 Preparation of restriction digested DHBV plasmid and viral DNA.....79

3.3 Results and discussion.....80

3.3.1 Separation efficiency.....80

3.3.2 Stacking of intercalating dye from sheath-flow buffer.....86

3.3.3 High-speed separation.....92

3.3.4 Calibration plots.....95

3.3.5 Analysis of DHBV DNA from congenitally infected ducklings...98

3.3.6 On-column labeling with two different intercalating dyes.....102

3.4 Conclusions.....106

3.5 Bibliography.....106

Chap. 4. Profiling HBV Infection in Ducks Exposed to Antiviral Compounds...111

4.1 Introduction.....112

4.1.1 Duck hepatitis B virus as a model for studying viral clearance..112

4.1.2 Detection of hepatitis B viral DNA in serum and liver.....112

4.1.3 Polymerase Chain Reaction with CE-LIF detection.....114

4.2 Experimental.....114

4.2.1 Preparation of plasmid DNA.....115

4.2.2 Treatment of ducks with antiviral compounds.....115

4.2.3 Extraction of DHBV DNA from serum.....116

4.2.4 Purification of core particles from liver.....116

4.2.5 Design of DHBV primers and probes.....118

4.2.6 PCR assays.....118

4.2.7 CE-LIF analysis.....121

4.3 Results and discussion.....121

4.3.1 Fluorescence detection of primer-extended oligonucleotides....121

4.3.2 Profiling of DHBV DNA in serum and liver.....124

4.3.3 Mechanism of inhibition of viral DNA synthesis.....127

4.4 Conclusions.....132

4.5 Bibliography.....133

Chap. 5. Probing Amplification Efficiency in Quantitative Competitive PCR.....138

5.1 Introduction.....139

5.1.1 Theoretical aspects of quantitative competitive PCR (QC-PCR).....139

5.1.2 Technical and mathematical considerations of QC-PCR.....141

5.2 Experimental.....144

5.2.1 Apparatus.....144

5.2.2 CE separation and post-column detection.....145
5.2.3 Preparation of DHBV DNA from duck sera.....146
5.2.4 Dot blot hybridization.....146
5.2.5 Construction of plasmid DNA templates.....147
5.2.6 Competitive PCR-CE-LIF.....147
5.2.7 Determination of limit of detection.....148
5.2.8 Quantitative considerations in QC-PCR.....148
5.3 Results and discussion.....150
5.3.1 Qualitative performance of CE-LIF.....150
5.3.2 Control of plasmid amplification and efficiency.....152
5.3.3 Quantification of cloned DHBV genome.....154
5.3.4 Limit of detection.....160
5.3.5 Measuring viral load.....163
5.4 Conclusions.....166
5.5 Bibliography.....170
Chap. 6. Analysis of Single Cells using CE-LIF.....175
6.1 Introduction.....176
6.2 Experimental.....178
6.2.1 Fluorophores and buffering conditions.....178
6.2.2 Incubation of yeast cells with triglucoside.....179
6.2.3 Generation of spheroplasts.....179
6.2.4 Confocal laser scanning microscopy.....180
6.2.5 Inhibition of substrate hydrolysis.....180

6.2.6 CE-LIF analysis.....181

6.2.7 Single spheroplast introduction.....182

6.2.8 Analysis of non-lyticase treated yeast cell.....184

6.2.9 Monitoring intra and extracellular substrate hydrolysis.....184

6.3 Results and discussion.....185

6.4 Conclusions.....198

6.5 Bibliography.....200

Chap. 7. Concluding Summary.....203

7.1 Closing remarks and future directions.....204

7.2 Bibliography.....208

Appendix.....210

List of Tables

Table 1.1 Methods of detection for CE.....20

Table 2.1 DHBV sequences designed for primer extension.....41

Table 2.2 Restriction fragments specific to HBVTa and HBVTb.....42

Table 3.1 Size determination of restriction fragment with ethidium bromide homodimer2.....100

Table 4.1 Construction of oligoprimers specific to DHBV genome.....119

Table 5.1 Competitive amplification as a function of input DNA and cycle number.....159

Table 5.2 Quantification of serum DHBV DNA in response to 3TC treatment.....165

Table 5.3 Experimental gradient of competitive amplification between T and C.....168

List of Figures

Figure 1.1 Schematic representation of the basic replication cycle of HBV....4

Figure 1.2 General scheme of a commercial CE instrument.....13

Figure 2.1 A typical structure of hydroxyethyl cellulose.....34

Figure 2.2 Schematic diagram of an in-house built CE instrument.....38

Figure 2.3 Anionic impurities of HEC polymer solution 0.8% (w/v).....45

Figure 2.4 Separation of DHBV DNA fragments.....46

Figure 2.5 Separation of 5' fluorescence-labeled, single-stranded DHBV DNA fragments.....49

Figure 2.6 Ferguson plot of 5' dye labeled DHBV DNA fragments.....50

Figure 2.7 The effect of HEC concentration on peak resolution and average migration time.....52

Figure 2.8 Plots of peak migration time (min) vs base number (nt).....54

Figure 2.9 Separation efficiency of single-stranded DHBV DNA fragments.....55

Figure 2.10 Adsorption of HEC on capillary.....57

Figure 2.11 A typical electropherogram of the current channel.....59

Figure 2.12 Stability of aged HEC polymer as measured by conductivity.....60

Figure 2.13 Stability of aged HEC polymer as measured by current flow.....61

Figure 2.14 Separation of 4 DHBV DNA fragments on an 8 day old HEC polymer.....62

Figure 2.15 Influence of polymer age on resolution of DNA fragments.....63

Figure 2.16 Influence of polymer age on relative migration time.....64

Figure 2.17 Separation of single-stranded DNA in various cellulose polymers.....66

Figure 3.1 Schematic diagram of a sheath-flow cuvette.....81

Figure 3.2 Separation of ϕX174/*HaeIII* restriction digest.....82

Figure 3.3 Separation of DNA size ladders in HEC matrix.....85

Figure 3.4 Effect of sample loading on separation efficiency.....87

Figure 3.5 Comparison of three different dye stacking conditions.....88

Figure 3.6 The 3021 bp duck hepatitis B virus insert.....90

Figure 3.7 Dependence of electropherotic mobility of DNA fragments.....91

Figure 3.8 Separation of ϕX174/*HaeIII* digest at high field strength.....93

Figure 3.9 Plots of mobility vs applied field strength.....94

Figure 3.10 Calibration plots of ϕX174/*HaeIII* DNA fragments.....96

Figure 3.11 Separation of duck hepatitis B virus DNA fragments.....99

Figure 3.12 Detection of PCR amplified DHBV DNA fragments.....101

Figure 3.13 Separation of 1 kb DNA ladder in 0.8% HEC.....103

Figure 3.14 Absorption of dye molecules on capillary coating.....105

Figure 4.1 PCR priming of partially double-stranded DHBV genome.....120

Figure 4.2 Separation of PCR amplified products using CE-LIF.....123

Figure 4.3 Simulated presentation of 16 PCR products.....124

Figure 4.4 Clearance of DHBV DNA in serum sample of infected animals treated with3TC.....126

Figure 4.5 Effect of 2-amino-6-methoxy on replicating cores.....129

Figure 4.6 Dependence of PCR amplification on concentration of input template.....130

Figure 4.7 Amplification of small PCR fragments from the 3' end of the minus strand of the DHBV genome.....131

Figure 5.1 CE separation of PCR products with or without sample purification.....151

Figure 5.2 Separation efficiency of plasmids pAlter-2-W and pT7Blue-3-M at various initial input template concentrations...154

Figure 5.3 Influence of cycle number on the accuracy of quantification.....157

Figure 5.4 Competition profile between target and competitor as a function of cycle number.....162

Figure 5.5 Working plot of pAlter-2-W.....163

Figure 5.6 Dot blot hybridization detection of DHBV DNA in serum.....166

Figure 6.1 A schematic diagram showing the introduction of Single cell into a capillary.....181

Figure 6.2 Photographs obtained by using confocal laser scanning microscopy.....187

Figure 6.3 Electropherograms obtained from CE-LIF of TMR-labeled sugars.....189

Figure 6.4 Intracellular inhibition of yeast glucosidase I by castanospermine.....191

Figure 6.5 Electropherograms of the contents of yeast spheroplasts.....193

Figure 6.6 CE separation of non-lyticase treated single yeast cell.....194

Figure 6.7 Hydrolysis of 50 μM Tri-Glc in Sabouraud dextrose media.....196

Figure 6.8 Step-wise hydrolysis of Tri-Glc.....197

Figure 6.9 Comparison of L/T ratio in culture media and total lysate.....199

List of Symbols and Abbreviations

Chapter 1

HBV	hepatitis B virus
HCC	hepatocellular carcinoma
DHBV	duck hepatitis B virus
cccDNA	covalently closed circular DNA
HBsAg	hepatitis surface antigen
HBcAb	hepatitis B core antibody
HBeAg	hepatitis B e antigen

Chapter 2

F_e	electrophoretic force
Q	net charge
E	electric field strength
F_d	drag force
f	translational friction coefficient
v	velocity
μ	electrophoretic mobility
ϕ	entanglement threshold
HEC	hydroxyethyl cellulose
N_b	the number of basepairs in a DNA fragment
M.S.	molar substitution
nt	nucleotide

Chapter 3

POPO3	POPO™-3 iodide
EthD2	ethidium homodimer II
V_{inj}	injection volume
V_i	injection voltage
V_r	running voltage
T_{inj}	injection time
T_m	migration time
V_{cap}	capillary volume
R_c	capillary radius
L_c	capillary length
C_{DL}	concentration detection limit
M_{DL}	mass detection limit
σ	standard deviation of background
S_c	slope of plot
C_a	concentration of analyte
P_h	peak height of analyte

Chapter 4

3TC	(-)-β-L-2',3'-dideoxy-3'-thiacytidine
2A6M	2-amino-6-methoxy purine 2' 3' dideoxyriboside

Chapter 5

N	PCR product formed after successive cycles
N_o	initial amount target DNA

E	efficiency of a PCR reaction
n	cycle number
T	target
C	competitor

Chapter 6

TMR	tetramethyl rhodamine
T	tri-saccharide-TMR
D	di-saccharide-TMR
M	mono-saccharide-TMR
L	linker-arm-TMR

Chapter 1. Introduction

1.1 Hepatitis B infection and advances in molecular diagnostics

1.1.1 Overview of hepatitis B infection

Infection with hepatitis B virus (HBV) is endemic throughout the world and is responsible for a variety of liver diseases. In North America, HBV infection occurs primarily as a result of horizontal transmission, which can occur via sexual contact between infected and uninfected individuals, parenteral drug abuse, and occupationally acquired infection. Cases imported by immigrants or travelers from high-prevalence countries represent an additional but less significant method of introduction of the infection. This is in contrast to Asia and Africa, where vertical transmission from infected mother to neonate plays a leading role in the spread of the infection [1,2].

The virus induces a spectrum of clinical manifestations, ranging from mild, inapparent disease to fulminant hepatitis, severe chronic liver disease and cirrhosis [1,2]. In addition, the virus has been clearly implicated in the development of primary hepatocellular carcinoma (HCC), one of the most common cancers in the world [1,3]. At the present time, over 300 million people worldwide are chronic carriers of the virus while the number of fatalities is estimated to be approximately two million individuals per year [4,5]. These individuals will not benefit from vaccination available for HBV infection. Hence there is an urgent need to speed the development of reliable and economical detection methods for routine HBV screening in order to prevent spread of the infection. Further, there is a growing need to investigate the significance of extrahepatic infection as this may have a bearing on antiviral therapy and potential cure of chronic viral infection.

1.1.2 Replication strategy of HBV

Understanding of HBV replication is largely derived from animal models such as the well characterized woodchuck hepatitis virus (WHV), ground squirrel hepatitis virus (GSHV) and duck hepatitis B virus (DHBV) isolated from Peking ducks [6,7]. The small HBV hepadnavirus contains only 3.2 kilo base pairs in its genome. The strategy of its replication is unique among double-stranded DNA viruses and more closely resembles that of the retroviruses [1,8-11]. Figure 1.1 depicts a schematic diagram of the HBV replication cycle. The genome of HBV is circular and partially double stranded. The full length, circular strand is known as the negative strand and contains overlapping genes that encode both structural proteins and replicative proteins. The positive strand is short and variable in length. Production of a complete virion begins with initial binding of the virus to the cell surface and penetration into the cell. The virus core is then transported to the nucleus, disassembled and followed by the conversion of the relaxed circular virus DNA into covalently closed circular DNA (cccDNA) which serves as the template for viral RNA synthesis. The transcription of viral RNA is carried out by cellular RNA polymerase. This transcription yields RNA of various sizes, among which, a 3.5 kb genomic RNA will serve as template for reverse transcription. This process is initiated at the 3' end of the template, with a terminal protein of the viral polymerase serving as a primer. The RNA template is simultaneously degraded by RNaseH activity as the negative strand synthesis progresses. The positive strand is primed by a small segment of the RNA template via primer translocation, and the synthesis continues until the terminal protein at the 5' end of the negative strand is passed. This produces an open circular DNA molecule similar to that in a mature HBV virus particle. In the final steps of the

assembly process, the mature nucleocapsids acquire the virion envelope by budding into the endoplasmic reticulum, and then exported from the cell to start a new round of

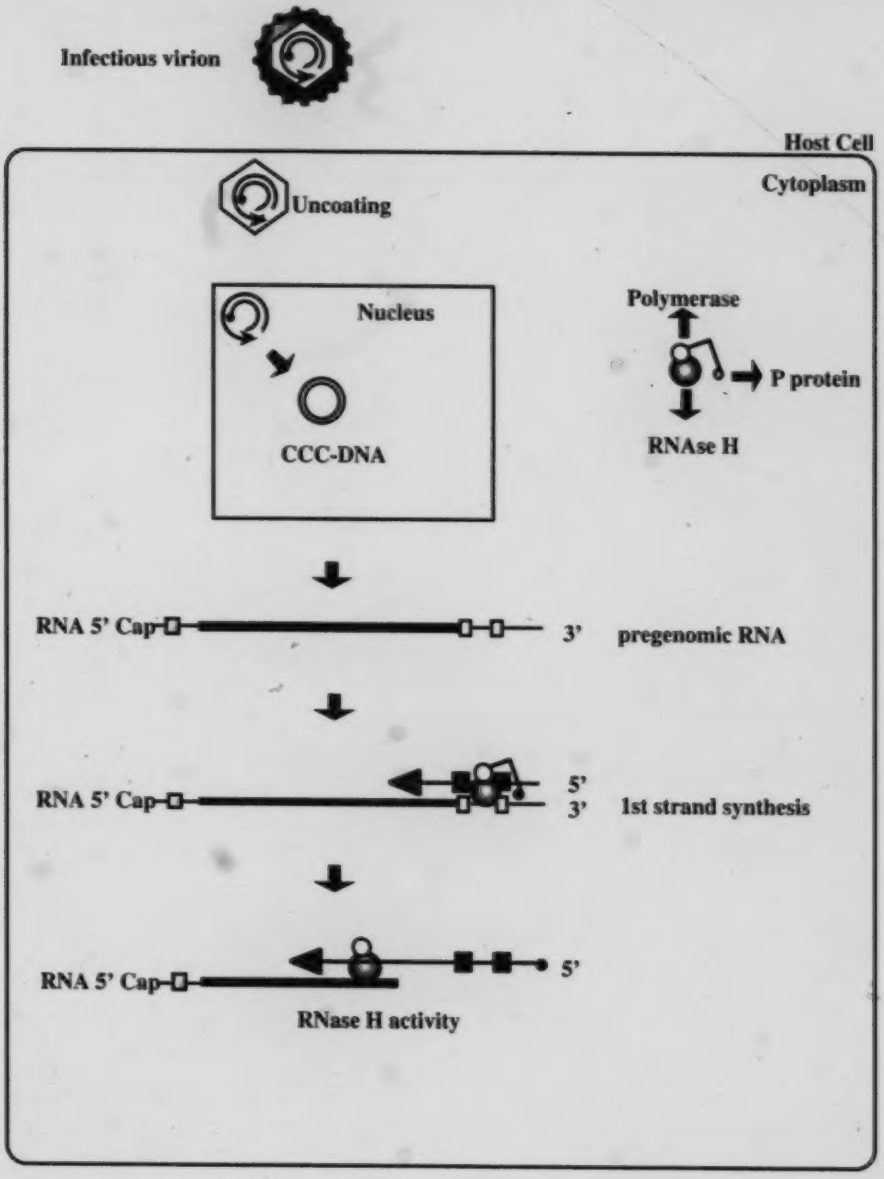

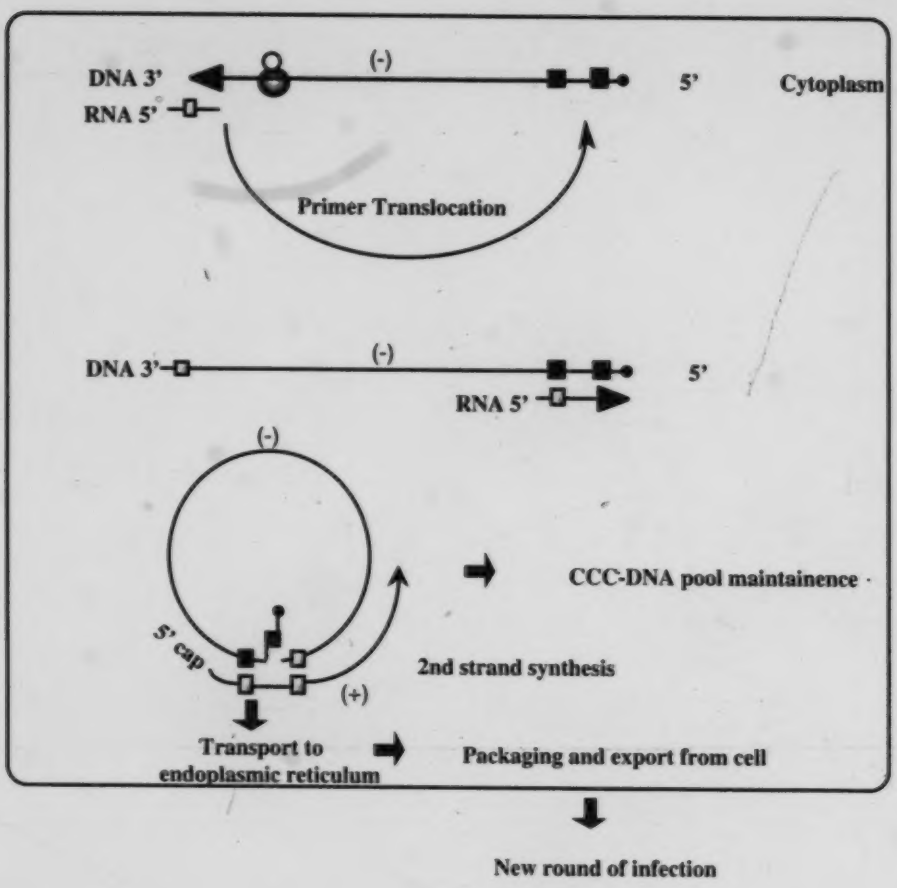

Figure 1.1 Schematic representation of the basic replication cycle of HBV. (1) Binding of intact virion to cell surface, (2) Uncoating of viral outer envelop follow by host cell penetration, (3) Removal of nucleocapside follow by transport of viral core into the nucleus, (4) Conversion of viral genome into CCC-DNA, (5) Transcription of CCC-DNA into pregenomic RNA by host RNA polymerase, (6) Reverse transcription of pregenomic RNA to generate first viral DNA strand, (7) Degradation of RNA template by RNAse H activity, (8) Primer translocation follow by second viral DNA strand synthesis, (9) Circularization of the partially double stranded genome, (10) Transport and packaging of viral genome in endoplasmic reticulum, (11) Export of fresh virus particles from the cell to initiate new round of infection.

infection. A stable pool of cccDNA molecules is maintained in the nuclei by transporting some of the newly synthesized HBV DNA back into the nucleus. Early after replication

begins, the cccDNA pool is amplified by recycling viral DNA to the nucleus whereas later in infection, the newly synthesized viral DNA is assembled into virions [1,9,12].

1.1.3 Treatment of chronic Hepatitis B

To date, antiviral chemotherapy remains the only option for controlling infection with HBV-induced chronic liver disease. Interferon (IFN)-α has proven benefit in a well-defined group of those with hepatitis B but has made little impact on the global burden of chronic liver disease [12]. In addition, the most radical approach such as liver transplantation has failed to eradicate the virus in many cases. In several studies, various antiviral agents such as levamisole [13], (-)-β-L-2',3'-dideoxy-3'-thiacytidine (lamivudine) [14,15], and immune modulators such as interleukin-2 [15] and interferon-α [12] have been evaluated in the treatment of chronic hepatitis. Thus far, most of the compounds tested has not produced effective response and could only suppress replication of virus during therapy. Among many of these compounds developed, lamivudine has been proven to be most effective and is associated with the least amount of host toxicity [14,15,17]. In preclinical studies, lamivudine has been reported as a potent inhibitor of HBV replication *in vitro*. The compound blocks HBV DNA synthesis in HBV transfected hepatoma cell lines but has no effect on viral RNA synthesis [12]. In clinical studies, this orally administered compound has been shown to markedly inhibit HBV replication and stabilize liver function in patients awaiting liver transplantation. Treatment with lamivudine results in a decrease in serum HBV DNA to undetectable levels in 100% of patients after 12 weeks of treatment [12].

HBV replication is most evident during the early phase of chronic infection. It is during this overt replicative phase that patients are most infectious [18]. Therefore

therapeutic efforts must be aimed at this group of patients with a goal of reducing the severity of liver disease and the probability of progressive liver injury. Accomplishment of this goal usually results in loss of serum HBV replication detectable by conventional hybridization assays, Southern blot or Polymerase Chain Reaction (PCR) amplification [19]. Monotherapy frequently leads to antiviral resistance and treatment with lamivudine has resulted in 25 - 35% of patients with mutant virus after 2 years of therapy. Clearly, other treatment strategies and/or new antiviral agents will need to be developed [20]. Assessment of these new treatments will require carefully designed clinical trials that are equipped with various diagnostic techniques which offer rapid, low cost and highly sensitive assays for HBV-DNA [21].

1.1.4 Detection of HBV DNA

Current strategies used in immunoassays involve the detection of Hepatitis surface antigen (HBsAg), hepatitis B core antibody (HBcAb) and antibodies. This indirect approach is subject to false-negative test results because of an absence of immunologic markers during early infection, or variations in the host immune response [21,22]. In addition, the presence of hepatitis B virus surface antigen (HBsAg) in serum or plasma may indicate HBV infection, but the detection of HBsAg does not provide information on the replicative activity of the virus. Furthermore, the link between viral replication and hepatitis B e antigen (HbeAg) is unreliable since HBV pre-core mutants replicate without producing HBeAg [23].

A more direct approach of analysis is the molecular hybridization of HBV DNA. HBV DNA determination for the assessment of ongoing viral replication and the effectiveness of antiviral therapy has been established as the most important method for

monitoring chronic hepatitis [23]. A variety of DNA hybridization techniques have been developed for detection of HBV DNA [21]. Many of the conventional methods are based on 'slot' [24] and 'dot' [25] blot hybridizations, which are slow and labor intensive because of long hybridization and autoradioraphic exposure times. This drawback makes dot / slot blot hybridization techniques unattractive for routine clinical applications. Solution hybridization assay, which has been found to be suitable for HBV DNA detection in serum, are now available in commercial test systems [26-29]. The Abbott HBV DNA assay (Abbott Laboratories, Chicago, IL) which is based on the separation of hybrids and free probe by column chromatography, appears to give satisfactory quantitative results, but sensitivity is low [27]. Detection methods that are more complicated involve affinity-based hybrid capture technique [30], DNA-enzyme immunoassay [31], branched DNA signal amplification assay [32] and some nonisotopic hybridization assays involving chemically modified probes [33]. Developement of the nonisotopic techniques is replacing the use of radiolabeled probes, which have limited application in clinical laboratories due to short half-life, as well as the potential hazard of radiation exposure and contamination.

Amplification techniques such as PCR are extremely sensitive for detecting nucleic acid sequences of HBV DNA in serum [34]. While PCR provides a direct and highly sensitive identification of HBV DNA in the serum, its limitations such as the risk of false-positive results due to contamination and difficulties in developing quantitative tests are limitations in the routine applications. The latter drawback is particularly severe when accurate quantitation of viral load is needed to study patient response to antiviral agents.

1.2 Non radio-labeled based detection of nucleic acids

1.2.1 Laser-induced fluorescence detection

The ability to detect ever smaller amounts of nucleic acid has improved viral diagnosis and monitoring of antiviral therapy to a level not previously envisioned. The use of radioactive compounds in radioimmunoassay and molecular biology assays has enabled measurement of target molecules in solutions with high specificity and sensitivity. The use of fluorescence holds the same level of requirement with the added power of directly visualizing simultaneously several molecular markers as they relate to each other [35].

Fluorescence detection is now gaining momentum in clinical analysis following developments in detector instrumentation and fluorescent dye chemistry. Both the superior concentration and mass sensitivity make this method of detection suitable for analysis of small quantity of analyte of interest, such as the measurement of viral DNA that is present in a background of contaminating host nucleic acids. Fluorescent tags provide a number of advantages for biomedical testing in addition to the high specificity and sensitivity. First, the quantification of fluorescence is linear over a wide range and it is not very susceptible to interfering substances. Second, unlike radio-labels, fluorescent reagents are stable for extended periods with proper storage. Third, the ability to examine fluorescent tags of different colors and correlate multiple parameters offers a superior way to perform multiparameter analysis in biological systems that are unsolved using single parameter analysis [36].

1.2.2 Utility of Laser-induced fluorescence in DNA analysis

The sensitivity and specificity advantages associated with LIF detection make it suitable for DNA analysis. Its sensitivity is 2 to 3 logs higher than UV detection [37,38]. Currently, slab gel-electrophoretic techniques in conjunction with ethidium bromide staining or autoradiography are the methods commonly used for the separation and quantitation of single and double stranded DNA. With the use of LIF detection as an alternative, ultrasensitive techniques are being developed to replace various nucleic acids separation and detection methods which invlove the use of autoradiography, such as Northern Blot for RNA and Southern Blot for DNA analysis. In the next three sections, three general methods to fluorescently label oligonucleotides and PCR products are discussed.

1.2.3 5' end labeling

The first method uses fluorescence-labeled primers that are prepared by coupling a fluorescent dye on the 5' end of an oligonucleotide primer using fluorescent amidite reagent, FAM amidite (Applied Biosystems) or by post-synthesis coupling using Aminolink 2 (Applied Biosystems) [39]. In DNA sequencing, Ansorge et al. [40] reported the use of 5' end rhodamine - labelled sequencing primer. The sequencing reactions proceeded normally, and the products of the four sequencing reactions were separated in adjacent lanes of a slab gel. The fluorophore was excited by a single laser beam. Fluorescence signal was detected from each lane. More sophisticated approaches in which primers were labelled with four different fluorescent tags have also been described [41]. Each labeled primer was used for one of the four different sequencing reactions and the products of the reaction were combined and separated in a single lane of

a slab gel or a multi-capillary system. An alternate method involved the use of fluor-labeled dideoxy nucleotide triphosphate terminators in the Sanger-Coulson chemistry. In this case, a spectrally different fluor is attached to each of the four terminators, and termination-type assignment is made via on-the-fly spectroscopy. This labelling approach is more convenient and reliable since only legitimately terminated fragments are labeled and detected [42].

1.2.4 Intercalating dyes

The second method relies on the use of fluorescent dyes, which involves the insertion of a conjugate ring system into the interior of the DNA helix, nestled in between the adjacent base pairs. The resulting dye-DNA complex usually creates up to a thousand fold enhanced fluorescence with increases in quatum yields to as high as 0.9. Intercalating dyes such as ethidium bromide and Hoechst 33258 [43] have been used over the years to enhance detection of DNA fragments in slab gel electrophoresis as well as CE [44]. They serve a dual role in the separation process, acting to enhance resolution as well as to improve detectability of the DNA. Recently more than a dozen cyanine dyes that bind with high affinity to nucleic acids have been marketed by Molecular Probes, Inc. (Eugene, OR, USA) [45]. Some common examples are POPO-3, YOYO-1, YOYO-3, TOTO-1, TOTO-3, YO-PRO, PO-PRO, TO-PRO, SYBR Green I and II, Pico Green and OliGreen (Molecular Probes). The properties of these dyes include selective binding to DNA, enhanced fluorescence upon binding, and minimal fluorescence in the unbound state. By using these dyes, the detection limit is as low as 4 pg of DNA in a single band in a slab gel system using a laser-excited confocal fluorescence gel scanner [46,47].

Some of these dyes have been shown to enhance sensitivity more than 500 times compared to conventional ethidium bromide staining of DNA [47].

1.2.5 Random labeling

In the third method, labelled nucleotide fluorescein 12-dUTP or F-dUTP (Boehringer Mannheim, Indianapolis. IN) [48] are incorporated into amplified products in the presence of cold deoxynucleoside triphosphates. This method is particularly useful in situations where covalent labeling of the PCR primer is not justified or possible, or where higher specific activity labeling is desired. All the three labeling techniques described have been applied to clinical analyses ranging from detection of abnormal genes to point mutations.

1.3 DNA separation technology

1.3.1 DNA Separation using capillary electrophoresis

The classical technique for DNA separation is slab gel electrophoresis. However, a gradual transition from slab gel to CE is likely in the near future. In its short history of a little more than a decade, CE has shown great applicability in modern bioanalytical, biopharmaceutical as well as molecular biology. These applications cover a wide range of research areas which include analysis of restriction DNA fragments [49-52], detection of point mutation in DNA and DNA damage [53-55], detection of fluorescently labelled polymerase chain reaction products [56-60].

CE has potentially many advantages over traditional slab gel electrophoresis. First, because of the small diameter of the capillaries, heat dissipation is very effective and band broadening due to joule heating is minimized. Second, strong electric fields of

400 V/cm and higher can be applied, and therefore reducing the run time and diffusion. Third, the diameter and length of the capillary can be chosen over a wide range, depending on the nature of the analysis. Fouth, for a capillary with small inner diameter (50 - 100 μm), minute amounts of sample can be analyzed with high sensitivity. Fifth, because of the reduced bandwidth, DNA separation efficiency is usually in the order of several million theoretical plates per meter. Figure 1.2 shows a schematic representation of a CE system.

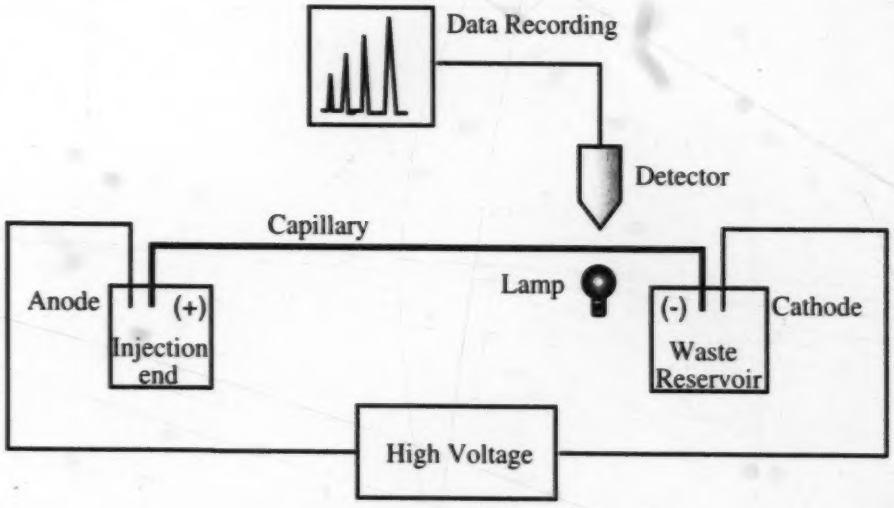

Figure 1.2 General scheme of a commercial CE instrument. Polarity at injection end is designated for separation driven by electro-osmotic flow. A reversed polarity at the injection end is necessary for DNA separatioin using a coated capillary. For laser-induced fluorescence detection, the lamp is replaced by a laser.

The basic instrumentation involves a fused silica capillary, two buffer reservoirs, one at the sample injection end and the other at the detector end, a detector and a high-

voltage power supply (0 to 30kV). This set up applies to most analyses using capillary zone electrophoresis. In the case of capillary gel electrophoresis with a coated capillary, the polarity of the system is reversed such that the injection end becomes the cathode while the detector end becomes the anode.

1.3.2 Separation media

For relatively short oligonucleotides, there is a need for single base resolution for DNA sequencing. For double-stranded DNA, analyzing and identifying DNA molecules in the form of restriction fragments or polymerase chain reaction (PCR) products may not require single base resolution.

At present, DNA fragments may be analyzed by two major CE approaches: a capillary-gel separation system [61-63] and a polymer-network capillary separation system [64-67]. The capillary-gel system uses an *in situ* polymerized acrylamide gel cross-linked to the walls of the capillary. This step is carried out by adding the catalysts to the monomer solution, which is then pumped into the capillary where the polymerization takes place. The inner wall of the capillary is usually treated with chemicals such as 3-methacryloxypropyltrimethoxysilane, which fixes the gel to the wall and prevents if from being extruded by electroosmotic forces [68]. The gel-filled columns currently being produced have a limited lifetime due to gel degradation caused by localized heating from the high electric field used in the CE separation [69]. The decomposition of additives such as urea in the buffer can also restrict the shelf life. There is also the potential for gel-filled columns to irreversibly bind high molecular weight DNA resulting in a reduction of performance over time [69]. Other disadvantages associated with gel-filled capillaries are the formation of air bubbles during gel

polymerization and the need to periodically trim the capillary due to clogging at the injection end [68].

The polymer-network system is based on buffers containing additives such as methylcellulose, hydroxypropylmethylcellulose, dextran or polyethylene glycol, which create a gel-like matrix inside the capillary. This idea of using polymer solutions to separate biopolymers is not new for it was proposed years ago in the pioneering work of Bode [70]. It has become particularly popular recently in combination with CE. Unlike gel filled capillary columns, non-gel sieving offers a clean and stable environment to be used each time a sample is run. The viscosity of the polymer solution is usually low enough that it can be replaced with fresh polymer solution by simple syringe pump methods. Thus, the same capillary column can be used for many runs before replacement is necessary. At very low viscosity (0.1 to 1%), the resolving power offered by some of the cellulose matrices may not be comparable to that of the high viscosity linear or polyacrylamide gels (6%). However, these low viscosity polymer solutions have been shown to provide excellent separation of restrtiction fragments and PCR products [68]. These advantages, in combination with low cost and low toxicity, have made cellulose polymer a seiving medium for routine application of CE.

1.3.3 Basic considerations for size-based separation

In free solution, all DNA molecules greater than 8 basepairs will migrate at the same, size-independent electrophoretic mobility [69]. Separation of DNA of different sizes can be achieved if electrophoresis is performed in gels or in polymer solutions. Most of the theoretical considerations used for capillary electrophoresis of DNA were derived from classical gel electrophoresis. These theoretical considerations for DNA

separation are well described [71-74]. In agarose or a crosslinked polymer matrix, the interaction between solute and matrix has the primary effect on the migration behavior of DNA. DNA separation is postulated to occur either by Ogston theory or by the Reptation model [69], depending on DNA size, field strength and gel concentration. These models allow migration times, plate numbers and resolution to be predicted.

The Ogston model treats the gel as a molecular sieve. The matrix is formed by randomly distributed fibers, which provide a system of randomly distributed pores. The probability that a DNA molecule will enter these pores depends on the pore size and diameter of the DNA at a spherical conformation. The higher the concentration of the gel, the lower the probability for the spherical DNA to enter the pore. The expression of this relationship is well explained by Dolnik [75]. As this model evolves, the extended Ogston model and the modified version of the Ogston model for separation of single stranded DNA have been developed to facilitate a growing interest in the behavior of DNA separation in various replaceble polymer solutions.

The Reptation model was developed to account for the fact that long DNA molecules, instead of migrating as undeformed, spherical particles of fixed radius of gyration, can be deformed and stretched according to conditions such as applied field strength and pore sizes that are too small for the DNA molecules. This model predicts that large DNA molecules move "head first" by a snakelike motion through the gel [76-78]. The Biased Reptation model states that at high electric fields or for DNA molecules larger than 40 Kbp, or a combination of both, field-induced orientation extends the stretching periods of DNA, causing their random walk to become strongly biased in the forward direction so that DNA is strecthed to a rodlike conformation. In a fully biased

reptation regime, mobility extended to saturation and size-based separation is lost. The mobility expression for this model has been described by Donik [75].

1.3.4 DNA separation in low viscosity polymer solutions

Apart from the important family of acrylamide, most of the polymers used in CE are modified polysaccharide such as agarose and its different alterations, various cellulose derivatives such as methylcellulose, hydroxyethylcellulose, hydroxypropylcellulose, hydroxypropyl-methylcellulose, glucomannan, polyethylene glyco and polyvinyl alcohol [79]. Solutions of these uncross-linked polymers have been found to have separation potential over a wide range of concentrations, from semi-dilute, low-viscosity solutions to extremely concentrated solutions that are impossible to be injected into a capillary, usually above 10% w/v.

To date, it has not been fully established whether the mechanism of DNA separation in an extremely dilute solution of cellulose derivatives is the same as that which occurs in a chemical gel. Further, in uncross-linked polymer solutions, the relationship between the resolution and the molecular weight and concentration of the polymer is not yet fully understood, and no theory exists to accurately predict the appropriate polymer size and concentration for a desired separation. Some groups have asserted that the mechanism is essentially the same as that in traditional slab gel electrophoresis [81,82], while others attribute separation to the attraction and interaction of DNA fragments with the cellulose derivatives in solution [83,84]. Still others have theorized that the separation involves a mechanism of exclusion from the polymer fiber network similar to that occurring in gel permeation chromatography [85]. Further investigation into the role of polymer properties and the mechanism of separation in

polymer solutions should lead to a rational design of polymer matrices for separations of nucleic acids by capillary electrophoresis.

1.4 Single cell analysis and CE-LIF

1.4.1 General aspects and areas of applications

The human body consists of approximately 10^{13} cells. A few hundred different cell types can be identified. However, even within one type of cells, there is variation in biological properties. Most evident is with the cells of the immune system, in which at any given time the human body contains B-cells with the potential to produce several million different antibodies. For other cell types this variation is less pronounced but still impressive.

To date, many biological techniques study cells in suspension. These experiments would give meaningful information when the level of variability in a population of cells is insignificant such that it can be described by Gaussian distribution. However, many transforming processes start with modifications of an individual cell, which results in a selective advantage of that cell over the prevailing population of cells. This is well reflected in tumorigenesis where cancer cells are clonal in nature. This means the final tumor is the progeny of only one or a few similar cells whose individual properties do not represent the properties of the majority of the cells of this type. Hence, it is important to have the ability to investigate cell properties on an individual basis.

With the development of miniaturization and automation for biological analyses, capillary electrophoresis (CE) has started to to be used for the analysis of individual cells. CE is well-suited for probing microenvironments due to the compatibility between the

dimensions of the capillary (inner diameters of 2 to 200 μm) and the size of most cells (5 to 500 μm). The technique also offers several advantages including much smaller sample size, extremely high separation efficiency, high analysis speed, possible on-capillary sample pretreatment such as enzymatic digestion and derivatization, and it is easy to couple with highly sensitive detection methods such as laser-induced fluorescence [86-88]. To date CE has not only been tested extensively for the separation of macromolecules such as DNA and proteins, but also has been made to conduct analytical separations of "particulate materials" at subcellular levels. These materials include colloidal organic or inorganic particles as well as biological subcellular vesicles, lipoprotein particles, liposomes, microsomes and viruses [89]. Further development of these techniques will find wide range of applications in the analysis of metabolic diseases as well as forensic and biochemical studies.

1.4.2 Detection methods

Optical detection systems for CE have been reviewed by Dovichi [90] and Pentoney and Sweedler [91]. Detection in CE is a significant challenge as a result of the small dimensions of the capillary. Although CE requires only nanoliter volumes of sample, it is not a "trace" analysis technique since relatively concentrated analyte solutions or pre-concentration methods are often necessary. A number of detection methods have been employed to meet this challenge, many of which are similar to those used in liquid column chromatography. Table 1.1 shows a list of many of the detection methods investigated [92].

From Table 1.1, it is obvious fluorescence detection in CE provides excellent mass detection sensitivity. Minimum detectable concentrations with LIF are typically

two to five orders of magnitude lower than UV detection, while superior linearity can be obtained. In some favorable cases, single-molecule detection can be achieved [93,94]. This property makes LIF a suitable choice for single cell analysis. Furthermore, compared to conventional non-LIF excitation sources such as lamps based on mercury-xenon, deuterium and tungsten, it is technically less challenging to focus a tight laser beam onto a tiny detection window of the capillary while minimizing light scatter from the capillary wall.

Table 1.1 Methods of detection for CE

Method	Mass detection limit (moles)	Concentration detection limit (molar)	Advantages/ disadvantages
Laser-induced fluorescence	10^{-18} - 10^{-20}	10^{-14} - 10^{-16}	° Extremely sensitive ° Needs sample derivatization
Amperometry	10^{-18} - 10^{-19}	10^{-10} - 10^{-11}	° Sensitive ° Selective but useful only for electroactive species ° Needs special electronics and capillary modification
UV-Vis absorption	10^{-13} - 10^{-16}	10^{-5} - 10^{-8}	° Universal ° Diode array offers spectral information
Mass spectrometry	10^{-16} - 10^{-17}	10^{-8} - 10^{-9}	° Sensitive and offers structural information ° Interface between CE and MS complicated
Conductivity	10^{-15} - 10^{-16}	10^{-7} - 10^{-8}	° Universal ° Needs special electronics and capillary modification

1.4.3 Future of single cell analysis

The analysis of intact cells by CE, either in their entirety or as subcellular compartments, has been very successful [95,96]. However to become clinically useful, great strides must be taken to improve on current cell injection and samplingtechniques, to increase throughput, i.e., the number of cells that can be analyzed in a given time, as well as to improve on sampling automation. The improvement in the production of diode lasers with useful wavelengths for native biomolecules and sensitive derivatizing agents, should lead to more compact and possibly portable devices. In adddition, subcellular compartmental analysis, kinetic studies of cell cycle and multiparametric determinations by CE-LIF should also find increased application in molecular and cell biology.

1.5 Bibliography

1. Yoffe, B. and Noonan, C.A. (1993) Prog. Med. Virol. **40**, 107-140.
2. Hilleman, M.R. (1994) AIDS Research & Human Retroviruses **10**, 1409-1419.
3. Ren, E.C. (1996) Ann. Acad. Med. Singapore **25**, 17-21.
4. Christofidou, M., Athanassiadou, A., Skoutelis, A. and Anastassiou, E.D. (1995) Eur. J. Clin. Microbiol. Infect. Dis. **14**, 464-468.
5. Yoffe, B. and Noonan, C.A. (1992) Digestive Diseases & Sciences **37**, 1-9.
6. Sherker, A.H. and Marion, P.L. (1991) Annu. Rev. Microbiol. **45**, 475-508.
7. Ganem, D. and Varmus, H.E. (1987) Ann. Rev. Biochem. **56**, 651-693.
8. Nassal, M. and Schaller, H. (1993) Trends in Microbiol. **1**, 221-228.
9. Lau, J.Y.N. and Wright, T.L. (1993) The Lancet **342**, 1335-1340.
10. Blum, H.E. (1995) Digestion **56**, 85-95.

11. Bruss, V., Gerhardt, E., Vieluf, K. and Wunderlich, G. (1996) Intervirology **39**, 23-31.

12. Torresi, J. and Locarnini, S. (2000) Gastroenterol. **118**, S83-S103.

13. Fattovich, G., Brollo, L., Pontisso, P., Pronaro, E., Rugge, M., Alberti, A. and Reali, G. (1991) Gastroenterol. **91**, 187-696.

14. Severini, A., Liu, X.Y., Wilson, J.S. and Tyrrell, D.L.J. (1995) Antimicrob. Agents. Chemother. **39**, 1430-1435.

15. Bain, V.G., Kneteman, N.M., Ma, M.M., Gutfreund, K., Shapiro, J.A., Fischer, K., Tipples, G., Lee, H., Jewell, L.D. and Tyrrell, D.L. (1996) Transplantation **62**, 1456-62.

16. Davis, G.L. (1991) Hepatology **14**, 567-569.

17. Frederik, N. (1998) Acta Gastro-Enterologica Belgica **I.X.I.**, 246.

18. Hoofnagle, J.H., Dusheiko, G.M., Seeff, L.B., Jones, E.A., Waggoner, J.G. and Bales, Z.B. (1986) Semin. Liver Dis. **6**, 1-10.

19. Korenman, J., Baker, B., Waggoner, J., Everhart, J.E., Di Bisceglie, A.M. and Hoofnagle, J.H. (1991) Ann. Intern. Med. **114**, 629-634.

20. Locarnini, S.A., Civitico, G.M. and Newbold, J.E. (1996) Antiviral Chem. Chemother. **7**, 53-64.

21. Main, J. and McDade, H.B. (1997) Int. J. Pharm. Med. **11**, 324-331.

22. Yang, G., Ulrich, P.P., Aiyer, R.A., Rawal, B.D. and Vyas, G.N. (1993) Blood **81**, 1083-1088.

23. Lieberman, H.M., LaBrecque, D.R., Kew, M.C., Hadziyannis, S.J. and Shafritz, D.A. (1983) Hepatology **3**, 285-291.

24. Scotto, J., Hadchouel, M., Hery,C., Yvart, J., Tiollais, P. and Brechot, C. (1983) Hepatology **3**, 279-282.

25. Weller, I., Fowler, M., Monjardino, J. and Thomas, H. (1982) J. Med. Virol. **9**, 273-280.

26. Barlet, V., Cohard, M., Thelu, M.A., Chaix, M.J., Baccard, C., Zarski, J.P. and Seigneurin, J.M. (1994) J. Virological Methods **49**, 141-152.

27. Kuhns, M.C., McNamara, A.L., Cabal, C.M., Decker, R.H., Thiers, V., Brechot, C. and Tiollais, P. (1988) In Zuckerman A.J. (ed): Viral Hepatitis Liver Disease; New York: Alan R. Liss, pp. 258-262.

28. Janssen, H.L.A., Schoenmaker-Weber, Y.A.M., Kruining, H., Schalm, S.W. and Heijtink, R.A. (1993) J. Med. Virol. **40**, 307-312.

29. Zaaijer, H., ter Borg, F., Cuypers, H, Hermus, M. and Leslie, P. (1994) J. Clin. Microbiol. **32**, 2088-2091.

30. Jalava, T., Ranki, M., Bengtstrom, M., Pohjanpelto, P. and Kallio, A. (1992) J. Virol. Methods **36**, 171-180.

31. Mantero, G., Zonaro, A., Albertini, A., Bertolo, P. and Primi, D. (1991) Clin. Chem. **37**, 422-429.

32. Kapke, G.F., Watson, G., Sheffler, S., Hunt, D. and Frederick, C. (1997) J. Viral Hepatitis **4**, 67-75.

33. Akar, A., Bournique, B. and Scholler, R. (1992) Clin. Chem. **38**, 1352-1355.

34. Quint, W.G.V., Heijtink, R.A., Schirm, J., Gerlich, W.H. and Niesters, H.G.M. (1995) J. Clin. Microbiol. **33**, 225-228.

35. MacTaylor, C.E. and Ewing, A.G. (1997) Electrophoresis **18**, 2279-2290.

36. Tao, L. and Kennedy, R.T. (1998) Trends Anal. Chem. **17**, 484-491.

37. Srinivasan, K., Morris, S.C., Girard, J.E., Kline, M.C. and Reeder, D.J. (1993) Appl. Theor. Electrophoresis **3**, 235.

38. Arakawa, H., Uetanaka, K., Maeda, M., Tsuji, A., Matsubara, Y. and Narisawa, K. (1994) J. Chromatogr. A. **680**, 517.

39. Gibbs, R.A., Nguyen, P.N., McBride, L.J., Koepf, S.M. and Caskey, C.T. (1989) Proc. Natl. Acad. Sci. USA **86**, 1919-1923.

40. Ansorge, W., Sproat, B., Stegemann, J. and Schwager, C. (1986) J. Biochem. Biophys. Meth. **13**, 315.

41. Smith, L.M., Sanders, J.Z., Kaiser, R.J., Hughes, P., Dodd, C., Connell, C.R., Heiner, C., Kent, S.B.H. and Hood, L.E. (1995) Nature **321**, 674.

42. Schwartz, H.E., Ulfelder, K.J., Chen, F.T.A. and Pentoney, S.L. (1994) J. Cap. Elec. **1**, 36-54.

43. Deflaun, M.F. and Paul, J.H. (1986) J. Microbiol. Methods **5**, 265-270.

44. Kasper, T.J., Melera, M., Gozel, P. and Brownlee, R.G. (1988) J. Chromatogr. **458**, 303-312.

45. Johnson, I.D., Marcus, E.M., Yue, S. and Haugland, R.P. (1992) Biophys. J. **61**, A314.

46. Rye, H.S., Quesada, M.A., Peck, K., Mathies, R.A. and Glazer, A.N. (1991) Nucl. Acids Res. **19**, 327, 333.

47. Quesada, M.A., Rye, H.S., Gingrich, J.C., Glazer, A.N. and Mathies, R.A. (1991) BioTechniques **10**, 616-625.

48. Voss, H., Schwager, C., Wirkner, U., Zimmermann, H., Erfle, H., Hewitt, N.A., Rupp, T., Stegemann, J. and Ansorge, W. (1992) Methods Mol. Cell Biol. **3**, 30-34.

49. Chan, K.C., Whang, C.W. and Yeung, E.S. (1993) J. Liq. Chromatogr. **16**, 1941-1962.

50. McGregor, D.A. and Yeung, E.S. (1993) J. Chromatogr. A. **652**, 67-73.

51. Kleemib, M.H., Gilges, M. and Schomburg, G. (1993) Electrophoresis **14**, 515-522.

52. Baba, Y., Ishimaru, N., Samata, K. and Tsuhako, M. (1993) J. Chromatogr. A. **653**, 329-335.

53. Mitchelson, K.R. and Cheng, J. (1995) J. Cap. Elec. **2**, 137-143.

54. Cadet, J. and Weinfeld, M. (1993) Anal. Chem. **65**, 675A-681A.

55. Kuypers, A.W.H.M., Willems, P.M.W., van der Schans, M.J., Linssen, P.C.M., Wessels, H.M.C., de Bruijn, C.H.M.M., Everaerts, F.M. and Mensink, E.J.B.M. (1993) J. Chromatogr. **621**, 149-156.

56. McCord, B.R., McClue, D.L. and Jung, J.M. (1993) J. Chromatogr. A. **652**, 75-82.

57. Williams, P.E., Marino, M.A., Del Rio, S.A., Turni, L.A. and Devaney, J.M. (1994) J. Chromatogr. A. **680**, 525-540.

58. Lu, W., Han, D.S., Yuan, J. and Andrieu, J.M. (1994) Nature **368**, 269-271.

59. Butler, J.M., McCord, B.R., Jung, J.M., Lee, J.A., Budowle, B. and Allen, R.O. (1995) Electrophoresis **16**, 974-980.

60. Hurni, W.M. and Miller, W.J. (1991) J. Chromatogr. **559**, 337-343.

61. Heiger, D.K., Cohen, A.S. and Karger, B.L. (1990) J. Chromatogr. **516**, 33.

62. Guttman, A. and Cooke, N. (1991) Anal. Chem. **63**, 2038.

63. Karger, B.L., Cohen, A.S. and Guttman, A. (1989) J. Chromatogr. **585**, 492.

64. Zhu, D., Hansen, D.L., Burd, S. and Gannon, F. (1989) J. Chromatogr. **480**, 311.

65. Strege, M. and Lagu, A. (1991) Anal. Chem. **63**, 1233.

66. MacCrehan, W.A., Rasmussen, H.T. and Northrop, D.M. (1992) J. Liq. Chromatogr. **15**, 1063.

67. Grossman, P.D. and Soanne, D.S. (1991) J. Chromatogr. **559**, 257.

68. Heller, C. (1995) J. Chromatogr. **698**, 19-31.

69. McCord, B.R., Jung, J.M. and Holleran, E.A. (1993) J. Liq. Chromatogr. **16**, 1963-1981.

70. Bode, H.J. (1977) Anal. Biochem. **83**, 204.

71. Giddings, J.C. (1969) Separ. Sci. **4**, 181.

72. Mikkers, F.E.P., Everaerts, F.M. and Verheggen, Th.P.E.M. (1979) J Chromatogr. **169**, 1.

73. Bocek, P., Demi, M., Gebauer, P. and Dolnik, V. (1988) Analytical Isotachophoresis (VCH Verlagsgesellschaft, Weinheim)

74. Hjerten, S. (1984) in Topics in Bioelectrochemistry and Bioenergetics, G. Milazzo, Ed. (John Wiley & Sons, Chichester), p 9.

75. Dolnik, V. (1994) J. Microcol. Sep. **6**, 315-330.

76. Slater, G.W. and Noolandi, J. (1993) Biopolymers **25**, 431.

77. Dejardin, P., Lumpkin, O.J. and Zimm, B.H. (1985) J. Polymer Sci., Polymer Symp. **73**, 67.

78. Lumpkin, O.J., Dejardin, P. and Zimm, B.H. (1985) Biopolymers **24**, 1573.

79. Righetti, P.G. and Gelfi, C. (1996) Capillary Electrophoresis of DNA in Capillary Electrophoresis in Analytical Biotechnology. CRC Press Inc. pp.477-508.

80. Barron, A.E., Soane, D.S. and Blanch, H.W. (1993) J. Chromatogr. A. **652**, 3-16.

81. Schwartz, H.E., Ulfelder, K., Sunzeri, F.J., Busch, M.P. and Brownlee, R.G. (1991), **559**, 267.

82. Grossman, P.D. and Soane, D.S. (1991) Biopolymers **31**, 1221.

83. Strege, M and Lagu, A. (1991) Anal. Chem. **63**, 1233.

84. Chin, A.M. and Colburn, J.C. (1989) Am. Biotech. Lab. **7**, 16.

85. Pulyaeva, H., Wheeler, D., Garner, M.M. and Chrambach, A. (1992) Electrophoresis **13**, 608.

86. Jankowski, J.A., Tracht, S. and Sweedler, J.V. (1995) Trends Anal. Chem. **14**, 170.

87. Yeung, E.S. (1994) Acc. Chem. Res. **27**, 409.

88. Hogan, B.L. and Yeung, E.S. (1993) Trends Anal. Chem. **66**, 527A.

89. Radko, S.P. and Chrambach, A. (1999) J. Chromatogr. B. 722, 1-10.

90. Dovichi, N. (1993) In: Camilleri, P. (ed). Capillary electrophoresis: theory and pratice. Boca Raton: CRC Press, p.25-64.

91. Pentoney, SL Jr. and Sweedler, JV. (1994) In: Landers J.P. (ed). Handbook of capillary electrophoresis. Boca Raton: CRC Press, p.147-83.

92. Ewing, A.G, Wallingford, R.A. and Olefirowicz, T.M. (1989) Anal. Chem. **61**, 292A-303A.

93. Castro, A., Fairfield, F.R. and Shera, E.B. (1993) Anal. Chem. **65**, 849-852.

94. Nguyen, D.C., Keller, R.A., Jett, J.H. and Martin, J.C. (1987) Anal. Chem. **59**, 2158-2161.

95. Yang, Q., Hidajat, K. and Li, S.F.Y. (1997) J. Chromatogr. Sci. **35**, 358-373.

Yeung, E.S. (1999) J. Chromatogr. A. **830**, 243-262.

Chapter 2. Hydroxyethyl Cellulose as a Replaceable Sieving Polymer for DNA Separation

2.1 Introduction

2.1.1 Theory of DNA separation

Theory of migration and separation of DNA is well described [1-5]. The basic principle of DNA separation in electrophoresis is that charged molecules migrate in the presence of an applied field strength. Under the influence of an electric field, a charged molecule experiences an electrophoretic force (F_e) equal to the product of its net charge (Q) and the electric field strength (E) as shown in equation 2.1.

$$F_e = Q \times E \qquad (2.1)$$

The charged molecule experiences a drag force (F_d) in the opposite direction of its motion. F_d is proportional to its velocity (v) and its translational friction coefficient (f) as shown in equation 2.2.

$$F_d = f \times v \qquad (2.2)$$

During electrophoresis, the drag force acting on the molecule will counterbalance the electrophoretic force (F_e). Hence the velocity of the molecule at steady state ($F_e = F_d$) can be described by equation 2.3.

$$v = Q \times E / f \qquad (2.3)$$

The electrophoretic mobility (μ) is defined as the velocity of the charged molecule divided by the field strength.

$$\mu = v / E = Q / f \qquad (2.4)$$

The differences in the mobility of molecules will arise from either differences in their frictional properties (sizes and shapes) or their net charges. It is these variations between molecules that make separation by electrophoresis possible.

In the absence of sieving medium, DNA molecules have virtually identical electrphoretic mobilities regardless of their size [6]. DNA acts as a free-draining coil during electrophoresis in which case all basepairs of a DNA fragment are accesible to solvent. Therefore, each base-pair contributes equally to the overall drag of the fragment such that the value f is compatible to the number of basepairs in a DNA fragment (N_b).

$$f \sim N_b \tag{2.5}$$

Since the two negatively charged phosphate groups per base-pair contribute to most of the charge of a DNA molecule, the net charge on a DNA molecule is approximately proportional to the number of basepairs in the DNA fragment (equation 2.6).

$$Q \sim N_b \tag{2.6}$$

From equations (2.5) and (2.6), it is thus suggested that the free-solution electrophoretic mobility of DNA is independent of the size of the DNA (equation 2.7).

$$\mu = (Q / f) \sim (N_b / N_b) \tag{2.7}$$

Hence, in order to achieve size-based separations of nucleic acids by electrophoresis, a separation matrix is needed to alter the dependence of the friction factor on molecular mass.

2.1.2 Polymer solutions

Several different types of polymers have been employed as DNA separation media for capillary electrophoresis, including polyacrylamide [7-9], methyl cellulose [10], hydroxyethyl cellulose [11-15], hydroxypropylcellulose [16], polyethylene glycol [17], polyethylene oxide [18], liquified agarose [19,20] and polyvinyl alcohol [17,20]. Attempts to perform CE separation of DNA in gel-filled capillaries have met with limited success, and have focused almost exclusively on the use of cross-linked polyacrylamide

gels. The preparation of gel-filled capillaries of uniform quality and stability has proven difficult and remains a problem [21-23]. In the last few years, there has been tremendous progress accomplished by optimizing and modifying the existing electrophoresis matrices [4,24-28]. Separations of an approximately ten-fold greater size range than achieved by conventional slab gel electrophoresis are now feasible.

CE in cellulose polymer solutions provides an alternative to the use of gel-filled capillaries. These polymer solutions have the advantages of ease of handling, and are replaceable separation matrices. In addition, these polymer solutions do not necessarily have a limited shelf life and in many instances have lower viscosity than polyacrylamide solutions [16,20,25,29,30]. These properties make cellulose polymers better candidates for CE separation. In general, polymer solutions can be separated into two different concentration regimes: dilute and entangled. A dilute solution is defined as a solution in which the polymer chains are hydrodynamically isolated from one another in solution, which occurs at a low concentration of the polymer. As the concentration of the polymer is increased, the polymer chains begin to overlap. A further increase in polymer concentration leads to entangled solutions, where the polymer molecules interact strongly with each other in solution, forming a physical network. The transition between dilute and entangled solutions is termed the semi-dilute regime, which occurs at concentrations near the entanglement threshold, ϕ. The theoretical expressions of ϕ have been proposed by several investigators [31-33]. For the purpose of our investigations, ϕ will not be described here in detail.

2.1.3 Hydroxyethyl Cellulose (HEC)

HEC is a non-ionic water-soluble, hydrophilic cellulose derivative used for a range of applications in the paint, building and textile industries as a stablilizing, thickening and emulsifying agent. It is synthesized commercially by reacting alkali cellulose with ethylene oxide at high temperature [34]. Substitution may be expressed in terms of the moles of ethylene oxide per anhydroglucose unit, designated as the molar substitution (M.S.). On average, HEC has a M.S. of 2.5, giving an average monomer molecular weight of 272 g / mol. A typical structural element of the HEC molecule is shown in Figure 2.1. In aqueous solutions, HEC is a linear, uncharged cellulose derivative. The dissolution of HEC in water is accomplished by the expansion of the structure by the bulky substituent groups, especially the polyethylene oxide side chains, which terminate in the hydrophilic hydroxyethyl group [34]. These hydrophilic side groups force HEC into a stiff, extended conformation. This property has been attributed to a unique sieving power of HEC for large DNA molecules between 2 and 23.1 kbp even at ultradilute polymer concentrations that are well below the entanglement threshold [35]. In addition, it was also noted that DNA molecules, being also stiff polymers, are able to engage with the short HEC rods by a mechanism of "transient entanglement coupling". This phenomenon is described as the ability of DNA molecules to intertwine with HECs and drag them along during electrophoresis [1]. Aqueous solutions of HEC exhibit pseudoplastic behavior with varying solution viscosity, depending upon the amount of stress applied. The extent of this pseudoplastic behaviour of HEC is dependent on the molecular weight distribution of the sample, which can be determined by gel filtration chromatography [34].

The use of HEC as a sieving polymer for CE has been studied by a number of groups [11,13,35-39]. The performance of HEC for optimum DNA separation has been found to be highly dependent on the manner in which the sieving medium is prepared. This includes degassing, filtration, dialysis of the sieving medium, and the presence of other additives such as urea, formamide and various intercalating dyes in the medium during DNA separation. Separation can be optimized by adjusting the concentration of HEC to match the desired size of DNA. In general, for HEC concentrations between 0.3 and 0.5%, separation of DNA fragments of 1000 bp or larger is found to be efficient.

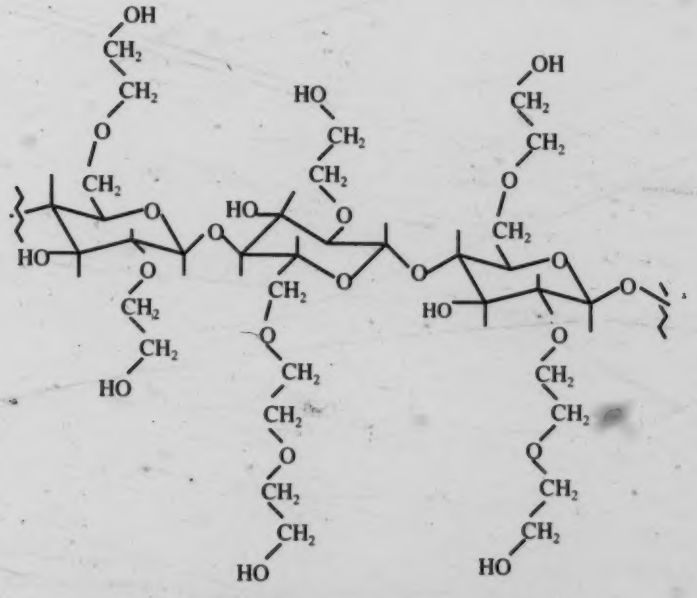

Figure 2.1 A typical structure of hydroxyethyl cellulose chain with three monomers shown.

For fragments that are 1000 bp and smaller, HEC concentrations between 0.5 and 1% is optimum. Selection of HEC polymer length is usually not critical as long as the polymer is within a size range that produces sufficient entanglement for DNA separation and yet not too viscous to properly fill the capillary at the desired concentration.

Migration time and separation efficiency of DNA fragments using HEC may be affected by other factors in addition to the quality of the HEC medium. For example, the addition of intercalating dyes into the medium as well as the type of capillary coating used can significantly influence DNA migration. These factors may account for the wide variation in separation of DNA fragments (the most common being *Hae III*-ϕX174 restriction fragments) observed in many publications [40-43]. Last, but not least, these variations may also be due to the fact that the cellulose matrix itself can serve as a dynamic coating on the inner surface of the capillary wall, resulting in a 'memory effect' that affects electroosmotic flow from run-to-run.

2.1.4 Polymer concentration

Although HEC has been consistently shown to be useful for the separation of PCR products between 50 and 500 bp [35], the choice of which polymer viscosity and concentration range to use for CE has often been arbitrary and less well defined. More over, this polymer is less frequently used with a denaturing agent in single-stranded DNA separation.

There are several systematic studies available to describe and to determine optimum entangled polymer concentration for DNA separation. The Ogston-Rodbard-Chrambach models [44-47] claim that size-exclusion separation is valid in entangled solutions with a concentration well above the entanglement threshold for biomolecules

with a radius of gyration smaller than the blob size. The Ogston model also says that the separation power decreases with decreasing concentration, and the concentration of a sieving polymer should stay close to the entanglement threshold in order to efficiently resolve small DNA molecules [11,48]. Based on the entanglement coupling theory of Bueche [49], Barron et al. proposed that separation is at its best for DNA fragments with a size comparable to the contour length between entanglements [13].

While many of these models focus on the theoretical aspect of separation of double-stranded DNA under nondenaturing condition, they are not necessarily applicable to the separation of single-stranded DNA fragments in the presence of denaturing agents, such as urea and formamide. In this section, experiments were carried out to investigate various cellulose derivatives of HEC and in particular, the role of polymer concentration in an effort to maximize separation efficiency and to ensure consistent and reproducible separation of single-stranded DNA fragments.

2.2 Experimental

2.2.1 CE Apparatus

The CE instrument for DNA separation was in-house built. It was equipped with a high voltage power supply (Model CZE 1000R, Spellman High Voltage Electronics Corporation, Plainview, NY) and a 543.5 nm green He-Ne laser system (Melles Griot) with a 5 mW maximum output. A Macintosh computer (Centris 650) was used to control the power supply via a NB-MIO-16XH-18 input/output board (National Instruments, Austin, TX). An interface box that transfers output from the instrument to the computer was used to digitize fluorescence signal. For safety purposes, a plexiglas box was

installed, with safety interlock over the injection end. A sheath-flow cuvette (1-mm thick walls, 200 μm x 200 μm square inner bore, 2 cm in length) was used as a post-column detector. An R1477 photomultiplier tube (Bridgewater, NJ) was employed in our system for detecting fluorescence signal. A schematic representation of the CE instrument is shown in Figure 2.2.

2.2.2 Post-Column Detection

As shown in Figure 2.2, the laser beam is focused by a 6.3X (N.A. 0.2) microscope objective (Melles Griot, Nepean, ON, Canada) into the sheath-flow cuvette, just below the capillary end. The fluorescence is collected at 90° from the direction of excitation by a 60X (N.A. 0.7) microscope objective (LWD-M Plan, Universe Kogaku, Japan) and directed to an iris which controls the diameter of the laser beam. The transmitted light is divided into two spectral channels with a dichroic beam splitter (XF40, 590DRLP). The reflected fluorescence in one channel is spectrally filtered with a 580DF40 band pass filter and the transmitted fluorescence in the other channel is filtered by a 630DF30 band pass filter (Omega Optical, Brattleboro, VT). The 580DF40 channel detects primarily N,N,N',N'-tetramethyl-6-carboxyrhodamine (Tamra) labeled oligonucleotides. The 630DF30 channel detects primarily 6-carboxy-X-rhodamine (Rox) labeled oligonucleotides. Data is collected at a sampling rate of 10 Hz.

2.2.3 Parameters for DNA separation

Capillary electrophoresis of the sample was performed using a 29-cm long, 50 μm i.d., 144 μm o.d. DB-210 coated fused-silica capillary (Polymicro Technologies Incorporated, Phoenix, AZ) purchased from J&W Scientific (Folsom, CA, USA). The capillary has a high polarity, 50%-trifluoropropyl-methylpolysiloxane coating bonded

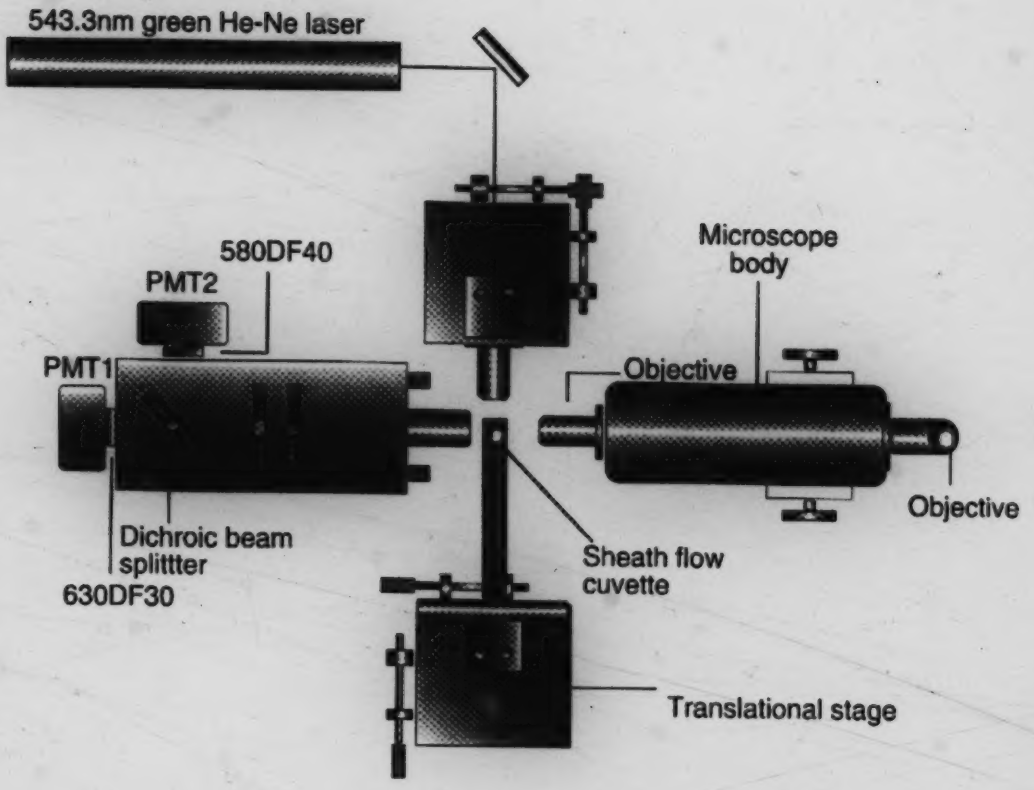

Figure 2.2 Schematic diagram of an in-house built CE instrument. Refer to Figure 3.1 for a schematic representation of a sheath-flow cuvette.

and cross-linked to the fused-silica surface according to manufacturer protocol. One end of the capillary was immersed in running buffer or sample along with a Pt wire electrode at the injection end (cathode) in the plexiglas box. The other end (anode) of the capillary was installed inside the sheath-flow cuvette. Sample introduction was performed by electrokinetic injection at 1000V for between 5 to 15 s. Separation was performed at an electric field of 200 V/cm. N-tris [Hydroxymethyl] methyl-3-aminopropane sulfonic acid

(TAPS; Sigma, St. Louis, MO) was dissolved in nanopure water and used to prepare a pH 8 running buffer using ethylamine (Sigma). Several cellulose polymers were purchased from Aldrich Chemical Co., Milwaukee, WI. They are sold in dry powder and are yellowish in appearence. A hydroxyethyl cellulose (Average Mw ca. 250,000) solution was prepared by dissolving measured quantity in filtered TAPS buffer, followed by a brief sonication. The mixture was then transferred to a rotor to mix at room temperature until completely dissolved. The final solution was filtered by a Millex-GS 0.45 μm filter and then transferred to a 3-mL syringe connected to a capillary connector. The polymer solution was then pushed into a DB-210 coated capillary using a syringe pump (Kazel, model A-99). Polymer solutions containing 7 M urea were prepared fresh and filtered by Millex-GS 0.45 μm filter unit (Millipore, Bedford, MA) prior to experiment. Other celluloses such as 2-hydroxyethyl cellulose (Average Mw 720,000) and hydroxypropyl cellulose (Average Mw ca. 1,000,000) were also prepared using a similar procedure.

2.2.4 Preparation of DHBV Plasmid DNA

Plasmid pAltD2-8 was a generous gift from K. Fischer of the Dept. of Medical Microbiology and Immunology. It contained a monomer of 3021 bp genome of the duck hepatitis B virus (DHBV) cloned into the *EcoRI* site of vector pAlter-1 (Promega). The pAltD2-8 was propagated in *Eschericheria coli* strain DH 5α grown in suspension broth culture. pAltD2-8 DNA was recovered using Qiagen Plasmid Purification Kit (Qiagen, Chatworth, CA). The isolated plasmid was digested with restriction endonuclease *EcoRI* to separate the 3021 bp DHBV fragments from the vector.

2.2.5 Indirect fluorescence labeling of restriction fragments

The purified *EcoRI* fragments of 3021 bp were further cut separately with restriction endonucleases *Taq I*, *Hpa II*, *Ava I* and *Afi III* to generate appropriate fragment sizes for subsequent chain extension using fluorescently labeled primers. The status of digestion was judged by running aliquots of each of the restriction digests on a 2% agarose gel. One microliter (ca. 25 ng of total DNA) of each of the restriction digests was then used for 25 cycles chain extension using the following parameters: denaturation at 96°C for 1 min, annealing at 55°C for 1 min, and extension at 72°C for 2 min on a PTC-100 thermal cycler, version 1.2 (MJ Research, Inc., Watertown, MA). Each sample contained 100 µL reaction mixture of 1.5 mM $MgCl_2$, 1x PCR buffer, 12 mM of dNTPs, 60 pmol of each forward and reverse primers, and 2.5 U of Taq DNA polymerase. The extended products were purified by QIAquick PCR Purification (Qiagen) to remove unbound probes and enzymes. Each of the purified products was resuspended in 30 µL of 10 mM Tris-HCl (pH 8). The Tamra or Rox labeled oligonucleotide primers as well as the cold primers specific to DHBV were ordered from University Core DNA Services (University of Calgary, AB, Canada). Using the Lightspeed Pascal software, Amplify 1.2 (W. Engels, Genetics Department, University of Wisconsin), the oligonucleotide primers were carefully selected to avoid nonspecific priming and formation of primer dimers. The sequences of the primers are listed in Table 2.1.

As shown in Table 2.2, the *Taq I* digest generates a 259 and a 533 bp restriction fragments that are primable by the HBVTa primer and the HBVTb primer. The *Hpa II* digest generated a 320 bp and a 703 bp fragments specific to HBVTb and HBVTa primers, respectively. The *Ava I* digest generated a 319 bp fragment for HBVTb and a

612 bp fragment for HBVTa; and the *Afi III* digest generated a 536 bp for HBVTb and a 933 bp for HBVTa. The length of each of the extended products is shown in the last column.

Table 2.1 DHBV sequences designed for primer extension

Name	Primer sequence	Location on genome	Fluorescence tag
HBVTa	5GTGACTGTACCTTTGGGTATG3	2599-2618	Tamra
HBVTb	5ACGAGGAATCACTGGATAGG3	32-51	Rox
H684	5GGCTCTATGAAGCAGGAATC3	687-707	____
T746	5GGTCAGCCTTATAATTGGGA3	746-765	Tamra
H1175	5GTTGTAGCTTCCACTGAGGA3	1157-1176	____
HBVW1	5ATCGGATAGTCGGGTTGGAA3	2989-3008	____
HBVW2	5CGTCTACATTGCTGTTGTCG3	2576-2595	____
HBVW3	5GAGATTGCTTTGGTGGCATT3	57-76	____
HBVW4	5ATTTCCTAGGCGAGGGAGAT3	393-412	____

Note: The genome sequence (HPUCGD accession no. K01834) was obtained from the National Center for Biotechnology Information (http://www3.ncbi.nlm.nih.gov/BankIt/)

The primer extended products were purified and pooled (except for the *Ava I* digest). Purity of each extended fragment was judged by CE-LIF using a 0.8% HEC with 7 M urea as sieving matrix. A 387 nucleotide (nt) fragment was also generated using HBVTb with a *BspM I* digest, and was added to the mix to generate a total of 7 fluorescent-labeled DHBV fragments ranging from 183 to 903 nt in length. The sequences of all 7 fragments were checked for possible hairpin and loop formations using

DNA Strider 2.1. Only fragments 229 and 290 nt were found to be able to generate 3 loops each. However in the presence of 7 M urea in the sieving matrix, formation of loops from the two fragments should be reduced.

Table 2.2 Restriction fragments specific to HBVTa and HBVTb and their corresponding extended products.

Restriction enzyme	Restriction fragment(bp)	Product length(nt)
Taq I	259	229(R)
	532	423(T)
Hpa II	320	290(R)
	703	307(T)
Ava I	319	289(R)
	612	423(T)
Afi III	536	183(T)
	933	903(R)
BspM I	418	387(R)

Note: (T) and (R) designate Tamra and Rox

2.2.6 Influence of HEC Concentration on DNA separation

To achieve good resolution and rapid separation of DNA fragments, the affect of HEC concentration under denaturing conditions was studied. A series of polymer solutions containing 0.1%, 0.2%, 0.4%, 0.8%, 1.2%, 1.6% and 2% HEC (Average Mw ca. 250,000) with 7 M urea were freshly prepared, sonicated and filtered. The purified sample containing 7 DHBV fragments was divided into several aliquots for subsequent

sample injections. This was to avoid sample contamination with running buffer, which could affect the ionic strength of the sample and subsequent sample injection efficiency. Contamination usually occurs when a vial containing running buffer is replaced with a vial containing DNA sample resuspended in water. This can be prevented by very briefly wiping the electrode and the capillary end with a cotton swab during the buffer-sample replacement step. Separation of the 7 DHBV fragments was carried out from low to high concentration (0.1% to 2%) HEC solutions. This was to avoid the possibility of adsorption of residual cellulose matrix at higher HEC concentration on the capillary wall, causing inaccurate measurement of DNA separation at lower HEC concentrations. For each concentration of HEC solution, three consecutive runs of the sample were performed, with sieving matrix replaced after each run. The capillary was conditioned by continuously flushing with HEC solution for 15 min after a new HEC concentration was being investigated. This was to ensure residual cellulose from the previous HEC matrix was completely removed from the capillary before the next concentration of HEC solution was introduced into the capillary. Separation of the DHBV fragments was carried out from high to low concentrations (2% to 0.8%) to demonstrate the adsorption of HEC cellulose on the capillary wall and its effect on DNA migration time. Parameters such as migration time, peak resolution and run-to-run reproducibility were examined. All data were collected and processed using Igor Pro (WaveMetrics, Inc., OR).

2.2.7 Stability of HEC under denaturing condition

The stability of HEC as a replaceable sieving polymer was investigated as a function of time. In this case 0.8% HEC with 7 M urea was employed to provide optimum separation in terms of resolution, current fluctuation and separation time. A 10

mL stock solution of 0.8% HEC with 7 M urea was prepared as described before and stored at 4°C. The stability of the polymer was monitored over a period of approximately 6 months. At each time interval of study, a freshly prepared polymer solution was used as a control to monitor column performance as well as variation of sample preparation. The DNA samples used in this study were prepared from the chain extended products of *Taq I* and *Hpa II* digests, which contain DNA fragments of 229(R), 290(R), 307(T) and 423(T) nucleotides (Table 2.2). For each time study, three consecutive runs were performed, followed by similar runs using the freshly prepared polymer solution. The polymer solution was replenished after each run.

2.3 Results & Discussion

2.3.1 Separation of DNA fragments using HEC polymer

Although the HEC polymer solution was filtered prior to the CE experiment, it was found to contain a trace amount of anionic contaminant, which consistently eluted at a given time during pre-sample electrophoresis (Figure 2.3). The anionic contaminant scattered light and could be easily detected by the 543.5 nm laser beam. The presence of this anionic impurity was also evident from a series of acid titration experiments with HCl (data not shown). Since a 10-min pre-run was always conducted after replacing each sieving medium, this impurity was eluted from the capillary prior to sample injection, and hence, did not influence the efficiency of DNA separation. As shown in Figure 2.4, a 0.8% HEC matrix was sufficient to separate the excess oligo probes from the extended product(s). The calculated efficiency was in excess of five to six million theoretical plates using a capillary as short as 29 cm and an electric field of only 200 V/cm.

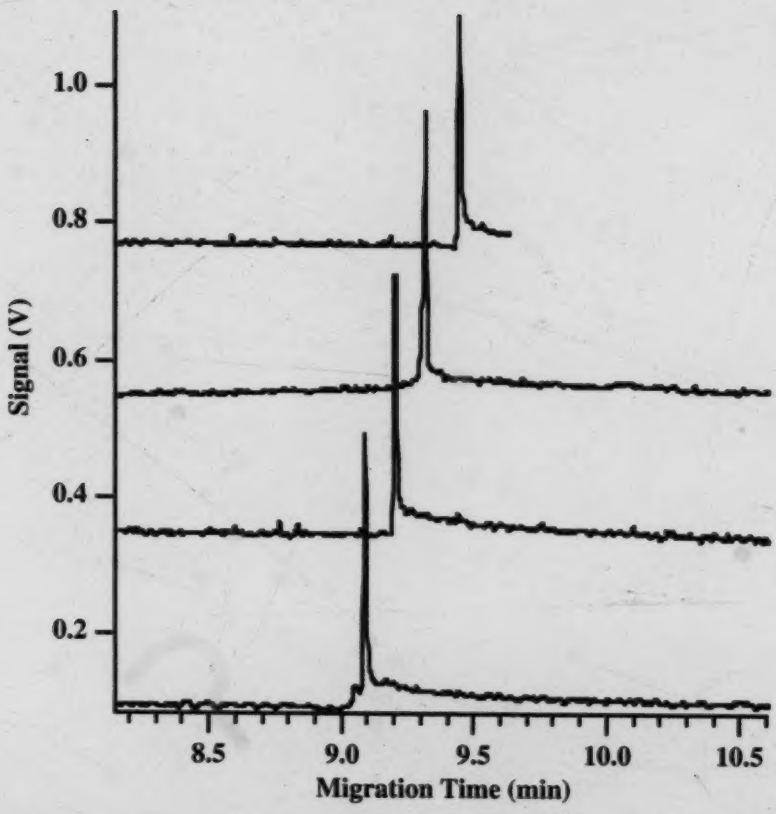

Figure 2.3 Anionic impurities of HEC polymer solution 0.8% (w/v). HEC polymer was prepared in 0.1M TAPS at pH8. The polymer solution was filtered and introduced into capillary with a syringe. The four electropherograms represent pre-runs of the HEC-filled capillary prior to sample injection.

Under non-denaturing conditions, the extended products were separated as a mixture of double-stranded (289 bp) and single-stranded (289 nt) fragments, in which case a portion of the 289 nt fragments still remained annealed to its template after primer extension. A population of the extended product was single-stranded, corresponding to a smaller peak (289 nt) which came out later than the double-stranded product-template DNA hybrid. This single-stranded product appeared when its copy number exceeded that of the

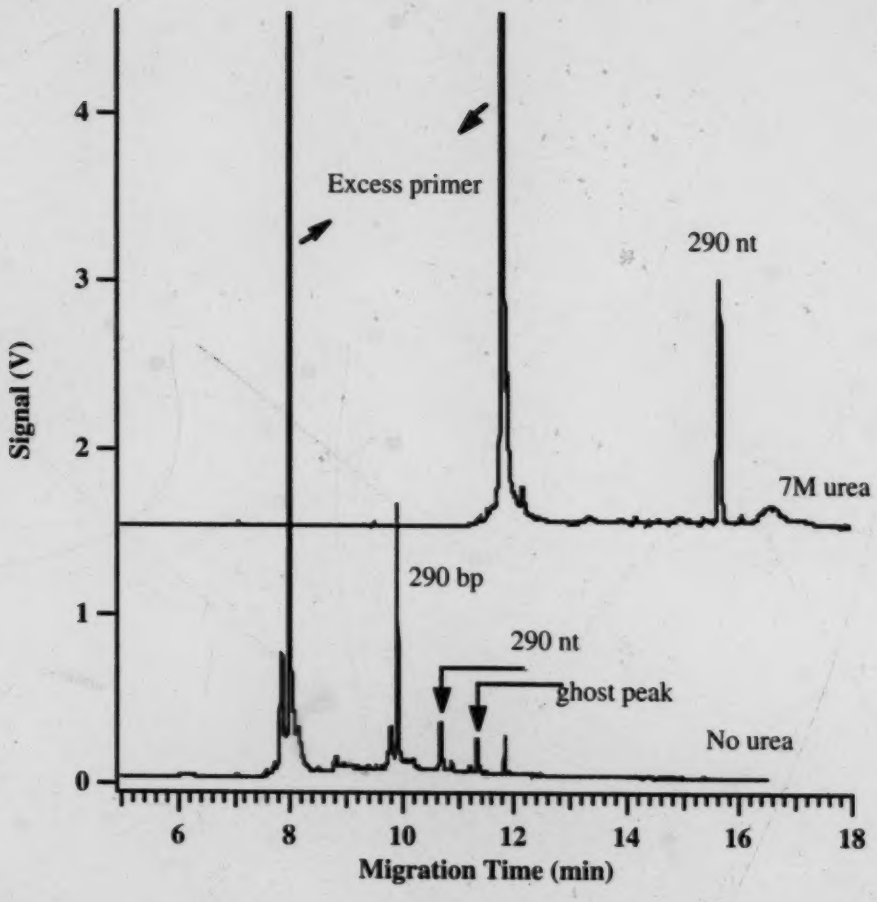

Figure 2.4 Separation of DHBV DNA fragments in the absence and presence of 7M urea. The 290 bp DNA fragment was generated using a *Hpa II* digested DHBV DNA template, followed by linear extension using a Rox-labeled primer. Separation was performed at room temperature in a 29cm, 50 µm I.D. coated capillary at 200 V/cm. Electropherograms were recorded from the Rox-channel.

template after 25 cycles of chain extension. The presence of "ghost peaks" in a non-denaturing run was probably the result of nonspecific hybridization of the fluorescence probe to contaminating DNA present in the sample as well as the formation of secondary

structures in the DNA fragments. The overall migration time was longer in the presence of 7 M urea than without the denaturant. This is due in part to the increased viscosity when urea was added to the sieving matrix. The presence of 7 M urea resulted in about 42% reduction of theoretical plates. However, in this case, the reduction did not affect peak resolution as the calculated efficiencies are still in excess of 5 million theoretical plates. We found that DNA fragments that were 5' labeled with Tamra showed much greater intensity compared to those that were labeled with Rox. This was attributed to the excitation wavelength of Rox (589 nm), which is further away from the HeNe laser (543.5 nm) when compared to the excitation wavelength of Tamra (547 nm). In addition, the bandpass filter (630DF-30) used in the Rox channel is not optimal for the detection of emission of Rox at 605 nm. The use of this particular filter in a two-channel detection system using Tamra and Rox labeled DNA was meant to cut down cross-talking between the two channels.

2.3.2 HEC concentration effect

Figure 2.5 shows seven electropherograms of separation of 7 single-stranded DNA fragments with various concentrations of HEC, from 0.8 to 2%. At concentrations as low as 0.1% HEC, separation of all 7 fragments was achieved in under 13 minutes with poor resolution. Resolution of all peaks improved dramatically from 0.1 to 0.4% HEC, with all 7 fragments fully resolved at 0.8% HEC. Migration time of the largest fragment (903 bases) increased by a factor of about 4 from 0.1 to 2% HEC. In contrast, migration time of a smaller fragment (423 nt) increased by a factor of about 3, and a factor of about 2 for the smallest fragment (183 nt). Therefore, at minimal expense of analysis time, a relatively high concentration of polymer solution can be employed to

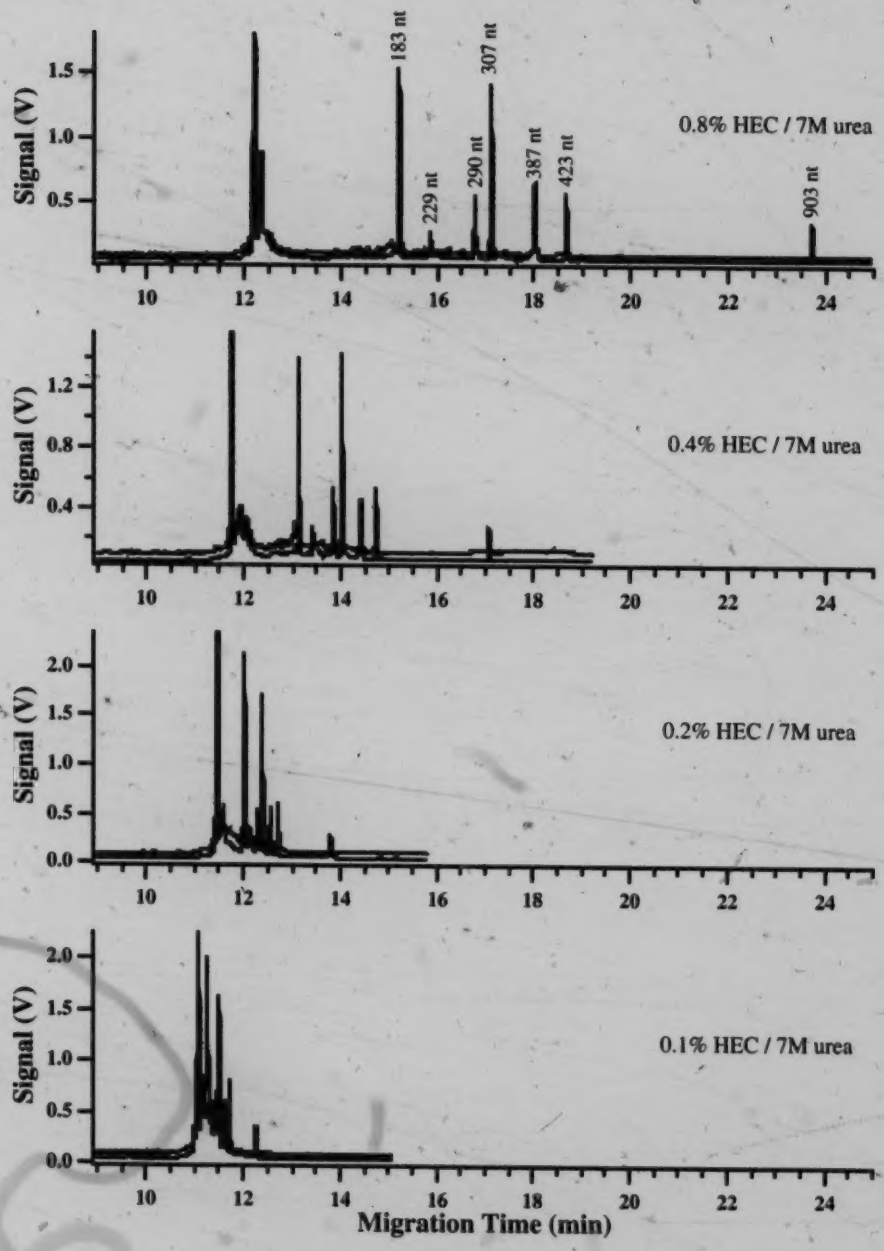
183 nt
229 nt
290 nt
307 nt
387 nt
423 nt
903 nt
0.8% HEC / 7M urea
0.4% HEC / 7M urea
0.2% HEC / 7M urea
0.1% HEC / 7M urea
Signal (V)
Migration Time (min)

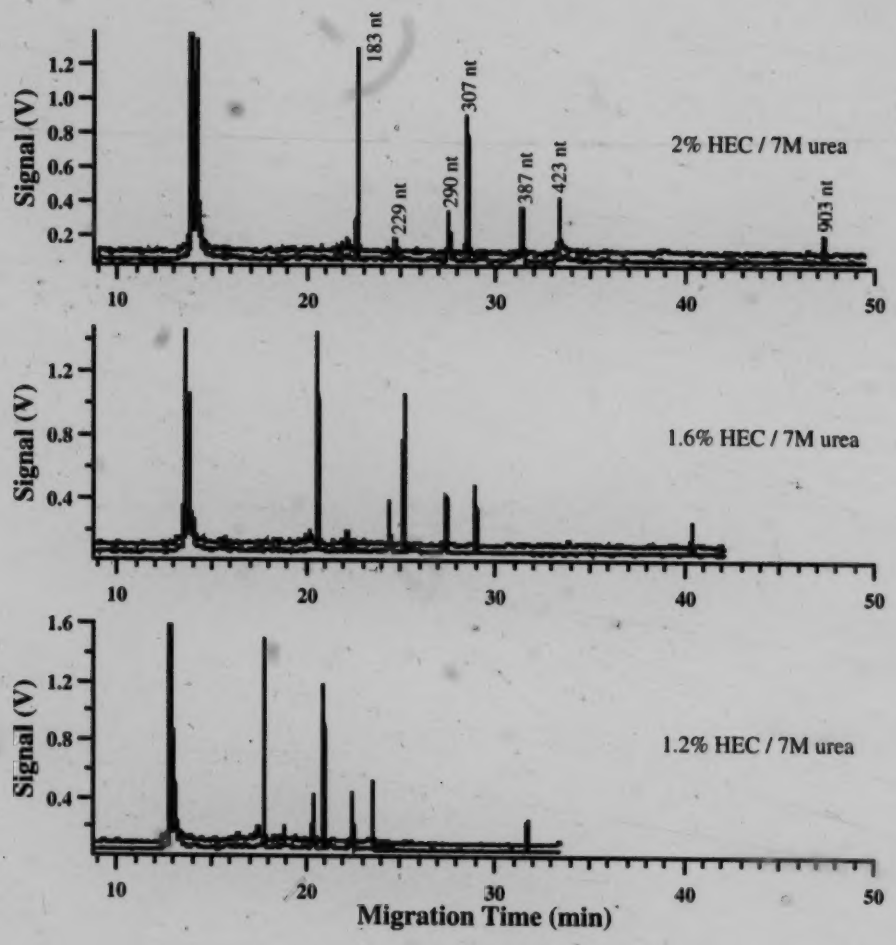

Figure 2.5 Separation of 5' fluorescence-labeled, single-stranded DHBV DNA fragments in various HEC concentrations (0.1, 0.2, 0.4, 0.8, 1.2, 1.6 and 2%) in 0.1 M TAPS, 7 M urea. Separation was performed at room temperature in a 29cm, 50 μm I.D. coated capillary at 200 V/cm. The dotted-trace corresponds to Tamra-channel and the solid-trace corresponds to Rox-channel.

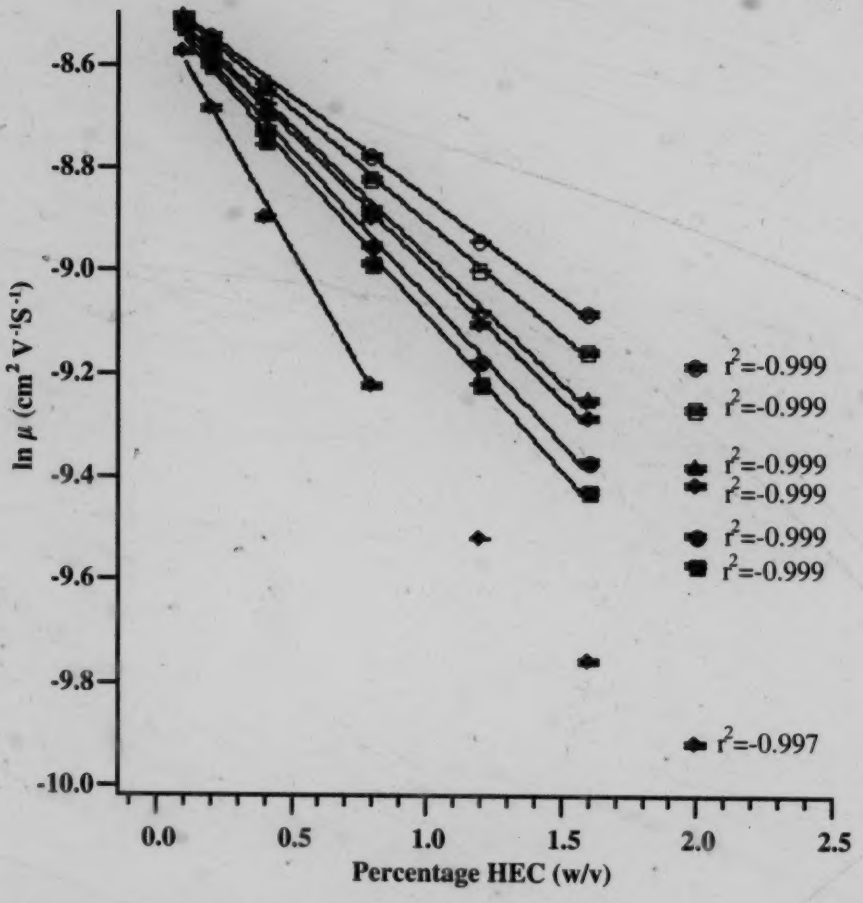

Figure 2.6 Ferguson plot of 5' dye labeled DHBV DNA fragments. Open circles: 183 nt; open squares: 229 nt; open triangles: 290 nt; open diamonds: 307 nt; closed circles: 387 nt; closed squares: 423 nt; closed diamonds: 903 nt.

increase the resolving power of small DNA fragments. Figure 2.6 illustrates these observations in more detail by comparing the mobility profile of each fragment at various HEC concentrations. Using the Ogston sieving model as a guideline, a plot of ln μ against % HEC (a Ferguson plot) should give a linear relationship with a slope equal to

the retardation coefficient. This behavior is indeed observed for DNA fragments of 423 nt and smaller in HEC concentrations as high as 1.5%. For DNA fragments larger than 423 nt, the linear relationship degrades, apparently due the gradual transition from Ogston to the Reptation regime for larger DNA. For the DNA fragment of 903 nt, the linear relationship is only valid at HEC concentrations under 0.8%. This indicates that when reptation becomes significant, the separation performance of the polymer solution at high concentration decreases rapidly, resulting in a saturated, size-independent mobility.

Figure 2.7 describes the effect of HEC concentration on the resolution of two fragments that are 290 and 307 nt in length. Resolution between the fragments improves with increasing concentration of HEC. The rate of increase slows with higher polymer concentrations. At HEC concentration between 1.6 and 2%, there is very little improvement in resolution. This may be the result of band broadening contributed by a longer retention time. In contrast, average migration time for the two fragments increases proportionally and no deviation from linearity was observed at 2% HEC. These observations indicate that polymer solution between 0.5% and 1.2% (w/v) should provide optimum separation with respect to resolution and analysis time for fragments 290 and 307 nt. At the lower end of this concentration range, efficient separation may be jeopardized by the unextended primers, which are usually present at high concentration. These primer peaks may overlap the target peaks that are eluted very early on. At a slightly higher HEC concentration such as 0.8%, there is a gap of at least 2 min between the primer peaks and the first eluting target peak. This ensures complete resolution of all

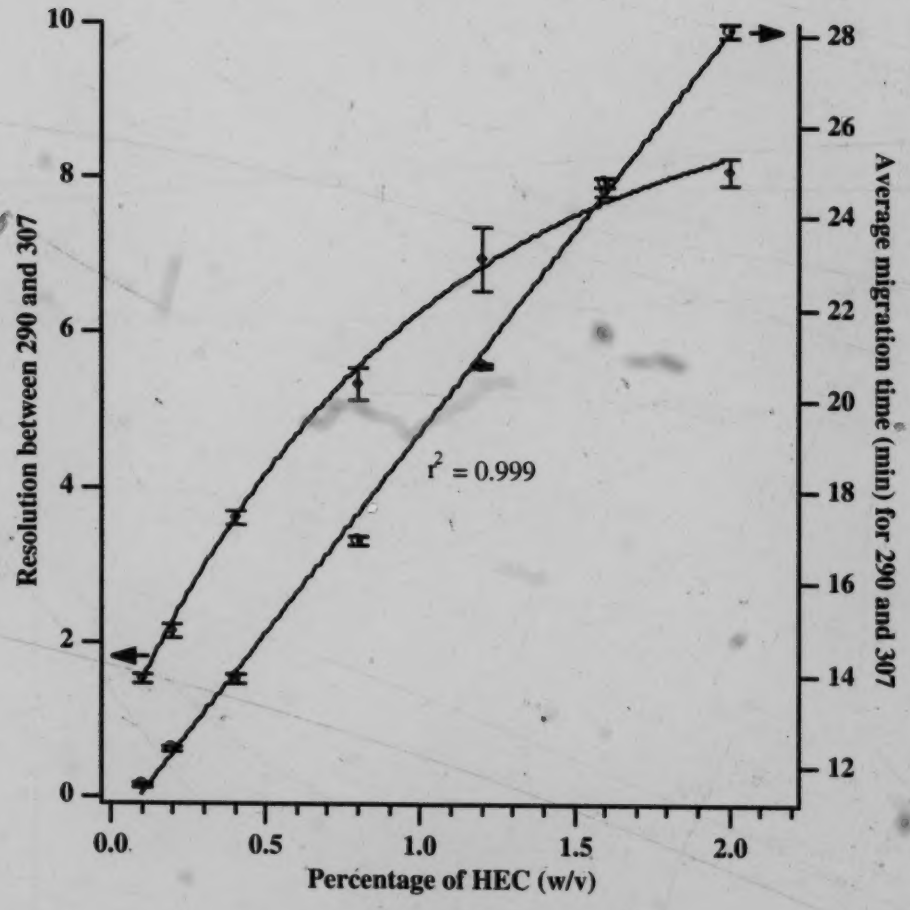

Figure 2.7 The effect of HEC concentration on peak resolution and average migration time for DHBV DNA fragments of 289 and 307 nt in length. Open diamonds: resolution (y-axis on the left); open circles: average migration time (y-axis on the right). The plot for resolution was derived from the equation y = 9.3 - 8.7e(-1.0x). The plot for avearage migration time was curve-fitted using least squares. Arrows indicate corresponding Y-axis of the plots.

DNA fragments with little background noise. HEC concentrations higher than 0.8% provide a similar advantage, but at the expense of longer analysis time.

2.3.3 Behavior of separation: 5' end labeled vs. intercalating dyes

Figure 2.8 compares the mobility behavior between the 5' end labeled, single-stranded DNA and double-stranded restriction DNA fragments of ϕX174 / *Hae III* digest labeled with Propidium Iodide. The contrast in migration time between the two separations was apparent. The single-stranded DNA fragments, which carried fewer negative charges, migrated to the detector end relatively slower than the double-stranded restriction fragments, which carried twice as many negative charges for the same fragment length. But in this case, the negative charges carried by the restriction fragments would be partially neutralized by the positively charged propidium iodide. Hence, a two-fold difference in migration time would not be expected for DNAs that are at approximately the same size (183 nt and 194 bp). The extent of linearity is slightly different between the two plots. In the case of the 5' end labeled, single-stranded fragments, deviation from linearity occurred between nucleotide length 423 and 903. In the intercalating dye labeled, double-stranded restriction fragments, linearity degrades more rapidly between 310 and 1358 bp.

2.3.4 Influence of polymer concentration on theoretical plates

Study on the separation efficiency of the single-stranded fragments showed no apparent correlation between the number of theoretical plates and viscosity of the sieving medium (Figure 2.9). Plate numbers of the 423 nt fragment increased by a factor of about 2 when the percentage of HEC increased from 0.2 to 2 %. Plate numbers of the

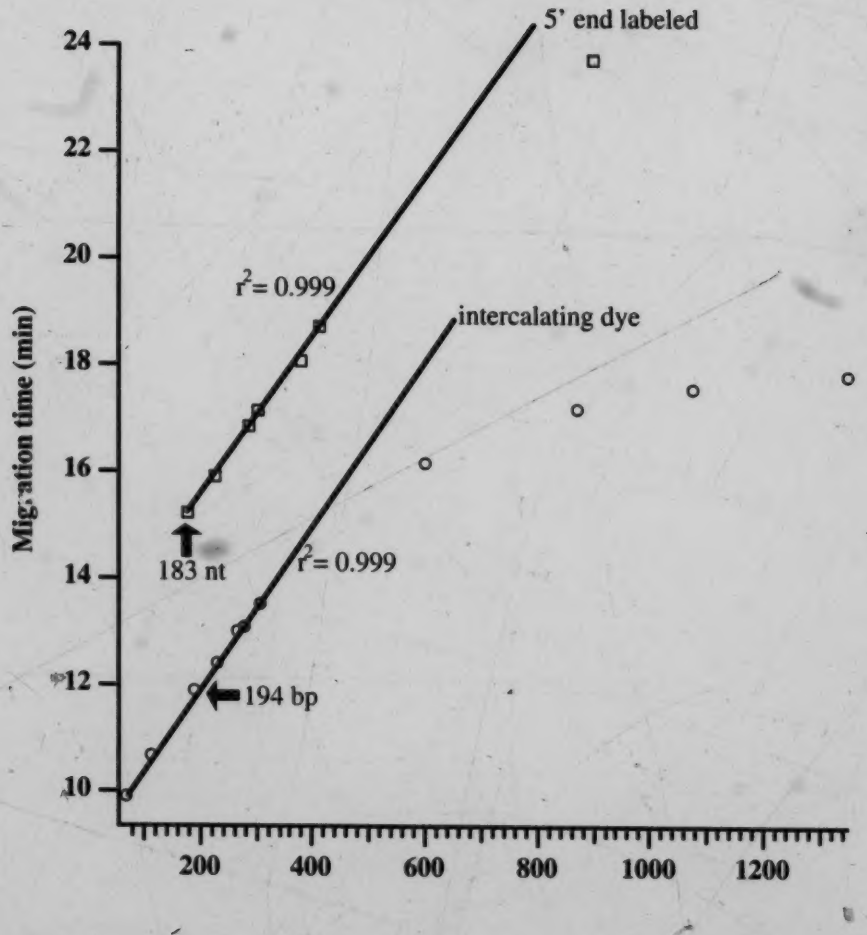

Figure 2.8 Plots of peak migration time (min) vs base number (nt). The lines are a least-squares fit to the data; Square: 5' end dye labeled DNA fragments, 0.8% HEC/7M urea in 0.1M TAPS (pH 8); Circle: ϕX174/*Hae III* restriction fragments labeled with propidium iodide, 0.8% HEC in 89 mM Tris-borate, 10 mM EDTA (pH 8.6).

smallest fragment 183 nt also increased by a similar factor from 0.2 to 2 % HEC. Interestingly, the largest fragment of 903 nt also presented similar behavior (up to 1.6% HEC) despite its significantly longer migration time relative to the rest of the fragments. However, there was an apparent drop in plate numbers for DNA fragment 903 nt when

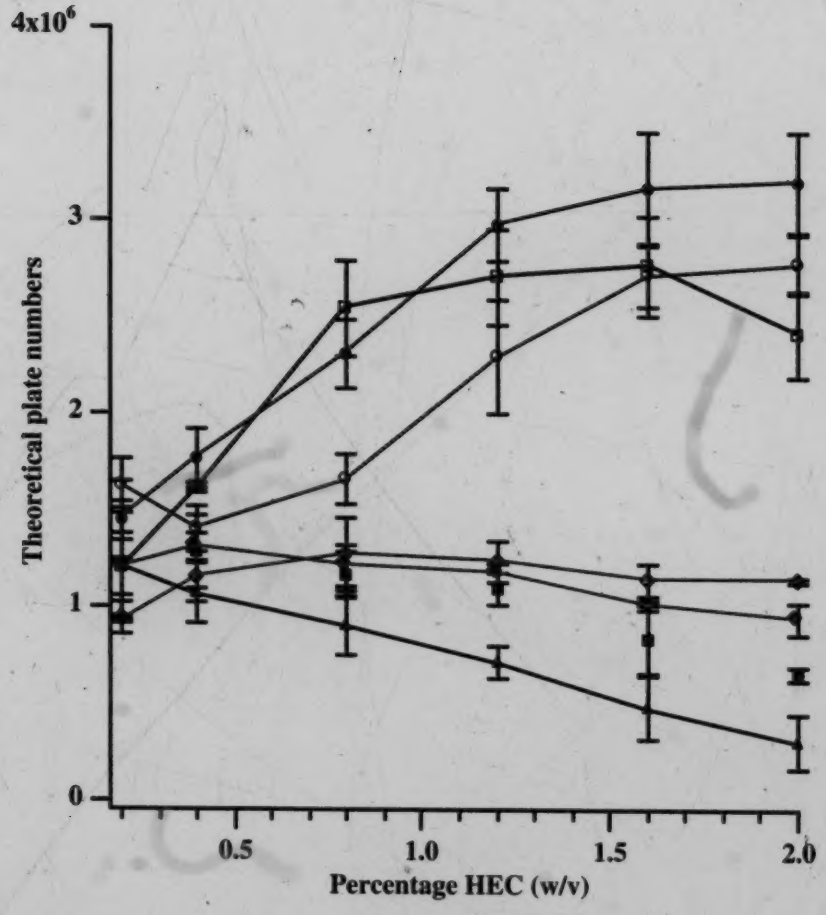

Figure 2.9 Separation efficiency of single-stranded DHBV fragments as measured by theoretical plate numbers vs percentage of HEC polymer. Open circles: 183 nucleotides (nt); open triangles: 229 nt; closed squars: 290 nt; closed diamonds: 307 nt; open diamonds: 387 nt; closed circles: 423 nt; open squares: 903 nt.

the percentage of HEC increased from 1.6 to 2%. This may indicate the onset of biased reptation, as predicted from the Ferguson plot in Figure 2.6. The plate numbers for DNA fragment 387 nt were not affected by the change in HEC concentration. For DNA

fragments 229 nt, 290 nt and 307 nt, the plate numbers actually dropped from lower to higher concentration of HEC matrix. Current separation theories such as Ogston sieving may not explain this behavior. This discrepancy was loosely attributed to a possible difference in the quality of primer extension on fragments 229, 290 and 307 nt.

2.3.5 Memory effect of HEC on capillary wall

When the order of the HEC concentration study was reversed such that HEC polymer with the highest concentration were introduced first into the capillary for DNA separation, followed by progressively lower concentrations, a memory effect of HEC on the capillary wall was observed. In Figure 2.10, the order of study was carried out with 2% HEC, followed by 1.6%, 1.2% and back to 0.8%. The apparent decrease in peak retention times were noticed in runs designated B2, C2 and D2. These runs were considerably shorter compared to their counterparts (B1, C1, D1), which was done in the order of increasing HEC concentration. This observation implies that when the HEC medium is being flushed out of the capillary, a small fraction of the polymer remains adsorbed onto the capillary wall. When the same polymer solution at a lower concentration is introduced into the capillary this adsorption is manifested. The result is a increased suppression of electroosmotic flow (EOF) and a decreased peak retention time. This memory effect would not be observed when using a low to high order of HEC concentration. Suppression of EOF (and a corresponding decrease in retention time) in this case maybe offset or masked by the effect of the increased viscosity at higher polymer concentration, which dramatically increases the retention time of the DNA fragments.

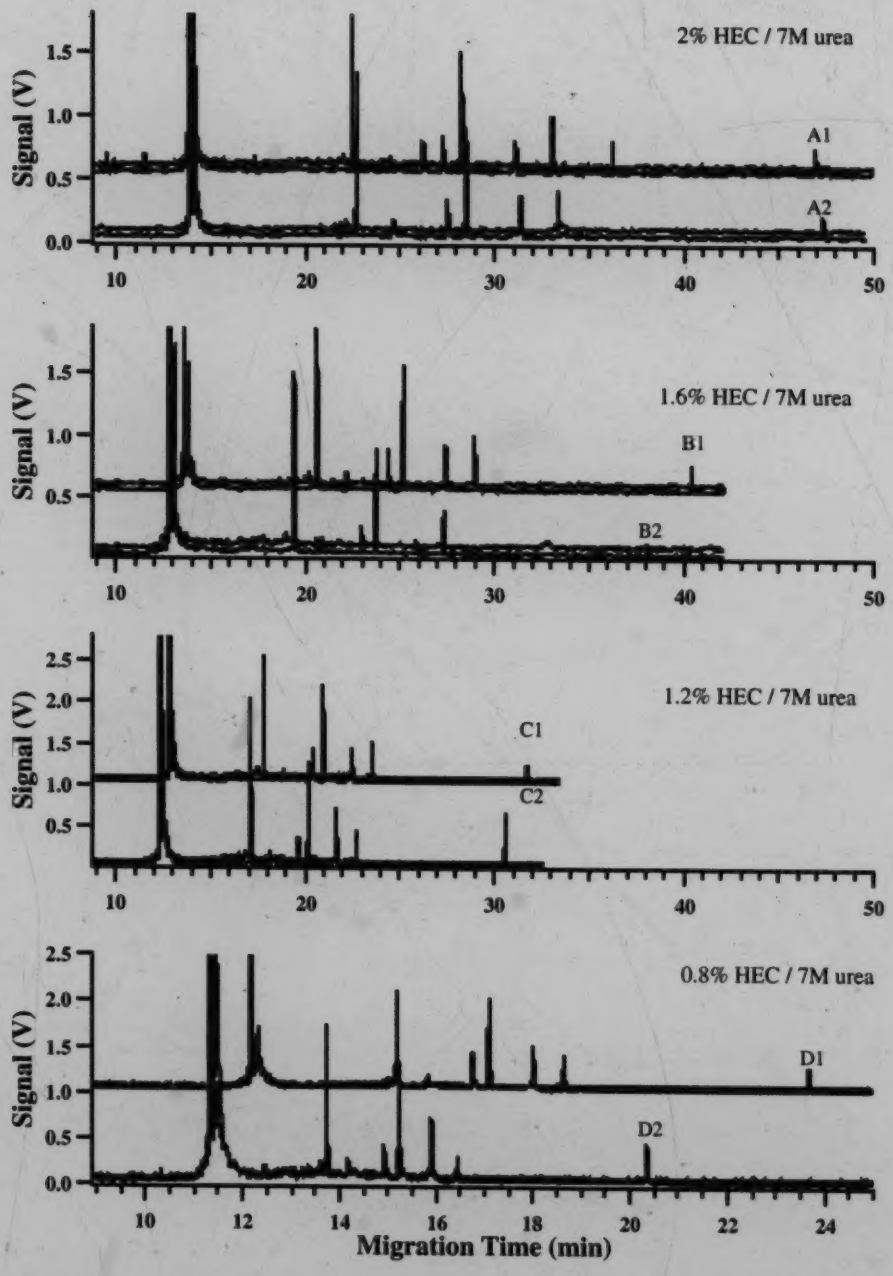

Figure 2.10 Adsorption of HEC on capillary wall. Electropherograms labeled with A1, B1, C1 and D1 were generated by a low-to-high HEC concentration study. A2, B2, C2 and D2 were generated in high-to-low HEC concentration study. Double lines on the plots indicate two channels detection.

2.3.6 Stability of HEC

Figure 2.11 depicts a typical electropherogram from the current channel. The current reading was recorded in voltage with a 100 KΩ resistor. Current profile of the aged polymer solution is shown in Figure 2.12. Current fluctuation at around 4 μA was recorded in polymer solutions that were between 8 and 194 days old. The fluctuation pattern was quite similar to that of the freshly prepared polymer solutions, indicating that current fluctuation was attributed to some parameters other than the aging process itself. The dependent parameters could be temperature fluctuation, adsorption of ions on the capillary wall, and minor siphoning effect, which occurs when the difference in height between the waste reservoir and the sample reservoir is not properly controlled. A graph of conductivity versus age of polymer (Figure 2.13) shows a similar trend as in the current plot (Figure 2.12). In this case, resistance across the capillary was considered and used as a reflection of the change in viscosity of the matrix during the aging process. The plots once again showed no obvious change in conductivity of the matrix, suggesting that the polymer solution was stable for at least six months when stored at 4°C and kept sterile. A Student's T test was conducted on data obtained from both the aged and fresh HEC polymers. The calculated T value (0.344) was compared to the tabulated value (2.576) at 99% confidence level. The result suggests that the difference between the two sets of data is insignificant.

Figure 2.14 shows the separation of 4 DHBV fragments in an 8 day old polymer solution. And again in this case, resolution between DHBV fragments 290 and 307 was used to judge the resolving power of the aged polymer solution. In Figure 2.15, a plot of

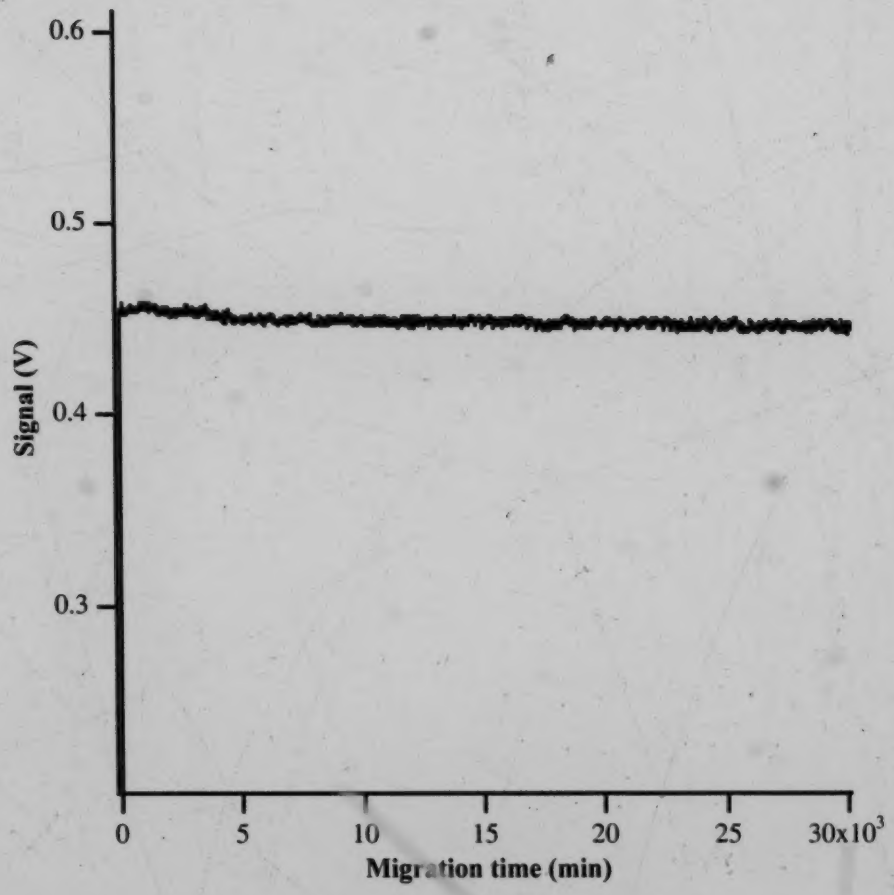

Figure 2.11 A typical electropherogram of the current channel obtained from a electrophoretic separation on an 8-day old HEC polymer solution. The current was recorded in voltage using a 100 KΩ resistor. Applied field strength: 200 V/cm on a 29 cm capillary, 50 μm I.D.

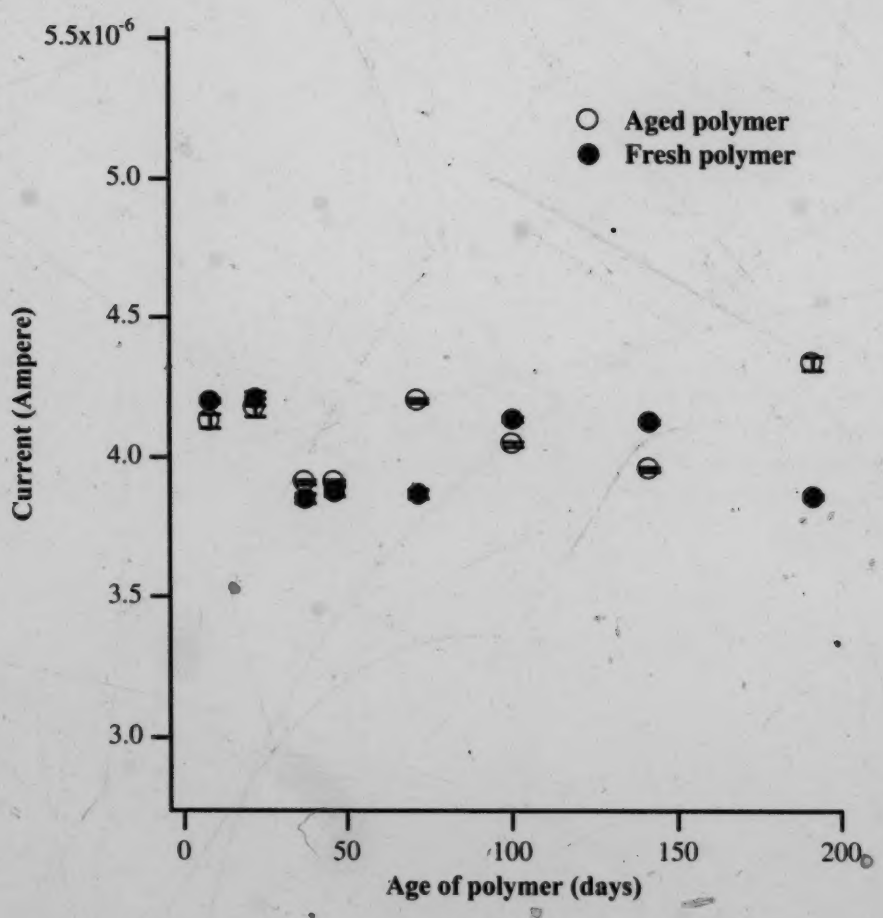

Figure 2.12 Stability of aged HEC polymer as measured by conductivity of the sieving matrix. Polymer solutions (0.8% HEC / 7 M Urea in 0.1 M TAPS, pH 8) were aged at 4 °C and fresh polymer solutions were prepared for each time point studied.

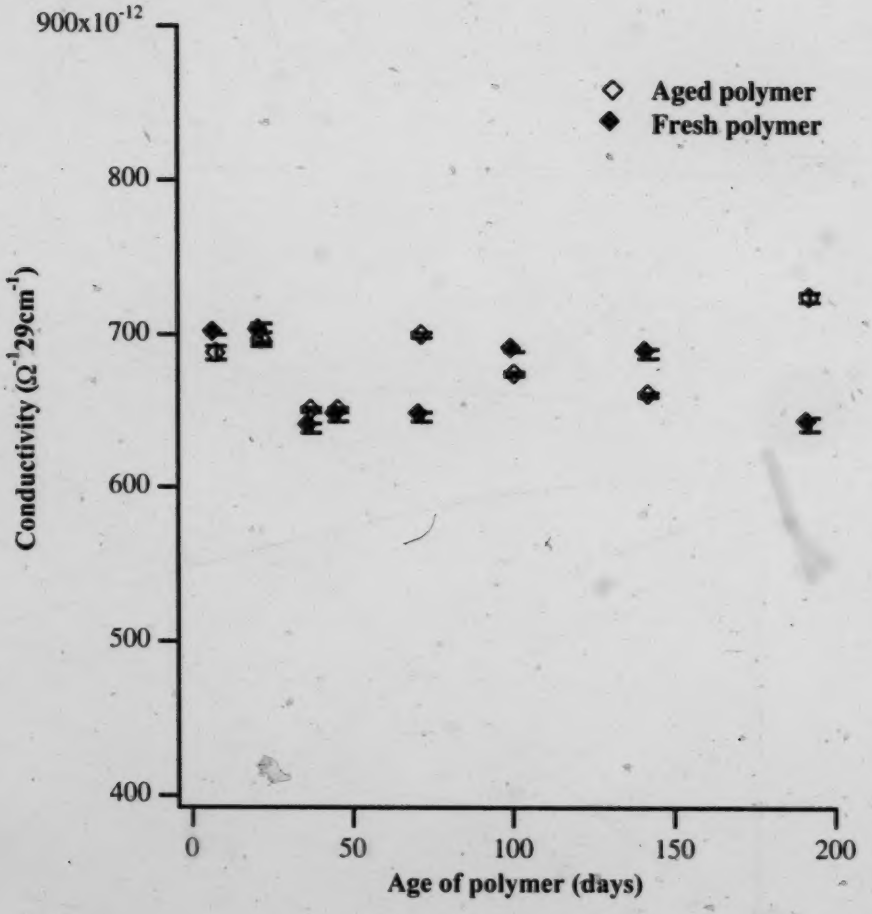

Figure 2.13 Stability of aged HEC polymer as measured by current flow across the capillary during electrophoretic separation. Polymer solutions were prepared as described in Figure 2.12.

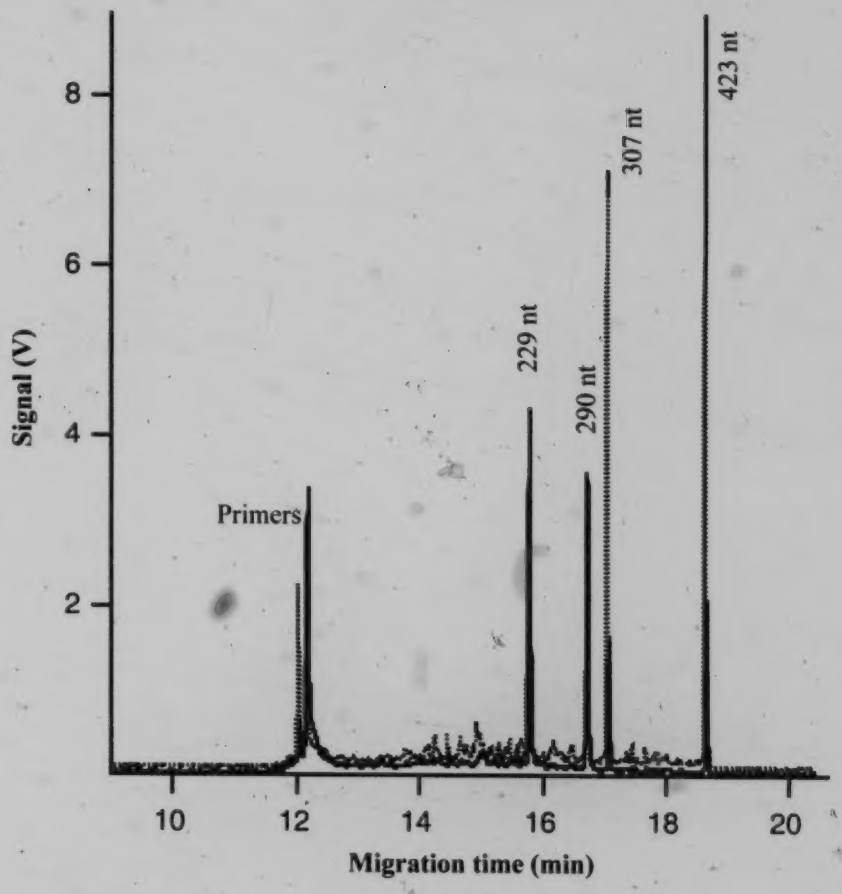

Figure 2.14 Separation of 4 DHBV DNA fragments on an 8 day old HEC polymer solution (0.8%) with 7M urea.

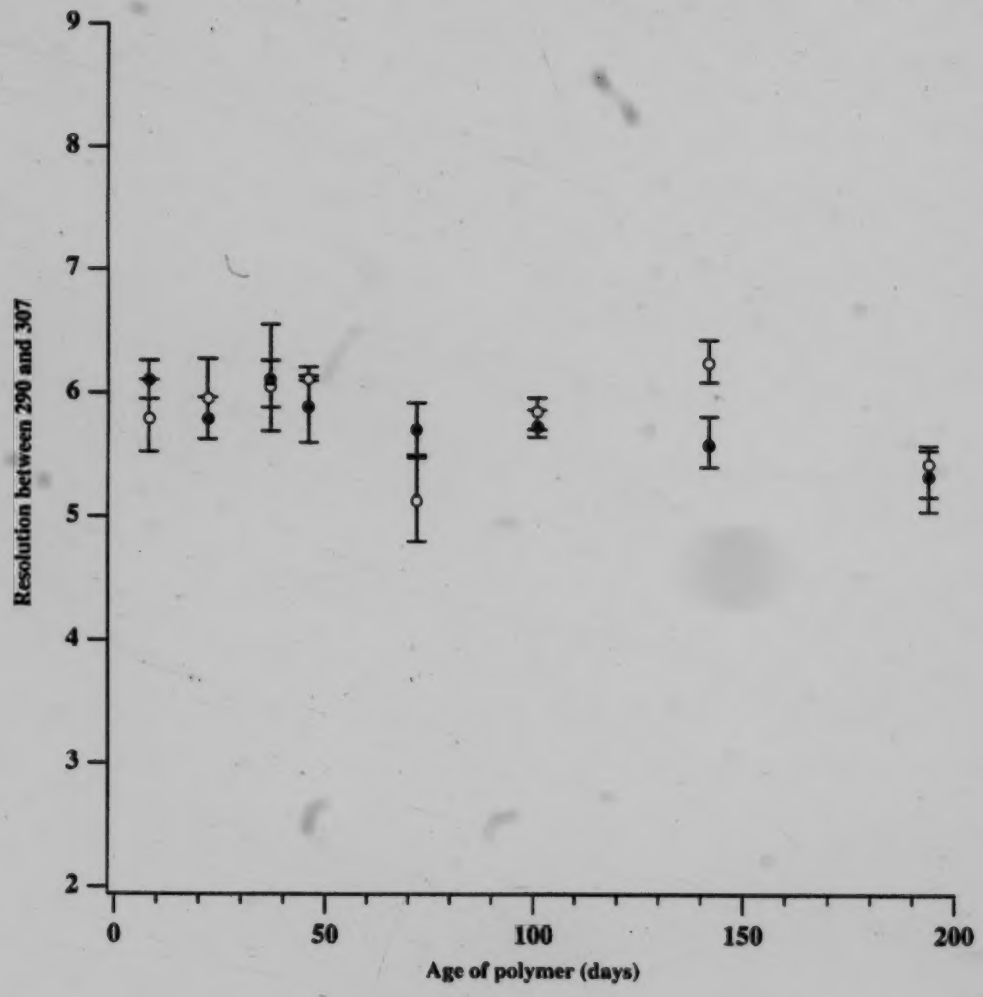

Figure 2.15 Influence of polymer age on resolution of DNA fragments of 290 nt and 307 nt. open circle: aged polymer; solid circle: fresh polymer.

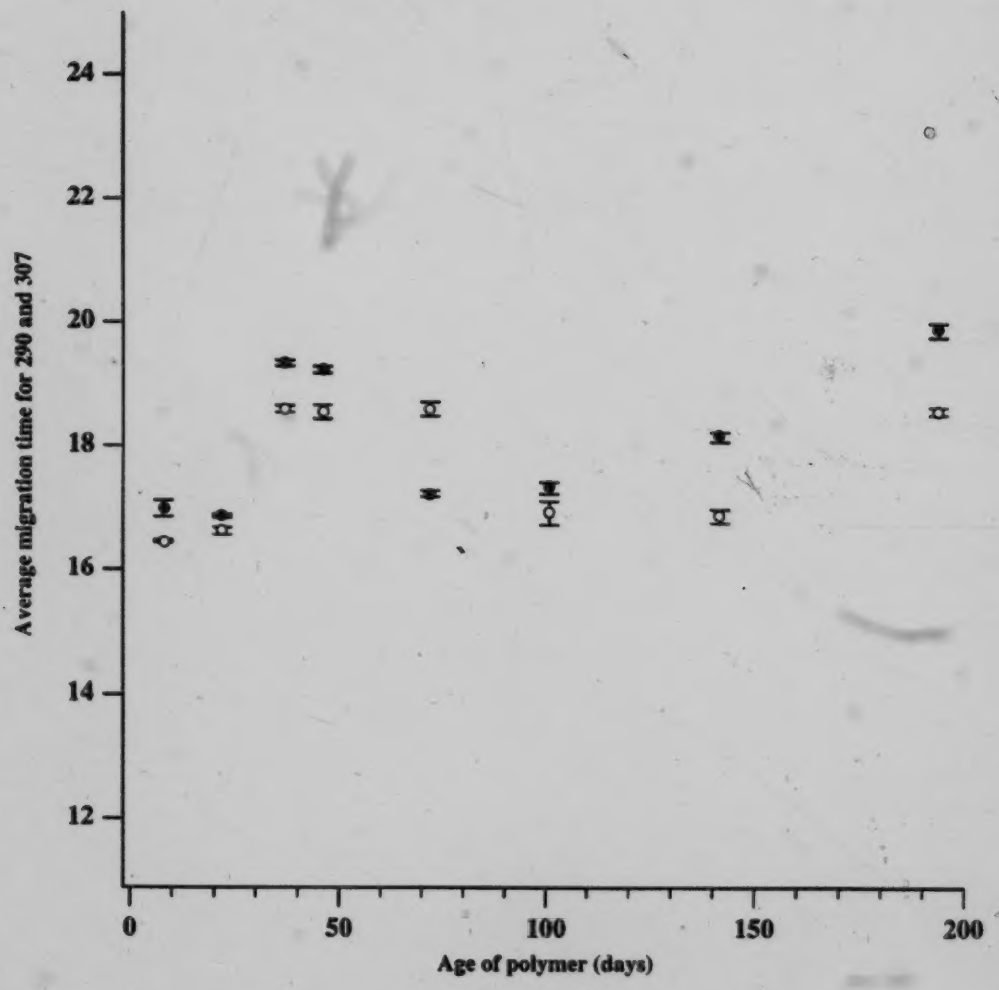

Figure 2.16 Influence of polymer age on relative migration time of DNA fragments 290 nt and 307 nt. open circle: aged polymer; solid crcle: fresh polymer.

resolution versus age of polymer shows no obvious degradation of resolution between the two closely migration DNA fragments over an aging process of about 200 days. The decrease of resolution on day 194 occurred in both the aged and fresh polymer, indicating that the degradation in resolution was not a function of the aging polymer. There was some noticeable change in migration time of the two fragments (as measured in average migration time for both fragments) between day 72, 142 and 194 (Figure 2.16). However, this difference does not correlate positively or negatively with the age of polymer. Hence the fluctuation of migration time between 16 and 20 minutes was likely the result of yet determined parameters rather than the age of the polymer itself. The presence of urea decreased the number of theoretical plates by about 42% (data not shown), and it is well known that urea is unstable and hydrolyzes readily in aqueous solution. However in this case, the instability of urea did not seem to affect the stability of HEC in TAPS buffer, and no apparent change in ionic strength of the aged polymer was manifested in this study. The stability of the polymer solution makes it suitable for long duration storage and helps avoid the inconvenience of repeatedly preparing fresh polymer solution. This will also help reduce batch-to-batch variation occurring from one preparation to the other.

2.3.7 Other cellulose polymers

Several other cellulose polymers that are available in the laboratory were also used to compare with hydroxyethyl cellulose (Mw 250,000). In Figure 2.17, using a 0.4% (w/v) polymer solution as a reference, 2-hydroxyethyl cellulose (Mw 720,000) was shown to retard DNA fragments the most. A separation using 0.4% (w/v) of this cellulose is approximately equivalent to a similar separation using a 0.8% HEC (Mw

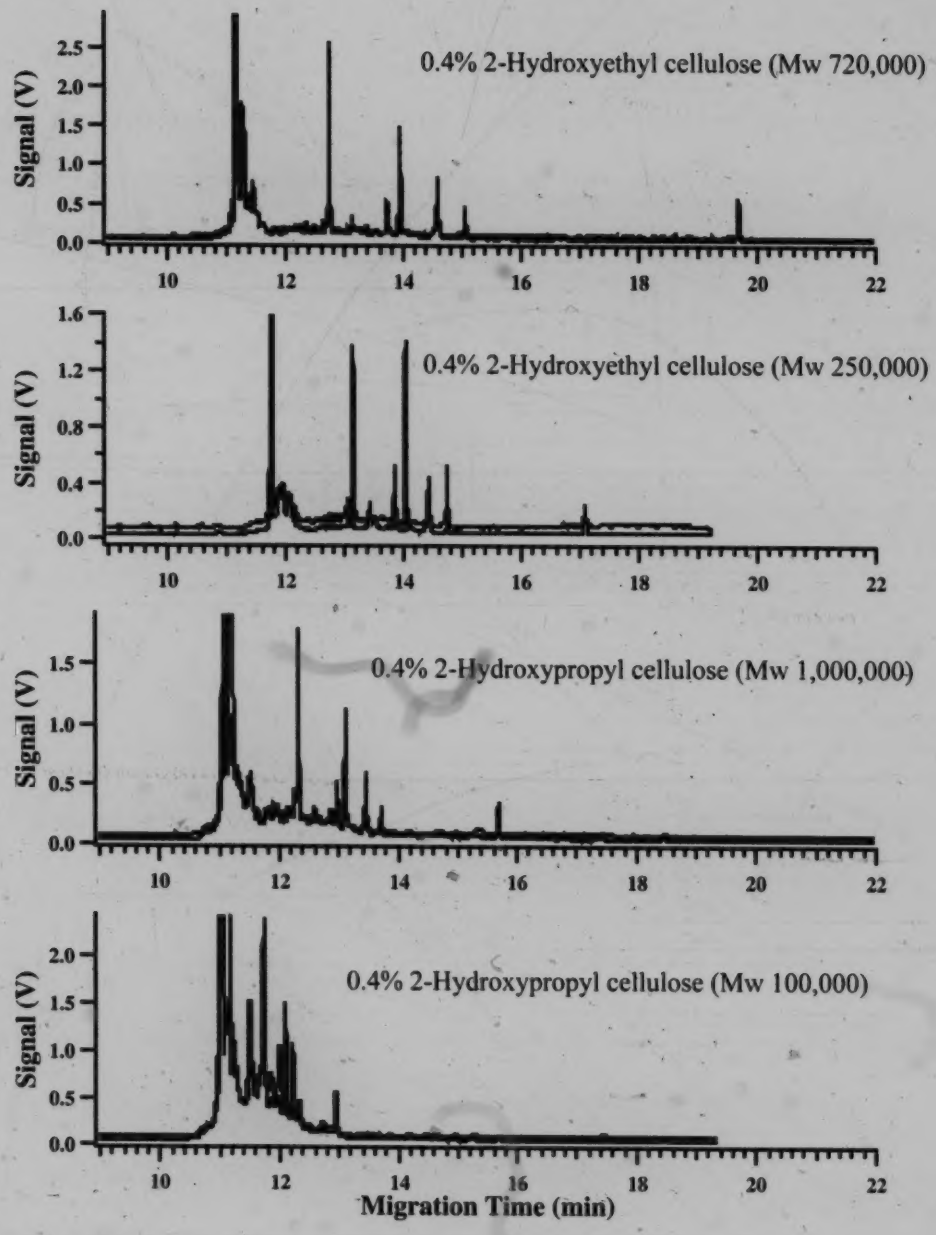
0.4% 2-Hydroxyethyl cellulose (Mw 720,000)
0.4% 2-Hydroxyethyl cellulose (Mw 250,000)
0.4% 2-Hydroxypropyl cellulose (Mw 1,000,000)
0.4% 2-Hydroxypropyl cellulose (Mw 100,000)
Signal (V)
Migration Time (min)

Figure 2.17 Separation of single-stranded DNA in various cellulose polymers. All polymer solutions were prepared in 0.1 M TAPS (pH 8)

250,000) in terms of peak resolution and migration time. Surprisingly, hydroxypropyl cellulose at Mw 1,000,000 did not provide separation power as high as hydroxyethyl cellulose at Mw 250,000. A similar cellulose at Mw 100,000 was shown to provide separation power equivalent to that of a 0.1% HEC at Mw 250,000.

2.4 Conclusions

The study of the effect of HEC concentration on single-stranded DNA separation indicates that the optimal polymer concentration for this type of analysis is 0.8%. This concentration allows complete separation of excess primers from the target DNA fragments and provides base-line resolution of all product peaks. Polymer solution at higher concentrations offer similar resolution, but at the expense of a much longer migration time. The resolution in this case may not be compatible to that of the high viscosity acrylamide matrices. However, unlike DNA sequencing technology, separation of PCR-amplified products for screening genetic diseases and laboratory diagnosis in most cases do not require single-base resolution, and resolution of fragments differing by 10 to 15 base pairs is generally sufficient. Hence there is no need to employ high viscosity sieving or rigid cross-linked gel matrices, which provide excellent resolution at the expense of a very long separation time. For the purpose of our study, the speed of analysis is a more important factor.

The stability study of HEC in the presence of urea has indicated that the polymer solution is very stable and can be stored at 4°C for at least 6 months. We initially expected reasonable hydrolysis of urea over long periods of storage time, but no effect of hydrolysis (if present) was observed in the resolution of all 4 DNA fragments. The

cellulose is uncharged and is highly stable at elevated temperature. The stability in this case is certainly advantageous compared to polymers which tends to break down in alkaline. In addition, the viscosity of a 0.8% HEC polymer solution is essentially compatible to that of water. This allows effortless replacement of sieving matrix on a capillary.

The melting point of the cellulose is between 288°C and 290°C. Using this property, an attempt was made to create a permanent capillay coating for this study by desiccating HEC (3% w/v) coated fused-silica capillary at 110°C for 6 hours. This unique coating showed significant suppression of EOF and was found to be effective for the separation of restriction DNA fragments as well as for high temperature sequencing (data in appendix). However, since there was no actual chemical bonding involved in the coating protocol, the capillary was not able to withstand repeated replacement of HEC polymer solution. As a result, this coating was found not desirable for the purpose of this study. The DB-210 coated fused-silica capillary that was employed subsequently has proven to be more durable and able to perform consistently. Although this commercially available capillary is costly (cost per unit length), the cost per run is inexpensive. A DB-210 capillary on average was able to perform between 250 to 350 runs in our hands without degradation of coating quality. In addition, the capillary can also be easily reconditioned by flushing with 20 mM NaOH and 10 volumes of methanol, followed by an overnight incubation at 37°C.

The present work demonstrated the efficient use of HEC as a replaceable sieving matrix for single stranded DNA analysis under denaturing condition. The short turnover

time of sieving replacement and DNA separation clearly suggests the advantage of this protocol for high speed, high resolution DNA analysis.

2.5 Bibliography

1. Righetti, P.G. and Gelfi, C. (1996) Capillary Electrophoresis of DNA in Capillary Electrophoresis in Analytical Biotechnology. CRC Press Inc. pp.431-450.
2. Dolnik, V. (1994) J. Microcol. Sep. **6**, 315-330.
3. Smisek, D.L. (1995) Electrophoresis **16**, 2094-2099.
4. Sunada, W.M. and Blanch, H.W. (1997) Electrophoresis **18**, 2243-2254.
5. Sunada, W.M. and Blanch, H.W. (1998) Electrophoresis **19**, 3128-3136.
6. Olivera, B.M., Baine, P. and Davidson, N. (1964) Biopolymer **2**, 245-257.
7. Pulyaeva, H., Wheeler, D., Garner, M.M. and Chrambach, A. (1992) **13**, 608-614.
8. Simo-Alfonso, E., Gelfi, C., Lucisano, M. and Righetti, P.G. (1996) J. Chromatogr. A **756**, 255-261.
9. Gelfi, C., Perego, M., Libbra, F. and Righetti, P.G. (1996) Electrophoresis **17**, 1342-1347.
10. Strege, M. and Lagu, A. (1991) Anal. Chem. **63**, 1233-1236.
11. Grossman, P.D. and Soane, D.S. (1991) J. Chromatogr. **559**, 257-266.
12. McCord, B.R., Jung, J.M. and Holleran, E.A. (1993) J. Liq. Chromatogr. **16**, 1963-1981.
13. Barron, A.E., Soane, D.S. and Blanch, H.W. (1993) J. Chromatogr. **652**, 3-16.
14. Zhu, H., Clark, S.M., Benson, S.C., Rye, H.S., Glazer, A.N. and Mathies, R.A. (1994) **66**, 1941-1948.

15. Butler, J.M., McCord, B.R., Jung, J.M. and Allen, R.O. (1994) **17**, 4-7.

16. Baba, Y., Isimaru, N., Samata, K. and Tsuhako, M. (1993) **653**, 329-335.

17. Dolnik, V. and Novotny, M. (1992) J. Microcol. Sep. **4**, 515-519.

18. Chang, H.T. and Yeung, E.S. (1995) J. Chromatogr. B **669**, 113-123.

19. Kleparnik, K., Foret, F., Carson, S. and Karger, B.L. (1996) Electrophoresis **17**, 1860-1866.

20. Chrambach, A. and Aldroubi, A. (1993) Electrophoresis **14**, 18-22.

21. Drossman, H., Luckey, J.A., Kostichka, A.J., D'Cunha, J. and Smith, L.M. (1990) Anal. Chem. **62**, 900-903.

22. Swerdlow, H., Dew-Jager, K.E., Grey, R., Dovichi, N.J., Gesteland, R. (1992) Electrophoresis **13**, 475-483.

23. Yin, H.F., Lux, J.A., Schomburg, G. (1990) J. High Resolut. Chromatogr. **13**, 624-627.

24. Chiari, M. and Righetti, P.G. (1995) Electrophoresis **16**, 1815-1829.

25. Barron, A.E., Sunada, W.M. and Blanch, H.W. (1996) Electrophoresis **17**, 744-757.

26. Madabhushi, R.S., Vainer, M., Dolnik, V., Enad, S., Barker, D.L., Harris, D.W. and Mansfield, E.S. (1997) Electrophoresis **17**, 104-111.

27. Heller, C. (1998) Electrophoresis **19**, 3114-3127.

28. Chiari, M., Damin, F., Melis, A. and Consonni, R. (1998) Electrophoresis **19**, 3154-3159.

29. Kleemib, M.H., Gilges, M. and Schomburg, G. (1993) Electrophoresis **14**, 512-522.

30. Singhal, R.P. and Xian, J. (1993) J. Chromatogr. **652**, 47-56.

31. Broseta, D., Leibler, L., Lapp, A., Strazielle, C. (1986) Europhys. Lett. **2**, 733-737.

32. Grossman, P.D. and Soane, D.S. (1991) Biopolymers **31**, 1221-1228.

33. De Gennes, P.G. (1979) Scaling Concepts in Polymer Physics, Cornell University Press, Ithaca, NY.

34. Kennedy, J.F., Rivera, Z.S., Lloyd, L.L., Warner, F.P. and da Silva, M.P.C. (1995) Carbohydrate Polymers **26**, 31-34.

35. Barron, A.E., Blanch, H.W. and Soane, D.S. (1994) Electrophoresis **15**, 597.

36. Grossman, P.D., Hino, T. and Soane, D.S. (1992) J. Chromatogr. **608**, 79.

37. Grossman, P.D. (1994) J. Chromatogr. A. **663**, 219.

38. Oefner, P.J., Bonn, G.K., Huber, C.G. and Nathakarnkitkool, S. (1992) J. Chromatogr. **625**, 331.

39. Oefner, P.J. and Bonn, G.K. (1994) Int. Lab. **14**, July/August.

40. Kim, Y. and Morris, M.D. (1994) Anal. Chem. **66**, 1168-1174.

41. Figeys, D., Arriaga, E., Renborg, A. and Dovichi, N.J. (1994) J. Chromatogr. A. **669**, 205-216.

42. Srinivasan, K., Morris, S.C., Girard, J.E., Kline, M.C. and Reeder, D.J. (1993) Appl. Theor. Elec. **3**, 235-239.

43. Zhu, H., Clark, S.M., Benson, S.C., Rye, H.S., Glazer, A.N. and Mathies, R.A. (1994) Anal. Chem. **66**, 1941-1948.

44. Ogston, A.G. (1958) Trans. Faraday Soc. **54**, 1754.

45. Rodbard, D. and Chrambach, A. (1970) Proc. Natl. Acad. Sci. U.S.A. **4**, 970.

46. Stellwagen, N.C. (1987) Electrophoresis of DNA in agarose and polyacrylamide gels, in Advances in Electrophoresis, Chrambach, A., Dunn, M., and Radola, Eds., 179.

47. Tietz, D., and Chrambach, A. (1992) Electrophoresis **13**, 286.

48. Viovy, J.L and Duke, T. (1993) Electrophoresis **14**, 322.

Bueche, F. (1962) Physical properties of polymers, John Wiley, New York.

Chapter 3. On-Column Labeling of DNA Fragments and Detection by CE-LIF

A shorter version of this chapter has been published.
W.G. Tan, D.L.J. Tyrrell and N.J. Dovichi. Detection of duck hepatitis B virus DNA fragments using on-column intercalating dye labeling with capillary electrophoresis-laser induced fluorescence (CE-LIF). 1999 J. Chromatography A. **853**, 309-319.

3.1 Introduction

3.1.1 Labeling of DNA with nucleic acid stains

In the past few years, many applications of CE in DNA separation have been demonstrated in analytical biochemistry as well as molecular biology, especially with the advent of mapping the human genome and high throughput screening. CE covers a wide range of research areas. They include analysis of restriction DNA fragments [1-7], detection of point mutation in DNA and DNA damage [8-10], detection of polymerase chain reaction (PCR) products [11-13], and identification of individuals in forensic applications [14,15].

One unique characteristic of CE is its requirement for low sample volume, typically in the low nano liter range. This makes practical application of CE highly dependent on detection sensitivity. Detection of DNA fragments using intercalating dyes has been well studied [1,12, 16-28]. These dyes usually insert themselves in between adjacent base pairs of the DNA, and the intercalative binding follows the 'neighboring exclusion principle' where every second site along the double helix remains unoccupied [29]. Many of these polycationic intercalators, in particular the dimeric analogs of acridines [30-32], 7-hydropyridocarbazoles [33] and 3,8-diamino-6-phenylphenanthridinium [34-36], demonstrate DNA-binding affinities several orders of magnitude higher than their corresponding monomers. Using an on-column staining method, Zhu et al. described the use of thiazole orange homodimer TOTO to detect DNA fragments as dilute as 40 fg/μL [21]. Figeys et al [18] showed detection limits of a few yoctomoles of fluorescently labelled DNA using a dimeric dye POPO3, oxazole yellow homodimer YOYO3 or YOYO1 in high salt buffer.

Detection limits of the dye itself are on the order of $1x10^{-21}$ moles. Skeidsvoll and Ueland [37] demonstrated the use of SYBR Green I, a monomeric fluorescent dye in the detection of DNA fragments in hydroxypropyl methylcellulose. Fluorescence intensity versus DNA concentration was linear over three orders of magnitude (4 pg/μL to 30 ng/μL), with a limit of detection of approximately 80 fg of double-stranded DNA (dsDNA).

3.1.2 Formation of DNA-dye complexes

In general, the binding constants of monointercalators to dsDNA are 10^5 - 10^6 M^{-1} in low salt buffer. Dyes with two potential intercalating moieties in a single molecule have been estimated to have association constants with dsDNA of 10^{10} - 10^{12} M^{-1} [38,39]. However, efficient separation using bis-intercalators are usually obtained over a narrow range of DNA-dye ratios. Peak-splitting and severe band-broadening [21,27,40] are frequently encountered in cases where DNA fragments are pre-stained prior to sample loading, and DNA separation is carried out in a continuous electrolyte system lacking intercalating dyes in the electrophoresis buffer [21,27,41]. This phenomenon is explained by a very simple Le Chatelier's principle, which states that concentration stress of a removed reactant is relieved by reaction in the direction that replenishes the removed substance. When the DNA-dye complexes migrate toward the detection end, they traverse a dye-depleted zone since the unbound dye molecules migrate toward to injection end. This drives the equilibrium towards the formation of free dye and non-intercalated DNA, resulting in the dissociation of dye molecules from the DNA-dye complexes.

3.1.3 Parameters affecting complex stability

Some groups [18,37,42] experienced greater success with the dimeric dyes and generated excellent DNA separation comparable to that achieved using monomeric dyes such as ethidium bromide, propidium iodide and SYBR Green I. This discrepancy in separation efficiency reflects the differences in the ways the DNA-dye complexes are formed. Parameters such as ionic strength and pH of separation buffer, sieving matrix and dye concentration may affect the stability of the complexes. In the case where NaCl is added to the separation buffer, DNA separation using POPO3 generated plate counts in excess of 2 million plates for small DNA fragments [18]. The addition of NaCl in the separation buffer increases the thermostability of the DNA double-helix. This promotes homogeneous distribution of dye molecules along DNA fragments of a given length, and the subsequent co-elution of all dye-complexed DNA fragments of the same size as a defined peak or band. However, like a great variety of metal ions, sodium ions interact with DNA via their hydrated shell [43,44], thus the ions compete with intercalated dyes for binding at DNA in an anti-cooperative fashion. A decrease in sensitivity of detection is thus expected as a result of intercalated dyes being displaced from the DNA-dye complexes. In cases where fluorescent dye is added to both, the electrophoresis and separation buffer, separation was shown to be desirable. DNA peaks generated are gaussian, and the separation efficiency for the large DNA fragments is on the order of 3 x 10^6 plates per meter [42].

Most of the DNA-dye intercalation studies usually require a lengthy period of DNA-dye incubation to allow the dye molecules to homogeneously distribute themselves along the DNA. Using bis-intercalating dyes, Carlsson et al. [40] have demontrated that

this equilibration process is extremely slow at room temperature (days), but can be improved if the temperature of incubation is raised to 50 °C, where the DNA-dye complexes equilibrate completely in 2 hours. To date, only a few reports have demonstrated satisfactory use of dimeric dyes for DNA separation while many have experienced unsatisfactory results in both capillary and slab gel electrophoresis.

In this study, we have employed an on-column labeling method which allows simultaneous labeling and separation of DNA restriction fragments without going through the pre-staining step. DNA separation is carried out in a discontinuous electrolyte system where sheath buffer at the detection end is added with intercalating dyes and carries ionic strength half of that present in the sieving matrix and the separation buffer. Detection of DNA fragments is achieved in a post-column configuration with a He-Ne laser using a sheath-flow cuvette system [45]. Application of high electric field strength separation is demonstrated using monomeric and dimeric intercalating dyes. Separation of DNA fragments from various sources are used to define DNA concentration linearity, dynamic range and detection limit. These parameters are used in turn to characterize viral nucleic acids purified from biological samples.

3.2 Experimental

3.2.1 Apparatus

The instrument for capillary electrophoresis was built in-house and has been described in detail elsewhere [46-48]. It is equipped with a high-voltage power supply (Model CZE 1000R, Spellman, Plainview, NY); a 543.5 nm green He-Ne laser system (Melles Griot) with a 5 mW maximum output; A Macintosh Centris 650 computer which

controls the power supply via a NB-MIO-16XH-18 input/output board (National Instruments, Austin, TX); an interface box (I-V converter) which transfers output from the instrument to the computer; a plexiglas box (with safety interlock) in which the injection end is installed; a sheath-flow cuvette (1-mm thick walls, 200 μm x 200 μm square inner bore, 2-cm long) which serves as a post-column detector; a R1477 photomultiplier tube (Bridgewater, NJ) for detecting fluorescence signals.

3.2.2 Parameters of CE separation

Capillary electrophoresis of the sample was performed using a 29-cm long, 50 μm i.d., 144 μm o.d. DB-210 coated fused-silica capillary (Polymicro Technologies, Phoenix, AZ) purchased from J&W Scientific (Folsom, CA). Electrophoresis buffer was TBE containing 90 mM Tris-Borate and 2 mM EDTA at pH 8.6. One end of the capillary was immersed in electrophoresis buffer or sample, with a Pt wire electrode at the injection end (cathode) in the plexiglas box. The other end of the capillary was installed inside the sheath-flow cuvette containing intercalating dye in 45 mM Tris-HCL and 1 mM EDTA buffer at pH 7. Sample introduction was performed by electrokinetic injection at 1000 V for 5 to 10 sec. Separation was performed with an electric field of 200 V/cm or higher. A 0.8% Hydroxyethylcellulose (HEC; MW 250,000) was prepared in electrophoresis buffer, filtered by Millex-GS 0.45 μm filter unit (Millipore, Bedford, MA) and used as sieving medium.

3.2.3 Post column detection

The laser beam was focused by a 6.3X (N.A. 0.2) microscope objective (Melles Griot) into the sheath-flow cuvette, just below the capillary end. The fluorescence was collected at 90° from the direction of excitation by a 60X (N.A. 0.7) microscope

objective (LWD-M Plan, Universe Kogaku, Japan). The transmitted light was divided into two spectral channels with a dichroic beam splitter (XF40, 590DRLP). The reflected fluorescence in one channel was spectrally filtered with a 580DF40 band-pass filter and the transmitted fluorescence in the other channel was filtered by a 630DF30 band-pass filter (Omega Optical, Brattleboro, VT). Both of the filtered fluorescence signals were detected by an R1477 photomultiplier tube (PMT). The PMT signal was transferred to the interface box and digitized by the input/output board. Data was collected at a sampling rate of 10 Hz.

3.2.4 Preparation of restriction DNA, DHBV plasmid and serum DNA

All the restriction DNA samples used in this study were purchased commercially; molecular size markers ϕX-174 / *HaeIII* digest were purchased from Pharmacia Biotech and 1kb DNA size markers were purchased from Gibco BRL. Dilution of DNA samples was carried out in deionized water unless otherwise indicated. Due to potential degradation of DNA in deionized water, all DNA samples were freshly prepared and stored on dry ice prior to sample injection.

Plasmid pAltD2-8 was a generous gift from K. Fischer (Dept. Medical Microbiology and Immunology). It contained a monomer of 3.2 kb genome of the duck hepatitis B virus (DHBV) cloned into the *EcoRI* site of vector pAlter-1 (Promega). The pAltD2-8 was propagated in *Eschericheria coli* strain DH 5α grown in suspension broth culture. pAltD2-8 DNA was recovered using Qiagen Plasmid Purification Kit (Qiagen, Chatworth, CA). The isolated plasmid was digested with restriction endonuclease *EcoRI* and electrophoresed on a 0.8% preparative agarose gel to purify the 3.2 kb DHBV

fragments from the vector. The concentration of the purified DHBV DNA was determined by optical absorbance at 260 nm.

Duck sera from 2 weeks old congenitally infected ducklings were collected. Viral DNA from serum was purified from a commercial QIAamp Blood Kit (Qiagen) using 200 μL of serum per infected duckling for direct DNA labeling using intercalating dyes.

3.3 Results & Discussion

3.3.1 Separation efficiency

Analysis of restriction fragments using intercalating dyes has been widely investigated. Many reports have indicated that unsatisfactory separation, in particular for the DNA fragments that are longer than 1000 base pairs, is a direct result of dye depletion and dissociation of DNA-dye complexes upon electrophoresis [25,37,42,50,51]. The results presented here indicate that these problems can be circumvented by an on-column, discontinuous electrolyte system as depicted by a schematic representation shown in Figure 3.1. The elimination of the pre-staining step could reduce the overall analysis time as well as the efficiency of sample injection and separation. Figure 3.2 contrasts the separation of DNA restriction fragments in the absence (a) and presence (b) of DNA-dye incubation prior to injection. In the absence of the pre-staining step, unlabeled DNA was present in the injection end. The partially negative charges carried by all 4 bases as well as the fully negative charged phosphate backbone on the DNA were not neutralized by the cationic dyes, and hence more DNA would be introduced into the capillary by electrokinetic injection. On the other hand, if DNA-dye complexes were injected, the

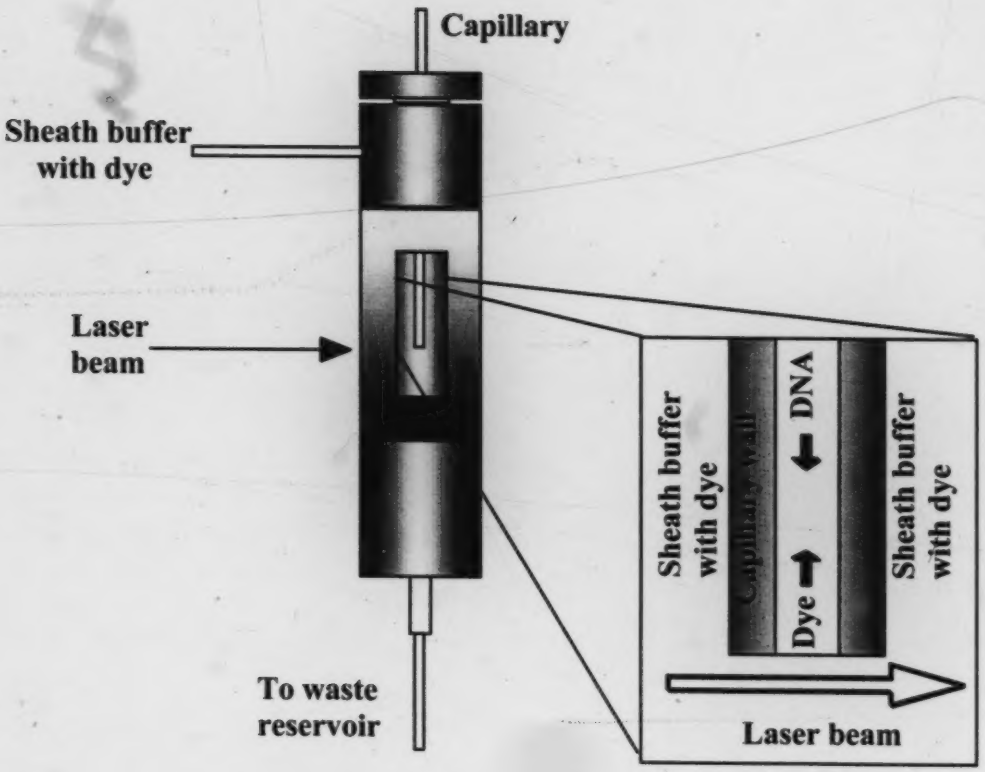

Figure 3.1 Schematic diagram of a sheath-flow cuvette. The sheath-flow cuvette is connected to a buffer reservoir via teflon tubing. The buffer reservoir carries electrophoresis buffer containing intercalating dyes. The buffer is siphoned into the cuvette chamber where the detection end of the capillary is secured. When voltage is applied across the capillary, the positively charged dye molecules migrate into the capillary at its detection end, moving towards the injection end. A difference in buffer ionic strength between the sieving matrix in the capillary and the electrophoresis buffer creates a stacking effect at the end of the capillary, resulting in rapid migration of dye molecules into the capillary.

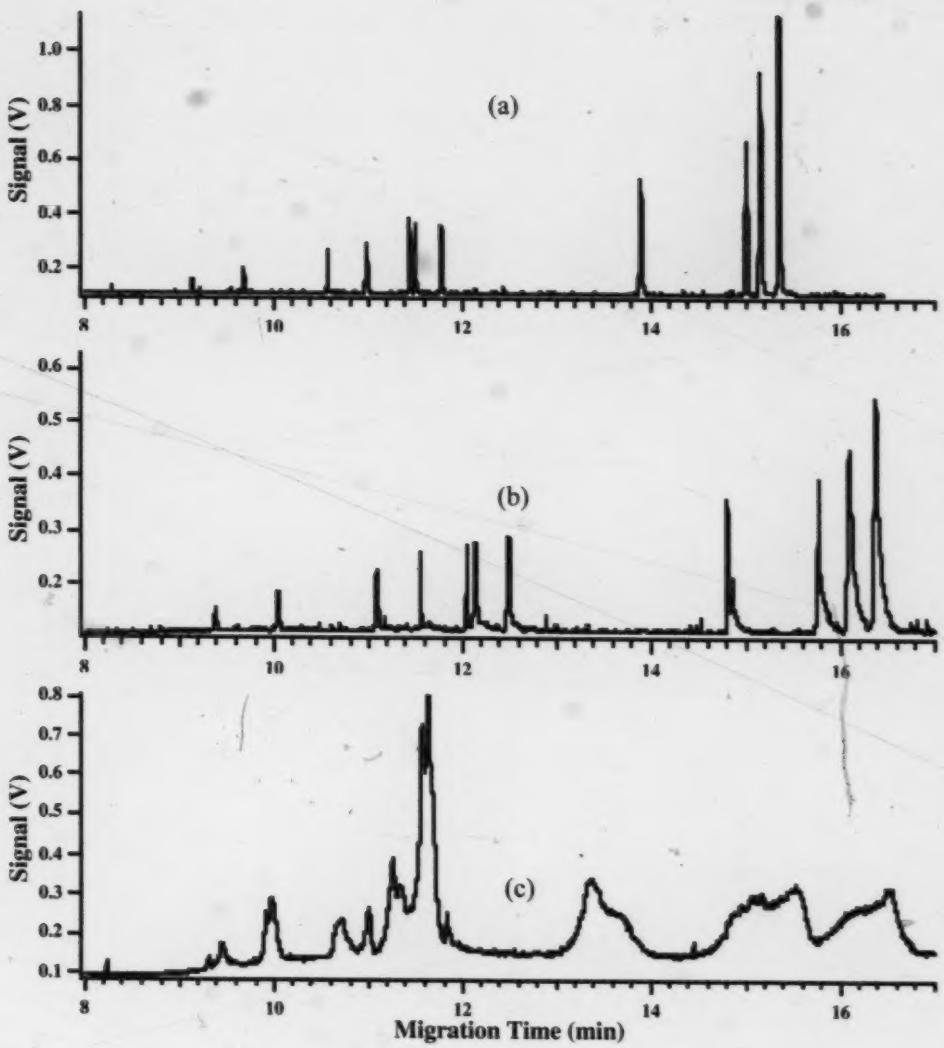

Figure 3.2 Separation of ϕX174/*HaeIII* restriction digest. (a) without DNA-dye pre-staining; (b) with DNA-dye pre-staining; (c) pre-staining without dye in sheath buffer. DNA sample was diluted to 200 pg/μL in 45 mM Tris-HCL and 1 mM EDTA at pH 7 prior to injection; POPO3 was diluted to 1 x 10^{-7} M in the same buffer and introduced into sheath-flow cuvette by siphoning. DNA-dye mixture was incubated for half hour at room temperature before sample injection.

partially neutralized DNA molecules would not be electrokinetically injected as efficiently. As a result, a slight reduction in sensitivity was noticed. The associated band broadening and longer migration time as shown in Figure 3.2(b) are explained by two possible modes of DNA-dye interaction. As indicated by Carlsson et al. [40] and Reese [52], when DNA-dye complexes are allowed enough time (hours) to equilibrate completely, the major mode of DNA-dye interaction is insertion. This was confirmed by a 42% increase in contour length of a T4-DNA incubated with ethidium bromide. The increase in DNA length in this case corresponds to the observation in Figure 3.2(b) in which the migration time of all 11 DNA fragments are relatively longer than those observed in Figure 3.2(a). In our study, complete equilibration was unlikely to occur in a 30 min DNA-dye incubation. Hence distribution of dye between DNA molecules for a DNA population of a defined length was not homogenous, resulting in band broadening and peak tailing. In the absence of pre-staining, intercalating dyes undergo a significant amount of secondary binding where the dye molecules attach to the external surface of DNA through electrostatic interactions [53-55]. This mode of binding will only contribute to reduction of the linear charge density of the DNA but will not alter the length of DNA, a scenario which matches well with the relatively shorter migration time observed in Figure 3.2(a) than in 3.2(b). In contrast to dye intercalation, electrostatic binding is typically a weak interaction and is easily disrupted above 100 mM NaCl [56]. According to Bloomfield et al. [57] and Bradley et al. [58], the coulombic interaction between the cationic dyes and the DNA promotes the formation of stacked dye aggregates along the DNA phosphate backbone. This weak external stacking is maintained only if equilibrium favors the formation of DNA-dye complexes. Since

electrostatic binding is weaker than insertion, the presence of free dye in the sheath buffer is unlikely to have a drastic effect on the incubated DNA-dye complexes. The possibility of technical difference between the two separations is ruled out in this case because the runs were carried out consecutively without changing the buffer system in the cuvette. As shown in Figure 3.2(c), the absence of intercalating dyes in the sheath buffer greatly decreases the efficiency of labeling even though the DNA sample was pre-stained with POPO3 (Molecular Probes). This observation strongly suggests that the formation of dye-DNA complexes under this condition is a dynamic process. The stability of these complexes can only be preserved in an environment where excess dye molecules are the predominant species, such as the continuous influx of dye molecules from the detection end of the capillary. Figure 3.3 shows the separation of various DNA size ladders using between 0.4 and 0.8% HEC matrix. DNA fragments between 50 and 23 kbp are mostly resolved. On a slab gel using agarose or polyacrylamide at a given sieving concentration, separation of the larger fragments is usually compromised by the efficient separation of the smaller fragments and vice versa. In CE using cellulose sieving, the larger fragments are often difficult to baseline resolve [7, 37]. We have attributed this problem to a combination of sample overloading and dye depletion. In the case of a 1 kb DNA size ladder, when there is an estimated 0.6 to 2.5 pg total DNA content injected into the capillary, all the DNA fragments experience excellent binding capacity. Hence the mobility shift caused by the intercalating dyes for each DNA fragment is very distinct for a given fragment size. This results in baseline resolution of all DNA fragments as shown in Figure 3.4. On the other hand if there is too much DNA (above 10 pg total DNA) in the injection plug, poor binding capacity is experienced, in particular for the larger

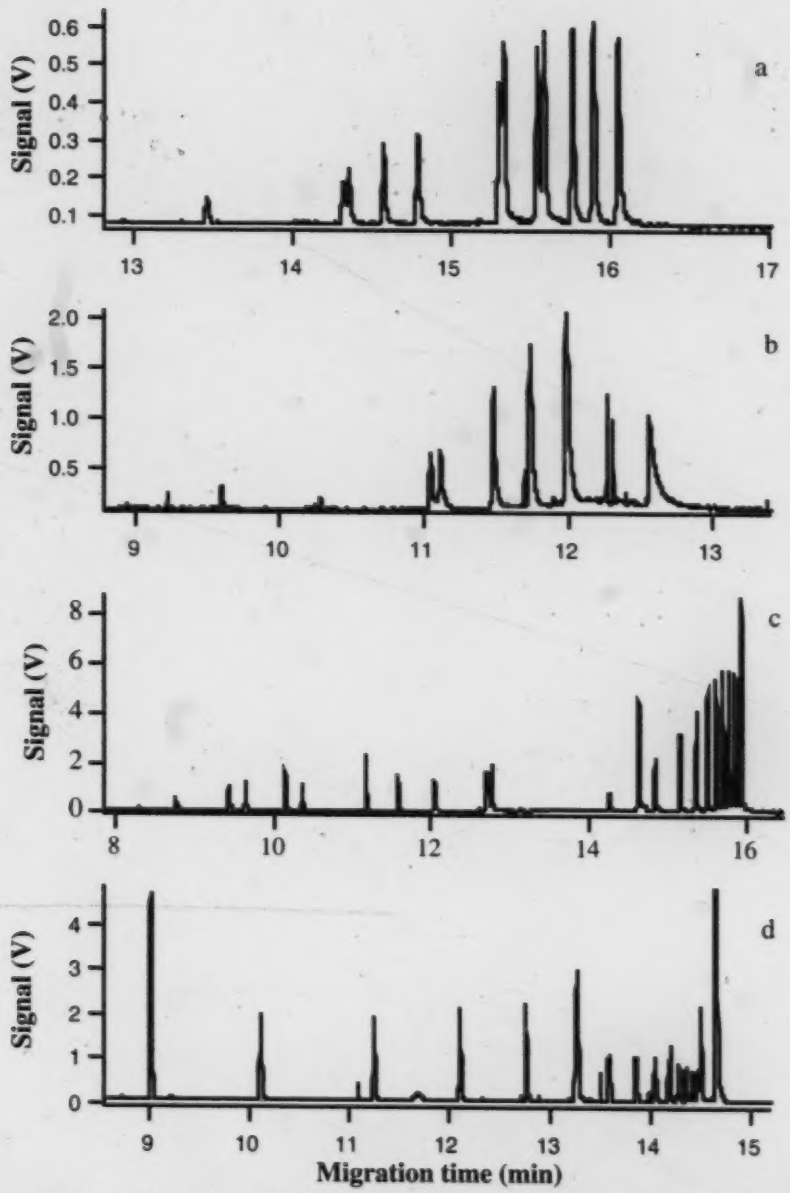

Figure 3.3 Separation of DNA size ladders in HEC matrix. Separation was carried out using between 0.4% and 0.8% polymer solution; (a) λ-BstEII (0.05 ng/μL); (b) λ-HindIII (0.25 ng/μL); (c) 1kb DNA ladder (2.5 ng/μL); (d) 100bp DNA ladder (8.5 ng/μL); capillary: 30 cm; field strength: 200 V/cm; sieving buffer: 90 mM Tris-borate and 2 mM EDTA (pH 8.6); POPO3 was diluted to 1 x 10^{-7} M in 45 mM Tris-HCL and 1 mM EDTA (pH 7).

fragments which require much more dyes for homogenous binding and efficient resolution. In Figure 3.4 (a), DNA fragments between 1018 and 12216 bp were baseline resolved. In Figure 3.4 (b) and (c) fragments 11198 and 12216 co-migrated. As the concentration of the DNA sample increased to 10 ng/μL (Figure 3.4d), fragments 10180, 11198 and 12216 co-eluted at a broad peak.

3.3.2 Stacking of intercalating dye from sheath-flow buffer

In order to detect minute amounts of DNA in the capillary, intercalating dye between $1x10^{-7}$ and $5x10^{-7}$ M must be added to the sheath buffer to provide optimum intercalation without increasing fluorescence background. To achieve low background and high binding capacity, the dye is diluted in sheath-flow buffer with an ionic strength lower than that of the running buffer. During electrophoresis, field amplification is expected to take place at the detection end of the capillary, causing the cationic dyes to migrate rapidly and stack as a tight plug at the boundary between the two buffer systems. As a result, the stacked dye zone at the detection end will have a concentration higher than that present in the sheath-flow buffer. This ensures that by using the least amount of dye in the sheath buffer (and hence a lower background fluorescence), effective labeling of all DNA fragments migrating towards the detection end can be achieved, regardless of their sizes. As shown in Figure 3.5, stacking of dye molecules at the detection end enhanced the sensitivity of detection by approximately 4 fold (using the 1636 bp fragment as a marker) when there was an approximately 2-fold ionic strength difference at the boundary of the two buffer systems (Figure 3.5b). No substantial increase in sensitivity is observed when the ionic strength difference is increased beyond 2 fold (Figure 3.5c). However, a further increase in ionic strength difference improved peak

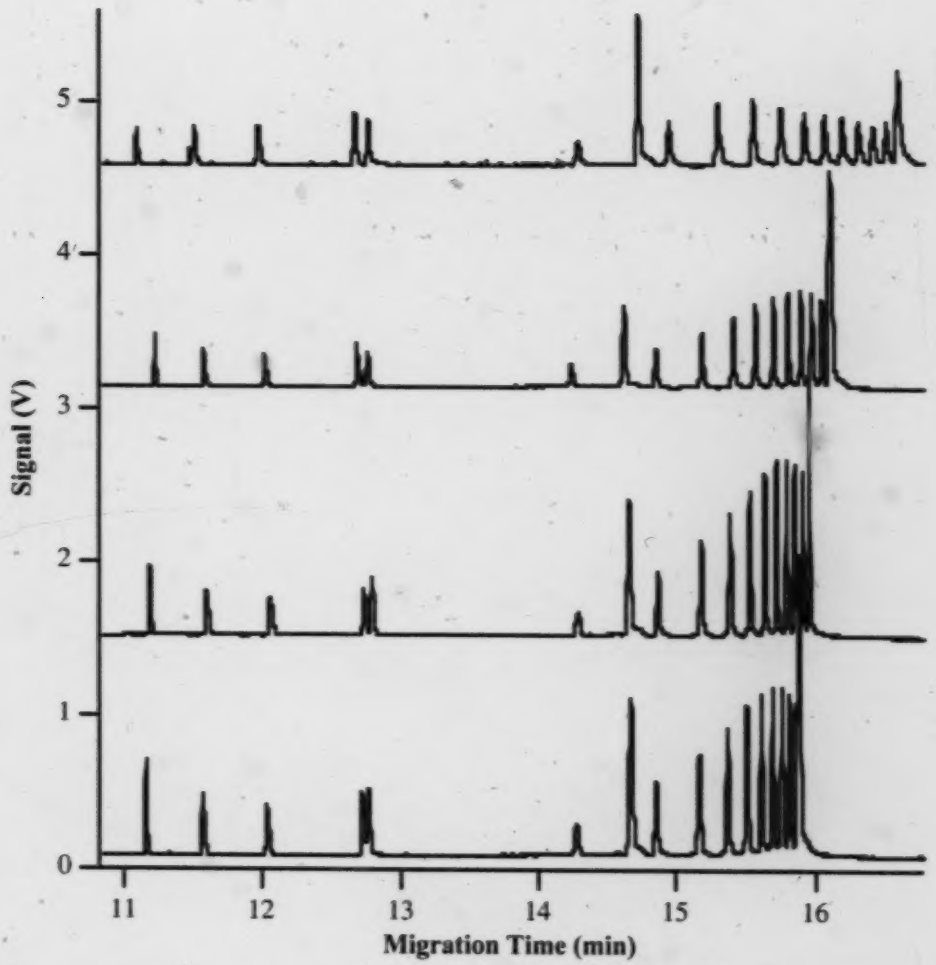

Figure 3.4 Effect of sample loading on separation efficiency. (a) to (d) represent a 1 kb DNA size ladders at 0.16, 0.63, 2.5 and 10 ng/µl respectively. 0.8% HEC was prepared in 90 mM Tris-borate and 2 mM EDTA (pH 8.6). POPO3 was diluted to 1 x 10^{-7} M in 45 mM Tris-HCL and 1 mM EDTA (pH 7.0). DNA was injected at 1000V for 5 s; separation at 200 V/cm. Sizes in base pairs of all 23 fragments are 72, 134, 154, 201, 220, 298, 344, 396, 506, 517, 1018, 1636, 2036, 3054, 4072, 5090, 6108, 7126, 8144, 9162, 10180, 11198 and 12216. Only fragments 298 to 12216 are shown. Peak heights in all electropherograms were adjusted to assist presentation.

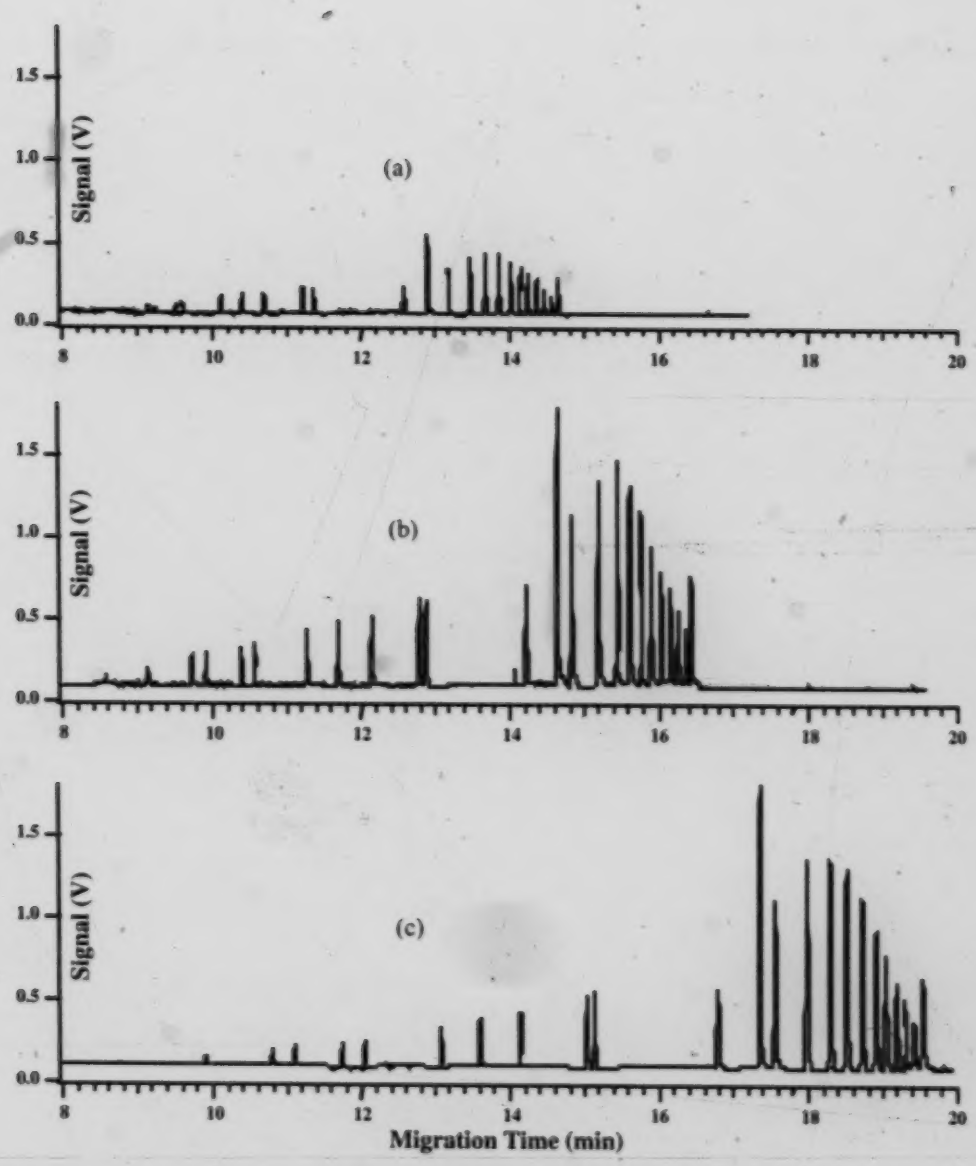

Figure 3.5 Comparison of three different dye stacking conditions at the detection end. The separation buffer was 90 mM Tris-borate/2 mM EDTA at pH 8.6. (a) sheath buffer was 90 mM Tris-borate/2 mM EDTA at pH 8.6 with 2×10^{-7} M ethidium homodimer II; (b) sheath buffer was 45 mM Tris-HCL/1 mM EDTA at pH 7 with 2×10^{-7} M ethidium homodimer II; (c) sheath buffer was 10 mM Tris-HCL/1mM EDTA at pH 7 with 2×10^{-7} M ethidium homodimer II.

resolution, in particular for the smaller DNA fragments. The presence of fewer counter ions for the dye molecules in the sheath buffer further increased the stacking phenomenon, and hence the velocity with which the dye molecules migrated into the capillary. This increase in velocity countered the migration of DNA from the opposite direction, resulting in a further decrease in migration time for all DNA fragments. Separation efficiency remained relatively consistent (6.25% RSD) for all three buffer systems, suggesting that the stacking of dye at the detection end has no observable influence on zone broadening. And since there was a continuous feeding of dye into the capillary from the sheath buffer, the equilibrium would be driven to the direction that favors the formation and preservation of DNA-dye complexes. The result is the formation of peaks that are nearly symmetrical, and plate counts that are in excess of 47 million plates per meter. This is among the highest efficiency reported for any separation technique (Figure 3.6). Figure 3.7 illustrates the mobility profile of DNA fragments resolved under different stacking conditions. The usual sigmoidal dependence of mobility on molecular mass was observed in all 3 stacking conditions. Transition from Ogston sieving to Reptation was obvious between 600 and 700 bp when a discontinuous electrolyte system with 10 mM Tris-HCL / 1 mM EDTA in the dye reservoir was used. As the ionic strength in the dye reservoir increased, the transition becomes less apparent. Transition was least apparent when a continuous electrolyte system without dye stacking was employed. The influence of ionic strength difference between the two buffers on mobility shift was more dramatic for larger as opposed to smaller DNA fragments. This suggests a more pronounced neutralization of the negative charges as the degree of dye stacking increases, which further promotes mobility retardation imposed on the DNA

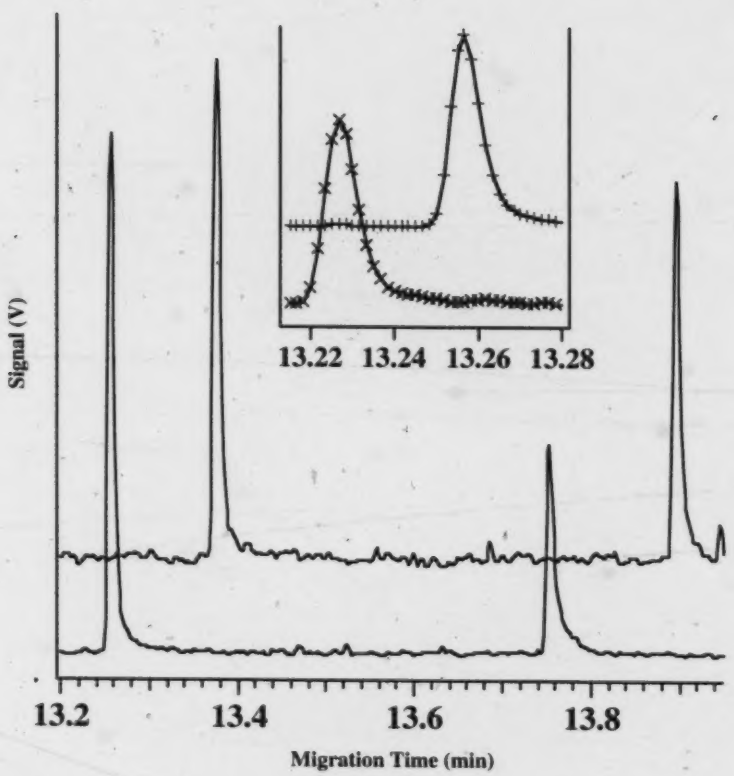

Figure 3.6 The 3021 bp duck hepatitis B virus insert was removed from the vector (PAlter-1) by endonuclease *EcoRI* digestion at 37°C for 3 hours. The electropherograms were obtained from two consecutive injections of the digested sample. The sieving matrix was 0.8% HEC. POPO-3 was diluted to 2 x 10^{-7} M in 45 mM Trisbase and 1 mM EDTA (pH 10.4) and introduced into the sheath-flow cuvette by siphoning. The shorter fragment is the 3021 bp insert and the larger fragment is the 5680 bp vector. The inset shows an expanded view of the peak generated by the 3021 bp fragment. Injection was at 1000 V for 5 s.

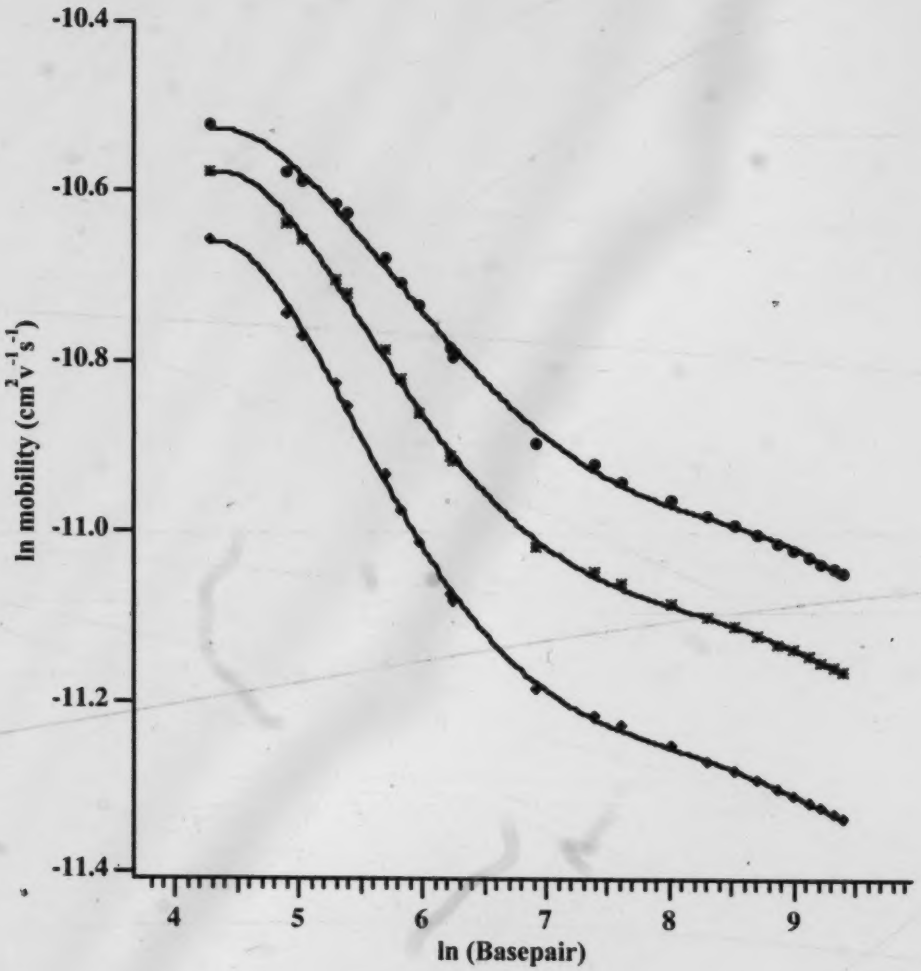

Figure 3.7 Dependence of electrophoretic mobility of restriction DNA fragments (72-12216 bp) on molecular mass in 3 different buffer systems. Closed diamonds: 10 mM Tris-HCL/1 mM EDTA at pH 7; asterisks: 45 mM Tris-HCL/1 mM EDTA at pH 7; closed circles: 90 mM Tris-borate/2 mM EDTA at pH 8.6. The double ln plots were curved fitted using a 6-term polynomial function.

fragments. Unlike sample stacking at the injection end, a continuous migration of dye into the capillary at the detection end was maintained for as long as voltage was applied across the capillary. This phenomenon ensured that equilibrium was always driven to

favor the formation and preservation of DNA-dye complexes. The continuous stacking of dye is attainable in a sheath-flow cuvette system that allows continuous replacement of dye containing buffer inside the cuvette compartment. However, the same stacking can not be achieved using a commercial CE instrument that is equipped with a post-column, closed end waste reservoir which does not allow continuous buffer replacement.

3.3.3 High speed separation

Separation of restriction DNA fragments using intercalating dyes has been demonstrated widely, but few have investigated this approach at high field strength separation. Here, we demonstrated the efficient separation of the 11 fragments from the ϕX174/*HaeIII* digest using a dimeric dye as the labeling agent (Figure 3.8). Separation of DNA-dye complexes was achievable at field strengths as high as 550 V/cm. High field strength was not problematic in this case as the power generated was usually no higher than 350 milli-watt per meter, a direct result of not adding sodium chloride into the TBE buffer. In cases where intercalating dyes were not added to the sieving medium and the electrophoresis buffer, sodium chloride was usually added to the running buffer to preserve the DNA-dye complexes during electrophoresis. In our set up, the continuous supply of dye from the sheath buffer into the capillary provides an environment that prevents the dissociation of dye molecules from the DNA-dye complexes in the absence of sodium chloride. The mobility profile of these DNA-dye complexes at various field strengths is presented in Figure 3.9. A linear relationship is observed between electrophoretic mobility of all 11 fragments and the applied field strength from 200 V/cm to 500 V/cm. The slopes of all 11 plots suggest that mobility of smaller DNA fragments experience little dependence on applied field strength. As the fragment length increases,

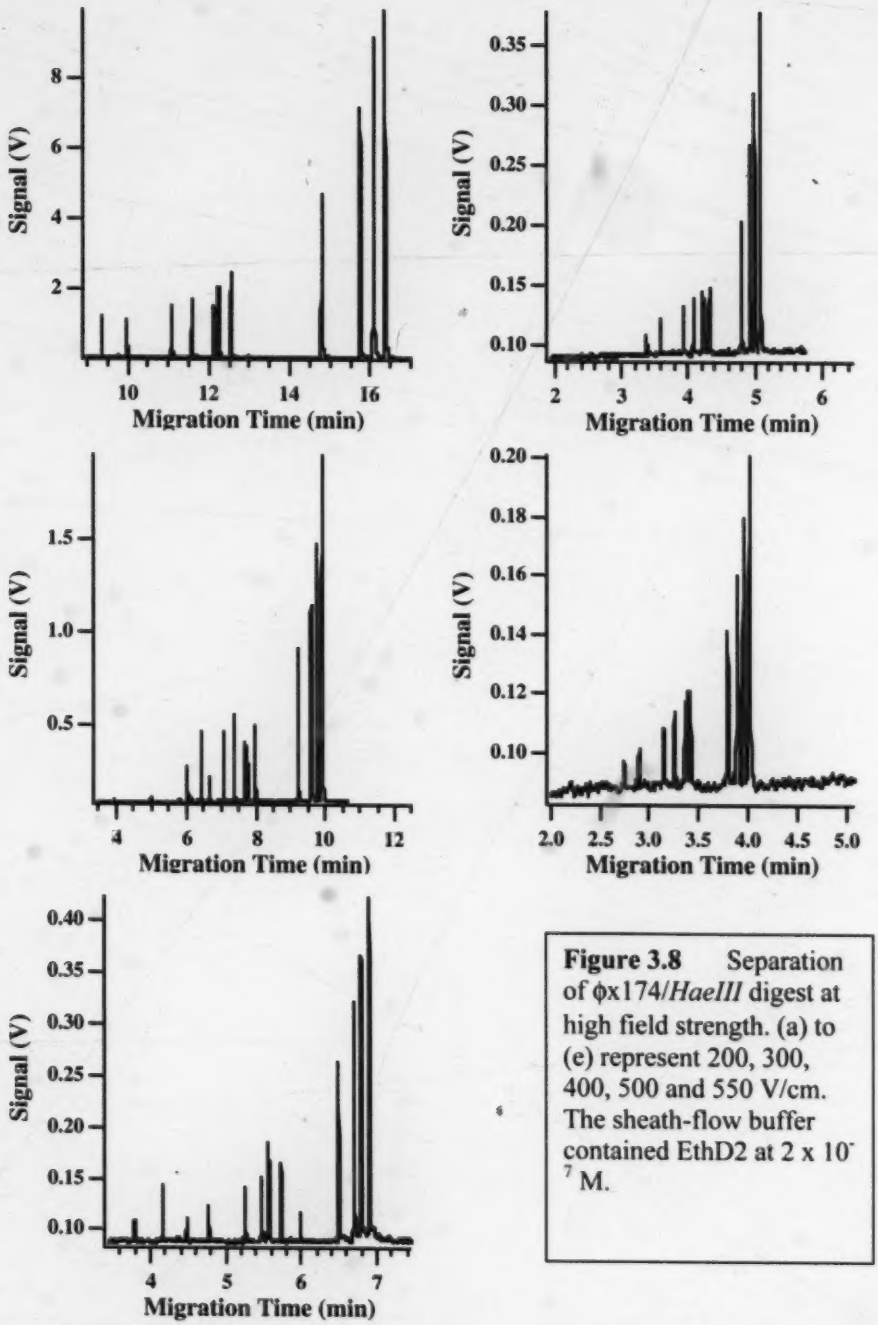

Figure 3.8 Separation of ϕx174/*HaeIII* digest at high field strength. (a) to (e) represent 200, 300, 400, 500 and 550 V/cm. The sheath-flow buffer contained EthD2 at 2 x 10^{-7} M.

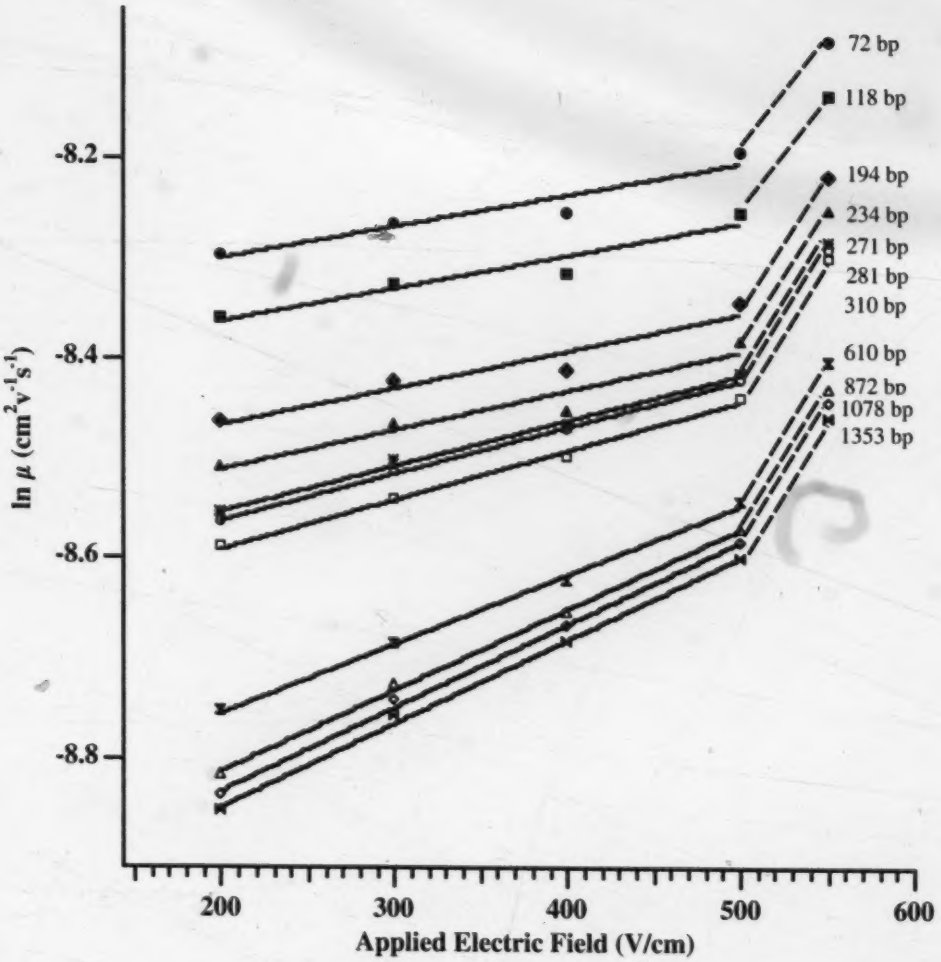

Figure 3.9 Plots of mobility vs applied field strength for the separation of ϕx174/*HaeIII* restriction fragments in 0.8% HEC. Mobility is derived from (ln μ = L2/Vt) in which 'L' denotes effective capillary length; 'V' denotes applied voltage and 't' denotes peak migration time. Line identification: 72bp (closed circles); 118bp (closed squares); 194bp (closed diamonds); 234bp (closed triangles); 271bp (astericks); 281bp (open circles); 310bp (open squares); 610bp (doubled-triangles/vertical); 872bp (open triangles); 1078bp (open diamonds); 1353bp (doubled-triangles/horizontal); r values (from smaller to larger fragments): 0.962, 0.961, 0.964, 0.966, 0.997, 0.999, 0.998, 0.999, 0.999, 0.999, 0.999.

mobility of the DNA becomes more and more dependent on applied field strength, a scenario well demonstrated by 610, 872, 1078 and 1353 bp fragments. The gradual increase in field strength dependency reflects the gradual transition from Ogston to Reptation regime for larger DNA fragments. Linearity degrades at 550 V/cm, in concordance with the degradation of peak resolution. Since deviation from linearity was consistent for all 11 DNA fragments, the cause is unlikely to be joule heating because of the entropy difference between a large and a small DNA molecule. A more likely reason for this deviation is the thermodynamic instability of DNA-dye interactions at elevated field strengths, which causes the dye molecules to dissociate from the complexes.

3.3.4 Calibration plots

As shown in Figure 3.10 (a), a linear relationship is observed between signal and DNA concentration over a relatively short dynamic concentration range (approximately an order of magnitude). The signal was measured for the ϕX174/*HaeIII* digest fragments for a total DNA concentration ranging from 5 to 140 pg/μL. The signal increased linearly with DNA concentration ($r > 0.987$, $n = 6$). Sensitivity is proportional to fragment length ($r = 0.990$), which results from the constant ratio of dye molecules per base pair. The concentration detection limit (3σ) ranged from 4.7×10^{-14} M for the 1353 bp fragment to 5.3×10^{-13} M for the 72 bp fragment. This linear relationship is consistent for all fragment sizes, suggesting that the affinity of dye molecules to DNA was not affected by the transition from Ogston to Reptation as DNA length increased. The linearity also suggests that dye depletion was not experienced by all DNA fragments, in particular for the larger fragments. The short dynamic range of this plot is a typical characteristic of CE-LIF when sensitivity of detection is of primary concern. This

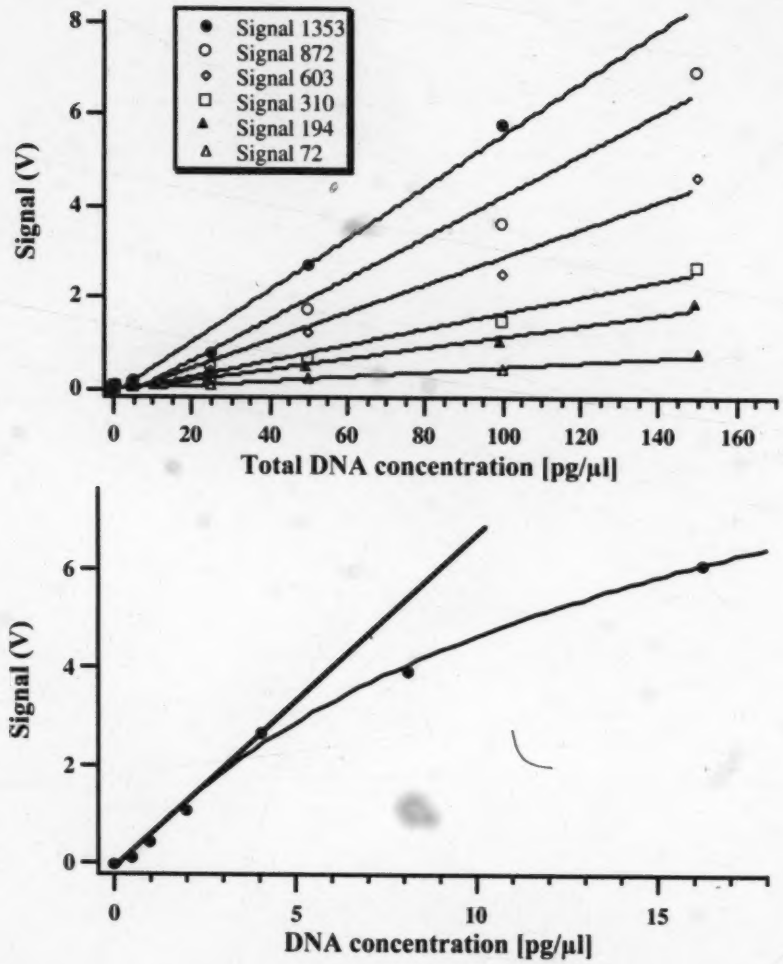

Figure 3.10 (a) Calibration plots of ϕx174/*HaeIII*. DNA samples were prepared in deionized water; 1 x 10^{-7} M POPO3 was prepared fresh and siphoned into the cuvette. Each sample was injected for 5 s at 1000 V. For clarity, only data derived from 1353, 872, 603, 310, 194 and 72 bp are shown; r values (from 1353 to 72 bp) are: 0.996, 0.988, 0.991, 0.991, 0.991 and 0.994. (b) Calibration plot of clone DHBV genome. The 3021 bp viral DNA was excised from its vector, total DNA concentration was measured by UV at 258 nm. Stock DNA was serially diluted to obtain suitable concentration range. 2 x 10^{-7} M EthD2 was prepared as in part (a). Each sample was injected for 20 s at 1000 V.

dynamic range is compatible to that demonstrated by Sepaniak and coworkers [42], but with an improvement of 3 orders of magnitude in concentration sensitivity. A longer dynamic range is desirable when sensitivity of detection is of secondary concern. This was achieved by reducing the bias of the photomultiplier tube. To improve detection limit further, a 3021 bp cloned DHBV genome was used to repeat the same calibration using 2 x 10^{-7} M EthD2 (Molecular Probes), and increasing the injection time to 20 s at 1 kV, Figure 3.10(b). The calibration curve deviated from linearity for DNA concentrations greater than about 5 pg/μL. In this experiment, the peak width increased dramatically for DNA concentration greater than 4.5 pg / μL. The long injection period reduced the efficiency to 3-4 million plates or ~10 million plates per meter. Equations 3.1 to 3.4 were employed to estimate the limit of concentration and mass detection sensitivity for the 3.2 kb fragment.

$$V_{inj} = V_{cap} [V_i / V_r] \times [t_{inj} / t_m] \quad (3.1)$$

$$V_{cap} = \pi \times (R_c)^2 \times L_c \quad (3.2)$$

$$C_{DL} = 3 \times \sigma / S_c \quad (3.3)$$

$$M_{DL} = V_{inj} \times 3 \times \sigma \times C_a / P_h \quad (3.4)$$

V_{inj} is injection volume; V_i: injection voltage; V_r: running voltage; t_{inj} : injection time; t_m: migration time; V_{cap}: capillary volume; R_c: capillary radius; L_c: capillary length; C_{DL}: concentration detection limit; M_{DL}: mass detection limit; σ: standarad deviation of background; S_c: slope of plot; C_a: concentration of analyte; P_h: peak height of analyte. By assuming a 2 nL injection volume from equation 3.1, the concentration detection limit was estimated at 3.9 x 10^{-16} M and the mass detection limit was estimated at approximately a single molecule of a 3.2 kb fragment.

3.3.5 Analysis of DHBV DNA from congenitally infected ducklings

Labeling with intercalating dyes is probably one of the most convenient and rugged ways to carry out direct detection of dsDNA. As reflected in Figure 3.10(a), an important property of DNA-dye complexes is that their fluorescence emission intensity is a linear function of the number of intercalated dye molecules. This allows quantitative detection of products from a restriction digest, a polymerase chain reaction as well as DNA purified from biological samples. Figure 3.11 depicts the separation of cloned duck hepatitis B virus DNA digested with restriction enzyme *Hpa II*. All 8 fragments generated from the digestion were resolved and clearly separated from the molecular weight markers containing 11 DNA fragments using one-step detection by CE-LIF. The plot of ln (mobility) vs 1/ln (basepair) shown in the inset of Figure 3.11 provides a conversion of mobility of the viral fragments to their corresponding sizes. In Table 3.1, a comparison of the calculated size of the viral DNA fragments with that obtained from the literature shows reasonable agreement. This agreement only holds when both the sample and the standard are analyzed as a mixture but not when they are analyzed separately. This is due to the migration time fluctuation commonly observed in capillary polymer electrophoresis where sieving matrix is replaced after each run. Previous studies have shown that single-base resolution is usually not possible using a 0.8% HEC polymer solution. However in this study, a 117 bp viral fragment and a 118 bp size marker were nearly base-line resolved. We have attributed this unusual separation efficiency to possible conformational difference between the two unrelated DNA fragments as a result of differences in preparation and purification of the nucleic acids.

An attempt to detect viral DNA purified from animal sera infected with DHBV was made using a similar on-column labeling approach. As expected, direct labeling

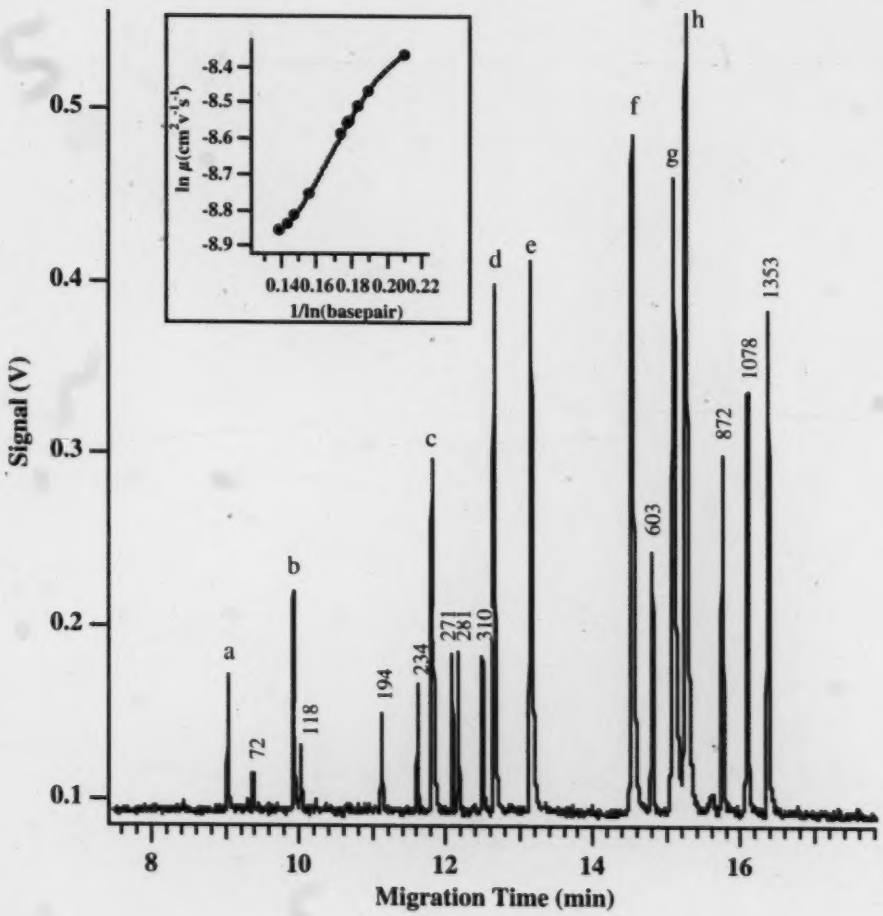

Figure 3.11 Separation of duck hepatitis B virus DNA; (a) to (h) represent 8 fragments generated from a *HpaII* digestion (52, 117, 251, 320, 379, 553, 646 and 703 bp). The sample was spiked with ϕX174/*Hae III* before injection. Final concentration of the molecular weight markers is 60 pg/μl; concentration of the sample was not determined. Injection was at 1000 V for 5 s; electric field at 200 V/cm. The calibration (ln μ vs. 1/ln bp) plot in the inset was prepared by least-squares analysis. Stock solution of EthD2 was diluted to $2x10^{-7}$ M in 45 mM Tris-HCL/1 mM EDTA at pH 7.

Table 3.1 Size determination of restriction fragment with ethidium homodimer2

Peak identity	Actual size*	Calculated size (bp)
a	52	nd
b	117	107
c	251	247
d	320	317
e	379	366
f	553	548
g	646	663
h	703	704

* Duck hepatitis B virus DNA sequence (HPUCGD accession no. K01834) was obtained from National Center for Biotechnology (http://www3.ncbi.nlm.nih.gov/BankIt/); restriction sites for HpaII and fragment sizes were obtained using DNA Strider® 1.2 (C. Marck)

resulted in the generation of a broad peak, suggesting possible non-specific interaction of the intercalating dyes with contaminating nucleic acids and proteins in addition to the viral DNA (Figure 3.12a). Alternatively, as shown in Figure 3.12(b), a PCR step was used to generate a product specific to the DHBV genome. The DNA product was spiked with a series of molecular size markers prior to sample injection. This approach provides cleaner separation and better identification of a PCR product specific to the DHBV genome.

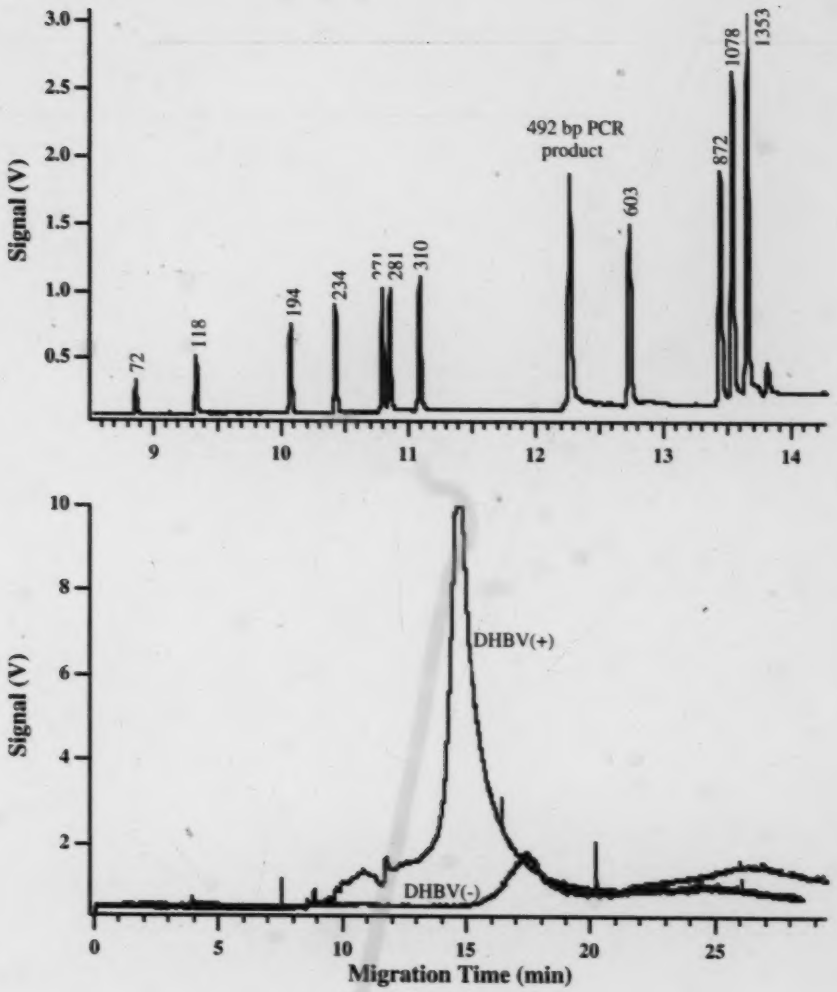

Figure 3.12 (a) Detection of PCR amplified DHBV DNA fragment by CE-LIF. The 492 bp fragment was amplified from an uncut vector containing the DHBV genome. The DHBV specific primer pair are H684 (GGCTCTATGAAGCAGGAATC) and H1175 (GTTGTAGCTTCCACTGAGGA). An aliquot of the PCR product was spiked with size stds ϕx174/*HaeIII* restriction fragments prior to injection. POPO3 was diluted to 2 x 10^{-7} M in 45 mM Tris-HCL and 1 mM EDTA (pH 7). (b) Direct analysis of viral DNA in serum. Viral DNA was prepared using Qiagen blood kit. DHBV(+) represents serum DNA from infected animal; DHBV(-) represents uninfected serum. DNA labeling was carried out on-column with 5 x 10^{-7} M EthD2.

The importance of using an optimum DNA-dye ratio to provide efficient labeling and subsequent separation has been implicated, but many investigations in this area have shown variation from one report to the other. One obvious reason is that successful sizing of DNA fragments requires knowledge of the DNA concentration so that an appropriate amount of dye can be added. This requirement varies, depending on the composition, size and binding constant of a particular intercalating dye. From a practical point of view, determining the optimum DNA-dye ratio becomes unattractive as other parameters that affect the ratio also need to be considered. In our study, measuring the DNA-dye ratio is unlikely because the amount of dye that migrates into the capillary can only be estimated.

3.3.6 On-column labeling with two different intercalating dyes

In a given condition, two intercalating dyes with different binding affinity should have different association constants for DNA, such as the case of mixing a monomeric with a dimeric intercalating dye. As a result of the stoichiometric difference between the two dyes, peak splitting and band broadening are expected if a mixture of two dyes is used to label DNA. In this study, we have employed a POPO3 / EthD2 mixture, and a propidium iodide / EthD2 mixture (both at 1:1 concentration ratio) to carry out DNA analysis as described above. In Figure 3.13(a), separation of the 1 kb DNA fragments using two dyes has a very similar separation efficiency as in using a single species of intercalating dye. However, retention time of all the fragments has increased considerably compared to labeling using POPO3 only (Figure 3.2). The increase in retention time is more pronounced as the fragment length increases. Fragments 506 and 517 are not resolved when a mixture of two dyes is used to label the 1 kb ladder. In

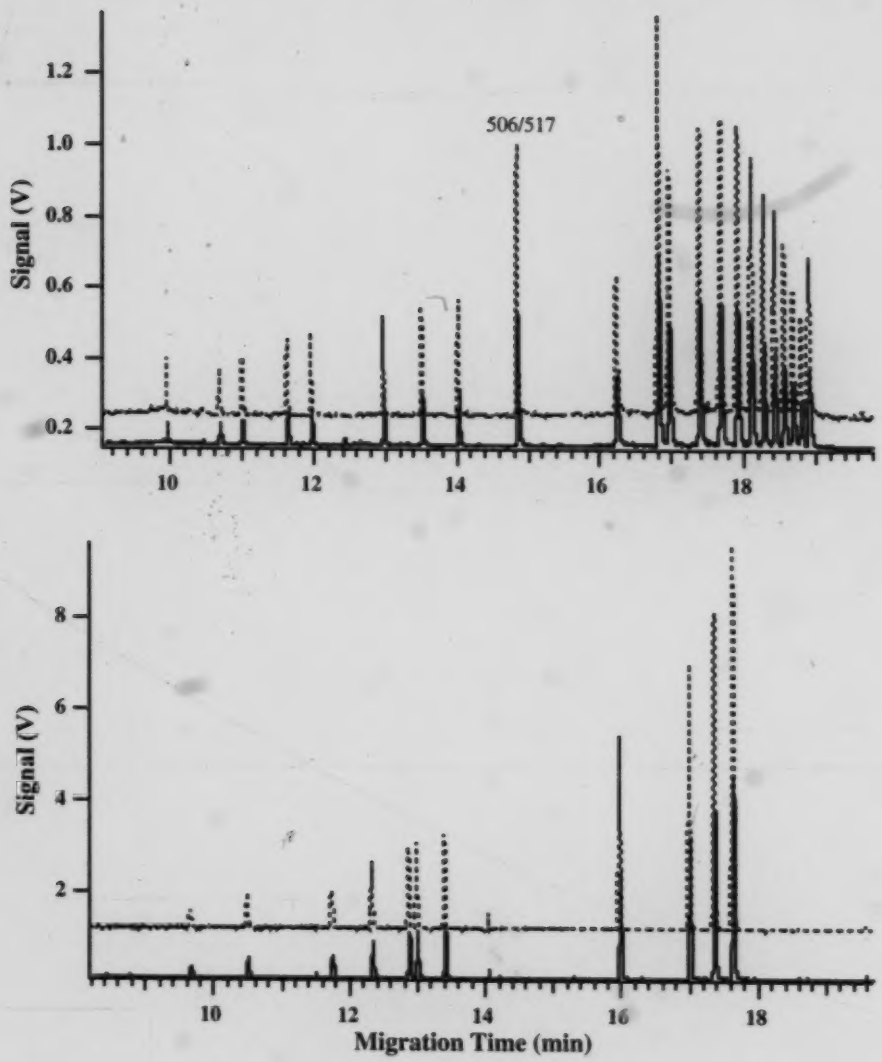

Figure 3.13 (a) Separation of 1 kb DNA ladder in 0.8% HEC. Stock DNA was diluted to 5 pg/μL in milliQ water prior to injection. POPO3 and EthD2 were mixed and diluted to 5 x 10^{-7} M as described in Figure 3.11; (b) Separation of ϕx174/*HaeIII* restriction fragments. Stock DNA was diluted to500 pg//μL in milliQ water. Propidium iodide and EthD2 mixture was prepared in similar concentrations. Data was collected from two channels; solid electropherograms obtained from 630DF30; dotted electropherogram obtained from 580DF40.

Figure 3.13(b), a similar finding was obtained in which no band broadening or splitting was observed even when mixture of a monomeric (propidium iodide) and a dimeric (EthD2) dye was used for DNA labeling. As in Figure 3.13(a), the retention time for all 11 fragments is considerably longer than compared to separation using only one dye (Figure 3.3). These phenomena suggest that when a mixture of two dyes are used, preferential labeling occurs, which results in a higher dye to DNA ratio of DNA-dye complexes and a further mobility retardation of the DNA fragments. Since the concentration of the intercalating dyes used in this part of the study was 5-fold higher relative to that used initially for the calibration curve, an interpretation of whether the use of a two-dye mixture provides better sensitivity than using one dye alone could not be determined. A more thorough study is needed to substantiate the advantage of using a two-dye system. In Figure 3.13(b), a decrease in detection sensitivity is observed when a propidium iodide / EthD2 mixture is used to label ϕX174/*HaeIII* restriction fragments at 500 pg/μL. As shown in Figure 3.10(a), a concentration of 500 pg/μL using POPO3 alone would saturate the detection system.

Capillary columns previously exposed to one dye were found to have some memory effect when a different dye was introduced. This memory effect severely affects DNA separation such that DNA fragments of a particular size are eluted in two closely migrating peaks. Figure 3.14(a) and (b) show two consecutive runs of a series of size markers of ϕX174/*HaeIII*. The larger DNA fragments were clearly duplicated while the smaller ones were not baseline resolved. In this case, the column was previously exposed to EthD2 at 5×10^{-7} M and was then used for labeling in the presence of POPO3 at the

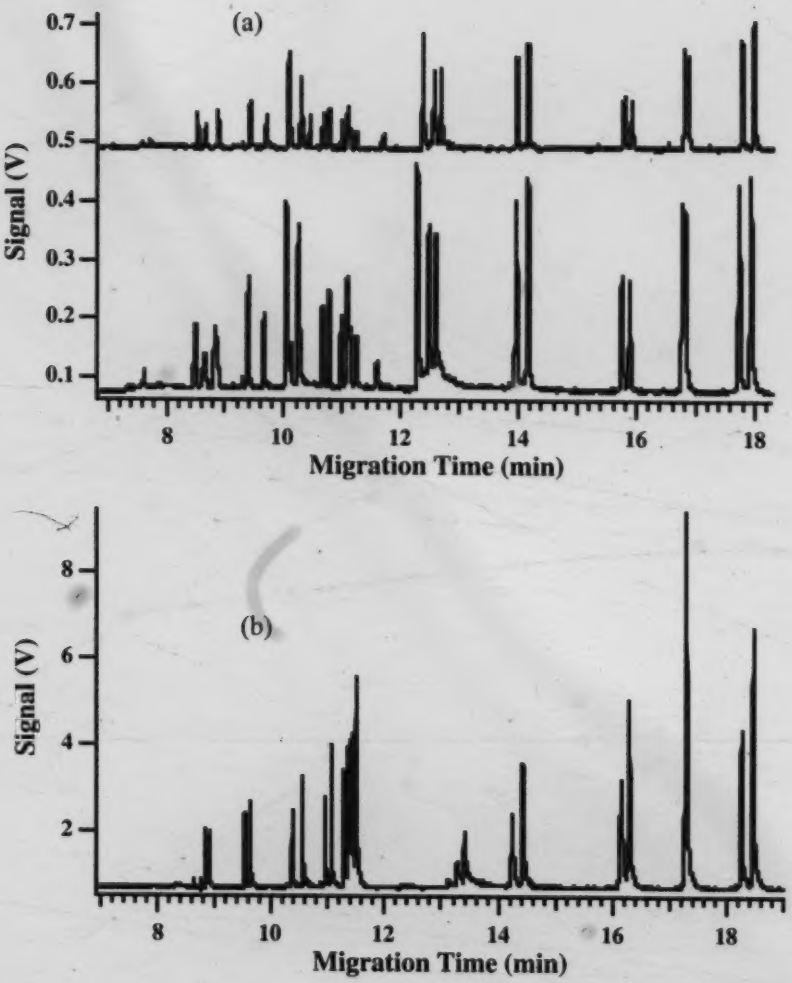

Figure 3.14 (a) The column was previously exposed to EthD2 at 5 x 10^{-7} M and then used for a 5 x 10^{-7} M POPO3 intercalation. Both electropherograms were obtained from two different ϕx174/*HaeIII* samples. (b) The sequence of exposure in this case was reversed, with initial exposure to POPO3, followed by exposure to EthD2 at the same concentration.

same concentration. The duplication manifested in a slightly different separation profile when column exposure to EthD2 and POPO3 was reversed in sequence (Figure 3.14b). The memory effect strongly suggests that the dye molecules bind tightly to the capillary

inner surface. Repeated flushing of the column with a 20mM NaOH solution and methanol is necessary in order to remove the bound dyes before a different intercalating dye is introduced for subsequent runs.

3.4 Conclusions

As more highly sensitive fluorescence detection apparatus evolves, the ability to use fluorescent dyes to replace radioisotopes for ultrasensitive detection of DNA will become important. This replacement will enhance the use of capillary electrophoresis, which has the ability to provide high speed and high throughput analysis. DNA-dye complexes represent a novel class of fluorescent labels with a wide range of spectroscopic properties that can be tailored to various applications. In the case of DNA analysis, we have demonstrated the sensitivity and versatility of this technique to detect minute amounts of restriction DNA fragments. The ability to combine the detection of DNA-dye complexes with high field strength CE separation will meet the detection criteria in clinical science. These include high sensitivity, high speed, and the potential to process many samples on a routine basis with the use of a minimum number of reagents and analytical steps. This in turn, provides minimal sample carry over and cross-contamination. The result is an analytical technique that is clinically reliable and comparable or better than some conventional methods.

3.5 Bibliography

1. K.C. Chan, C.W. Whang and E.S. Yeung, J. (1993) Liquid Chromatogr. **16**, 1941.

2. D.A. McGregor and E.S. Yeung. (1993) J. Chromatogr. A. **652**, 67.

3. M.H. Kleemi§, M. Gilges and G. Schomburg. (1993) Electrophoresis **14**, 515.

4. P.E. Williams, M.A. Marino, S.A. Del Rio, L.A. Turni and J.M. Devaney. (1994) J. Chromatogr. A. **680**, 525.

5. D.A. McGregor and E.S. Yeung. (1994) J. Chromatogr. A. **680**, 491.

6. W. Lu, D.S. Han, J. Yuan and J.M. Andrieu. (1994) Nature **368**, 269.

7. Y. Baba, N. Ishimaru, K. Samata and M. Tsuhako. (1993) J. Chromatogr. A. **653**, 329.

8. A.W.H.M. Kuypers, P.M.W. Willems, M.J. van der Schans, P.C.M. Linssen, H.M.C. Wessels, C.H.M.M. de Bruijn, F.M. Everaerts and E.J.B.M. Mensink. (1993) J. Chromatogr. **621**, 149.

9. K.R. Mitchelson and J. Cheng. (1995) J. Cap. Elec. **002:3**, 137.

10. J. Cadet and M. Weinfeld. (1993) Anal. Chem. **65**, 675A.

11. J.M. Butler, B.R. McCord, J.M. Jung, J.A. Lee, B.Budowle and R.O. Allen. (1995) Electrophoresis **16**, 974.

12. B.R. McCord, D.L. McClure and J.M. Jung. (1993) J. Chromatogr. A. **652**, 75.

13. W.M. Hurni and W.J. Miller. (1991) J. Chromatogr. **559**, 337.

14. D.M. Northrop, B.R. McCord and J.M. Butler. (1994) J. Cap. Elec. **001:2**, 137.

15. R.R. Chadwick, J.C. Hsieh, K.S. Resham, R. Brett Nelson. (1994) J. Chromatogr. A. **671**, 403.

16. J.P. Landers, R.P. Oda, T.C. Spelsberg, J.A. Nolan and K.J. Ulfelder. (1993) Bio Techniques **14**, 98.

17. H.E. Schwartz and K.J. Ulfelder. (1992) Anal. Chem. **64**, 1737.

18. D. Figeys, E. Arriaga, E. Renborg and N.J. Dovichi. (1994) J. Chromatogr. A. **669**, 205.

19. B.R. McCord, J.M. Jung, E.A. Holleran and D.M. McClure, Proc. 2nd Int. Symp. (in press).

20. K. Srinivasan, J.E. Girard, P. Williams, R.K. Roby, V.W. Weedn, S.C. Morris, M.C. Kline and D.J. Reeder. (1993) J. Chromatogr. A. **652**, 83.

21. H. Zhu, S.M. Clark, S.C. Benson, H.S. Rye, A.N. Glazer and R.A. Mathies. (1994) Anal. Chem. **66**, 1941.

22. R.P. Haugland. (1992) Molecular Probes. Inc., Eugene, OR, 221.

23. A.N. Glazer and H.S. Rye. (1992) Nature **359**, 859.

24. J. Berka, Y.F. Pariat, O. Muller, K. Hebenbrock, D.N. Heiger, F. Foret and L.B. Karger. (1995) Electrophoresis **16**, 377.

25. A.N. Glazer, K. Peck and R.A. Mathies. (1990) Proc. Natl. Acad. Sci. USA **87**, 3851.

26. B.R. McCord, J.M. Jung and E.A. Holleran. (1993) J. Liquid Chromatogr. **16**, 1963.

27. Y. Kim and M.D. Morris. (1994) Anal. Chem. **66**, 1168.

28. H.S. Rye, S. Yue, M.A. Quesada, R.P. Haugland, R.A. Mathies and A.N. Glazer (1993) Methods in Enzymology **217**, 414.

29. D.M. Crothers. (1968) Biopolymers **6**, 575.

30. R.G.M. Wright, L.P.G. Wakelin, A. Fieldes, R.M. Acheson and M.J. Waring. (1980) Biochemistry **19**. 5825.

31. N. Assa-Munt, W.A. Denny, W. Leupin and D.R. Kearns. (1985) Biochemistry **24**, 1441.

32. N. Assa-Munt, W. Leupin, W.A. Denny and D.R. Kearns. (1985) Biochemistry **24**, 1449.

33. D. Delaprat, A. Delbarre, I. Le Guen, B.P. Roques and J.B. Le Pecq. (1980) J. Med. Chem. **23**, 1336.

34. B. Gaugain, J. Barbet, R. Oberlin, B.P. Roques and J.B Le Pecq. (1978) Biochemistry **17**, 5071.

35. B. Gaugain, J. Barbet, N. Capelle, B.P. Roques , J.B Le Pecq and M. Le Bret. (1978) Biochemistry **17**, 5078.

36. J. Markovits, B.P. Roques and J.B. Le Pecq. (1979) Anal. Chem. **94**, 259.

37. J. Skeidsvoll and P.M. Ueland. (1995) Anal. Biochem. **231**, 359.

38. L.P.G. Wakelin. (1986) Med. Res. Revs. **6**, 275.

39. L.H. Hurley. (1989) J. Med. Chem. **32**, 2027.

40. C. Carlsson, M. Jonsson and B. Akerman. (1995) Nucleic Acids Res. **23**, 2413.

41. K. Srinivasan, S.C. Morris, J.E. Girard, M.C. Kline and D.J. Reeder. (1993) Appl. Theor. Electrophoresis **3**, 235.

42. B.K. Clark and M.J. SepaniaK. (1993) J. Microcol. Sep. **5**, 275.

43. G.L Eichhorn. (1978) in Inorganic Biochemistry. (Vol. **2**, Mir, Moscow, Chap 34)

44. V.G. Bregadze (1996) in Metal Ions in Biological Systems. (Vol. 32, Marcel Dekker, New York, Chap 12).

45. D.H. Baker. (1995) in Capillary Electrophoresis. (John Wiley & Sons, Inc.).

46. Y.F. Cheng and N.J. Dovichi (1988) Science **242**, 562.

47. D.Y. Chen, H.R. Harke and N.J. Dovichi. (1992) Nucleic Acids Res. **20**, 4873.

48. S. Wu and N.J. Dovichi. (1989) J. Chromatogr. **480**, 141.

49. X. de Lamballerie, C. Zandotti, C. Vignoli, C. Bollet and P. de Micco. (1992) Res. Microbiol. 143, 785.

50. H.E. Schwartz and K.J. Ulfelder. (1992) Anal. Chem. **64**, 1737.

51. H.S. Rye, S. Yue, D.E. Wemmer, M.A. Quesada, R.P. Haugland, R.A. Mathies and A.N. Glazer. (1992) Nucleic Acids Res. **20**, 2803.

52. H.R. Reese. (1994) Biopolymers **34**, 1349.

53. W.Y. Chou, L.A. Marky, D. Zaunvzkowski and K.J. Breslauer. (1981) J. Biomol. Struct. Dynam. **5**, 345.

54. R.B.Jr. Macgregor, R.M. Clegg and T.M. Jovin. (1985) Biochemistry **24**, 5503.

55. M.T.Jr. Record, C.F. Anderson and T.M. Lohman. (1978) Quart. Rev. Biophys. 11, 103.

56. W.D. Wilson. (1990) Intercalation Chemistry. In M.S. Whittingham and A.J. Jacobsen (ed); IRL Press, Oxford, Chap. 8.

57. V.A. Bloomfield, D.M. Crothers and I.J. Tinoco. (1974) Physical Chemistry of Nucleic Acids; Harpet & Row, New York, Chap. 7.

58. D.F. Bradley and M.K. Wolf. (1966) Proc. Natl. Acad. Sci. USA **45**, 944.

59. J.M. Andrieu. (1991) in Viral Quantitation in HIV Infection. (John Libbey Eurotext, Paris).

Chapter 4. Profiling HBV Infection in Ducks Exposed to Antiviral Compounds

4.1 Introduction

4.1.1 Duck hepatitis B virus as a model for studying viral clearance

Since only humans and primates are susceptible to infection with hepatitis B virus (HBV), studies on treatment of persistent infection with HBV have been limited. The inability of HBV to infect cultured cells has also made study of virus neutralization difficult. HBV is a member of the hepadnavirus family, a category of DNA viruses that also includes related hepatitis B viruses found in woodchucks, ground squirrels and Pekin ducks. Duck hepatitis B virus (DHBV), which infects Pekin ducks naturally and other birds experimentally, provides a useful *in vivo* system to study a hepadnavirus since ducks are easy to breed and maintain and persistent infection can be readily established. Most importantly, since DHBV is similar to HBV in terms of morphology, genomic structure and replication mechanism [1-6], it has been used quite extensively as a model for HBV infection [7-9]. The feasibility of using DHBV-carrier Pekin ducks to evaluate the therapeutic potential of antiviral drugs has been described [10-11]. In the DHBV model titers of greater than 10^7 infectious units per ml of DHBV are readily obtainable. In addition, the kinetics of inhibition can easily be studied using the DHBV model, making it a convenient system to study the response of a hepadnavirus to anti-viral treatment [12].

4.1.2 Detection of hepatitis B viral DNA in serum and liver

Detection of HBV-DNA in serum and liver of HBsAg positive carriers has shown that many carriers do not have active HBV replication. The presence of HBeAg in the serum is often associated with viral replication while the presence of HBeAb is often associated with an inactive phase of infection. Free forms of viral nucleic acid have been

found in the serum and liver of the majority of HBeAg-positive individuals but also in a significant proportion of HBsAg carriers with circulating HBeAb. For patients with acute HBV infection, HBV DNA is usually present during the acute phase of infection and it is cleared before or simultaneously with seroconversion from HbeAg to HBeAb [13-15]. In some cases, the natural history of chronic HBV infection is one of slow transition from the phase of active HBV multiplication to the phase of inactive viral infection [16-18]. During chronic HBV infection, a discrepancy between the presence of serum HBV DNA and that of HBeAg is possible. This occurs with pre-core mutants in which patients can have high levels of HBV DNA and HbeAb. The viral DNA in serum is a direct measure of virion particles while detection of HBeAg is highly dependent on the relative excess of the antigen over the homologous antibody at the time of testing and does not predict viral replication as well as HBV DNA levels.

Serum levels of HBV DNA vary considerably, from 1 to 2000 pg/ml, the lowest values most often found in sera of patients with HBeAb [18, 19-21]. Most conventional tests for HBV DNA rely on nucleic acid hybridization methods using cDNA clones of HBV DNA [22]. These techniques are based on spot/dot hybridization or on solution hybridization. Solution hybridization techniques that use either radioisotopic [^{125}I] or non-radioisotopic detection systems for HBV DNA are available commercially. Two common examples are Genostics™ (Abbott Laboratories, Chicago, IL) and Digene Hybrid-Capture™ (Murex Diagnostics Ltd, Dartford, UK). These tests are standardized and easy to use, but they detect amounts of HBV DNA higher than 4×10^4 genomes (1.5pg) and thus lack sensitivity. More sensitive assays have been developed in recent years. Quantification of HBV DNA in human serum using a the Chiron Quantiplex

branched DNA (bDNA) signal amplification assay (Chiron Corp., Emeryville, CA) with a detection sensitivity of 7×10^5 equivalents per ml has been reported [22,23]. Second-generation bDNA assays have a lower limit of sensitivity of 3.5×10^5 equivalents per ml [24]. In contrast to PCR, bDNA "signal amplification" boosts the strength of the signal rather than expanding the target. The assay is rapid, easy to perform, reproducible, and does not require radioactive material. However, it is limited by its inability to detect low levels of viremia relative to the sensitivity attained by a standard PCR (~100 molecules/ml) assay.

4.1.3 Polymerase Chain Reaction with CE-LIF detection

The polymerase chain reaction (PCR) is in theory capable of detecting low numbers of HBV DNA copies in clinical samples [25]. Indeed, detection of HBV DNA sequences in serum for diagnostic purposes is currently performed by PCR in many laboratories [26-31]. There are, however, drawbacks to the high sensitivity of the PCR method. First, PCR assays detect extremely low levels of HBV DNA molecules, the clinical relevance of which is still unclear [32]. Second, PCR results are usually qualitative and therefore not suitable for monitoring antiviral treatment. Third, current procedures for analyzing PCR products are time consuming and labor intensive [33]. These disadvantages make screening and monitoring large numbers of samples to determine the efficacy of antiviral therapy difficult and costly.

In this report, using DHBV as a model, we evaluated the use of PCR with CE-LIF detection to monitor viral DNA synthesis in response to antiviral treatment. The purpose was to develop a methodology that could be used to evaluate the effect of certain antiviral compounds on viral DNA synthesis. We believe it will be advantageous if a technique

used to monitor the level of viral DNA in response to therapy is very sensitive. In addition, this technique may be valuable in leading to an understanding of the mechanism of an antiviral compound in inhibiting viral DNA synthesis.

4.2 Experimental

4.2.1 Preparation of plasmid DNA

Plasmid pAltD2-8 was a generous gift from K. Fischer. It contains a monomer of 3,021 bp genome of the duck hepatitis B virus (DHBV) cloned into the *Eco*RI site of vector pAlter-1 (Promega). The pAltD2-8 was propagated in *Eschericheria coli* strain DH 5α grown in suspension broth culture. pAltD2-8 DNA was recovered using a Qiagen Plasmid Purification Kit (Qiagen Inc., Chatworth, CA). The isolated plasmid was digested with restriction endonuclease *Eco*RI and electrophoresed on a 0.8% agarose gel to purify the 3,021 bp DHBV fragments from the vector. The concentration of the purified DHBV DNA was determined by optical absorbance at 260 nm. Purity of plasmid was assessed by the 260/280 nm ratio. The purified plasmid was aliquoted and stored at -20°C in 10 mM Tris-EDTA buffer at pH 8.

4.2.2 Treatment of ducks with antiviral compounds

For the study of (-)-β-L-2',3'-dideoxy-3'-thiacytidine (3TC), 10 day-old congenitally infected ducklings were subjected to 3TC treatment with a dosage of 40mg / kg body weight. The compound was obtained as a powder from Glaxo Inc. (USA). The animals were treated intramuscularly 4 times daily for 72 hours. In separate studies, ducklings between 10 to 14 days old were divided into 2 groups of 3 and treated intramuscularly twice daily with 3TC or 2-amino-6-methoxy purine 2' 3' dideoxyriboside

(2A6M) at 20 mg / kg for 2 weeks. Sera samples were collected prior to and after the termination of treatment. The 2A6M powder was synthesized by Dr. J. Wilson (Dept. Medical Microbiology and Immunology). All animal handling protocols were reviewed and approved by the Animal Ethics Committees at the University of Alberta.

4.2.3 Extraction of DHBV DNA from serum

Serum samples were obtained from each duck at 0, 6, 18, 30, 42, 54, 66 and 78 hours after treatment was initiated. A 200 µl sample of serum collected at each time point and serum DHBV-DNA was concentrated in 100 µl of elution buffer using a commercial QIAamp Blood Kit (Qiagen Inc., Chatworth, CA). The serum samples were treated with a 200 µl extraction cocktail containing QIAamp protease at 70 °C for 20 min. The incubated mixture was added with 210 µl of 99% ethanol before loading onto a chromatography column. After two washes with 500 µl of wash buffer, extracellular DHBV DNA was eluted from the column by centrifugation in 100 µl elution buffer pre-heated to 70 °C.

4.2.4 Purification of core particles from liver

The protocol for purifying core particles was obtained from Summers & Mason [4] with some modification. Briefly, immediately after ducklings were sacrificed, the liver tissues (4g per duckling) were excised and homogenized in an extraction buffer containing 50 mM sodium chloride, 20 mM Tris-HCL (pH 7.5), 7 mM $MgSO_4$ 250 mM sucrose, 0.5% NP-40 and 0.1% of 2-mercaptoethanol. The homogenate was transferred into 30 ml corex glass tubes and centrifuged (Beckman model J-21C; JA-20 rotor) at 10,000 g for 20 min., at 4 °C. After the centrifugation step, the fat residue and liver tissue were removed to obtain a cloudy liver homogenate. The semi-purified homogenate

was transferred to an ultra-clear centrifuge tube (25x89mm) containing a discontinuous sucrose gradient of 15, 22.5 and 30%. The sucrose was prepared in the same buffer used to homogenize the liver tissue. The samples were centrifuged for 7 hours at 23,000 g and 4 °C in an SW27 rotor in a Beckman LB80 ultracentrifuge. After the centrifugation, a syringe with a blunt end needle was used to withdraw the band within the 22.5% sucrose fraction containing DHBV core particles. The core particles were centrifuged for 15 hours at 23,000 g and 4 °C. After centrifugation, the supernatant was removed and the pellet of purified DHBV core particles was resuspended in an elution buffer containing 10 mM Tris-EDTA buffer at pH 8. The suspensions were incubated overnight at 4 °C. To remove contaminating nucleic acids, DNAase I was added to the suspension at 1µg/ml and incubated at 37 °C for an hour. RNAase A at a final concentration 0.1 µg/ml and 20 mM EDTA, were added and the mixture reincubated for 30 min at 37 °C. After the RNAase digestion, the mixture was centrifuged at 2500 rpm for 10 min at 4 °C using a refrigerated centrifuge (Sorvall RT6000B). Following centrifugation, the supernatant was transferred to a clean tube for subsequent DNA extraction. The purified core particle preparation was added to 10 volumes of a DNA extraction buffer containing 1% sarkosyl, 10 mM Tris, 10 mM EDTA and proteinase K at 800 µg /ml. The digestion was carried out in a 42 °C water bath for at least 12 hours. The digest was extracted 3 times with phenol/ chloroform (1:1 volume), and the DHBV DNA was precipitated with 100 mM NaCl followed by 2 volumes of 96% ethanol. The mixture was incubated at -20 °C for at least 30 min (longer incubation times are advisible). The precipitated DHBV DNA sample was centrifuged (SW60 rotor) at 30,000 g force for 30 minutes at 4 °C. The DNA

pellet obtained was dried in a 37 °C incubator for 10 - 15 min and resuspended in 50 µl of Milli Q water.

4.2.5 Design of DHBV primers and probes

A DHBV DNA sequence (HPUCGD accession no. K01834) was obtained from National Center for Biotechnology at http://www3.ncbi.nlm.nih.gov/BankIt/ and processed using DNA Strider® 1.2 (C. Marck). To facilitate proper design of primers and probes specific to the DHBV sequence, we employed a Lightspeed Pascal software Amplify 1.2 (W. Engels, Genetics Department, University of Wisconsin) to construct a set of 17 oligoprimers that are distributed evenly along the entire 3,021 bp DHBV template. The primer sequences and their corresponding locations on the DHBV genome are listed in Table 4.1. The primers were synthesized locally by the DNA lab in the Department of Biochemistry (University of Alberta). Fluorescently labeled primers were synthesized by the Core DNA Services at the University of Calgary. Figure 4.1 depicts a schematic representation of the DHBV genome and the orientation of the primers upon annealing to the DHBV template.

4.2.6 PCR assays

To avoid complication in PCR multiplexing and potential primer-dimer formation, we conducted PCR amplification using 16 primers in 16 separate tubes. To each reaction cocktail containing 100 µl of a pre-mixed PCR buffer (Gibco), we added 28 pmol of the Tamra-labeled H2481 primer, 36 pmol of one of the 16 cold primers (listed in Table 4.1), 200 µmol of each of the four deoxyribonucleoside triphosphates (dNTPs), 1.5 mM $MgCl_2$, 3 U of Taq DNA Polymerase and DNA templates to be amplified. The mixture was amplified for 25 cycles (unless otherwise indicated) using the following

Table 4.1 Construction of oligoprimers specific to DHBV genome

Name	Primer sequence	Amplicon length (nt)	GC (%)♣	Location of genome (nt)
H2481	GTGTATGGAAAAGCCGTCCA	_____	____	2462_2481*
H56	GGAGATTGCTTTGGTGGCAT	2428	43.7	56_75
H246	AAAACCTCGTGGACTCGAAC	2238	50.0	246_265
H375	TTCGAGCAGCCACCATAGAT	2109	43.0	375_394
H532	AGTTAATGAGTGCCCTTCCC	1952	43.4	532_551
H687	GGCTCTATGAAGCAGGAATC	1797	43.7	687_706
H824	AATGGACGTCAGACGGATAG	1660	44.1	824_843
H1006	CGGGAAGGAGAGTAGGATTA	1478	43.5	1006_1025
H1156	CTCCTCAGTGGAAGCTACAA	1328	42.4	1156_1175
H1312	CTGGCCTAATCGGATTACTG	1172	41.1	1312_1331
H1498	TCTTTGGACCTATCTCAGGC	985	40.4	1499_1518
H1656	TCGGATCCGAAATCTCTCGT	828	38.7	1656_1675
H1816	GCCTTCTCCGGTGAATGAAA	668	37.6	1816_1835
H1927	AGTAGGAGAATGGTATGACTG	557	38.8	1927_1947
H2062	CTTCTCTTCATCCTATAGGAC	422	41.5	2062_2082
H2185	CGCAATATCCCATATCACCG	299	41.7	2185_2204
H2328	GCCATAAGCGTTATCAGACG	156	44.8	2328_2347

Note: ♣ represents GC content of the amplicon; * denotes a fluorescently labeled reverse primer that primes the incomplete (+) strand of the viral genome. The remainder of the 16 cold primers are specific to the complete (-) strand of the viral genome. All primers have 100% primability and 75% stability of match.

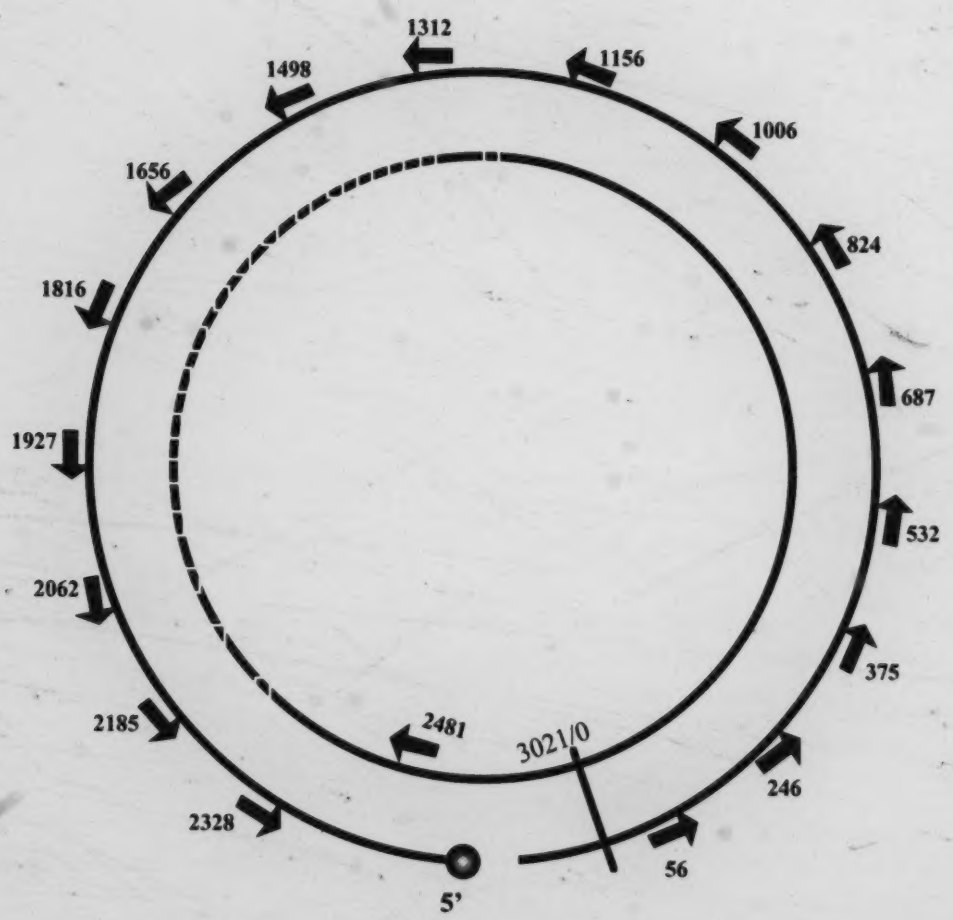

Figure 4.1 PCR priming of partially double-stranded duck hepatitis B virus genome. 16 primers were designed to prime the primer protein-bound virus DNA template (minus strand); a reverse primer was designed to prime the incomplete template (plus strand).

cycling parameters: Initial denaturation at 95°C for 5 min, 20 cycles at 95°C for 60s, 55°C for 60s and 72°C for 120s. The last extension step was at 72°C for 5 min. This last extension step is to ensure complete extension of the longer PCR fragments. A PTC-100

thermal cycler, version 1.2 (MJ Research, Inc., Watertown, Ma) was used in these experiments.

4.2.7 CE-LIF analysis

The electrophoresis apparatus was built in-house and is described in Chapter 3. In this case, 0.1 M TAPS (pH 8) was used as the sheath buffer. The capillary used was a 30 cm, 50 μm I.D., 144 μm O.D. DB-210 coated capillary with 0.2 μm coating (J&W Scientific, Folsom, CA, USA). The 5' end labeled PCR fragments were excited by a 543.5 nm green He-Ne laser system (Melles Griot). The excitation source was directed through the sheath flow cuvette at approximately 0.5 mm below the tip of the capillary. Fluorescence was collected at right angles to the excitation beam by a 60x (N.A. 0.7) microscope objective and directed to a photomultiplier tube at 1100V through a 580DF40 band pass filter. The HEC sieving medium was prepared similarly as described in chapter 3 except that in this case, the 0.8% HEC matrix was added with 7% urea to facilitate separation of DNA fragments under denaturing condition. The low viscosity polymer solution was introduced into the capillary using a 10-ml syringe connected to a low-pressure syringe. Prior to CE analysis, all the PCR samples were purified and desalted using a QIAquick PCR Purification Kit (Qiagen). CE injection modes and parameters were the same as previously described.

4.3 Results and Discussions

4.3.1 Fluorescence detection of primer extended oligonucleotides

The sensitivity of laser induced fluorescence detection permits minimal sample requirements for PCR product analysis. As a comparison, between 5 to 10 μl of a PCR

sample is usually necessary in the case of slab-gel analysis for qualitative as well as quantitative measurement which current CE technology furnishes the same information with consumption of between 1 to 2 nl of the same sample. The low sampling volume requirement greatly facilitates subsequent development of nano-scale technology. Figure 4.2 depicts the separation of the 16 PCR amplified products. In addtion to the advantage of real time monitoring of DNA separation, the resolving power of CE is clearly demonstrated in this case. PCR fragments between 156 bp and 2428 bp were all baselined resolved using a very diluted polymer concentration (0.8% w/v). As expected, the addition of 7% urea to the sieving medium increased the overall viscosity of the polymer solution, which resulted in longer separation times. In addition, separation of DNA fragments under denaturing condition reduced the negative charge per unit length by half. The reduction in negative charge reduces the overall mobility of the DNA fragments towards the detection end of the capillary. Figure 4.3 represents a schematic diagram of the 16 PCR fragments ranging from 156 bp to 2428 bp. The variable primer H56 binds furthest away from the 5' end of the minus DNA strand. The thickness of each bar indicates efficiency of amplification, and the results suggest an inverse relationship between the extent of amplification and amplicon length. Exploiting the ability of this method to probe the entire length of the DHBV genome is considered a unique approach. In addition to monitoring the presence of virus DNA, this is also an alternative way to provide information in studies where the mechanism of a particular antiviral compound is to be investigated. In the case of chain termination by incorporation of terminators on the growing viral DNA strand, a progressive shortening of viral DNA as a function of duration and dosage of treatment is expected.

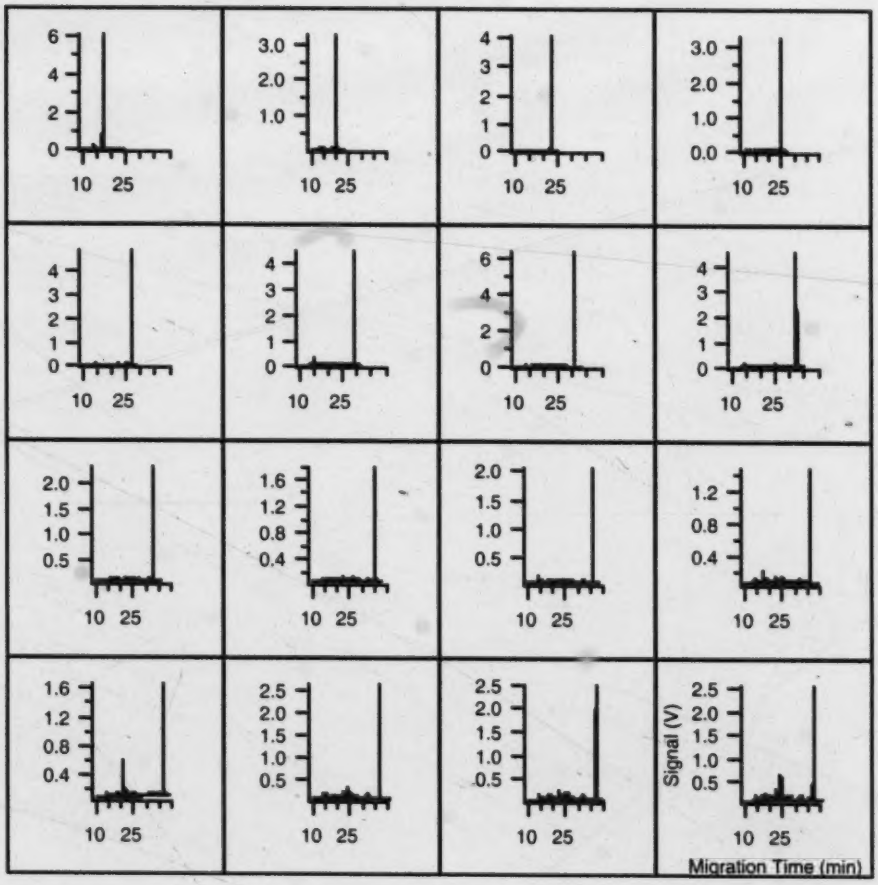

Figure 4.2 Separation of PCR amplified products using CE with LIF detection. Separation parameters: 0.8% HEC/7M urea; capillary length: 29 cm; field strength: 200 V/cm. Each of the 16 PCR products was injected separately. Data points acquired from each DNA fragment were processed and presented in a separate panel as shown above.

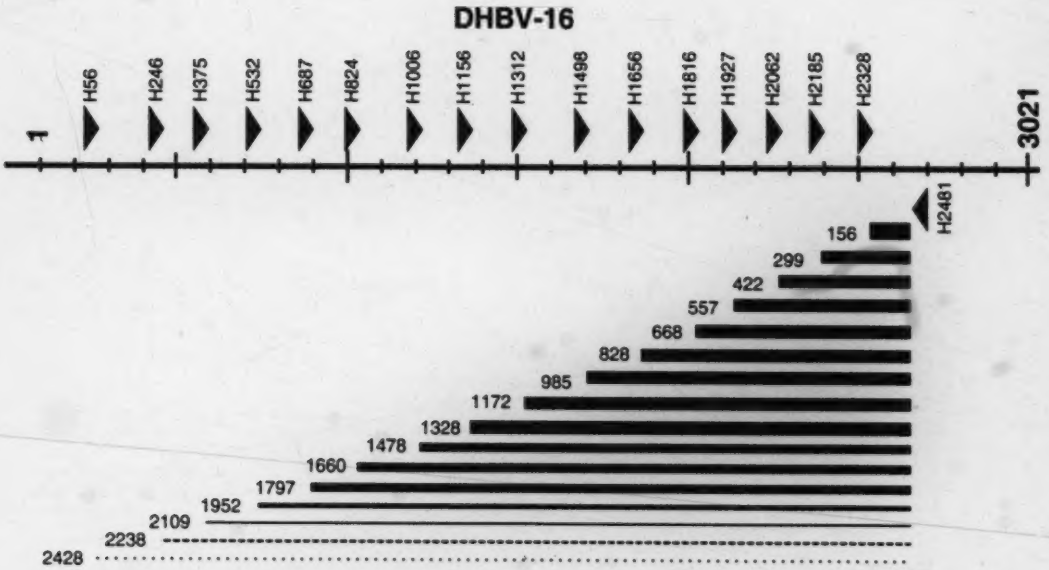

Figure 4.3 Simulated presentation of 16 PCR products amplified by 16 forward primers and a dye-labeled reverse primer. Thickness of each bar represents amplification efficiency of each fragment. Number listed on left hand side of each bar represent size of amplifiedproducts. Simulation was conducted by Amplify 1.2 as described in Experimental.

4.3.2 Profiling of DHBV DNA in liver and serum

As described in Chapter 1, during the initial phase of infection the viral DNA genome is transported into the nucleus, and incomplete strands are completed and ligated to yield the ccc-DNA. Transcription of the ccc-DNA produces pregenomic RNA that is transported to the cytoplasm and packaged in cores with the polymerase. Genome replication occurs within the cores. Only mature cores are packaged and exported from the infected cell. Hence in theory, both complete DHBV genomes and replication intermediates such as incomplete minus strands will be detectable in the liver. Only

extracellular viruses carrying complete DHBV genomes will be detected in the serum. Based on these differences, we predicted that amplification of the DHBV genome in the serum should yield positive signals for all the 16 primer sets as long as DHBV genome is detectable in the serum. Due to the absence of replication intermediates in the serum, amplification using the 16 primer sets would be an "all or none" scenario in animals undergoing antiviral therapy. We predicted that the presence of replication intermediates in the liver of the same animals would yield a larger proportion of PCR products generated from primers located closer to the initiation site of the minus DNA strand. Primers that bind further down stream may not be extendable, depending on the completeness of the inhibition of viral DNA synthesis.

Figure 4.4(a and b) illustrates the results obtained when a series of serum samples were amplified prior to and at the end of treatment with 3TC. The DNA was analyzed using conventional slab gel electrophoresis. As expected, the 3-day high dosage treatment by intramuscular injection of 3TC significantly reduced the level of serum DNA. However, the PCR products demonstrated "all or none" amplification, suggesting that genome templates in the sera contained some full-length genome. Since DHBV DNA was not completely cleared from the serum, full-length genomes were expected to be still present in the liver at the end of the treatment. This was clearly demonstrated when liver tissue of an animal was investigated. The animal was sacrificed 6 hours after the last administration of 3TC and core particles were prepared from the liver for PCR amplification. The results (Figure 4.4e) showed that all 16 PCR products were being amplified, and suggest that the majority of the viral templates present in the liver were still intact. A longer duration of treatment may be necessary to demonstrate truncation of

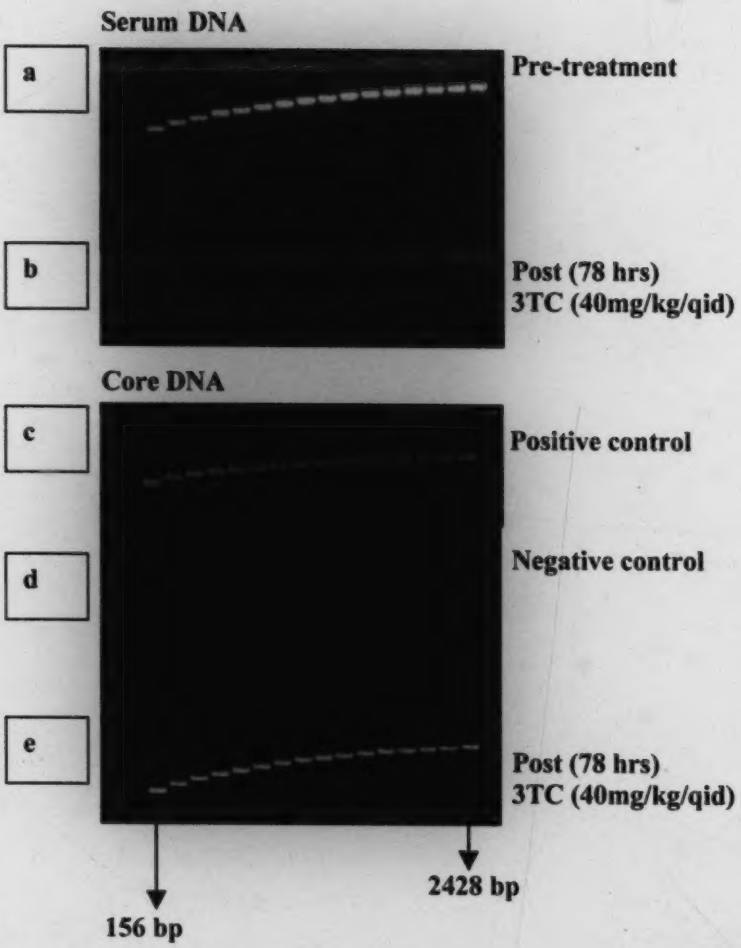

Figure 4.4 Clearance of DHBV DNA in serum and liver samples of an infected animal treated with 3TC. Panel (a) represents serum of an animal prior to treatment, panel (b) represents serum of the same animal after 78 hours treatment. The last serum sample was collected 6 hours after the last administration of 3TC by intramuscular injection. PCR products of 15 µl each was loaded on to and resolved by a 2 % agarose gel. The gel was stained with ethidium bromide for detection. Each band on the gel represents PCR product of each of the 16 PCR amplifications. Panels (c) to (e) demonstrate chain termination of intracellular virus genome in replicating cores of the same animal. Panel (c) represents a positive control (infected, untreated cores); panel (d) represents a negative control (non infected cores) and panel (e) represents cores purified from the animal after 78 hours treatment with 3TC.

the viral genome in the liver of 3TC treated animals. Furthermore, to show the decreased synthesis of longer DNA relative to the shorter DNA PCR products, it would be necessary to conduct quantitative PCR for each DNA fragment.

4.3.3 Mechanism of inhibition of viral DNA synthesis

The nucleoside 3TC is a deoxycytidine analog in which the 3' carbon is replaced by a sulfur atom with loss of 3' OH group necessary for the elongation of a growing DNA chain. Previous work by others as well as our group showed that the compound is highly effective against HBV [34-36], DHBV [36] as well as HIV [37-40]. The inhibitory mechanism of 3TC requires phosphorylation of the compound to 3TC-5'-triphosphate (3TC-TP) which specifically inhibits the viral polymerases [41-43].

Another compound found to be effective against DHBV in our lab [44,45] is 2',3' -dideoxyguanosine (ddG). Using a pro-drug of ddG, 2A6M, Howe et al. [45] showed that the inhibition mediated by 2A6M took place at a very early stage of viral reverse transcripition. The results of further studies by the same authors suggest that the phosphorylated form of ddG binds to the DHBV polymerase and blocks the initiation of DNA synthesis. Based on this information, we predicted that, in animals treated with 2A6M for a longer time, the majority of the replication intermediates would be truncated due to binding of the nucleoside analogue at the initiation site of DNA synthesis and PCR amplification using the 16 DHBV primers would not yield any product.

In a preliminary study using slab-gel electrophoresis, we found results that did not support our prediction. As shown in Figure 4.5(a), animals that were exposed to 2A6M for two weeks showed marked decreases in viral DNA in the liver such that PCR products generated by primers that bind further downstream of the minus DNA strand

were no longer amplified. However, the presence of PCR products in excess of 1100 bp indicated reasonable amounts of elongation of DNA from the initiation site of the minus DNA strand template. This observation suggests that complete inhibition of initial DNA synthesis at the 5' end of the minus strand was not achieved by the treatment with 2A6M. The disappearance of the PCR products longer than 1300 bp in this case could be explained by either of two ways. First, the disappearance of the longer PCR products was a direct result of chain termination mediated by 2A6M. Second, the disappearance of the longer PCR products was caused by a decrease in template as a result of drug treatment.

To rule out the second possibility, the initial input target for PCR amplification was increased from 5 µl of purified core DNA per tube to 10 µl and 15 µl per tube. As shown in Figure 4.5b-c, the increase in input target clearly suggested the significance of template dosage. Due to the inverse relationship between amplicon length and amplification efficiency, longer PCR fragments are amplified at lower frequencies than shorter ones. As the pool of viral DNA in the liver decreases, fewer templates are available for amplification and the frequency of amplification of the longer PCR product is reduced. As shown in Figure 4.5(c), a 3-fold increase in input target clearly indicated that even after 2 weeks exposure to 2A6M, all three animals still carried significant amount of full-length viral genome in their livers. A control experiment demonstrating the effect of template dosage on amplification of large PCR products is depicted in Figure 4.6.

To further support the importance of template dosage in this study, two primer sets were designed to amplify small DNA fragments (169 and 356 bp respectively) from

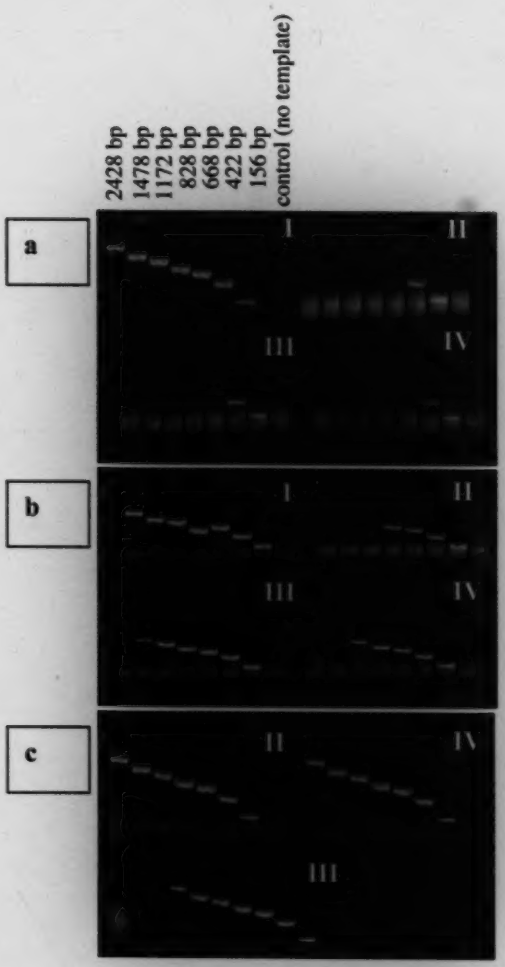

Figure 4.5 Effect of 2-amino-6-methoxy on replicating cores in 2 weeks old ducks treated for 2 weeks. I represents an animal infected, not treated; II-IV represent 3 animals, infected and treated. Panels (a) to (c) show increasing dose of initial input template for PCR amplification, respectively, 5, 10 and 15 µl of purified DNA from replicating cores. Seven PCR products were amplified from primers H56, H1006, H1312, H1656, H1816, H2062 and H2328. The same reverse primer (H2481) was used in each amplification.

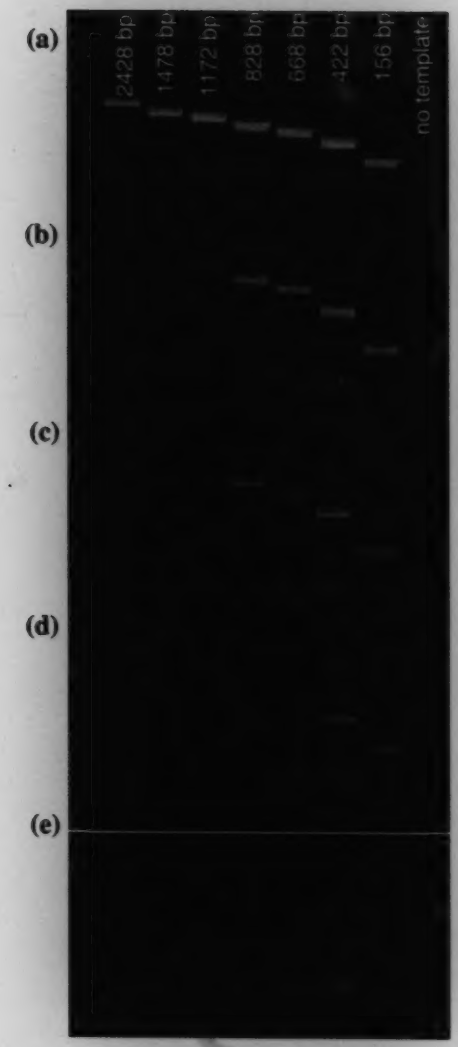

Figure 4.6 Dependence of PCR amplification on concentration of input template. (a) to (e) represent decrease in amplification as a function of initial input template 16, 6, 3, 1, 1(1:10) µl per panel respectively. The last panel represents one µl of a 1:10 diluted template. PCR primers used in this experiment are identical to that described in Figure 4.5

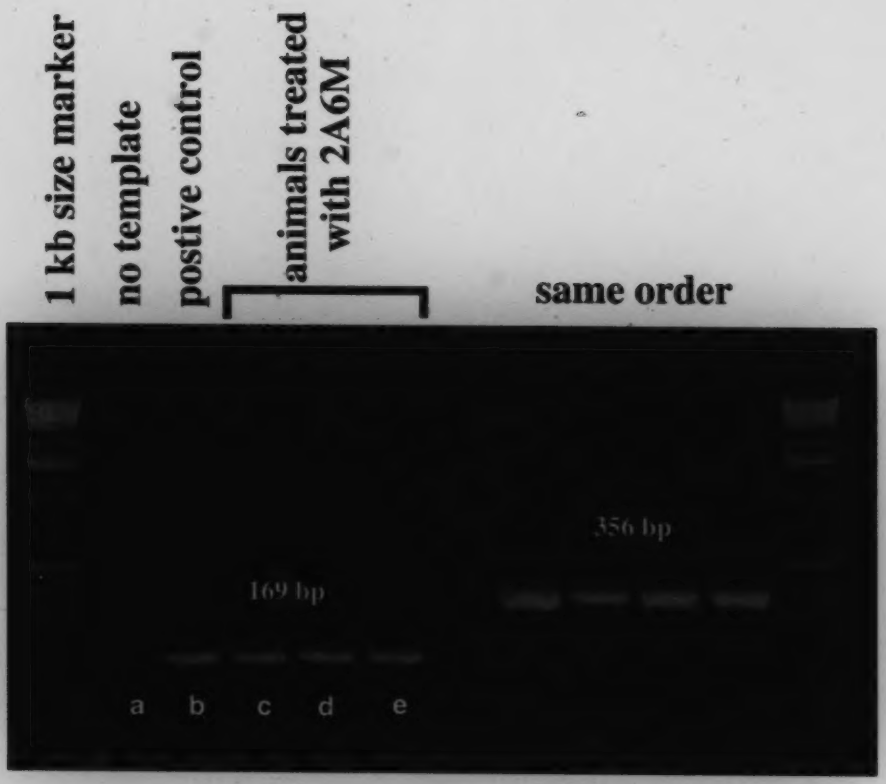

Figure 4.7 Amplification of small PCR fragments from the 3' end of the minus strand of the DHBV genome. Lanes 'a' and 'b' represent a negative control (no template) and a positive control (replicating core from a congenitally infected animal) respectively. Lanes 'c' to 'e' represent the animals treated with 2A6M as described in Figure 4.5. Samples were loaded in the same order to produce the panel corresponding to 356 bp PCR prodcuts.

the 3' end of the minus DNA strand. This experiment served two purposes. First, by selectively amplifying the 3' end of the minus DNA strand, the presence of full-length templates of the minus strand could be substantiated. Second, by amplifying shorter PCR

products, the disappearance of longer PCR products caused by a decrease in template dosage could be ruled out. As anticipated, the work illustrated in Figure 4.7 showed that full-length minus DNA strands were still present in all three animals after 2 weeks of treatment with 2A6M. This observation strongly suggests that a much longer duration of treatment as well as increase dosage is perhaps necessary to completely inhibit DNA synthesis. This would reduce background amplification arising from full-length templates and allow truncated viral DNA fragments to be detected more efficiently. Alternatively, quantitative PCR with primers from each end of the genome might show a relative decrease of full-length genome in 3TC treated animals and less gradient in 2A6M treated ducklings.

4.4 Conclusions

To date, therapy for hepatitis B infection is frequently monitored by measuring viral DNA by various hybridization methods. These methods are usually expensive and require radioisotope facilities. In addition, other drawbacks of current DNA diagnostics are the need for labor intensive, time consuming separation and detection methods such as gel electrophoresis, labeling or staining, membrane transfer, hybridization and autoradiography. With the development of automated, rapid and high throughput technologies, CE may evolve into a diagnosic tool that can be used routinely to detect HBV-DNA in patients treated with newer antiviral drugs for HBV.

The feasibility of PCR with CE-LIF detection as a diagnostic tool was investigated in this study. The current CE technology coupled with PCR was found to be capable of real time analysis and separation of viral specific DNA fragments using fluorescence

based detection. From the experiments conducted in this study, it can be concluded that PCR coupled with CE-LIF provides an easy-to-use, rapid and inexpensive method for the identification of DHBV DNA in serum and liver.

The multi-primer approach of priming the DHBV genome provides information on the mechanism of viral neutralization in response to antiviral therapy. In this study, the use of the 16 primer sets did not demonstrate truncation of the minus DNA strand in response to treatment with 3TC. Also the same experiment did not indicate that 2A6M is able to completely inhibit viral DNA synthesis by blocking the 5' end of the minus DNA strand. We attributed these results to a relatively short duration of exposure to the antiviral compounds, which left a significant background level of full-length genomes in the treated animals.

In the liver, turn over of hepatocytes is a dynamic process. New cells are continuously infected as viral infection persists. Using PCR, it is difficult to qualitatively demonstrate truncation of viral DNA imposed by antiviral compounds 3TC and 2A6M during early periods of treatment. Ultimately, quantification of the 16 PCR products will be necessary to compare the relative amount of the long and short DNA fragments in order to demonstrate truncation of viral DNA in response to 3TC treatment.

4.5 Bibliography

1. Marion, P.L., Oshiro, L.S., Regnery, D.C., Scullard, G. and Robinson, W.S. (1980) Proc. Natl. Acad. Sci. USA **77**, 2941-2945.
2. Mason, W.S., Seal, G. and Summers, J. (1980) J. Virol. **36**, 829-836.
3. Seeger, C., Ganem, D. and Varmus, H.E. (1986) Science **232**, 477-484.

4. Summers, J. and Mason, W.S. (1982) Cell **29**, 403-415.

5. Summers, J., Smolec, J.M. and Snyder, R. (1978) Proc. Natl. Acad. Sci. USA **75**, 4533-4537.

6. Will, H., Reiser, W., Weimer, T., Pfaff, E., Buscher, M., Sprengel, R., Cattaneo, R. and Schaller, H. (1987) J. Virol. **61**, 904-911.

7. Yokosuka, O., Omata, M., Zhou, Y., Imazeki, F. and Okuda, K. (1985) Proc. Natl. Acad. Sci. USA **82**, 5180-5184.

8. Urban, M.K., O'Connell, A.P., and London, T.W. (1985) J. Virol. **55**, 16-22.

9. Freiman, J.S., Jilbert, A.R., Dixon, R.J., Holmes, M., Gowans, E.J., Burrell, C.J., Wills, E.J. and Cossart, Y.E. (1988) Hepatol. **8**, 507-513.

10. Tsiquaye, K. and Zuckerman, A. (1985) J. Hepatol. **1**, 663-669.

11. Tsiquaye, K.N., Collins, P. and Zuckerman, A. (1986) J. Antimicrob. Chemother. **18**, (suppl.B), 223-228.

12. Severini, A., Liu, X.Y., Wilson, J.S. and Tyrrell, D.L.J. (1995) J. Antimicrob. Chemother. **39**, 1430-1435.

13. Bonino, F., Chiaberge, E. and Negro, F. (1985) DNA by molecular hybridization-Clinical sifnificance. In: Biotechnology in Diagnostics, pp.163-172.

14. Berninger, M., Hammer, M,, Hoyer, B. and Gerin, J.L. (1982) J. Med. Virol. **9**, 57-68.

15. Krogsgaard, K., Aldershville, J. and Kryger, P. (1985) Hepatol. **5**, 778-782.

16. Bonino, F., Chiaberge, E. and Negro, F. (1985) J. Gastroenterol. **17**, 235.

17. Bonino, F., Hoyer, B. and Nelson, J. (1981) Hepatol. **1**, 386-391.

18. Negro, F., Chiaberge, E. and Oliviero, S. (1984) Liver **4**, 177-183.

19. Hadziyannis, S.J., Lieberman, H.M., Karvountzis, G.G. and Shafritz, D.A. (1983) Hepatol. **3**, 656-662.

20. Bonino, F., Rosina, F. and Rizzetto, M. (1986) Gastroenterol. **90**, May

21. Chu, C.M., Karayiannis, P. and Fowler, M.J.F. (1985) **5**, 431-434.

22. Pawlotsky, J.M., Bastie, A., Lonjon, I., Remire, J., Darthuy, F., Soussy, C.J. and Dhumeaux, D. (1997) J. Virol. Methods **65**, 245-253.

23. Hendricks, D.A., Stowe, B.J., Hoo, B.S., Kolberg, J., Irvine, B., Neuwald, P.D., Urdea, M.S. and Perrillo R.P. (1995) Clin. Microbiol. Infect. Dis. **104**, 537-546.

24. Kapke, G.F., Watson, G., Sheffler, S., Hunt, D. and Frederick, C. (1997) J. Viral Hepatitis **4**, 67-75.

25. Klein, A., Barsuk, R., Dagan, S., Nusbaum, O., Shouval, D. and Galun, E. (1997) J. Clin. Microbiol. **35**, 1897-1899.

26. Kaneko, H.L. and Schwartz, I. (1994) BioTechniques **16**, 84-92.

27. Paterlini, P., Gerken, G., Nakajima, E., Terre, S., D'Errico, A., Grigioni, W., Nalpas, B., Franco, D.,Wands, J., Kew, M., Pisi, E., Tiollais, P. and Brechot, C. (1990) N. Engl. J. Med. **323**, 80-85.

28. Aspinall, A., Steele, D., Peenze, I. And Mphahlele, M.J. (1995) J. Viral Hepatitis **2**, 107-111.

29. Payan, C., Veal, N., Crescenzo-Chaigne, B., Belec, L. and Pilot, J. (1997) J. Virol. Methods **65**, 299-305

30. Pardoe, I.U., and Michalak, T.I. (1995) J. Virol. Methods **51**, 277-288

31. Jardi, R., Buti, M., Rodriguez-Frias, F., Cortina, M., Esteban, R., Guardia, J. and Pascual, C. (1996) J. Hepatol. **24**, 680-685.

32. Carman, W.F., Dourakis, S., Karayiannis, P., Crossey, M., Drobner, R. and Thomas, H.C. (1991) J. Med. Virol. **34**, 114-118.

33. Kaneko, S., Miller, R.H. Bisceglie, A.M., Feinstone, S., Hoofnagle, J.H. and Purcell, R.H. (1990) Gastroenterol. **99**, 799-804.

34. Chang, C.N., Doong, S.L., Zhou, J.H., Beach, J.W., Jeong, L.S., Chu, C.K., Tsai, C.H., Cheng, Y.C., Liotta, D.C. and Schinazi, R.F. (1992) J. Biol. Chem. **267**, 13938-13942.

35. Doong, S.L., Tsai, C.H., Schinazi, R.F. and Liotta, D.C. (1991) **88**, 8495-8499.

36. Tyrrell, D.L.J., Fischer, K. and Cameron, J. (1993) 18th International Symposium on Viral Hepatitis and Liver Diseases. Viral Hepatitis Research Foundation of Japan, Tokyo.

37. Coates, J.A.V., Cammack, N., Jenkinson, H.J., Jowett, A.J., Jowett, M.I., Pearson, B.A., Penn, C.R., Rouse, P.L., Viner, K.C. and Cameron, J.M. (1992) Antimicrob. Agents Chemother. **36**, 733-739.

38. Greenberg, M.L., Allaudeen, H.S. and Hershfield, M.S. (1990) Ann. N. Y. Acad. Sci. **616**, 517-518.

39. Soudeyns, H., Yao, X.J., Gao, Q., Belleau, B., Kraus, J.L., Nguyen-Ba, N., Spira, B. and Wainberg, M.A. (1991) Antimicrob. Agents Chemother. **35**, 1386-1390.

40. Wainberg, M.A., Tremblay, M., Rooke, R., Blain, N., Soudeyns, H., Parniak, M.A., Yao, X.J., Li, X.G., Fanning, M., Montaner, J.S.G., O'Shaughnessy, M., Tsoukas, C., Falutz, J., Dionne, G., Belleau, B. and Ruedy, J. (1990) Ann. N. Y. Acad. Sci. **616**, 346-355.

41. Cammack, N., Rouse, P., Marr, C.L.P., Reid, P.J., Boehme, R.E., Coates, J.A.V., Penn, C.R. and Cameron, J.M. (1992) Biochem. Pharmacol. **43**, 2059-2064.

42. Chang, C.N., Skalski, V., Zhou, J.H. and Cheng, Y.C. (1992) J. Biol. Chem. **267**, 22414-22420.

43. Hao, Z., Cooney, D.A., Hartman, N.R., Perno, C.F., Fridland, A., DeVico, A.L., Sarngadharan, M.G., Broder, S. and Johns, D.G. (1988) Mol. Pharmacol. **34**, 431-435.

44. Kitos, T.E. and Tyrrell, D.L.J. (1995) Biochem. Pharmacol. **49**, 1291-13302.

45. Howe, A.Y.M., Robins, M., Wilson, J.S. and Tyrrell, D.L.J. (1996) Hepatol. **92**, 87-96.

Chapter 5. Probing Amplification Efficiency in Quantitative Competitive PCR

A shorter version of this chapter has been submitted as conference proceeding. 83rd CSC Conference and Exhibition, Calgary, Alberta, Canada (2000). Profiling Amplification Efficiency of Competitive Polymerase Chain Reaction Using Capillary Electrophoresis with Laser-Induced-Fluorescence Detection.
W. G. Tan, N. Li, D. L. J. Tyrrell and N. J. Dovichi.

5.1 Introduction

5.1.1 Theoretical aspects of quantitative competitive PCR (QC-PCR)

In the last few years, capillary electrophoresis has become a mature technique. It has been shown that CE instruments work reliably. Good quantitative results may be obtained and validation guidelines have been outlined [1-3]. CE is now widely used in routine analysis, leading to a rapidly increasing number of successful applications of this technique. On the other hand, it is nearly 15 years since the polymerase chain reaction (PCR) was described by Saiki et al [4]. The amplification of DNA sequences using PCR is now a widespread routine that is being used for the qualitative detection of viral infection such as HBV while methods of applying this technique for quantification are more difficult and continue to be improved. A quantitative PCR methodology would be valuable in HBV infection, for instance, when assessing the correlation of clinical outcome to viral loads. Another application is in monitoring response to antiviral therapy.

Initially, PCR was not viewed as having great quantitative as illustrated by the fact that early description of PCR technology made no mention of quantification [5, 6]. Indeed, it should come as no surprise that the factor that makes PCR so powerful, i.e., its ability to amplify small amounts of nucleic acids exponentially, is also the factor that makes the technique so challenging as a quantitative method. Anything that is capable of interfering with the exponential amplification might ruin the intrinsic quantitative ability of PCR. This interference may be overcome by normalizing the amount of PCR product of a specific template with respect to an internal standard that is amplified in the same reaction tube. Template from an internal standard can be derived from the cellular genes,

for example, pyruvate dehydrogenase [7], proenkephalin [8], β actin [9] or β-globin [10]. The most precise quantification of DNA can be obtained by competitive PCR [12-17]. This assay is based on competitive co-amplification of a specific target sequence together with an internal standard of known concentration in the lane reaction tube. The internal standard (hereafter referred to as competitor) shares primer recognition sites with the specific template. Both specific target and competitor must be PCR-amplified with the same efficiency and it must be possible to analyze the PCR-amplified products of the target and the competitor separately. Quantification is then performed by comparing the PCR signal of the specific template with the PCR signals obtained with known concentrations of the competitor.

Competitors for competitive PCR can be constructed in several ways. For initial attempts, competitors were used that differ from the wild-type target by only a point mutation. In most cases, these point mutations were introduced in such a way that new restriction enzyme recognition sites were created within the competitor nucleic acid sequence [18, 19]. Following restriction enzyme cleavage, the resulting products of competitor and primary target are separated by electrophoresis on an agarose gel and quantified by hybridization with a labeled probe or with the help of a labeled PCR primer. Although these competitors are showing a very high degree of similarity to the wild-type product, it is cautioned that in cases of unpredictable efficiency of enzyme digestion, the amplification products of the competitor may not be cut completely. This can strongly influence the results of the assay.

More recently, deletions of a part of the wild-type sequence or insertions of foreign sequences have been used for the *de novo* construction of competitors, followed

by analysis by gel electrophoresis [20]. Reviewing the literature, it seems obvious that there are no general rules or strategies for the construction of these modifications [21-25]. Often a critical analysis of precision and reproducibility is found in the literature, but evaluation of the amplification efficiencies of the target and the competitor is often lacking.

5.1.2 Technical and Mathematical Considerations of QC-PCR

The most critical prerequisite for the proper performance of quantitative competitive-PCR (QC-PCR) is a comparable amplification efficiency of the target and the competitor, and it is especially important to carefully control for this when setting up a new PCR-based quantification procedure. The easiest mode of control is to repeatedly quantify several known amounts of specific wild-type template with the help of the newly constructed competitor. If these analyses result in the calculated copy numbers, comparable amplification efficiencies between the target and the competitor can be assumed, and the newly constructed competitor can be safely used for quantification. If the result of such quantification experiments point to minor differences in amplification efficiency between the target and the competitor, it may be compensated for by using a correction factor [26].

In addition to the commonly used ethidium bromide staining method on gel electrophoresis, another frequently used procedure for the determination of amplification efficiency is the analysis of known amounts of target and competitor in a PCR protocol that uses fluorescence or radioactive labeled primers. After various numbers of cycles, the PCR products are separated and quantified by measuring their fluorescence or radioactivity [27, 28]. When controlling for amplification efficiencies of the target and

competitor, it is also important to keep in mind that minor variation in amplification efficiency may become more pronounced when the amplification reaction is driven to the post-exponential phase [26, 29]. To ensure proper quantification, it has therefore been suggested that the amplification be measured during the exponential and post-exponential phases. In general, it can be concluded that a minor difference in sequences of the target and competitor as well as small differences in size do not substantially affect amplification efficiency [31]. However, as an inverse exponential relationship between template size and amplification efficiency has been observed, it is obviously important to keep the size difference between the target and the competitor as small as possible [26, 30]. Another problem to be dealt with concerns the possible formation of heteroduplexes. These structures can occur when the target and the competitor differ in only one or a few bases, either small differences in size or small diversities in the nucleotide sequences [26, 29, 31]. Since heteroduplexes interfere with subsequent quantification procedures, great care should be taken to avoid their formation [32-34].

PCR quantification in general relies on end-point measurement of PCR products. As mentioned, the principle condition that must be fulfilled to derive absolute quantitative information is that the target and the competitor be amplified with equal efficiency. Under this condition, the initial ratio of target to competitor is assumed to remain constant throughout the amplification, and it is not necessary to restrict a PCR reaction to the exponential phase for the purpose of quantification. However, according to the mathematical expression of $N = N_o(1 + E)^n$, where N is the PCR product formed after n successive cycles, N_o is the initial amount target DNA and E is the mean efficiency of the reaction, E will only be identical for both the target and the competitor if

similar template sequences as well as lengths are used during amplification. These restrictions render PCR products of both the target and the competitor indistinguishable. In practice, because of the nature of QC-PCR, the competitor is always constructed such that its amplified products can be separated from that of the target. This is carried out by either manipulating the size or introduction of a restriction site in the competitor. Either way would alter the nature of the competitor such that it is physically different from the target. While the difference in amplification efficiency between the target and competitor can be reduced to a minimum, it is theoretically incorrect to assume that both the target and the competitor share an identical efficiency of amplification using experimental protocols that rely on end point measurement.

Recent developments of real-time PCR such as the TaqMan [35, 36] and the LightCycler [37, 38] has allowed PCR products accumulated at each cycle to be monitored. Real-time PCR in the case of TaqMan is compatible with a quantitative comparative PCR approach with the advantage that it eliminates the need to design individual internal or external control templates. The instrumentation also permits end point measurement in addition to measurement of PCR products at each cycle [39]. However, there is precaution that needs to be considered when quantification of nucleic acid is conducted using TaqMan. First, to ensure correct quenching in the intact probe, optimal hybridization efficiency and high efficiency of cleavage by Taq Polymerase, a hybridization probe and the flanking primers usually have to be designed via a stringent process such that it limits sequence selection for both the probe and the primers. Second, in the TaqMan assay, the donor and the quencher are preferably located on the 3' and 5' ends of the probe, because the requirement that 5' to 3' hydrolysis be performed between

the fluorophore and quencher. This can be met only when these two moieties are not too close to each other. However, this requirement is a serious drawback of the assay since the efficiency of energy transfer decreases with increasing distance between the reporter and the quencher. As a consequence, the background emission from unhybridized probe can be quite high. Third, in practice the current approach in QC-PCR is not applicable to real-time PCR such as TaqMan because of restrictions in the instrument design that does not allow a double reading in the same tube.

In this study, we describe an alternative approach to QC-PCR using Capillary Electrophoresis-Laser Induced Fluorescence (CE-LIF) detection. The aim is to improve current technologies in QC-PCR as well as to promote eventual automation of DNA quantification in clinical diagnosis. The target for this assay was the duck hepatitis B virus (DHBV), whose level in the serum of infected animals was monitored during antiviral therapy.

5.2 Experimental

5.2.1 Apparatus

The instrument for capillary electrophoresis was built in-house and has been described in detail in Chapter 2. The instrument is equipped with a high voltage power supply (Model CZE 1000R, Spellman, NY); a 543.5 nm green He-Ne laser system (Melles Griot) with a 5 mW maximum output; A Macintosh Centris 650 computer which controls the power supply via a NB-MIO-16XH-18 input/output board (National Instruments, Austin, TX); an interface box (I-V converter) which transfers output from the instrument to the computer; a plexiglas box (with safety interlock) in which the

injection end is installed; a sheath-flow cuvette (1 mm thick walls, 200 μm x 200 μm square inner bore, 2 cm in length) which serves as a post-column detector; a R1477 PMT (Bridgewater, NJ) for detecting fluorescence signals.

5.2.2 CE separation and post-column detection

Capillary electrophoresis of the sample was performed using a 30 cm long, 50 μm i.d., 144 μm o.d. DB-210 coated fused-silica capillary (Polymicro Technologies, Phoenix, AZ) purchased from J&W Scientific (Folsom, CA, USA). Electrophoresis buffer was 100 mM of TAPS at pH 8.0 (Sigma). One end of the capillary was immersed in electrophoresis buffer or sample, with a Pt wire electrode at the injection end (cathode) in the plexiglas box. The other end of the capillary was installed inside the sheath-flow cuvette containing electrophoresis buffer siphoned from a buffer reservoir. Sample introduction was performed by electrokinetic injection at 1000 V for 10 sec., and separation was performed with an electric field of 200 V/cm. A 0.8% HEC was dissolved in electrophoresis buffer, filtered by a Millex-GS 0.45 μm filter unit (Millipore, Bedford, MA) and introduced into the capillary via a syringe.

The laser beam was focused by a 6.3X (N.A. 0.2) microscope objective (Melles Griot, Nepean, Canada) into the sheath-flow cuvette, just below the capillary end. The fluorescence was collected at 90 degrees from the direction of excitation by a 60x (N.A. 0.7) microscope objective (LWD-M Plan, Universe Kogaku, Japan). The transmitted fluorescence light was spectrally filtered with a 580DF40 bandpass filter (Omega Optical, Brattleboro, VT) and detected by an R1477 PMT. The PMT signal was transferred to the interface box and digitized by the input/output board. Data was collected at a sampling rate of 10 Hz.

5.2.3 Preparation of DHBV DNA from duck sera

Ten day old congenitally infected ducklings were subjected to 3TC treatment with a dosage of 40 mg/kg body weight. The animals were treated intramuscularly 4 times daily for 72 hours. Serum samples were obtained from each duck at 0, 6, 18, 30, 42, 54, 66 hours and 78 hours after treatment was initiated. A 200 μL of serum collected from each time point was purified and concentrated in a 100 μL elution buffer using a commercial QIAamp Blood Kit (Qiagen). Briefly, the serum samples were treated with QIAamp protease before loading onto the chromatography column. After two washes with 500 μL of wash buffer, extracellular DHBV DNA was eluted from the column by centrifugation in a 100 μL elution buffer pre-heated to 70 °C.

5.2.4 Dot blot hybridization

Serum samples collected from the animals were also subjected to dot blot hybridization. This technique, which relies on the use of radiolabeled detection, is a routine method employed by our laboratory to screen animals for DHBV DNA in serum. Serum samples were spotted onto nylon membrane (Hybond – N; Amersham) filtered with a Bio-Dot microfiltration apparatus (Bio-Rad). DNA from the membrane was denatured with 0.5 M NaOH and 1.5 M NaCl at room temperature for 20 min, followed by neutralization in 1 M Tris-HCl and 1.5 M NaCl (pH 8). The membrane was exposed to UV for 3 min, followed by pre-hybridization for 3 hours at 65 °C in a cocktail containing 6x SSC (20x SSC contains 3 M NaCl and 0.3 M Sodium citrate, pH 7) plus 7% SDS. Hybridization was initiated by adding ^{32}P labeled DHBV DNA at approximately 10^6 cpm per ml under the same hybridization conditions for at least 12 hours. The hybridized membrane was washed in 1x SSC plus 0.1% SDS at 65 °C for 40

min (twice) and 0.1x SSC plus 0.1% SDS at room temperature for 15 min. The membrane was dried and autoradiographied at -70 °C with an enhancer screen.

5.2.5 Construction of plasmid DNA templates

A pAlter-2-W plasmid containing a wild type DHBV genome of 3021 bp was kindly donated by K.Fischer (Dept. Medical Microbiology & Immunology, University of Alberta). It contained a 3021 bp monomer of a DHBV genome cloned into the *EcoRI* site of pAlter-1 (Promega). PCR amplification of pAlter-2-W using primers T2481(5'gtgtatggaaaagccgtcca 3') and H2328(5'gccataagcgttatcagacg 3') gave rise to a single PCR product of 156 bp. A second plasmid pT7Blue-3-M containing a mutant DHBV sequence was constructed by insertion of a 44 bp foreign sequence in a unique restriction site internal to the primer binding sites on the DHBV genome. Screening of the mutant was carried out by PCR amplification of the mutant sequence (156 + 44 bp) prior to cloning into a plasmid using the pT7Blue-3 Blunt Vector cloning system (Novagen, Madison, WI). The plasmid was propagated in *E. coli* strain DH 5α grown in suspension broth culture. Recovery of plasmid was carried out using Qiagen Plasmid Maxi Kit (Qiagen, Chatworth, CA).

5.2.6 Competitive PCR-CE-LIF

A 50-μL reaction mixture containing 1.5 mM $MgCl_2$, standard PCR buffer (Gibco), 200 μM of dNTPs mix, 16 and 20 pmol of each T2481 and H2328 primers respectively was prepared for each sample. T2481 was 5'-rhodamide-labeled. Both primers are 20 nucleotides in length. The reaction mixture was chilled at 0 °C prior to the addition of Taq DNA polymerase. For quantitative analysis, a master mix was prepared and 50 μL aliquots were dispensed into a series of PCR tubes that were placed

out in a thermal cycler (MJ Research) for a single program (5 min at 95 °C, up to 50 cycles of 50 s at 95 °C, 1 min at 56 °C, 1 min at 72 °C). After each PCR cycle, a tube will be withdrawn for CE-LIF quantification. The PCR product was purified by QIAquick PCR Purification (Qiagen, CA) prior to capillary electrophoresis. To correct for variation in sample introduction, an injection standard of 235 bp was added into the purified PCR product. Aliquots of the purified target and competitor templates were stored in 10mM Tris-HCl (pH. 8) at -20 °C. Each aliquot was only thawed and used once to avoid carryover of contamination. Concentration of the templates was monitored regularly by absorbance at 260 nm to check for sample degradation.

5.2.7 Determination of limit of detection

To determine the detection limit of this assay, the target template was serially diluted and amplified using the framing oligonucleotide primers, T2481 and H2328 respectively. To ensure better sensitivity of detection, the PCR was carried out for 30 cycles using the same amplification parameters as described above. The concentration of the stock target template was measured by optical absorbance at 260 nm. The range of initial input template used was between 5 and $5x10^8$ copies.

5.2.8 Quantitative description of QC-PCR

The use of competitive PCR is well documented. In this study, we have employed the theoretical considerations as described mathematically by Raeymaekers [40] and Santagati [41]. We denote the initial input target and competitor respectively as T_o and C_o, the amount of products following a number of n cycles as T_n and C_n, and the efficiency of amplification as E_t and E_c. From these parameters we obtain

$$T_n = T_o (1 + E_t)^n \quad (5.1)$$

$$C_n = C_o (1 + E_c)^n \quad (5.2)$$

At a given cycle where equations 5.1 and 5.2 intercept, the initial input template of the target T_o can be determined. In this case, the accuracy of using the point of intercept to determine T_o is dictated by the accuracy of measuring the initial input of known competitor concentration. As well, it is equally crucial to ensure that at this point of intercept E_t and E_c are compatible.

Alternatively, by dividing equation (5.1) with (5.2), the following equation is generated:

$$\text{Log}(T_n / C_n) = \text{Log } T_o - \text{Log } C_o + n\text{Log}[(1+ E_t)/(1+ E_c)] \quad (5.3)$$

If E_t and E_c are identical, a basic assumption for absolute quantification, equation (5.3) can be simplified to

$$\text{Log}(T_n / C_n) = \text{Log } T_o - \text{Log } C_o \quad (5.4)$$

Equation (5.4) predicts a straight line in the form of $y = c - x$ when different amounts C_o are co-amplified with a constant amount of the target T_o for a fixed number of cycles. When $\text{Log}(T_n / C_n)$ is plotted as a function of $\text{Log } C_o$, a line with a theoretical gradient of -1 is expected. Under ideal conditions the number of copies of T_o can be quantified by interpolating the X-axis value when the final number of the target and competitor copies are identical where $\text{Log}(T_n / C_n) = 0$ and $\text{Log } T_o = \text{Log } C_o$.

5.3 Results and Discussion

5.3.1 Qualitative performance of CE-LIF

From a qualitative point of view, our results suggest that the 0.8% low viscosity hydroxyethyl-cellulose sieving medium was able to baseline resolve the reaction products in a very short separation time (10 min). The results of the study also showed that CE could be performed without sample purification because excess primers could be separated from the products. As shown in Figure 5.1 (a) and (b), the product peaks of 157 bp and 201 bp were resolved, indicating that the presence of Taq polymerase as well as excess primers and dNTPs did not seem to significantly affect resolution. However, in PCR reactions in which the amount of initial input template was low (< 100 copies), large excess of primers and dNTPs were present in the samples. Injection of such samples without sample purification may sometimes complicate separation due to primer flooding in the injection plug. Injection without sample purification was also found to reduce the amount of DNA fragments injected. In the absence of sample purification, a large molar excess of primer would out-compete PCR products for injection. In addition, the presence of salt in the PCR sample would also reduce the efficiency of sample injection, as clearly depicted in Figure 5.1 (a) and (b) versus (c) and (d). To avoid these problems, all the samples used in quantitative analysis were purified prior to CE analysis.

In contrast to conventional slab gel electrophoresis, CE run times are short, the capillary can be re-used for at least 250 runs and automation using array technology is feasible. Consecutive injections of purified CE samples on average yielded 4.0 % RSD for peak height and between 2.3 % RSD for peak area. These values, which combine the variability of PCR and capillary electrophoresis separation, are reasonably acceptable for

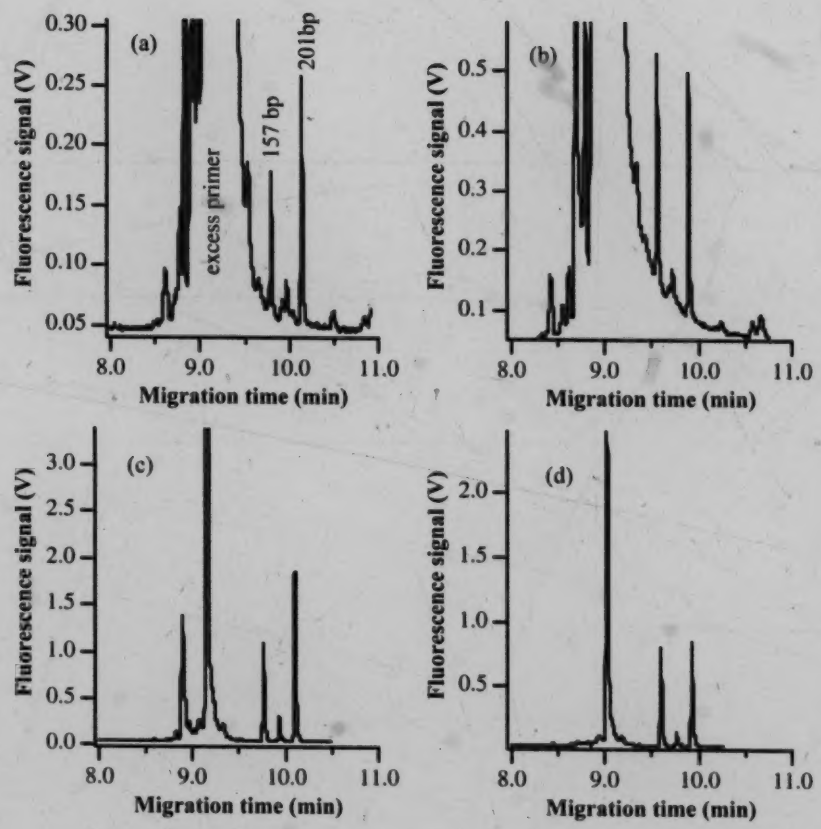

Figure 5.1 CE separation of PCR products in the presence and absence of sample purification using Qiagen protocol. (a) and (b) represent non-Qiagen purified products amplified at different input templates and cycle numbers; (c) and (d) represent the same samples after Qiagen purification. A 29cm, DB-210 capillary with an i.d . of 50 um was filled with 0.8% HEC. PCR products were electrokinetically injected at 1000 V for 5 s at room temperature.

bioassay validation. In addition, data acquisition and analysis are computer-controlled. This reduces data processing error especially when large numbers of PCR products need to be analyzed.

5.3.2 Control of plasmid amplification and efficiency

pAlter-2-W and pT7Blue-3-M plasmid concentrations were evaluated by spectrophotometric measurement after gel electrophoresis. To ensure accurate quantification of the purified plasmid, the concentrations were measured once a week for 7 weeks and mean and standard deviation of measurement were obtained. At 260 nm, pAlter-2-W and pT7Blue-3-M plasmid were at 1.5×10^{11} and $(3.0 \pm 0.3) \times 10^{10}$ copies per μL respectively. To check for protein contamination, the 260 / 280 nm ratios of the purified plasmid were also determined. When subjected to different amplification cycles, both pAlter-2-W and pT7Blue-3-M demonstrated compatible amplification efficiency as indicated by identical slopes from plots constructed relating Log T_n or Log C_n to number of cycles. Figure 5.2(a) shows a typical electropherogram of pAlter-2-W co-amplified with pT7Blue-3-M (hereafter referred as target and competitor respectively). The peak height of the target and the competitor were normalized against a DNA marker added at the end of each cycle. This step corrects for variations in sample loading and detector sensitivity due to differences in instrument alignment accuracy. Figure 5.2(b) to (f) depicts the progression of PCR reaction with different initial input target and competitor templates in relation to cycle numbers. The amplification ratio between the target and the competitor was consistent in all five panels until the PCR reaction was driven into the plateau phase. The PCR products of pAlter-2-W and pT7Blue-3-M were essentially identical except for a 44 bp insert in the competitor. This difference was not manifested

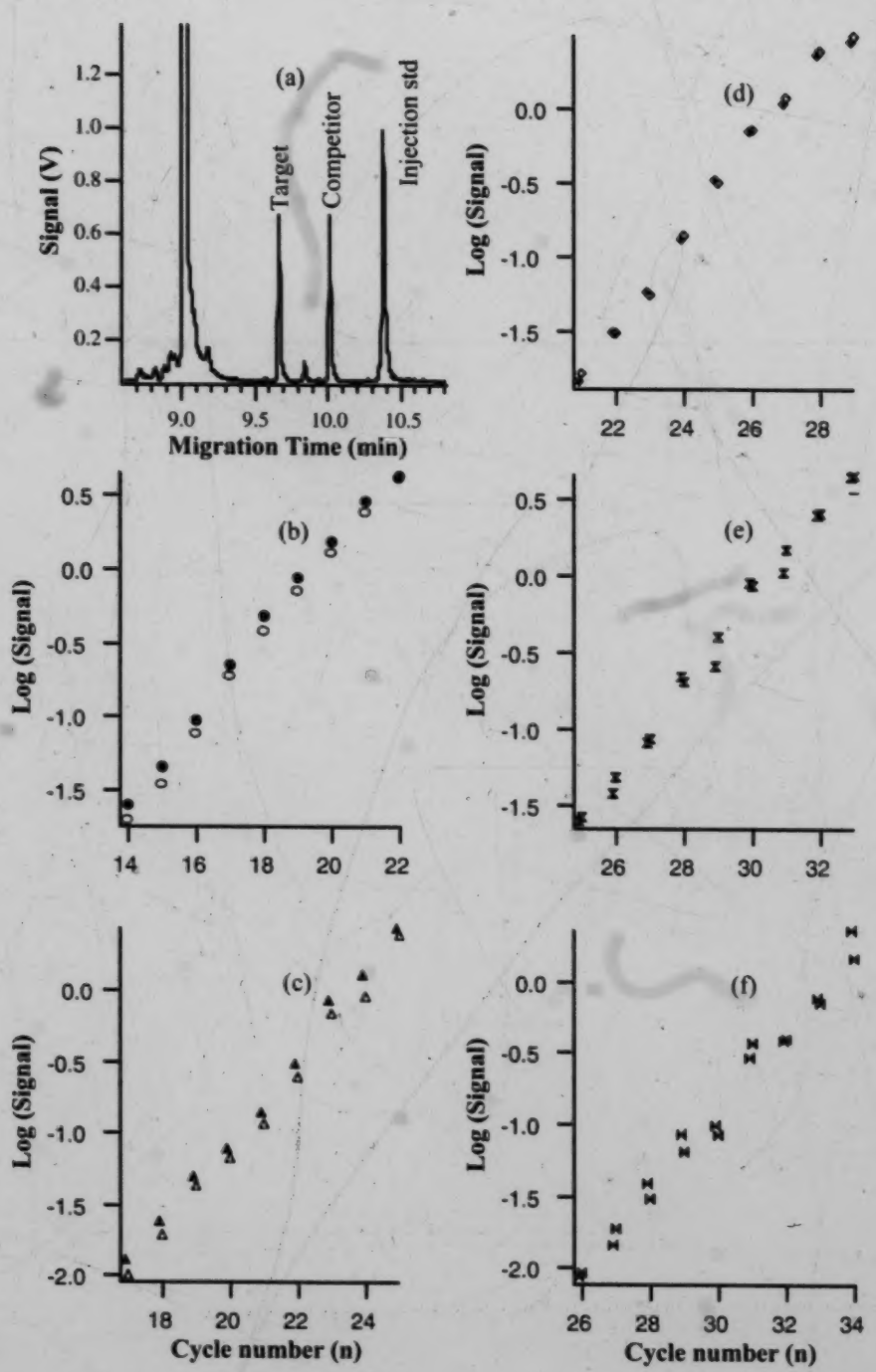
(a)
Target
Competitor
Injection std
Signal (V)
Migration Time (min)
(b)
(c)
(d)
(e)
(f)
Log (Signal)
Cycle number (n)

Figure 5.2 Separation efficiency of plasmids pAlter-2-W and pT7Blue-3-M at various initial input template concentrations. (a) Separation profile of PCR products with an injection standard added at the end of a PCR amplification; (b) to (f) represent progression of PCR reaction at different input target and competitor templates in relation to cycle number. All data points were generated by normalizing the peak height of both plasmids by the peak height of the injection standard. Input template of pAlter-2-W and pT7Blue-3-M started 1.5 x 10^6 copies respectively, and was reduced by one log sequentially from (c) to (f). Filled dots denote pAlter-2-W and opened dots denotes pT7Blue-3-M. Only data points within linear range were shown in each plot.

during early PCR cycles, but was increasingly obvious when PCR reaction was driven into the plateau phase where the variation in amplification efficiency would be further compounded by parameters such as substrate depletion and inefficient denaturation of DNA templates. As a result, it is important not to sample a PCR reaction at the plateau phase where quantification can be ambiguous.

5.3.3 Quantification of cloned DHBV genome

In this experiment, we evaluated the accuracy of measuring a known concentration of input target from a range of cycles as well as end point measurement. According to the mathematical model described above, E_t and E_c are identical provided if both the target and the competitor share a similar template size and sequence internal to the framing primers. We have shown that a minor difference in amplification efficiency had a negligible effect on quantification at early PCR cycles but tended to be significant at terminal stages of the reaction when actual competition for reagents started to take place. In Figure 5.3, using an initial input target template of 1.5 x 10^4 copies, we showed that competitive amplification between the target and the competitor was consistent only over a range of cycles. Within cycles 21 to 30, average accuracy of quantification was 100%. This value would drop dramatically when the PCR products were sampled

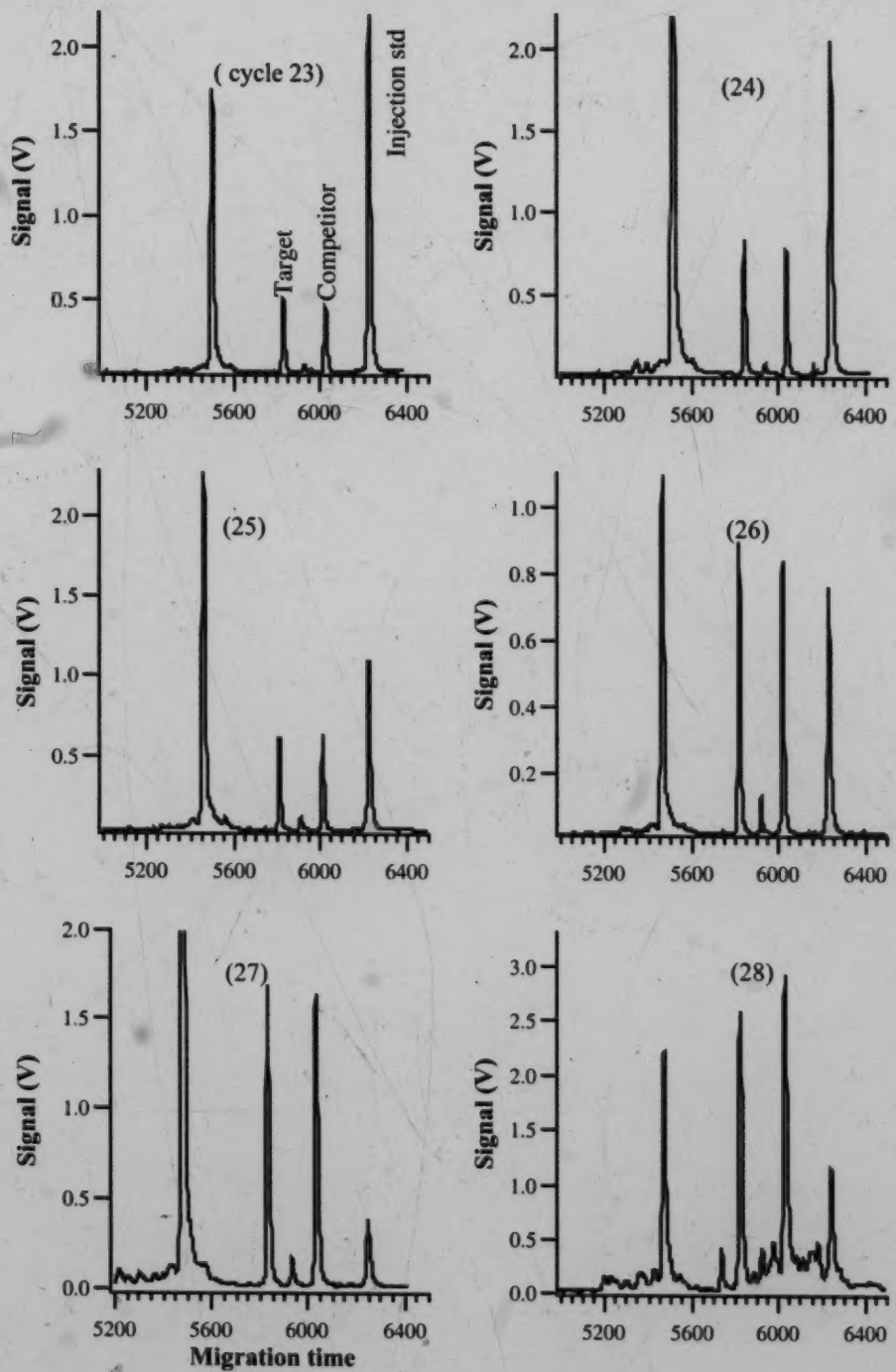
(cycle 23)
Target
Competitor
Injection std
(24)
(25)
(26)
(27)
(28)
Signal (V)
Migration time
5200
5600
6000
6400

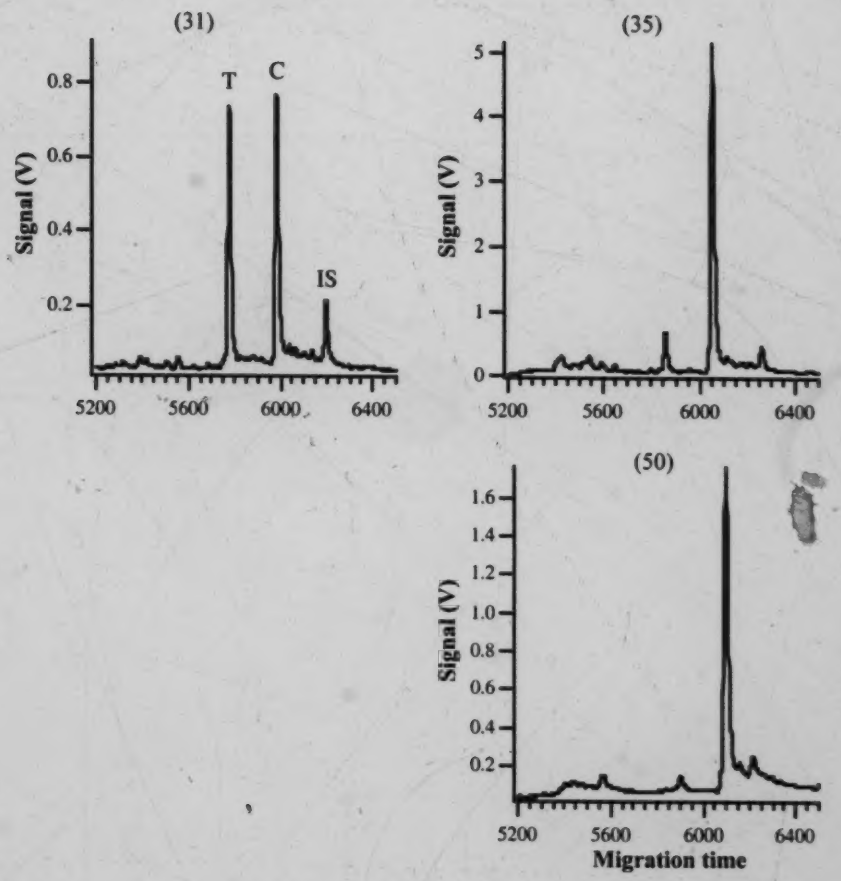

Figure 5.3(a) Influence of cycle number on the accuracy of quantification. Initial input of target and competitor at 1.5 x 10^4 copies, respectively, were PCR amplified. PCR products from cycle 23 to 28, 31, 35 and 50 were compared; T: Target, C: Competitor.

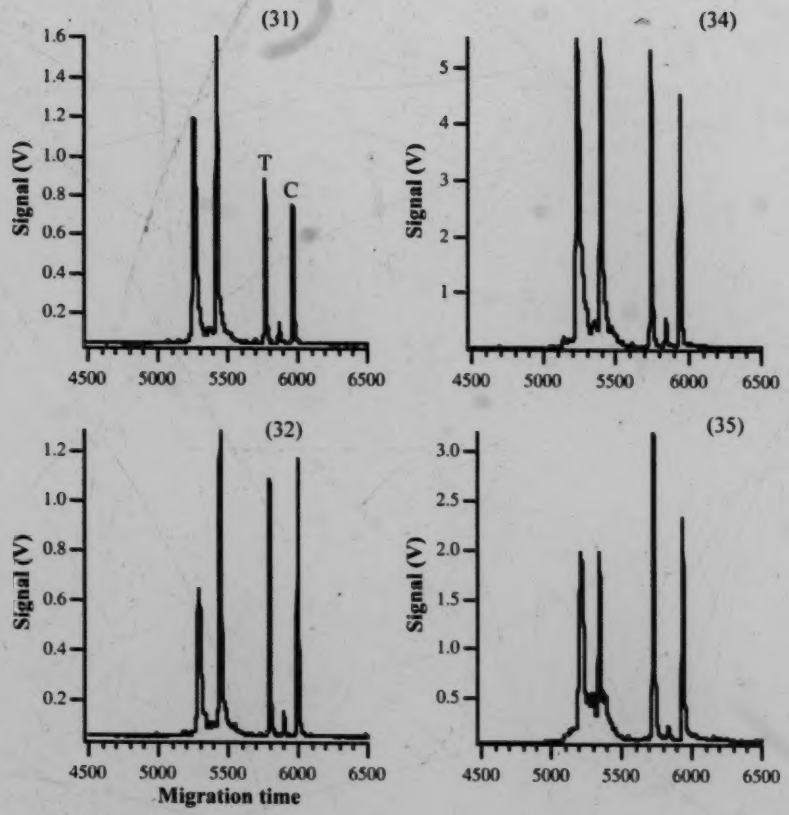

Figure 5.3(b) Influence of cycle number on the accuracy of quantification. Initial input of target and competitor at 150 copies respectively were PCR amplified. PCR products from cycle 31 to 35 were compared; T: Target, C: Competitor.

beyond 30 cycles. Table 5.1 shows the tabulated results of all cycles at high (1.5×10^4 copies) and low (1.5×10^2 copies) initial input templates. As in the case of high initial input template, a similar trend of decline in accuracy was observed when an initial input target template of only 1.5×10^2 copies was used. At lower initial input template, the range of cycles in which PCR products became measurable starting at cycle 26. Between cycles 26 and 40 the ratio of target to competitor remained relatively consistent. As the cycle number increased from 43 to 50, the ratio deviated significantly in favor of the amplification of the competitor. Contrary to the inverse relationship between amplification efficiency and fragment size of amplicon, the 201 bp competitor was shown to be amplified at a better efficiency relative to the 157 bp target. This discrepancy in amplification efficiency was not manifested at early cycles but became significant at higher cycle numbers. We attribute this unusual phenomenon to some possible conformational constraint on the target during denaturation of template. A drop in the efficiency of denaturation hence affects subsequent primer annealing and extension. The above observation suggests that sampling of PCR products at cycle numbers where there is a heavy build up of amplicon is disadvantageous. First, saturation of the reaction chamber with PCR product may affect the denaturation of templates as well as primer annealing. Second, minor differences between the target and the competitor may be more prominent at the plateau phase and third, degradation of the quality of Taq polymerase after repeated cycles of heating and cooling may result in unpredictable error due to a decrease in the fidelity of amplification.

Table 5.1 Competitive amplification as a function of input DNA and cycle number

1.5×10^2 copies initial input target		1.5×10^4 copies initial input target	
Cycle no.	T to C ratio	Cycle no.	T to C ratio
26	1.0	21	1.0
27	0.9	22	1.0
28	1.2	23	1.1
29	1.4	24	1.1
30	1.2	25	1.0
31	1.2	26	1.1
32	0.9	27	1.0
33	1.2	28	0.9
34	1.2	29	0.9
35	1.3	30	0.9
36	0.9	31	0.8
40	0.9	32	0.6
43	0.1	33	0.5
45	0.2	34	0.4
50	0.0	35	0.2
		36	0.9
		50	0.4

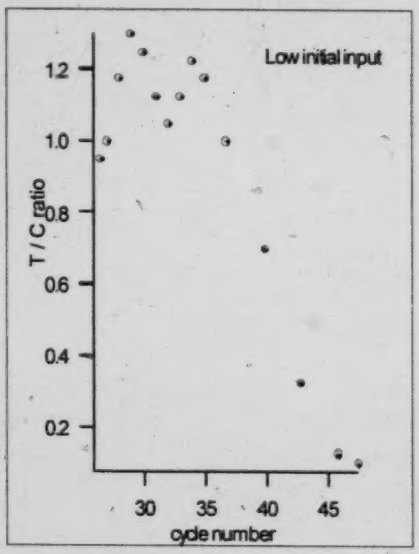

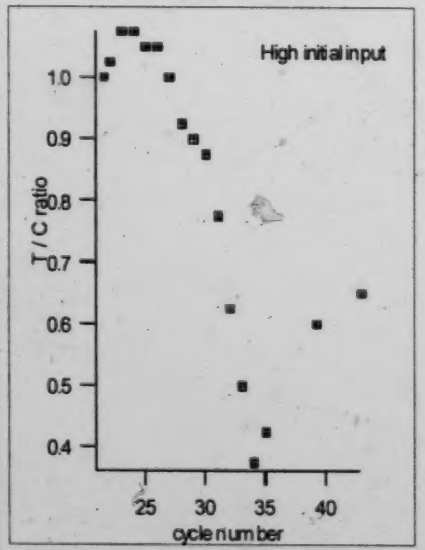

Note: Cycle numbers before 26 in low initial input and cycle numbers before 21 in high initial input did not have enough amplicon that were detectable by QC-PCR-CE-LIF. "T to C" denotes Target to Competitor ratio. Initial input competitor was set at 1.5×10^2 and 1.5×10^4 copies for low and high initial input respectively. The theoretical ratio for both inputs is 1.0.

In Figure 5.4, using an initial input target DNA of 1.5×10^4 copies in the presence of a range of input competitors, we showed a gradual transition from linear to competitive amplification. In contrast to theoretical prediction, the point of intercept as determined from each of the cycles was not identical to each other. This point of intercept is closely comparable from cycles 24 to 27. Outside of this cycle range, the point of intercept deviates significantly from the expected copy number of the input target. Hence a standard QC-PCR where end-point measurement is used will most likely result in larger error as compared to sampling using only a range of cycles in which the difference in efficiency of amplification between the target and competitor is negligible. By using only a range of cycles, estimation of the initial input DNA is expected to be more accurate.

5.3.4 Limit of detection

In practice, the mass sensitivity of LIF detection can be pushed to the attomole (10^{-18} mole) level. Hence assuming maximum efficiency of amplification and an initial input target DNA of at least 2 copies of pAlter-2-W plasmid, 30 cycles of amplification should yield no more than 3.6 fentomole of PCR products. This amount was detectable by our system using a relatively inexpensive He-Ne laser. Figure 5.5 shows a double-log working plot of pAlter-2-W. The log-peak height of the amplified product increased proportionally with the log input copy number. From the plot, linearity was observed between log 0 and 3 input target. Between log 3 and 8, the slope of the plot decreased, in accordance with a change in amplification efficiency as the input target concentration increased. At a high concentration of initial input target, the reaction was rapidly driven to plateau, resulting in deviation from linearity of amplification at low copy number. The

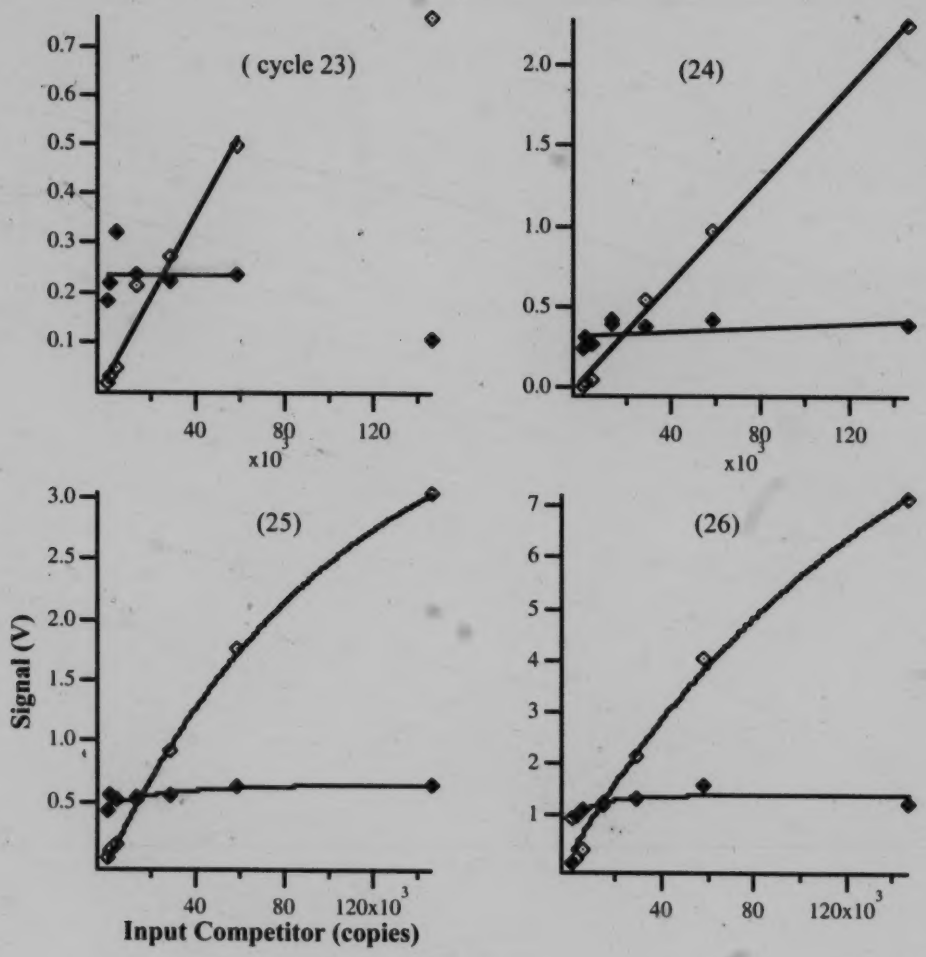

Figure 5.4 Competition profile between target and competitor as a function of cycle number. Cycle numbers 23 to 26 depict amplification of 1.5×10^4 copies of target in the presence of competitor between 1.5×10^3 and 1.5×10^5 copies. Closed diamonds: target; Opened diamonds: competitor.

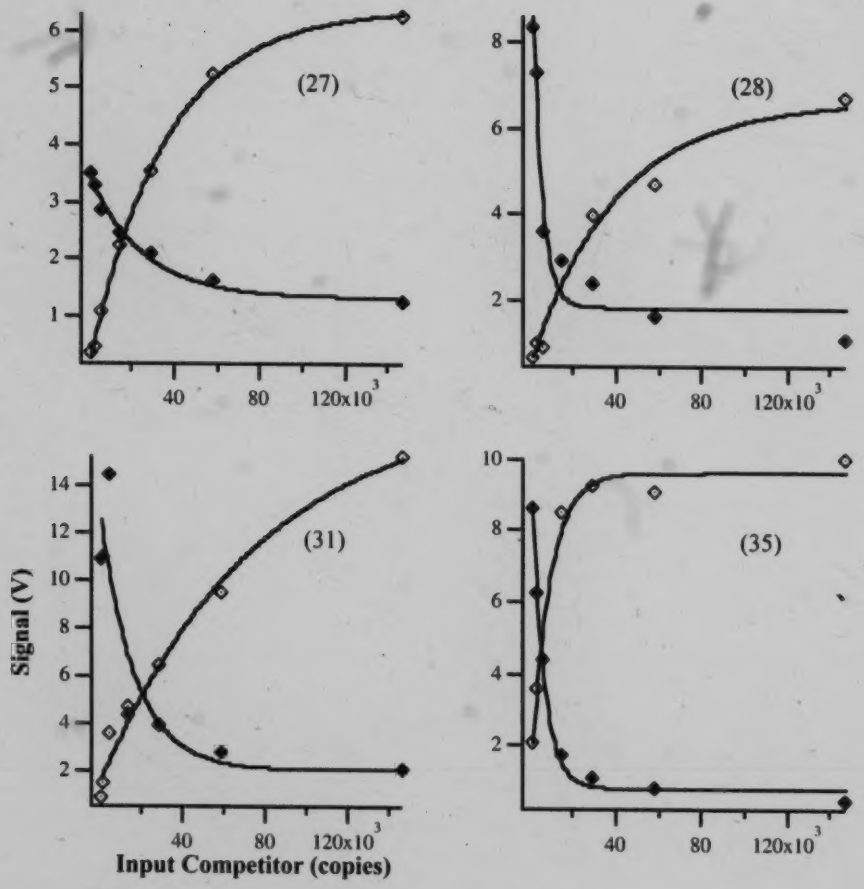

Figure 5.4 Competition profile between target and competitor as a function of cycle number. Cycle numbers 27, 28, 31 and 35 depict amplification of 1.5×10^4 copies of target in the presence of competitor between 1.5×10^3 and 1.5×10^5 copies. Closed diamonds: target; Opened diamonds: competitor.

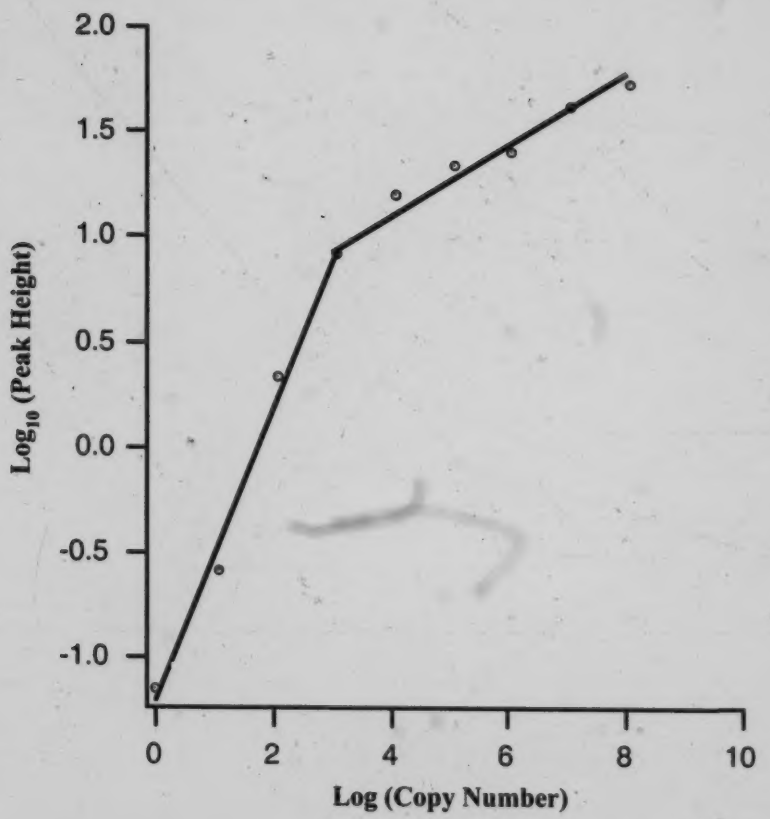

Figure 5.5 Working plot of pAlter-2-W. Serial dilutions of the plasmid were subjected to 30 cycles of amplification. PCR parameters are described in text. PCR products were purified by QIAquick PCR purification. Purified products were added with an internal standard to correct for variation in sample injection. Each data point was derived from PCR sample injected at 1000 V for 10 s. Other CE parameters were similar to that described in Figure 5.1.

first linear range has a dynamic range of 3 logs while the second linear range has 5 orders of magnitude.

5.3.5 Measuring viral load

To measure the level of viral load in sera of animals treated with 3TC, the QC-PCR-CE-LIF protocol described above was used to quantify viral DNA purified from

serum, prior to and after the administration of 3TC. As shown in Table 5.2, serum DHBV DNA as determined from cycles 22 to 29 gives an average value of 1×10^9 genome equivalence per mL of serum in a 10 week old congenitally infected duckling. There was a consistent trend in which the value determined from each cycle decreased with increasing cycle numbers. The value determined from cycle 29 was found to differ by almost 3 fold relative to cycle 22. This observation again suggests that even in the presence of a competitor with comparable amplification efficiency, sampling of PCR products at different cycles may not always produce compatible results. Sampling of PCR products from a range of cycles in which amplification efficiency of both the target and the competitor is consistent will improve accuracy of quantification. Serum sample collected from the same animal 72 hours after the administration of 3TC was shown to have an average of 7×10^7 genome equivalence per ml of serum, a reduction of approximately 14-fold. This estimation is compatible to a 13-fold reduction as determined from an assay using dot blot hybridization (Figure 5.6). A panel of serum samples collected from other animals infected and treated with 3TC indicates significant reduction of viral DNA over a 3-day period of high dosage treatment. Traces of viral DNA were almost undetectable in serum samples collected 6 hours after the treatment was terminated. The extent of reduction in viral DNA in this case was determined from the animal designated P8 and from the serum sample collected prior to the start of the treatment and the serum sample collected at the end of the treatment. By relating the last serum sample directly to the pre-serum level on the basis of ratio, instrumental and quantitative variations between QC-PCR-CE-LIF and dot blot hybridization can be ignored.

The level of viral DNA in serum was also determined from parallel amplification of the pre-treatment samples and the sera samples collected post-treament. The calculated level of reduction from 2 animals investigated was approximately 6-fold. This value was incomparable to the values obtained from QC-PCR-CE-LIF and dot blot hybridization. We attributed this discrepancy to possible variation in amplification when the same target template is being subjected to PCR amplification in separate tubes.

Table 5.2 Quantification of serum DHBV DNA in response to 3TC treatment.

Cycle number	Pre-treatment	Post (72 hours)
22	2×10^9	*
23	2×10^9	*
24	2×10^9	9×10^7
25	1×10^9	8×10^7
26	9×10^8	5×10^7
27	Nd	9×10^7
28	6×10^8	6×10^7
29	8×10^8	Nd
30	Nd	2×10^7

* Quantitative values could not be determined because the range (similar to that used for the pre-serum) of input competitor used for these two cycles is outside the point of intercept. A range with lower input competitor was for the post serum. Unit of virus titer is defined as genome equivalence per mL of serum; cycles 27 and 30 of pre-treatment and cycle 29 of post-treatment were not determined.

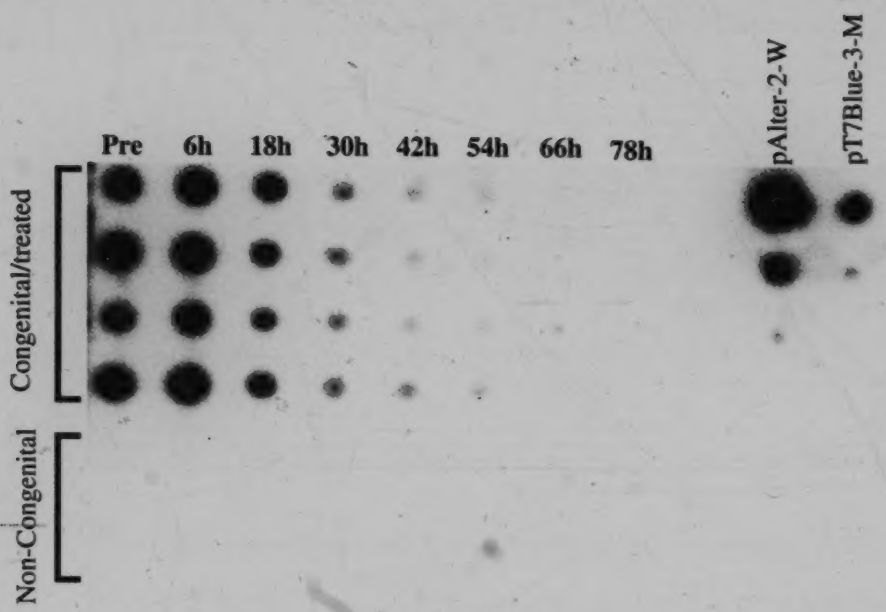

Figure 5.6 Dot blot hybridization detection of DHBV DNA in serum samples of 10 week old ducklings treated with 3TC. Each dot on the blot represents 10 µl of serum. The drug was dissolved in phosphate buffered saline (PBS) at 40 mg/mL. The drug solution was administered intramuscularly at 40 mg/kg, 4 times daily. The placebo group (non-congenitally infected) was given PBS. Serum samples were collected on day 6, 18, 30, 42, 54, 66 and 78 hours after treatment was initiated. Plasmids pAlter-2-W and pT7Blue-3-M were serially diluted and dotted as positive controls.

5.4 Conclusions

Quantitative PCR analysis of HBV viremia in samples from asymptomatic and symptomatic HBV-infected patients suggest a high proportion of these patients are viremic [42, 43]. Quantitative methods for the precise evaluation of HBV DNA levels in serum samples [23] are important for the pathogenic investigation of chronic HBV liver disease.

Using DHBV as a model, we reported excellent separation efficiency for the PCR products of the DHBV genome and their easy quantification using CE-LIF detection. We

believe CE, with its excellent sensitivity and precise measurement of small amounts of amplified DNA, could be valuable in serving as an alternative to conventional slab gel electrophoresis. We analyzed the efficiency of amplification of the target and the competitor for QC-PCR-CE-LIF using a well characterized mathematical model of PCR. The accuracy of this method was tested using carefully quantified cloned DHBV plasmid, and the basic mathematical requirements predicted by the theoretical model of competitive PCR was assessed. As anticipated, differences in the rate of amplification between the target and the competitor limit the accuracy of quantification. These differences fluctuate from cycle to cycle, and tend to present an amplification profile that gives rise to discrepancy in quantification at high cycle numbers. The amplification efficiency of the target relative to the competitor was investigated by comparing our experimental data to eq. 5.3 and eq. 5.4. Equation 5.4 predicts a straight line in the form of $y = mx + c$ when different amounts of the competitor are co-amplified with a constant amount of the target for a given number of cycles. When the ratio of PCR products (T_n/C_n) is plotted as a function of the competitor copy number (C_o) added into eachreaction prior to amplification, a line with a theoretical gradient of -1 is expected. Under this condition, the number of input target (T_o) can be interpolated from the x-axis when $\log T_o = \log C_o$. However in the case where $E_t \neq E_c$, the plot of T_n/C_n as a function of C_o produced error in predicting the initial input T_o. As shown in Table 5.3, the gradients determined from cycles investigated were between 1 and 24 % of the value -1. A gradient of -1 reflects similar efficiency between E_t and E_c. A gradient that deviates from -1 indicates non-compatibility between E_t and E_c. The value of T_o estimated under this condition was shown to be less accurate than the T_o values derived from plots

Table 5.3 Experimental gradient of competitive amplification between T and C

Cycle no.	Gradient	R value	$T_{o\ (estimated)}$	Relative error
23	-1.04	-0.986	2.5×10^4	66.7
23	-1.11	-0.988	2.4×10^4	60.0
24	-1.08	-0.988	1.9×10^4	26.7
24	-1.06	-0.983	2.5×10^4	66.7
25	-0.90	-0.992	1.8×10^4	20.0
25	-0.92	-0.995	2.0×10^4	33.3
26	-1.00	-0.996	1.8×10^4	20.0
26	-1.00	-0.996	1.8×10^4	20.0
27	-1.01	-0.994	1.8×10^4	20.0
27	-1.10	-0.994	1.8×10^4	20.0
28	-0.97	-0.995	1.8×10^4	20.2
31	-1.03	-0.995	1.9×10^4	26.7
35	-1.24	-0.962	7.8×10^3	48.0
35	-1.02	-0.985	4.8×10^3	68.0

Note: All cycles presented here (except cycle 31) were repeated to show reproducibility. Initial input target was set up 1.5×10^4 copies. The values of the gradient were derived from plots of the ratio of PCR products (T_n/C_n) plotted as a function of the competitor copy number (C_o) added into each reaction prior to amplification. R value denotes correlation coefficient of the plot.

(shown in Figure 5.4 and Table 5.1) where the point at which the target and competitor plots intercept. From Table 5.3, there was no direct correlation between the value of the gradient and the accuracy of predicting T_o. We found that the plot of (T_n/C_n) versus (C_o)

consistently produced T_o values that were at least 10% less accurate compared to using the point of intercept. The discrepancy between these two plotting methods could be explained in terms of the fluctuation of E_t and E_c. In the case of (T_n/C_n) versus (C_o), when $E_t \neq E_c$, and the values of E_t and E_c fluctuate (as demonstrated in Figure. 5.2) in such a way that the ratio of E_t / E_c is constant, the plot obeying eq. 5.4 would be shifted in parallel without change of the slope. The amplitude of the shift and hence the error in the quantification of T_o is independent of the gradient of the plot.

Our data suggest that the point of intercept between two independently plotted target and competitor curves is a more reliable approach in predicting the value of T_o. By plotting the target and the competitor curves separately as opposed to constructing a single plot using T/C, parallel shift and hence error described above can be easily avoided.

Since the amplification pattern stays constant for only a limited number of cycles, we investigated the point of intercept from a range of cycles. By obtaining an average value of T_o from a range of cycles, quantitative error commonly associated with the conventional approach of using end point measurement at a given cycle can be minimized.

In order to increase throughput, the current technology has to be applied to a semi or fully automated system. With the implementation of a multi-capillary format, the point of intercept can be observed from a range of cycles in a single CE run, followed by real time data processing. This is one important criterion that has to be met to allow quantitative competitive PCR to be carried out on a routine basis. The impact of this aspect may be dramatic in the near future in medical virology laboratories. This is

particularly true if an increasing number of specific anti-viral compounds or new efficient strategies for the treatment of viral infections are introduced in clinical practice.

5.5 Bibliography

1. Altria, K.D. and Rudd, D.R. (1995) Chromatographia **41**, 325-331.
2. Altria, K.D. (Ed.). (1996) Capillary Electrophoresis Guidebook, Humana, Totowa (NJ)
3. Kunkel, A., Degenhardt, M., Schirm, B. and Watzig, H. (1997) J. Chromatogr. A **768**, 17-27.
4. Saiki, R.K., Scharf, S., Faloona, F., Mullis, K.B., Horn, G.T., Erlich, H.A. and Arnheim, N. (1985) Science **230**, 1350-1354.
5. Erlich, H.A., Gibbs, R. and Kazazian H.H. (1989) Polymerase chain reaction. Current communications in molecular biology. Cold Spring Harbor Laboratory, Cold Spring Harbor, New York.
6. Erlich, H.A., ed. (1989). PCR technology: Principles and applications for DNA amplification. Stockton Press.
7. Rolfs, A, Schuller, I., Finckh, U. and Weber, R.I. (1992) PCR. Clinical Diagnostics and Research. Springer-Verlag, Berlin, Germany, p.11.
8. Wackym, P.A., Simpson, T.A., Gantz. B.J. and Smith, J.H. (1993) Laryngpscope **103**, 583-588.
9. Hruza, C., Dobianer, K., Beck, A. et al. (1993) Eur. J. Cancer **29**. 1593-1597.

10. Coutlee, F., He, Y., Saint-Antonie, P., Olivier, C. and Kessous, A. (1995) Hum. Retroviruses **11**, 363-371.

11. Clementi, M.P., Bagnarelli, P., Manzin, A. and Menzo, S. (1994) Genet. Anal. Tech. Appl. **11**, 1-6.

12. Clementi, M.P., Menzo, S., Bagnarelli, P., Manzin, A., Valenza, A. and Varaldo, P.E. (1993) PCR Methods Appl. **2**, 191-196.

13. Clementi, M.P., Menzo, S., Manzin, A. and Bagnarelli, P. (1995) Arch. Virol. **140**, 1523-1539.

14. Cross, N.C.P. (1995) Br. J. Haematol. **89**, 693-697.

15. Ferre, F. (1992) PCR Methods Appl. **2**, 1-9.

16. Foley, K.P., Leonard, M.W. and Engel, J.D. (1993) Trends Genet. **9**, 380-385.

17. Siebert, P.D. and Larrick, J.W. (1992) Nature. **359**, 557-558.

18. Becker-Andre, M. (1993) Methods Enzymol. **218**, 420-445.

19. Gilliand, G, Perrin, S. and Bunn, H.F. (1990) Proc. Natl. Acad. Sci. USA **87**, 2725-2729.

20. Gilliand, G, Perrin, S. and Bunn, H.F. (1992) A Guide to Methods and Applications, Academic, San Diego, CA, pp. 60-69.

21. Huang, S.K., Essayan, D.M., Krishnaswamy, G., Yi, M., Kumai, M., Su, S.N., Xiao, H.Q., Lichtenstein, L.M. and Liu, M.C. (1994) J. Immunol. Methods **168**, 167-181.

22. Kumar, U., Thomas, H.C. and Monjardino, J. (1994) J. Virol. Methods **47**, 95-102.

23. Lehtovaara, P., Uusi-Oukari, M., Buchert, P., Laaksonen, M., Bengtstrom, M. and Ranki, M. (1993) PCR Methods Appl. **3**, 169-175.

24. Scheuermann R.H. and Bauer S.R. (1993) Methods Enzymol. **218**, 446-473.

25. Zipeto, D., Baldanti, F., Zella, D., Furione, M., Cavicchini, A., Melanesi, G. and Gerna, G. (1993) J. Virol. Methods **44**, 45-56.

26. McCulloch, R.K., Choong, C.S. and Hurley, D.M. (1995) PCR Methods Appl. **4**, 219-226.

27. Cottrez, F., Auriault, C., Capron, A. and Groux, H. (1994) Nucleic Acids Res. **22**, 2712-2713.

28. Scadden, D.T., Wang, Z. and Groopman J.E. (1992) J. Infect. Dis. **165**, 1119-1123.

29. Becker-Andre, M. and Hahlbrock, K. (1989) Nucleic Acids Res. **17**, 9437-9446.

30. Menzo, S.P., Bagnarelli, P., Giacca, M, Manzin, A., Varaldo, P.E. and Clementi, M. (1992) J. Clin. Microbiol. **30**, 1752-1757.

31. Piatak, M., Saag, Jr. M.S., Yang, L.C., Clark, S.J., Kappes, J.C., Luk, K.C., Hahn, B.H., Shaw, G.M. and Lifson, J.D. (1993) Science **259**, 1749-1754.

32. Apostolakos, M.J., Schuermann, W.H.T., Frampton, M.W., Utell, M.J. and Willey, J.C. (1993) Anal. Biochem. **213**, 277-284.

33. De-Kant, E., Rochlitz, C.F. and Herrmann, R. (1994) BioTechniques **17**, 934-942.

34. Hahn, M., Dorsam, V., Friedhoff, P., Fritz, A. and Pingoud, A (1995) Anal. Biochem. **229**, 236-248.

35. Heid, C.A., Stevens, J., Livak, K.J. and Williams, P.M. (1996) Genome Res. **6**, 987-994.

36. Gibson, U.E.M., Heid, C.A. and Williams, P.M. (1996) Genome Res. **6**, 995-1001

37. Wittwer, C., Ririe, K., Andrew, R., David, D., Gundry, R. and Balis, U. (1997) BioTechniques **22**, 176-181.

38. Wittwer, C., Herrmann, M., Moss, A. and Rasmussen, R. (1997) BioTechniques **22**, 130-138.

39. Orlando, C., Pinzani, P. and Pazzagli, M. (1998) Clin. Chem. Lab. Med. **36**(5), 255-269.

40. Raeymaekers, L. (1993) Anal. Biochem. **214**, 582-585.

41. Santagati, S., Bettini, E., Asdente, M., Muramatsu, M. and Maggi, A (1993) Biochem. Pharmacol. **46**, 1797-1803.

42. Gerken, G., Paterlini, P., Manns, M., Housset, C., Terre, S., Dienes, H-P., Hess, G., Gerlich, W.H., Berthelot, P., Meyer zum Buschenfelde, K.H. and Brechot, C. (1991) Hepatology **13**, 158-166.

43. Manzin, A., Salvoni, G., Bagnarelli, P., Menzo, S., Carloni, G. and Clementi, M. (1991) J. Virol. Methods **32**, 245-253.

Chapter 6. Analysis of Single Cells using CE-LIF

A shorter version of this chapter has been published.
X.C. Le, W. Tan, C.H. Scaman, A. Szpacenko, E. Arriaga, Y. Zhang, N.J. Dovichi, O. Hindsgaul and M.M. Palcic. 1999 Glycobiology **9**, 219-225.

6.1 Introduction

In 1953, Edstrom used fine silk fibers of 15-μm diameter and 1 to 2 cm in length for the electrophoretic determination of a hundred picograms of RNA contained within a single cell [1]. Since then, the study of the chemical contents of individual biological cells has attracted increasing attention. These studies arise from a fundamental interest in cell heterogeneity and potential applications of single-cell assays to clinical diagnosis and pharmaceutical research. There has been much activity in the analysis of neurotransmitters [2,3] contained within individual neurons because of interest in neurochemistry and also the availability of sensitive electrochemical detectors for neuroactive amines. Much of this work has relied on the use of large (200-μm) ganglia from snails. There are a number of other single-cell analytical techniques. Neher and coworkers have used microinjection to load a cell with a calcium-sensitive fluorescence dye and subsequently used fluorescence microscopy to measure the calcium concentration in single rat peritoneal mast cells [4]. They further developed patch-clamping techniques, which can provide information on ion channels and signaling networks, within an individual cell [5]. Flow cytometry also provides a rapid method for counting and sorting normal and abnormal cell populations [6]. Yeung and colleagues [7-9] have assayed lactate dehydrogenase and glucose-6-phosphate dehydrogenase in single human erythrocytes using capillary electrophoresis with laser induced fluorescence detection (CE-LIF), demonstrating the utility of CE-LIF for single-cell analysis. More recently Chiu and coworkers [10] have combined CE-LIF with optical trapping to study single secretory vesicles from the atrial gland of the gastopod mollusk *Aplysia californica*. They identified taurine, a possible neuromodulator or hormone, as one of the

most abundant molecules present in atrial gland vesicles. Capillary electrophoresis techniques for the analysis of single cells have been recently reviewed [11,12].

Glycosyltransferases and glycosidases are important enzymes responsible for the formation and hydrolysis of oligosaccharides, respectively. Assay of the activity of these enzymes is essential to understanding their roles in biology. There have been several reports on the detection of glycosidase activity in single cells using non-fluorescent substrates that are enzymatically hydrolyzed to yield the detectable fluorophores [13-16]. These assays require 4000 molecules of hydrolase, yielding ~1 femtomole of product, which is detected within the cells [16]. Some of these assays further require that lipophilic substrates pass through a cell membrane. As a result, there is ambiguity in the assays because the fluorescence signal is related to both the uptake of the substrate by the cell and the enzyme activity within the cell.

Several reports have demonstrated the use of capillary electrophoresis separation and analysis of labeled oligosaccharides. Honda et al. [17] derivatized monosaccharides to N-2-pyridylglycamines and analyzed these derivatives using capillary electrophoresis with UV detection. They obtained a detection limit of 10 picomoles. Novotny's group pioneered the use of CBQCA as a fluorogenic reagent to label oligosaccharides [18-21]. They achieved detection limits of 0.5 attomole (300,000 molecules) of labeled monosaccharides using on-column laser-induced fluorescence detection. It is not clear if these derivatized monosaccharides would act as substrates for enzymes. Lee *et al.* [22] developed an electrophoresis-based assay for glycosyltransferases. Using capillary electrophoresis separation and laser-induced fluorescence detection of fluorescent-sugar

conjugates (7-amino-1,3-naphthalenedisulfonic acid), they obtained a detection limit of 80 femtomole.

We have previously developed ultrasensitive assays for glycosidases and glycosyltransferases, using CE-LIF detection [23-25]. The CE-LIF technique can resolve isomeric oligosaccharides at a detection limit of $8x10^{-23}$ mole (or 50 molecules) of tetramethylrhodamine-labeled saccharides. The conversion of a fluorescent substrate to more than one product can also be monitored. Our techniques are several orders of magnitude more sensitive than the most sensitive technique previously reported for these enzymes [22]. The rate limiting enzyme activity can be measured by the action of either competing or sequential enzymes because of the efficient separation and sensitive detection of the fluorescent substrate and products. We report here our studies of enzyme assay in single yeast cells, by CE-LIF. We also present results on the uptake of fluorescently labeled substrate by yeast cells using confocal laser scanning microscopy.

6.2 Experimental

6.2.1 Fluorophores and buffering condition

Fluorescent dye tetramethylrhodamine N-hydroxysuccinimide ester was obtained from Molecular Probes (Eugene, OR). Fluorescently labeled oligosaccharides were prepared as described previously [25,26]. Stock solutions including 0.1 M Na_2HPO_4 (Fisher), 0.1 M tetraborate (Fisher), 0.1 M sodium dodecyl sulfate (BDH) and 0.1 M phenylboronic acid (Sigma) were prepared in deionized water (Barnstead NANO pure system) and filtered with 0.2 μm pore size disposable filter (Nalgene). The electrophoresis running buffer was prepared by mixing these stock solutions to final

concentrations of 10 mM Na_2HPO_4, 10 mM tetraborate, 10 mM sodium dodecyl sulfate and 10 mM phenylboronic acid (pH 9.3). Unless otherwise indicated, all reagents were of analytical reagent grade.

6.2.2 Incubation of yeast cells with triglucoside

Saccharomyces cerevisiae (baker's yeast, Fleischman) was grown on Sabouraud dextrose agar plates (Difco) at 37°C, and then stored at 4°C. A typical colony was inoculated into 1 mL sterile Sabouraud dextrose media and grown over night at room temperature with shaking. A subsample of 200 µL was transferred to a sterile micro-centrifuge tube and pelleted by centrifugation at 14,000 rpm for 2 min. Old media was removed and fresh media (1 mL) was added to the pelleted cells along with sterile filtered TMR-trisaccharide, α-D-Glc(1→2) α-D-Glc(1→3) α-D-Glc-$O(CH_2)_8CONHCH_2CH_2NHCO$-TMR, from a 5 mM stock solution. The final concentration of the labeled trisaccharide was 50 µM. The cell suspension was incubated at 37°C for a measured time period. At incubation intervals of 5 min, 1, 2, 3, 4, 5 and 24 hours, 100 µL of the cell suspension sample was withdrawn and washed thoroughly with phosphate buffered saline (PBS). The cells were then subject to confocal laser scanning microscopy analysis to study the uptake of the TMR labeled trisaccharide by the yeast cells. A parallel control containing the same amount of the yeast cells and media but without the TMR-triglucoside substrate was carried out under the identical conditions.

6.2.3 Generation of spheroplasts

Cells from parallel 1 mL incubations were transferred to the surface of a 0.45 µm 47-mm HVLP filter (Millipore) and washed under vacuum with 500 mL of PBS, pH 6.0 containing 2% sucrose. A final fraction of the filtrate was collected for analysis by

capillary electrophoresis, ensuring that extracellular substrate was completely washed out. Cells were then washed from the membrane into a test tube with the same buffer, pelleted, and washed with 200 µL of 25 mM Tris-HCl, pH 7.5, and 2 M sorbitol. Spheroplasts were generated from the cells by incubating in 25 mM Tris-HCl, pH 7.5, and 2 M sorbitol containing 770 U/100µL lyticase (*Arthrobacter luteus*, Sigma) for 2 hours at 25°C.

6.2.4 Confocal laser scanning microscopy

A 20 µL aliquot of each cell sample was examined by a Model 2001 confocal laser scanning microscope (Molecular Dynamics, Sunnyvale, CA). An argon / krypton gas laser was used as the excitation source, with 568 nm wavelength selected for TMR. The fluorescence was collected using a 100x objective with oil immersion. The fluorescence intensity of TMR was measured at 590 nm. Data were digitized using the Image Space 3.1 software of the Model 2001 confocal microscope.

6.2.5 Inhibition of substrate hydrolysis

Castanospermine (Boehringer Mannheim), a competitive inhibitor of α-glucosidase I, was used to inhibit the hydrolysis of the trisaccharide substrate. *S. cerevisiae* was grown on Sabouraud dextrose broth at 25°C with shaking for 72 hours in an Erlenmeyer flask. The cell densitiy of the culture was measured at between 32.0 and 37.0 OD_{600} after 72 hours incubation. A 2 mL aliquot of the 72-hour culture was then transferred into a 10 mL glass tube. The cells were spun and replaced with 1 mL of fresh media containing 12 µM of castanospermine. Following 24 hours of exposure to castanospermine alone, fresh media was again replaced, and the same concentration of the inhibitor as well as 50 µM trisaccharide substrate were added. The cells were grown

for another 24 hours prior to processing and sampling. Control experiments were carried out in parallel with only the addition of trisaccharide substrate. The cells were washed thoroughly and subjected to a 17-hour lyticase treatment as described above to facilitate cell lysis. The lysate was filtered thorough a 0.45 μm PVDF filter (Millipore) to remove cell debris. The filter membrane was then washed with 2 mL of methanol to remove bound dye-labeled substrate or product. The methanol filtrate and the filtrate from the lysate were combined for lyophilization. The dried pellet was resuspended in electrophoresis buffer as described above.

6.2.6 Capillary electrophoresis laser-induced fluorescence analysis

All CE-LIF analyses reported in this study were carried out by using a locally constructed CE instrument as described previously [25]. Briefly, the electrophoresis was driven by a CZE1000R high voltage power supply (Spellman, Plainview, NY). Separation was carried out in a 50-cm long, 10 μm or 30 μm inner diameter fused-silica capillary (Polymicro, Phoenix, AZ) at an electric field of 400 V/cm. The aqueous electrophoresis buffer contained 10 mM each of phosphate, tetraborate, phenylboronic acid, and sodium dodecylsulfate (SDS), at pH 9.3. The sheath fluid was identical to the running buffer and was gravity fed from a 250-mL wash bottle. A 1.0-mW helium-neon laser (Melles Griot, Nepean, Canada) beam, λ=543.5 nm was focused into a post-column sheath-flow cuvette. Fluorescence was collected at a right angle with a high numerical aperture (0.7 N.A.) microscope objective (60X) (Universe Kogaku Model 60X-LWD, Oyster Bay, NY), spectrally filtered with a band-pass filter (580DF40) (Omega Optical, Brattleboro, VT), imaged onto one end of a SELFOC fiber collimator (p-type, NSG America, Somerset, NJ), and detected at the other end of the fiber collimator with a

R1477 photomultiplier tube (Hamamatsu, Bridgewater, NJ). Data was digitized by a NB-MIO-16X data acquisition board (National Instruments, Austin, TX) in a Macintosh Quadra 650 computer.

6.2.7 Single spheroplast introduction

Figure 6.1 shows a schematic diagram for the introduction of a single cell into a capillary for electrophoresis analysis. Approximately 1 cm of coating from one end of the 50-cm separation capillary was removed. This end was then etched by using hydrofluoric acid (39%) for 10-15 min. The capillary was filled with aqueous electrophoresis buffer prior to the etching and periodically flushed with the buffer during the etching, in order to minimize the damage of the inner wall and to maximize the etching of the outer wall of the capillary. The etched, sharp tip (approximately 1-5 μm wall thickness) of the capillary was positioned at the injection end, and the other end of the capillary was inserted into the sheath flow cuvette. The etched, injection end of the capillary was held to a coarse micro-manipulator MX100R and a hydraulic-controlled fine micro-manipulator MX630R (Newport/Klinger, Mississauga, ON), both of which could be used to move the capillary in three dimensions. A cell suspension (2-5 μL) was placed on the center of a depressed glass slide. An inverted fluorescence microscope IMT-2 (Olympus, Lake Success, NY) was used to view the cells and the injection end of the capillary. When an appropriate cell was located, the capillary tip was moved close to the cell, with the aid of the micro-manipulator. A gentle suction from the detection end of the capillary was created by using an air-tight syringe or a syringe pump. A single cell along with minimum surrounding solution was introduced into the capillary under the microscope view. Immediately after the cell was introduced into the capillary, suction

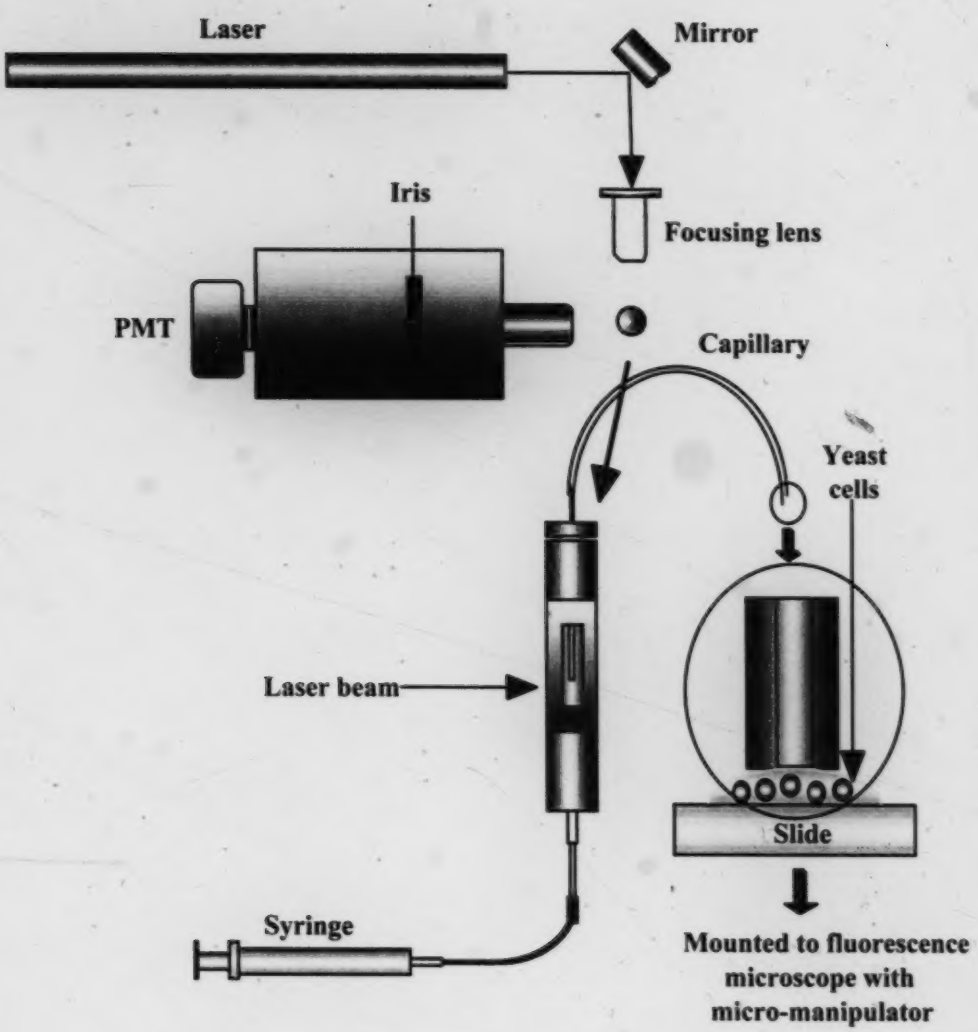

Figure 6.1 A schematic diagram showing the introduction of a single cell into a capillary for subsequent analysis by capillary electrophoresis with laser induced fluorescence detection. Inset is an expanded view of capillary-sample interface.

was stopped, the injection end of the capillary was removed from the glass slide and placed into an electrophoresis buffer vial. A high voltage (20,000 V) was applied for 10 seconds to drive the electrophoresis buffer flowing into the capillary. The high voltage was stopped for one minute before reapplied. At this moment, the electrophoresis buffer, containing 10 mM each of phosphate, tetraborate, phenylboronic acid, and sodium dodecylsulfate (SDS), surrounds the spheroplast. The single spheroplast was lysed inside the capillary by non-physiological buffer and the presence of SDS. The intracellular substrate and enzyme products from the single cell were electrophoretically separated in the capillary and were detected by laser-induced fluorescence. A similar amount of solution surrounding the cells in the cell suspension was also injected separately and analyzed in a similar manner, confirming undetectable fluorescence in the solution.

6.2.8 Analysis of non-lyticase treated yeast cells

In this section, a yeast culture incubated with TMR-trisaccharide was prepared using a similar procedure as described in section 6.2.2. The cell suspension after 24 hours incubation was washed thoroughly with PBS prior to single-cell analysis. Selection of single cell was based on the criterion of fluorescence or non-fluorescence microscopic visualization. An electric field of 600 V/cm was applied across a 40-cm capillary to drive the separation after cell injection.

6.2.9 Monitoring intra and extracellular substrate hydrolysis

To further determine the fate of the hydrolytic products, the yeast media and lysate were analysed in parallel on a time course basis. A stationary-phase culture of *S. cerevisiae* was prepared by subculturing an isolated colony from a Sabouraud dextrose agar plate (Difco) into Sabouraud dextrose media on a rotor in a 37°C incubator. The

culture was then incubated with 50μM of TMR-trisaccharide in the same media. A 200 μL aliquot of the culture was withdrawn at specified intervals. The media from each aliquot was kept for CE analysis. The cells were washed thoroughly with PBS containing 10% ethanol. The washed cells were converted into spheroplasts using the protocol as described above. Following an overnight lyticase incubation at room temperature, the sample was subjected to a 1.5 hour sonication (Cole-Parmer, Model 8890) to ensure complete lysis of all spheroplasts. The lysate was filtered by a 0.45 μm ultrafree-MC filter to remove large fragments of cell debris.

6.3 Results and Discussion

Figure 6.2 shows typical photographs from confocal laser scanning microscopy study of the yeast cells that were incubated with TMR-triglucoside, α-D-Glc(1→2) α-D-Glc(1→3) α-D-Glc-O$(CH_2)_8$CONHCH_2CH_2NHCO-TMR, for 5 min, 1 hour and 24 hours. By 1 hour of incubation many cells are fluorescent and some show intense fluorescence. The difference in fluorescent intensity is attributed to the heterogeneity of the cells; for instance, uptake may vary with the age and the viability of the cells, which are different in a cell population. Further incubation to 2, 3, 4, 5, and 24 hours resulted in increased uptake of the fluorescent substrate. Intense fluorescence from the cells after 24 hours of incubation is shown in Figure 6.2. Control experiments where the cells were incubated without the fluorescent substrate did not show detectable fluorescence.

If dye adherence to the cell surface contributes substantially to the fluorescence of the cell, incubation of the cells with the dye for as short as several minutes should result in cell fluorescence. This is clearly not the case, since cells incubated for 5 minutes with

the TMR-labeled trisaccharide show no detectable fluorescence. It is expected that adsorption of the dye by the cell surface would be much faster than the uptake process. Thus, the fluorescence observed in the yeast cells following 1 hour and 24 hours incubation is primarily due to the uptake of the TMR-labeled trisaccharide and not due to the adsorption of the dye on the cell surface.

A detailed examination of a single yeast cell shows that the fluorescence is localized throughout the cell (Figure 6.2d, 24h/0.5 μm), indicating that the TMR analogue can pass through the cell wall and membrane, and accumulate inside the cell. The resolution from the confocal scanning system does not provide details of organelle localization. Therefore organelle-specific accumulation of the substrate could not be interpreted from the photographs. However, the design of the substrate described below eliminates a requirement for exact cellular localization in monitoring *in vivo* transformation since its hydrolysis is controlled by α-glucosidase I, found only in the endoplasmic reticulum.

Since confocal laser scanning microscopy does not allow for the identification of the fluorescent species, CE-LIF analysis was employed to characterize the fluorescent substrate and any conversion products from enzymatic transformation within the cells. Hydrolysis of α-D-Glc(1→2) α-D-Glc(1→3) α-D-Glc-O$(CH_2)_8$CONHCH_2CH_2NHCO-TMR by α-glucosidase I gives TMR- disaccharide, α-D-Glc(1→3) α-D-Glc-O$(CH_2)_8$CONHCH_2CH_2NHCO-TMR. The disaccharide can either be sequentially hydrolyzed to monosaccharide α-D-Glc-O$(CH_2)_8$CONHCH_2CH_2NHCO-TMR and the linking arm by α-glucosidase II and/or other α-glucosidases or converted directly to the

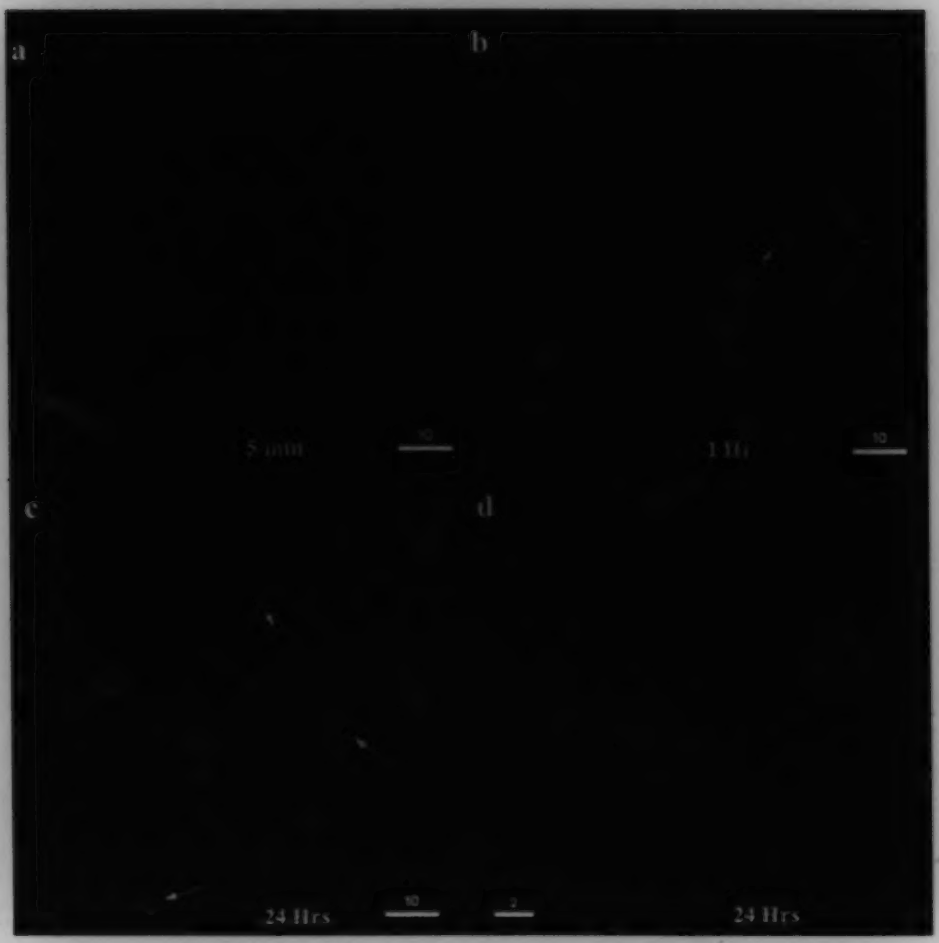

Figure 6.2 Photographs obtained by using confocal laser scanning microscopy. Yeast cells were incubated with 50 μM of the tetramethylrhodamine (TMR) labeled triglucoside, α-D-Glc(1→2)α-D-Glc(1→3)α-D-Glc-O$(CH_2)_8$CONHCH_2CH_2NHCO-TMR, at 37 °C for (a) 5 min, (b) 1 hr, (c) and (d) 24 hr. The scale bars in (a), (b), and (c) represent 5 μm, and in (d) 0.5 μm. Intensity of orange color corresponds to the intensity of fluorescence from TMR. (λ_{ex}=568 nm and λ_{em}=590 nm)

linking arm by endo-glucosidases. Figure 6.3 shows an electropherogram obtained from the analysis of the standard mixture of substrate and all potential hydrolytic products. TMR-trisaccharide (T) substrate is well resolved from the expected products, TMR-disaccharide (D), TMR-monosaccharide (M), and the TMR-linker arm (L). The baseline separation was achieved by using micelles (SDS) as well as borate and phenylboronic acid in the running buffer solution. The use of borate and phenylboronic acid enhances resolution because their complexation with sugar hydroxyl groups results in the electrophoretic differences between the neutral saccharides [17,27,28]. The detection limit for the TMR-labeled saccharides using the CE-LIF system was approximately 8×10^{-23} moles (or 50 molecules). The excellent detection and resolution make the present technique suitable for the determination of enzyme products and substrate in single cells.

Figure 6.3b and c show electropherograms of the supernatant of the incubation media that contains only unmodified trisaccharide substrate and the final cell-wash solution prior to preparing spheroplasts. The analysis of the last PBS wash solution does not show a detectable level of saccharides. This ensures that results from spheroplast analysis were due only to the compounds present inside the cells. Only background fluorescence was detected in the solution surrounding the spheroplasts.

Figure 6.4a shows electropherograms of the contents of spheroplasts prepared from yeast cells grown in the presence of 50 μM trisaccharide for 24 hours. Hydrolysis of substrate produced mainly the linker arm, with minor amounts of monosaccharide and disaccharide intermediates. The peak intensity of the linker arm was normalized against the substrate with a 0.78 linker arm / trisaccharide (L/T) ratio. This ratio represents the

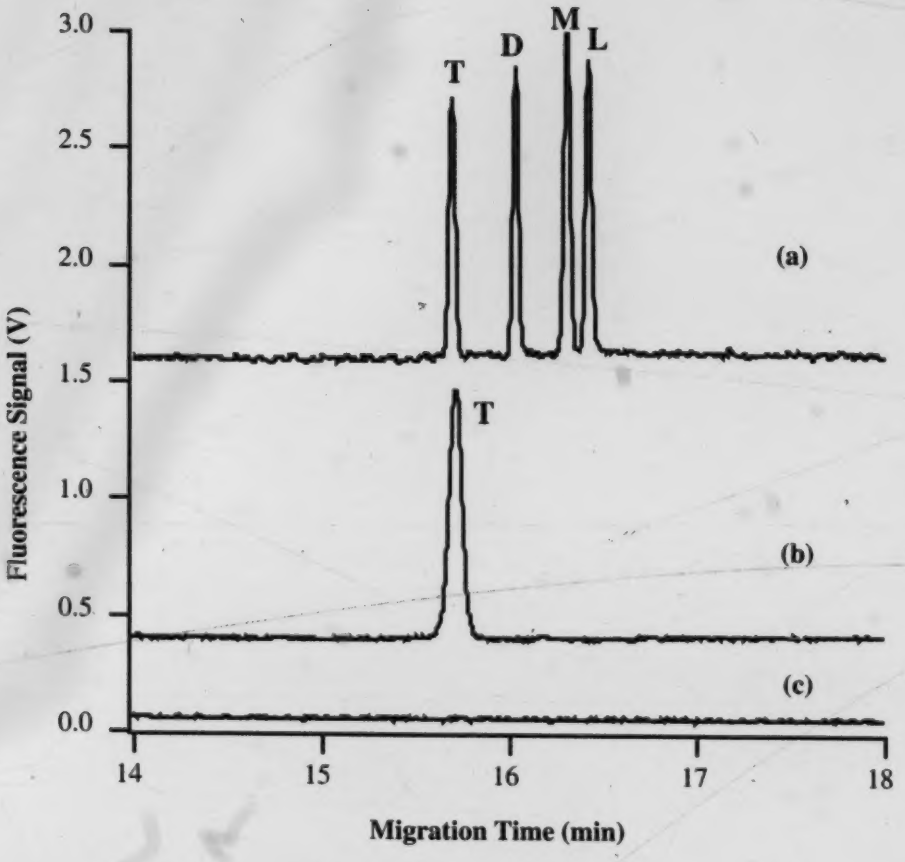

Figure 6.3 Electropherograms obtained from CE-LIF analysis of : (a) standards containing 10-9 M of each of the TMR derivatiaves: α-D-Glc(1→2) α-D-Glc(1→3) α-D-Glc-O(CH2)8CONHCH2CH2NHCO-TMR(T); α-D-Glc(1→3) α-D-Glc-O(CH2)8CONHCH2CH2NHCO-TMR(D); α-D-Glc-O(CH2)8CONHCH2CH2NHCO-TMR(M); and the TMR-linker arm HO(CH2)8CONHCH2CH2NHCO-TMR (L), (b) supernatant from the incubation media, (c) wash solution. A 50 cm capillary (10 μm i.d.) was used for electrophoretic separation under 20,000 V. The electrophoresis buffer contained 10 mM each of phosphate, tetraborate, phenylboronic acid, and sodium dodecyl sulfate (SDS).

extent of hydrolysis as a function of the initial substrate concentration. The ratio ranged from 0.5 to 0.9 in repeated experiments. This variation is attributed to cell-to-cell differences in the uptake and localization of substrate in the endoplasmic reticulum. To date no other enzymes besides α-glucosidases I have been found which hydrolyze this trisaccharide substrate. No glucose release was detected in a standard assay [29] when the trisaccharide was incubated with commercial brewers yeast α-glucosidase, bakers yeast α-glucosidase, and isolated yeast α-glucosidase II.

To confirm that hydrolysis of TMR-trisaccharide to the TMR-linker arm occurred in a stepwise fashion with initial conversion to TMR-disaccharide, the cells were incubated with 12 μM castanospermine. Castanospermine is a competitive inhibitor of purified yeast α-glucosidase I with a K_i of 12 μM. The production of the linker arm was reduced approximately 6-fold as a result of the inhibition of α-glucosidase I (Figure 6.4b). When the concentration of castanospermine was increased to 60 μM, no further reduction of the amount of linker arm was apparent (Figure 6.4c). As expected, the inhibition of α-glucosidase I activity did not result in the accumulation of di- and monosaccharides.

Analysis of the contents of individual spheroplasts introduced into a capillary and monitored by CE-LIF is shown in Figure 6.5. Each of the three electropherograms was obtained from the analysis of fluorescent molecules in one individual spheroplast. A single spheroplast was introduced via a micromanipulator set-up (Figure 6.1), into the CE separation capillary that was filled with running buffer. The non-physiological buffer containing 10 mM SDS lysed the spheroplast inside the capillary. Subsequent CE-LIF analysis was the result of the lysate from the single spheroplast.

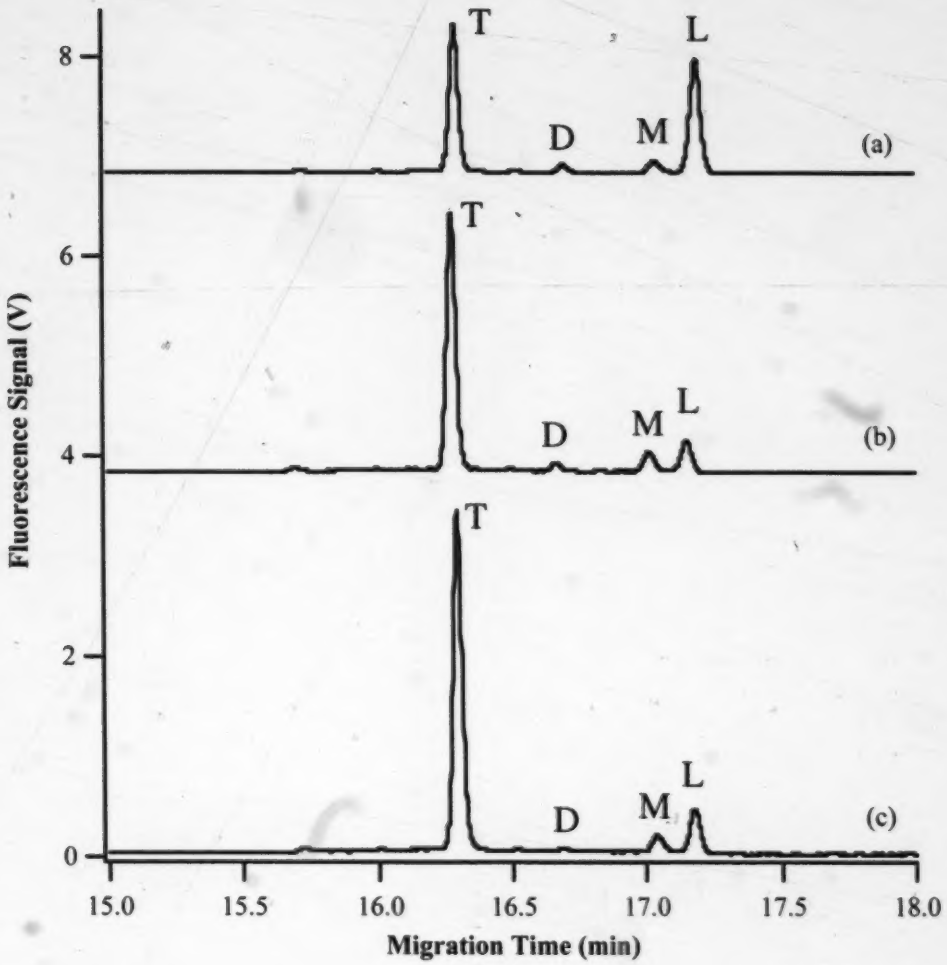

Figure 6.4 Intracellular inhibition of yeast glucosidase I by castanospermine. (a) Hydrolysis of 50 μM TMR-trisaccharide; (b) Hydrolysis of TMR-trisaccharide in the presence of 12 μM inhibitor, (c) Hydrolysis of TMR-trisaccharide in the presence of 60 μM inhibitor. A 40-cm capillary was used for electrophoretic separation under 16,000 V. The electrophoresis buffer contained 10 mM each of phosphate, tetraborate, phenylboronic acid and SDS.

As shown in Figure 6.5, the major fluorescent compounds in the single spheroplasts appear to be the TMR labeled trisaccharide and the free linker arm. Approximately 500-1000 molecules TMR-labeled trisaccharide and free linker arm molecules were present in a single spheroplast, although the absolute number varied among the individual spheroplasts as indicated by the intensity of the two peaks (T and L) in each of the electropherograms. Fewer than 100 molecules of intermediate TMR-labeled di- and monosaccharide were also detected. The overall peak patterns, as governed by the enzymatic hydrolysis of TMR-labeled triglucoside, are generally consistent with those previously reported [24] and the results of Figure 6.4, where a population of cells was examined. However, variation between individual spheroplasts is evident.

Additional CE-LIF analysis of other individual spheroplasts from the same cell suspension also showed differences in fluorescence intensity and in the levels of substrate and intermediate products within different cells. These differences probably reflect the heterogeneous nature of the cellular population, such as different stages of maturity. Analysis using non-lyticase treated single yeast cell was also explored. In this case, osmotic lysis of the cell in the capillary is unlikely. Intact yeast cells do not lyse easily in isotonic solution and a sample of yeast culture was found to last several days at 4°C even in buffer suspension containing a lysing agent such as sodium dodecyl sulfate (SDS). Instead, we propose that high electric field caused the cell to elongate with or without cell lysis as it migrates toward the detection window. In Figure 6.6 the relatively low peak intensity obtained from these runs may also suggest two other possibilities. First, no lysis occured when the intact cell migrated toward the detection window, but the high electric

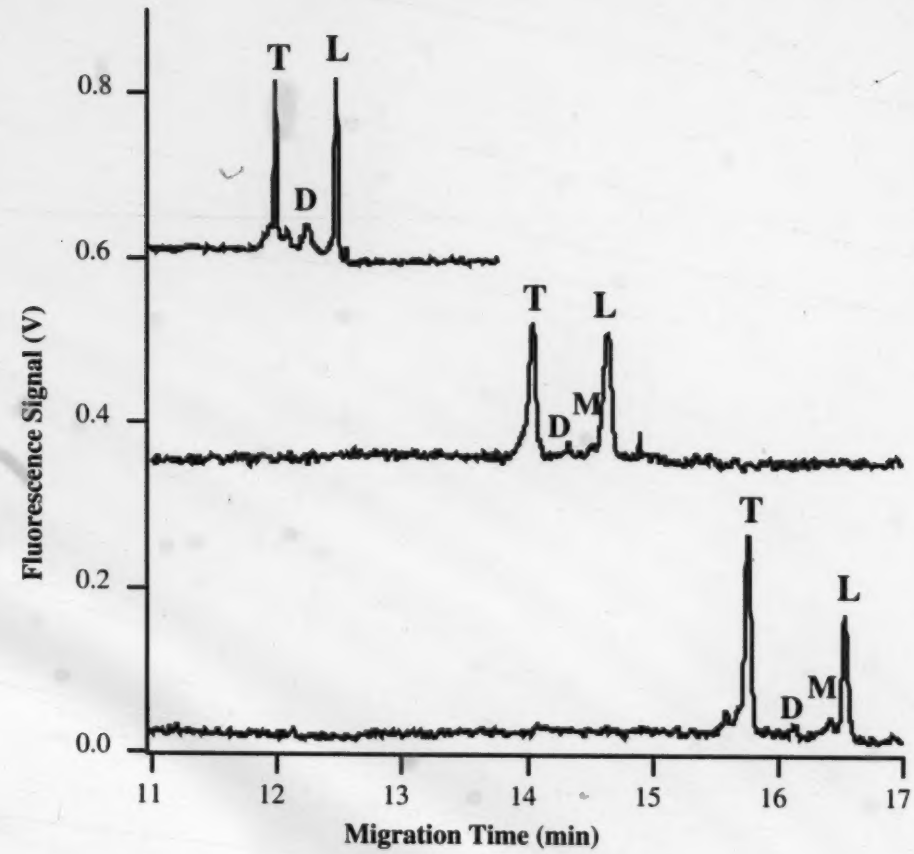

Figure 6.5 Electropherograms of the contents of three individual yeast spheroplasts separately introduced in a capillary. A 40-50 cm capillary (10 μm i.d.) was used for electrophoretic separation under 20,000 V. The electrophoresis buffer contained 10 mM each of phosphate, tetraborate, phenylboronic acid and SDS. Each spheroplast was injected into the buffer filled capillary. The spheroplast was lysed inside the capillary by the nonphysiological buffer and SDS and the lysate from the single spheroplast was analyzed with CE-LIF. For clarity, the electropherograms have been manually shifted. T,D,M,L are as described in Figure 6.3.

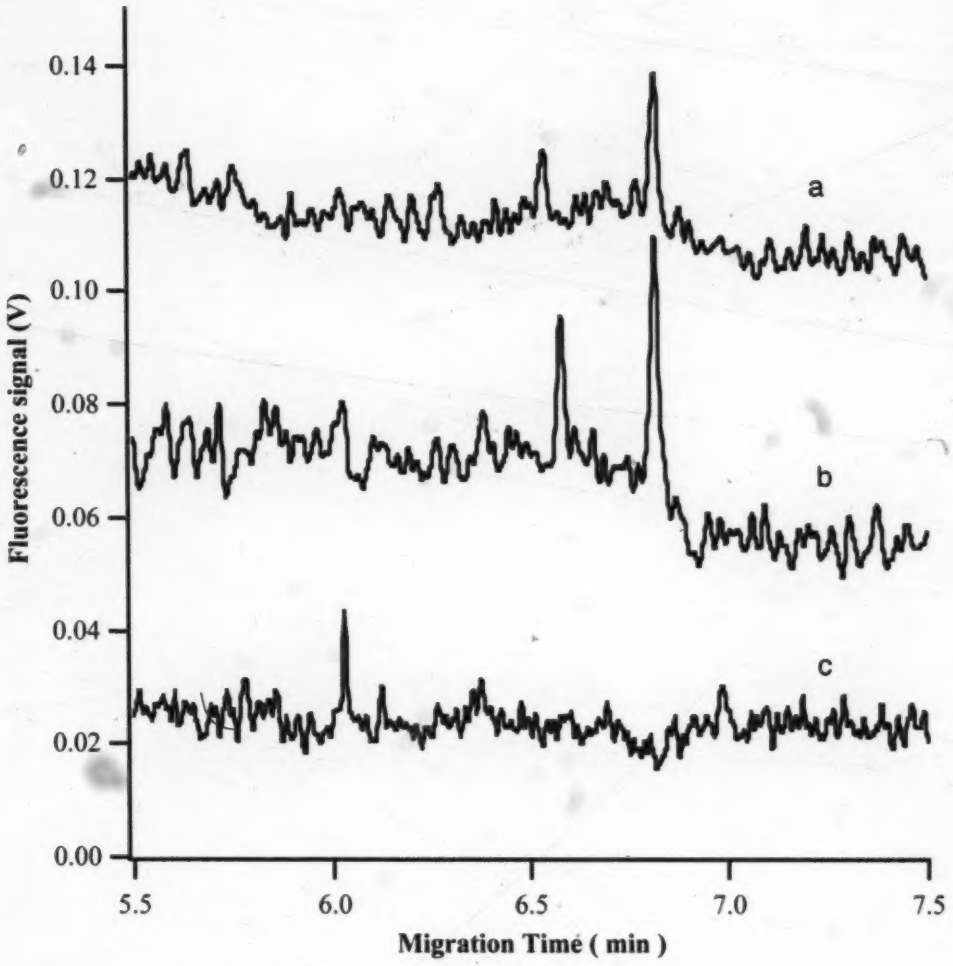

Figure 6.6 CE separation of non-lyticase treated single yeast cell. Cells were incubated in 50 µM Tri-Glc for 48 h. Separation parameters: 40 cm capillary length, 10 µm i.d. and 600 V/cm electric field; Buffer: 10 mM tetraborate, 10 mM SDS, 10mM phenylboronic acid, 10 mM phosphate (dibasic), pH 9.3. Electropherograms a and b were obtained from individual cells; Electropherogram c represent buffer wash prior to single-cell analysis.

field may cause the 'transport channels' on the cell membrane to open as in the case of electroporation of bacterial cells. As a result, some of the fluorescence labeled species might have leaked out into the running buffer. The second possibility is based on the fact that the TMR is relatively hydrophobic and will adhere to cell wall very tightly. Simple washing of the cells using PBS may not be successful in removing all the TMR-labeled material adsorbed on the cell surface. However when the cell comes into contact with SDS present in the electrophoresis buffer, some of this adsorbed TMR-labeled material on the cell wall may dissociate from the cell surface. The smaller peak intensity may support this hypothesis.

Analysis of the media has shown little substrate hydrolysis outside the cells. Fig. 6.7a was generated after 71 h incubation of the yeast culture with 50 μM Tri-Glc at 37°C. The increase in linker-arm/Tri-Glc (L/T) ratio was found to be higher in the culture when compared to incubation of substrate in media alone. In the control, the L/T ratio was found to be stable relative to the culture media. The stability of the substrate at long incubation time is shown in Figure 6.7b and c. The slope calculated from the control is $(0.6\pm0.4) \times 10^{-7}\ h^{-1}$ and that calculated from the culture media is $(2.9\pm0.3) \times 10^{-6}\ h^{-1}$. Similar trends were observed with Mono-Glc/ Tri-Glc (M/T) and Di-Glc / Tri-Glc (D/T). The insignificant increase of the hydrolytic products in the culture media justified the absence of the intracellular hydrolytic enzymes glucosidases I and II in the media during incubation.

Figure 6.8 depicts the sequential hydrolysis of Tri-Glc by glucosidases I and II in yeast cells [12]. The enzymes are specific for Tri-Glc and show unique catalytic activity on the substrate. Glucosidase I converts Tri-Glc to Di-Glc while Glucosidase II converts

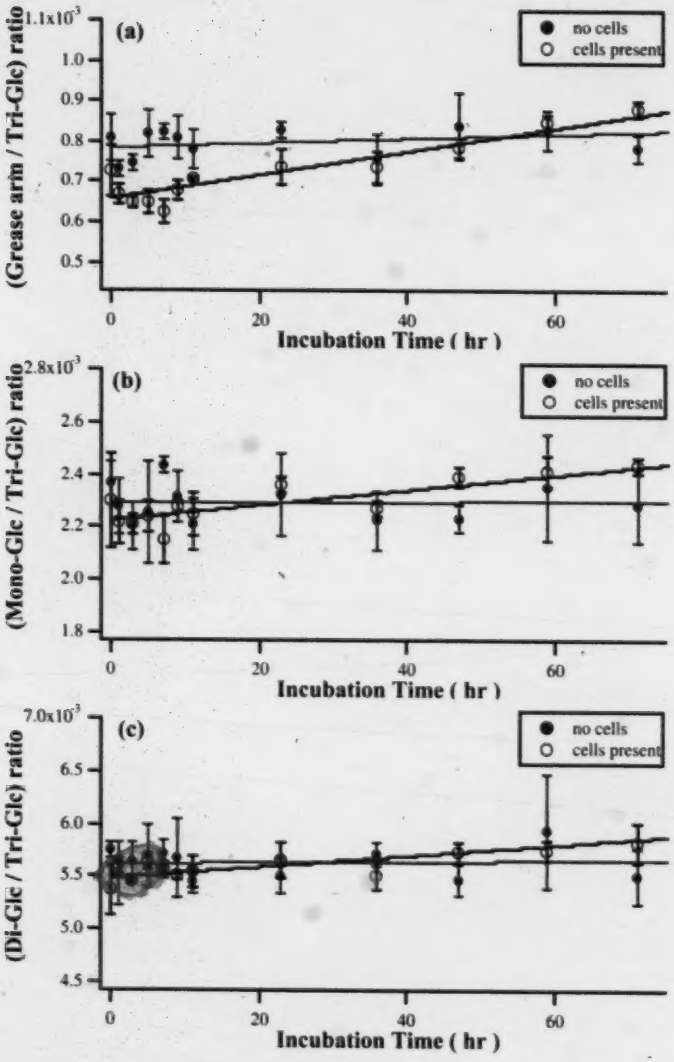

Figure 6.7 Hydrolysis of 50 μM Tri-Glc in Sabouraud dextrose media. All samples collected were analyzed by CE using the same conditions as described in Figure 6.3. Each data point on the plot represents average ratio (n=3) of each sample. Error bars indicate standard deviation. Plots a, b and c represent changes in L/T, M/T and D/T ratios respectively.

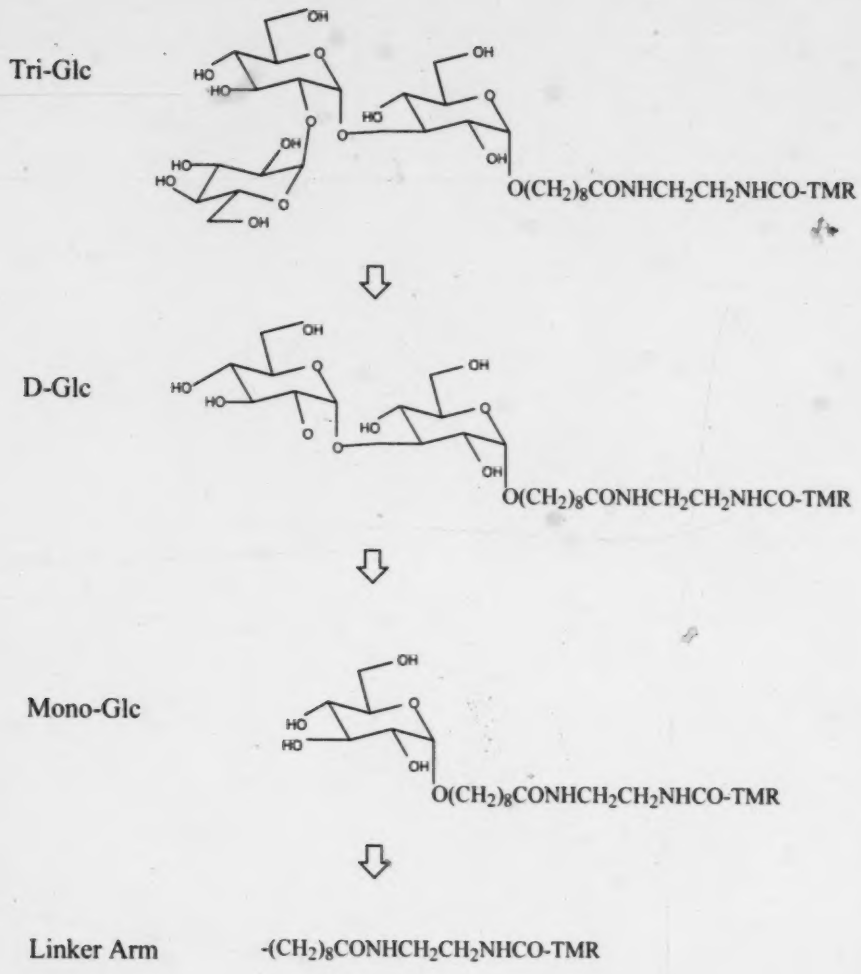

Figure 6.8 Step-wise hydrolysis of Tri-Glc by glucosidases I and II to generate Di-Glc, Mono-Glc and a Linker Arm.

the intermediate to Mono-Glc and the linker arm. Glucosidase II alone has not activity on the substrate. Glucosidase I is specific for the cleavage at the α-1,2 position and Glucosidase II is specific for cleavage at the α-1,3 position [25, 26]. The presence of Glucosidase II in excess of Glucosidase I (personal communication with Dr. A.Szpacenko, Dept. Chemistry) corresponds to the rapid accumulation of linker-arm in the yeast cells (Figures 6.4 and 6.5).

Figure 6.9 shows the change of L/T ratio of the 12 culture samples collected over 71 hours incubation periods. The reduction of L/T ratio in the lysate reached plateau after 10 hours of incubation while the L/T ratio in the media increased slowly with time. These observations suggest that the influx of Tri-Glc into the cells is rapid upon initial exposure of the cells to the substrate and the concentration build up of linker-arm inside the cells and in the media may have negative feedback on the uptake of Tri-Glc by the cells.

6.4 Conclusions

We have shown that CE-LIF could be used as a rapid and cost effective approach to monitor enzyme activity *in vivo* using batch and whole-cell sampling methods. This technique requires fluorescent derivatization of the substrate, CE separation and identification of fluorescence species within cells. It offers the capability of detecting and separating minute amounts of hydrolytic products in individual cells. The present methodology can be expended to assay virtually any class of enzymes for which a

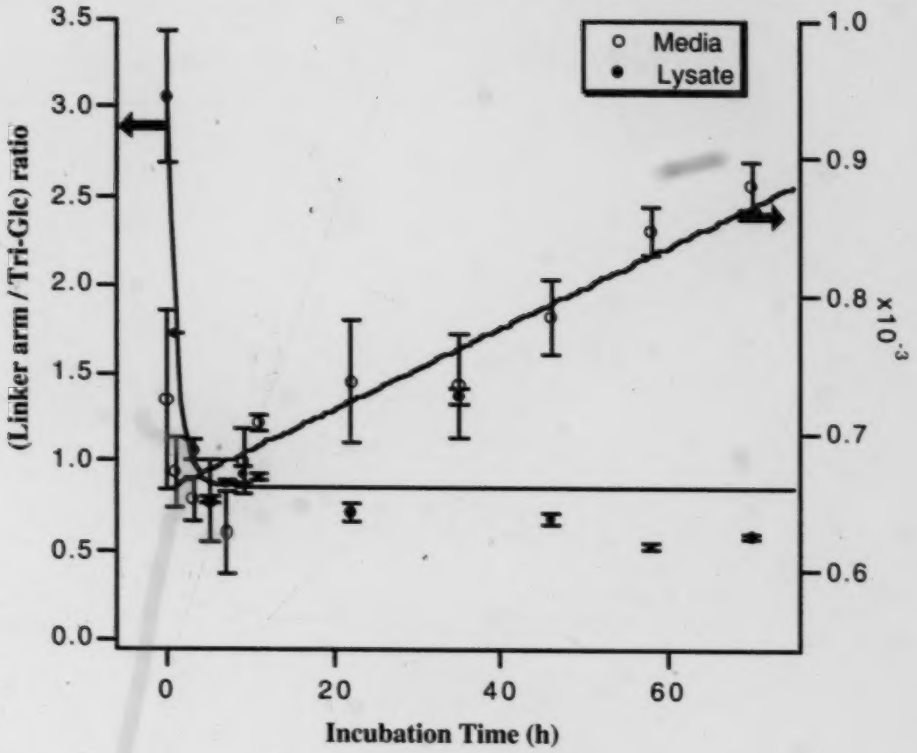

Figure 6.9 Comparison of L/T ratio in culture media and total lysate. Experimental parameters for media and lysate are described in experimental.
Arrows in the plot represent scales on Y axis.

fluorescent substrate can be synthesized. The assay of enzyme activity on a cell-by-cell basis allows the use of the distribution of activity in the cellular population as a diagnostic and prognostic indicator of cancer and other diseases. The assay may also be used in the pharmaceutical industry as a tool in the development and *in vivo* evaluation of novel enzyme inhibitors. The methodologies described here are the foundation for CE analysis of enzyme activity in single cells, identification of novel enzyme activity *in vivo*,

intracellular biosynthesis, metabolite channeling and studies of various macromolecules within sub cellular organelles. Operation of a system with a series of capillaries will be desirable to overcome the fundamental limitation of throughput analysis in single cell study.

6.5 Bibliography

1. Edstrom, J-E. (1953) *Nature* **172**, 809.
2. Kennedy, R.T., Oates, M.D., Cooper, B.R., Nickerson, B. and Jorgenson, J.W. (1989) *Science* **246**, 57-63.
3. Ewing, A.G., Strein, T.G. and Lau, Y.Y. (1992) *Acc. Chem. Res.* **25**, 440-447.
4. Almers, W. and Neher, E. (1985) FEBS Lett., **192**, 13-18.
5. Neher, E. and Sakmann, B. (1992) *Sci. Amer.* **226**, 44-51.
6. Steinkamp, J.A. (1984) *Rev. Sci. Instrum.* **55**, 1375-1400.
7. Yeung, E.S. (1994) *Acc. Chem. Res.* **27**, 409-414.
8. Rosenzweig, Z. and Yeung, E.S. (1994) *Anal. Chem.* **66**, 1771-1776.
9. Xue, Q. and Yeung, E.S. (1994) *Anal. Chem.* **66**, 1175-1178.
10. Chiu, D.T., Lillard, S.J., Scheller, R.H., Zare, R.N., Rodriguez-Cruz, S.E., Williams, E.R., Orwar, O., Sandberg, M. and Lundqvist, J.A.(1998) Science, **279**, 1190-1193.
11. Lillard, S.J. and Yeung, E.S. (1997) Capillary electrophoresis for the analysis of single cells: Laser-induced fluorescence detection. In Landers, J.P. (ed.), Handbook of Capillary Electrophoresis, 2nd ed. CRC Press, Boca Raton, FL, pp. 523-544.
12. Swanek, F.D., Ferris, S.S. and Ewing, A.G. (1997) Capillary electrophoresis for the analysis of single cells: electrochemical, mass spectrometric, and radiochemical

detection. In Landers, J.P. (ed.). Handbook of Capillary Electrophoresis, 2nd ed. CRC press, Boca Raton, FL, pp. 495-521.

13. Rotman, B. (1961) Proc. Natl. Acad. Sci. USA, 47, 1981-1991.

14. Yashphe, J. and Halvorson, H.O. (1976) *Science* **191**, 1283-1284.

15. Luyten, G.P.M., Hoogeveen, A.T. and Galjaard, H. (1985) *J. Histochem. Cytochem.* **33**, 965-968.

16. Jain, V.K. and Magrath, I.T. (1991) *Anal. Biochem.* **199**, 119-124.

17. Honda, S., Iwase, S., Makino, A. and Fujiwara, S. (1989) *Anal. Biochem.* **176**, 72-77.

18. Liu, J., Shirota, O., Wiesler, D. and Novotny, M. (1991) *Proc. Natl. Acad. Sci. USA* **88**, 2302-2306.

19. Liu, J., Shirota, O. and Novotny, M. (1992) *Anal. Chem.* **64**, 973-975.

20. Novotny, M. and Sudor, J. (1993) *Electrophoresis* **14**, 373-389.

21. Stefansson, M. and Novotny, M. (1994) *Anal. Chem.* **66**, 1134-1140.

22. Lee, K.B., Desai, U.R., Palcic, M.M., Hindsgaul, O. and Linhardt, R.J. (1992) *Anal. Biochem.* **205**, 108-114.

23. Liao, J.Y., Dovichi, N.J., Hindsgaul, O., Gosselin, S. and Palcic, M.M. (1994) *Glycobiology* **4**, 239-242.

24. Le, X.C., Scaman, C., Zhang, Y., Zhang, J., Dovichi, N.J., Hindsgaul, O. and Palcic, M.M. (1995) *J. Chromatogr. A* **716**, 215-220.

25. Zhang, Y., Le, X.C., Dovichi, N.J., Compston, C.A., Palcic, M.M., Diedrich, P. and Hindsgaul, O. (1995) *Anal. Biochem.* **227**, 368-376.

26. Scaman, S.H., Hindsgaul, O., Palcic, M.M. and Srivastava, O.P. (1996) *Carbohydrate Res.* **296**, 203-213.

27. Hoffstetter-Kuhn, S., Paulus, A., Gassmann, E. and Widmer, H.M. (1991) *Anal. Chem.* **63**, 1541-1547.

28. Le, X.C., Zhang, Y., Dovichi, N.J., Compston, C.A., Palcic, M.M., Beever, R.J. and Hindsgaul, O (1997) *J. Chromatogr. A* **781**, 512-522.

29. Neverova, I., Scaman, C.H., Srivastava, O.P., Szweda, R., Vijay I.K. and Palcic, M.M. (1994) *Anal. Biochem.* **222,** 190-195.

Chapter 7. Concluding Summary

7.1 Closing remarks and future direction

The most optimistic forecast predicts that high throughput and automated nucleic acid screening methods will soon replace conventional culture and immunoassays in the diagnosis of infectious diseases. A more realistic approach to the future, however, is based on the recognition that there is a long way to go to achieve this goal. Molecular methods no doubt have an enormous potential in the diagnosis of infectious diseases, because they may offer exquisite sensitivity and specificity and sufficient rapidity. Nevertheless major improvements must be achieved in automation, assay simplicity and reproducibility, short analysis time and high throughput fashion. It may be safely predicted that once these factors are refined, new molecular diagnostic methods will be widely accepted and implemented routinely in clinical microbiology laboratories, leading to great improvements in their capabilities to diagnose infectious diseases.

In this thesis, the use of capillary cellulose polymer electrophoresis to detect, profile and quantify DHBV DNA was investigated. The tremendous resolving power of CE and the excellent mass sensitivity of LIF detection were demonstrated in chapter 2 and 3. Separation of both single and doubled-stranded DNA fragments was found to be equally efficient in a low viscosity HEC polymer solution. These advantages make CE a useful technique in the field of DNA sizing and profiling.

HEC concentration at 0.8% (w/v) was shown to be optimal for the separation of 5' end labeled, single stranded DNA fragments between 183 and 903 nt. In this case, the presence of 7M urea in the HEC polymer solution was found to be necessary to ensure separation of the primer extended products from their corresponding templates as well as to prevent formation of secondary structures on the products. The addition of urea into

the seiving matrix is not without disadvantage. First, the added urea reduced the conductivity and increased the overall viscosity of the HEC polymer solution. These combinations prolong migration time and reduce separation of DNA fragments.

The selection of optimal polymer length for HEC has been arbitrary in this study. The influence of polymer chain length on resolution was not investigated in detail. However, a significant difference in resolution was noticed when the molecular mass (mw) of HEC was increased from 250,000 to 720,000. A similar trend was also observed in hydroxypropyl cellulose mw 100,000 versus 1,000,000. Further elucidation of polymer chain length in conjunction with better understanding of the mechanism of DNA separation in these polymers will provide a more universal and systematic set of guidelines for the selection of the right polymer for a particular application.

In constrast to the separation of 5' end labeled, single stranded DNA fragments, separation of double stranded DNA fragments in the presence of intercalating dyes was found to be interesting different, but comparatively efficient. A 0.8% (w/v) HEC concentration in this case appeared to accommodate a wider range of DNA sizes in a considerably shorter migration time. The presence of intercalating dyes may play an important role in the efficient separation of the large DNA fragments (10,180 bp and up), as has been demonstrated by other authors. The unique on-column labeling approach described in chapter 3 has significantly improved the ease and performance of using cationic dyes to label DNA fragments. The ability to detect minute amount of DNA fragments, to separate them at high field strength and to generate plate counts in excess of 47 million plates per meter will make this technique look attractive in high speed DNA sizing. Further development involving improved stringency of labeling, automation as

well as high throughput coupled to high diagnostic precision will be required to make this technique reliable for DNA sizing.

In chapter 4, profiling of viral DNA in infected animals undergoing antiviral therapy was addressed. The objective of this work is to simplify current technologies to investigate the mechanisms of viral neutralization using a variety of antiviral compounds, in this case specifically effective against Hepatitis B infection. We showed that, with strategic design of PCR primers, a relatively simple protocol could be developed to follow the disappearance of virus DNA in response to drug treatment. In addition, the same approach using the 16 PCR primers may also be used to investigate the kinetics and mechanisms of termination in viral DNA synthesis. However, the inhibitory mechanisms of 3TC and 2A6M were not successfully demonstrated in this study. A relatively high background of full length genomes was still detectable when the drug treatment was terminated, masking the presentation of the truncated viral DNA genomes. A more detailed experimental set up based on quantification of the short and long PCR products will be necessary in order to make this alternative approach more informative in probing the efficacy of an antiviral therapy.

To improve current technologies in the quantification of nucleic acids, we developed quantitative PCR techniques with CE-LIF detection (chapter 5). The goal is to further refine conventional quantitative PCR for eventual automation and high throughput analysis to facilitate routine application of these techniques in clinical settings. The basic concepts of QC-PCR-CE-LIF were described and the logic and practicality of the technique for reliable quantification of DNA were demonstrated. A large scale study of clinical samples including single blind investigation will be necessary to further establish

reliability of this novel approach. In addition, this technique involves a larger sampling numbers, and it will be necessary also to conduct the analysis in a high throughput and automated environment. The fulfillment of these requirements, and hence, the success of this technique, will have major impact on the growing importance of studying viral dynamics and measurement of viral load in response to antiviral therapy.

The single cell technologies as described in chapter 6 represent the initial design of an in house built CE instrument with single cell sampling set up. The instrument is practically functional and can be applied for the *in vivo* assay of virtually any enzyme with a fluorescent substrate. However, the nature of the current injection and detection methods suffers from several drawbacks. First, it takes an average of over 2 minutes (for an experienced worker) to complete a cell injection process. Second, due to the nature of the syringe suction applied during cell injection, the exact location of a cell inside the capillary can not be pin-pointed. In this case, a visual confirmation of the cell inside the capillary using a CCD camera will be advantageous. Third, the current CE set up does not allow multiple cells injection. This limits the throughput of analysis. Fouth, *in vivo* assay of enzymatic hydrolysis described in this study is only feasible for enzyme with a fluorescent substrate. Therefore, future improvements would involve further instrumentation and automation in cell injection with emphasis on high throughput screening. The improvement and development of diode lasers with useful wavelengths for native biomolecules and sensitive derivatizing agents, should lead to more efficient sub-cellular compartmental and multi-parametric analyses using CE-LIF. It is anticipated that future single cell analysis in virology will involve sampling of infectious virus particles in the cytoplasm of individual infected cells.

To date, electrophoresis is still the main laboratory technique that allows molecular biologist to separate, sequence, map and purify nucleic acids. And it is likely to remain so for at least another decade. Although it is a mature technology, it certainly remains a very active field of investigation for the scientists and technologists, as this thesis has tried to illustrate. The Human Genome Project has increased the visibility and usefulness of CE. The magnitude of this project has led to the automation of most steps in DNA sequencing as well as genome analysis for genetic testing, forensic investigation and clinical diagnosis.

Development of automated technologies has now become major commercial directions that rely heavily on high throughput and robust DNA analysis. In this respect, CE has clearly established itself as the way of the future for nucleic acid analysis.

Although first routine applications have been reported [1,2,3], further developments are needed for widespread adoption of CE in routine settings. High throughput, inexpensive autoanalyzers featuring automated sample loading, simple, reliable software for data evaluation and protocols with test kits should be developed and become commercially available. The introduction of 3700 DNA Analyzer (P.E. ABI), BioFocus 2000 (BioRad) and MegaBACE 1000 (Molecular Dynamics), with data management software, that provides not only real time analysis, but also user-defined methods that can be set up quickly and easily, represents a first step in the right direction.

7.2 Biobliography

1. Jenkins, M.A. and Guerin, M.D. (1996) J. Chromatogr. B. **682**, 23-34.

2. Thormann, W., Zhang, C.X. and Schmutz, A. (1996) Ther. Drug Monit. **18**, 506-520.

3. Jenkins, M.A., O'Leary, T.D. and Guerin, M.D. (1994) J. Chromatogr. B. **662**, 108-112.

Appendix

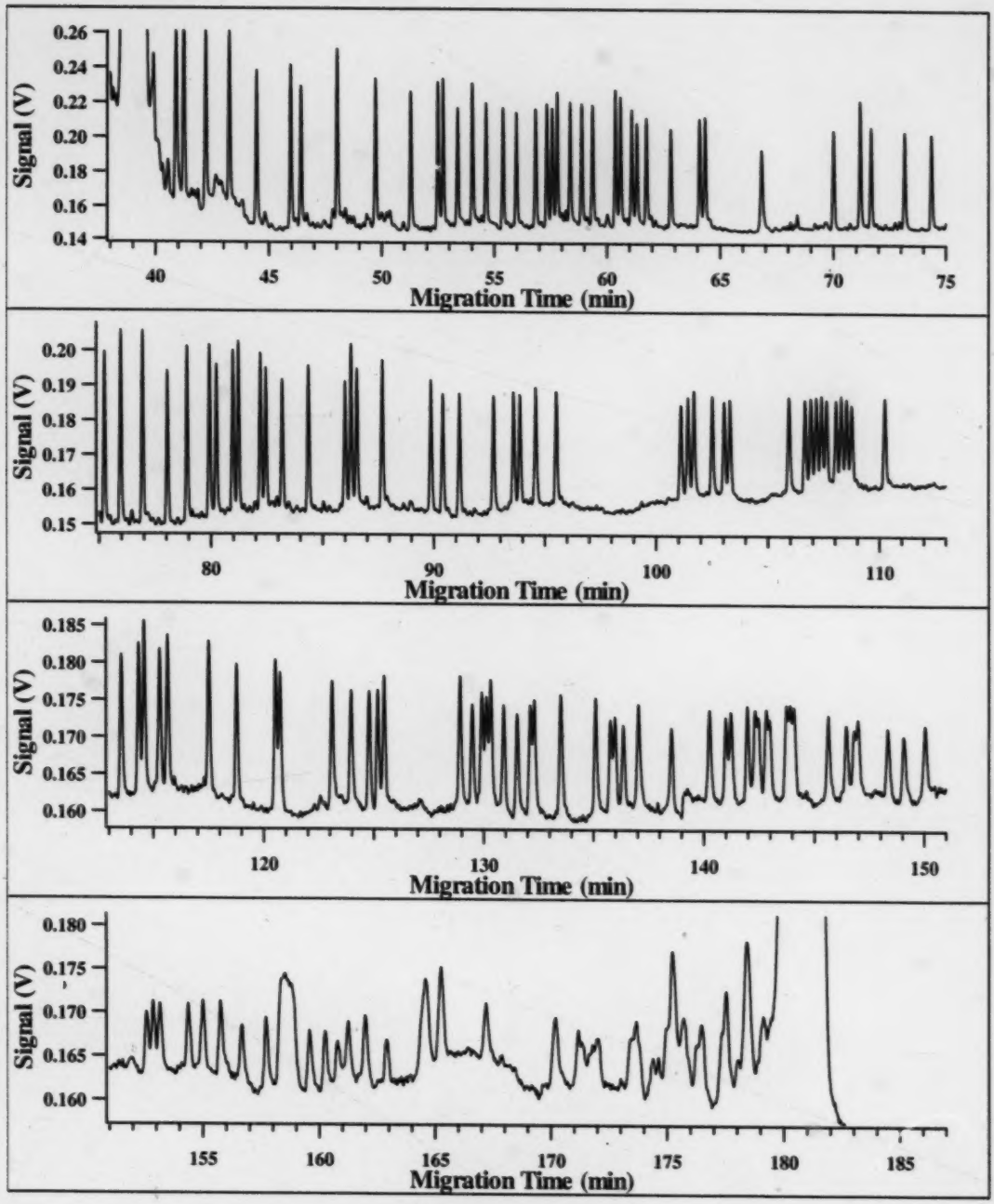

2A. T-termination sequencing reaction. CE parameters: capillary length: 45 cm; capillary coating: 2% HEC (Mw 250,000); sieving: 4% linear polyacrylamide ambient temperature at 150 V / cm.

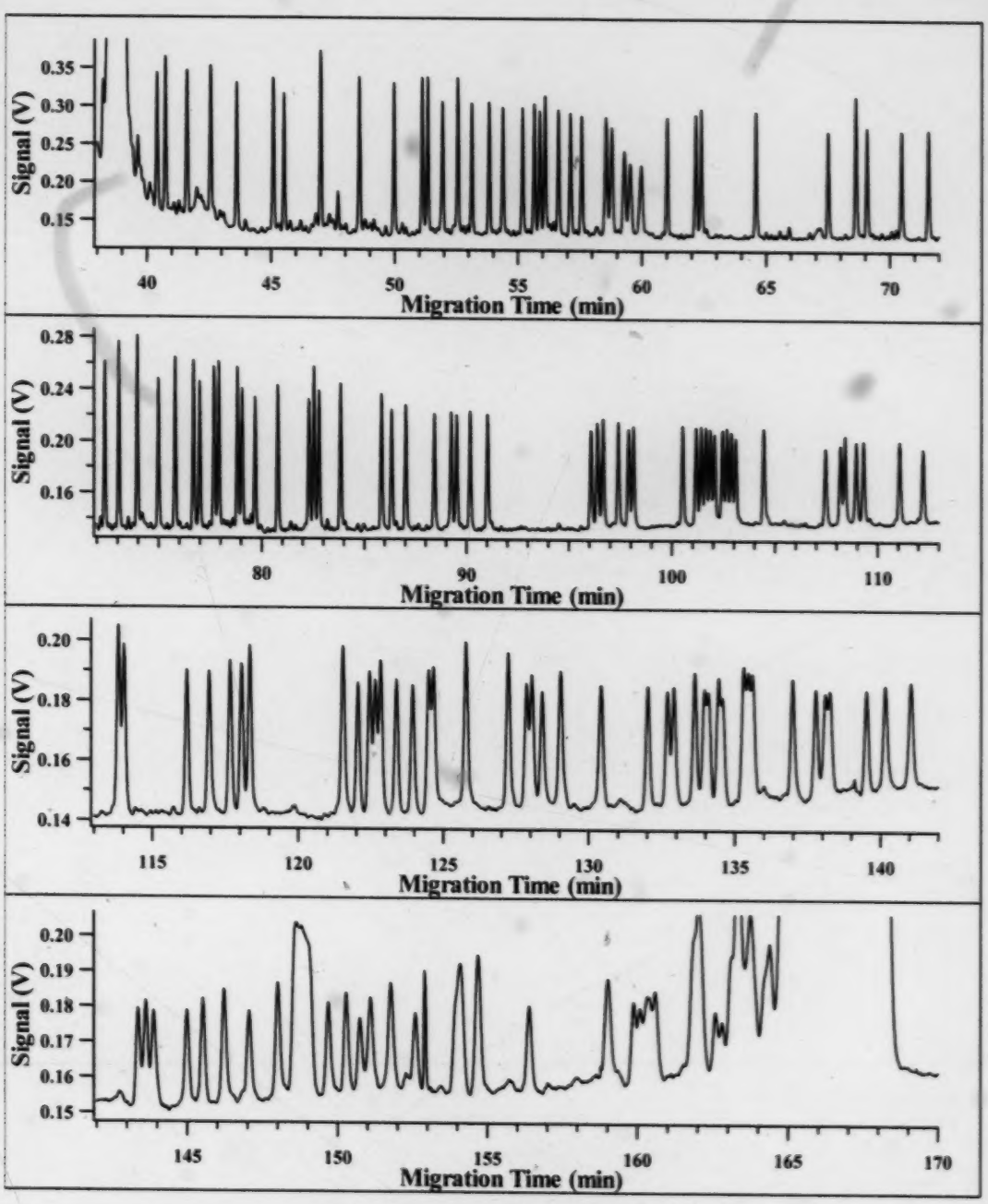

2B. T-termination sequencing reaction. CE parameters: capillary length: 45 cm; capillary coating: 2% HEC (Mw 250,000); sieving: 4% linear polyacrylamide ambient temperature at 150 V / cm.

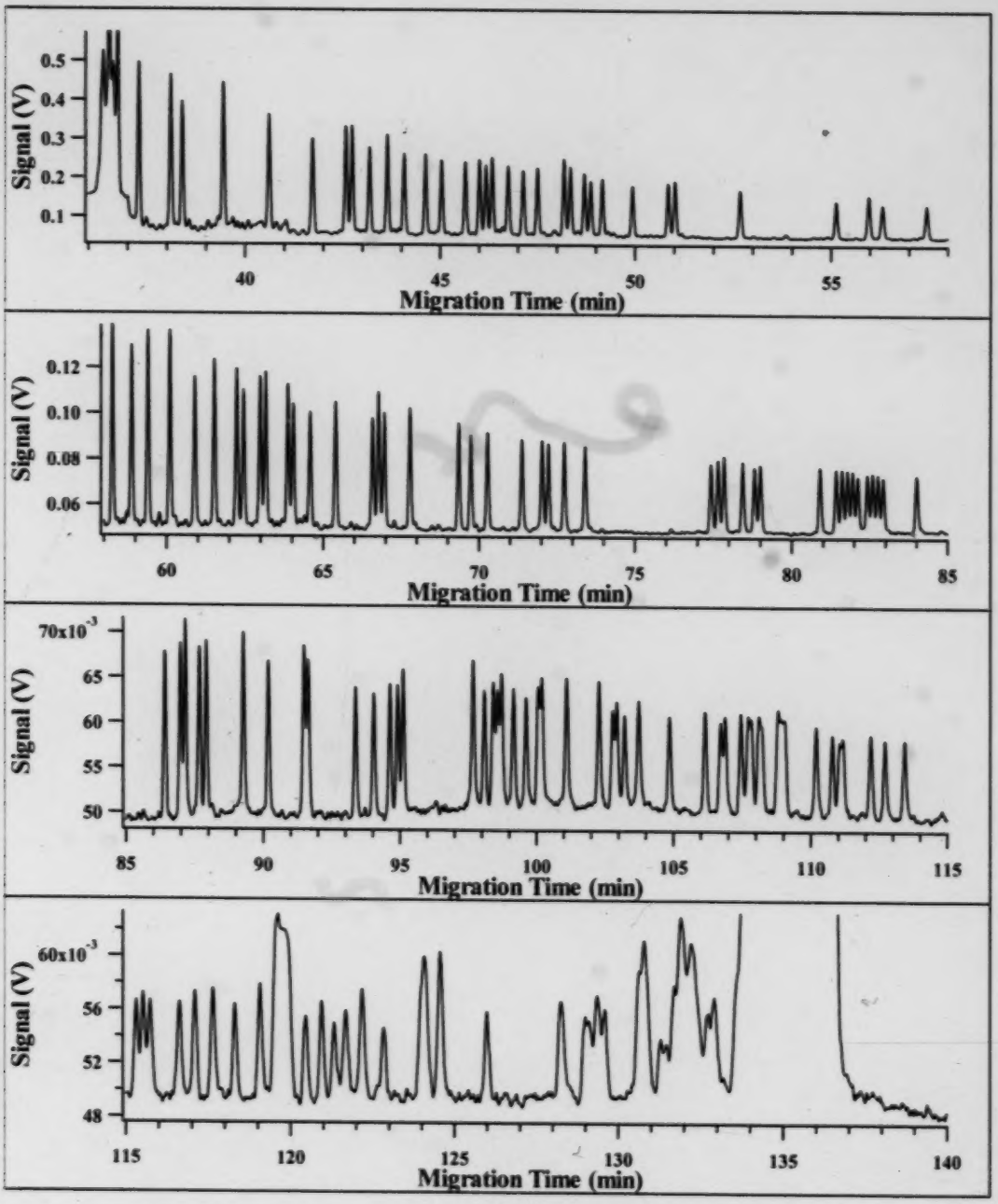

2C. T-termination sequencing reaction. CE parameters: capillary length: 45 cm; capillary coating: 2% HEC (Mw 250,000); sieving: 4% linear polyacrylamide; temperature: 45 °C; run voltage: 100 V / cm.

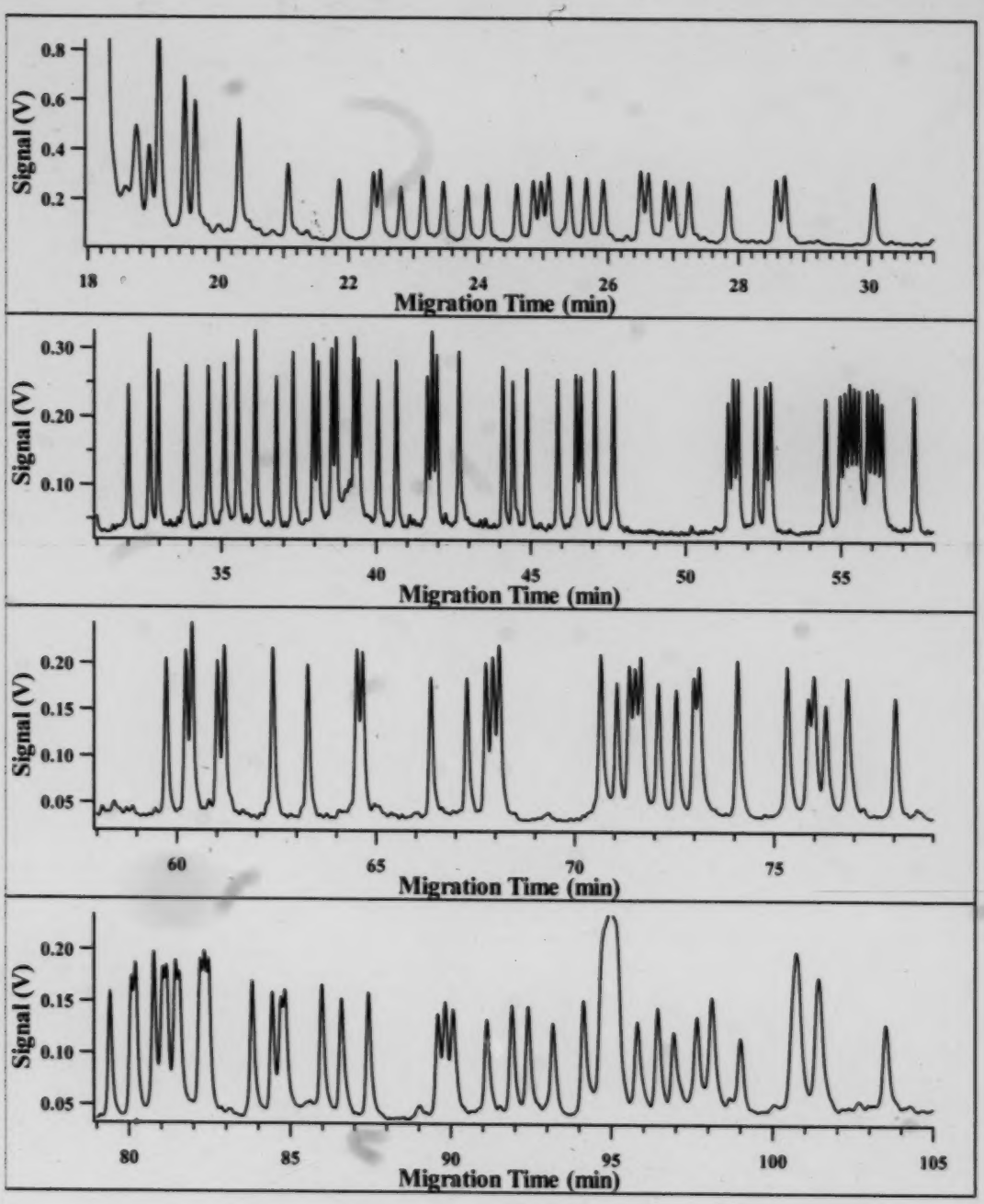

2D. T-termination sequencing reaction. CE parameters: capillary length: 45 cm; capillary coating: 2% HEC (Mw 250,000); sieving: 4% linear polyacrylamide; temperature: 65 °C; run voltage: 100 V / cm.

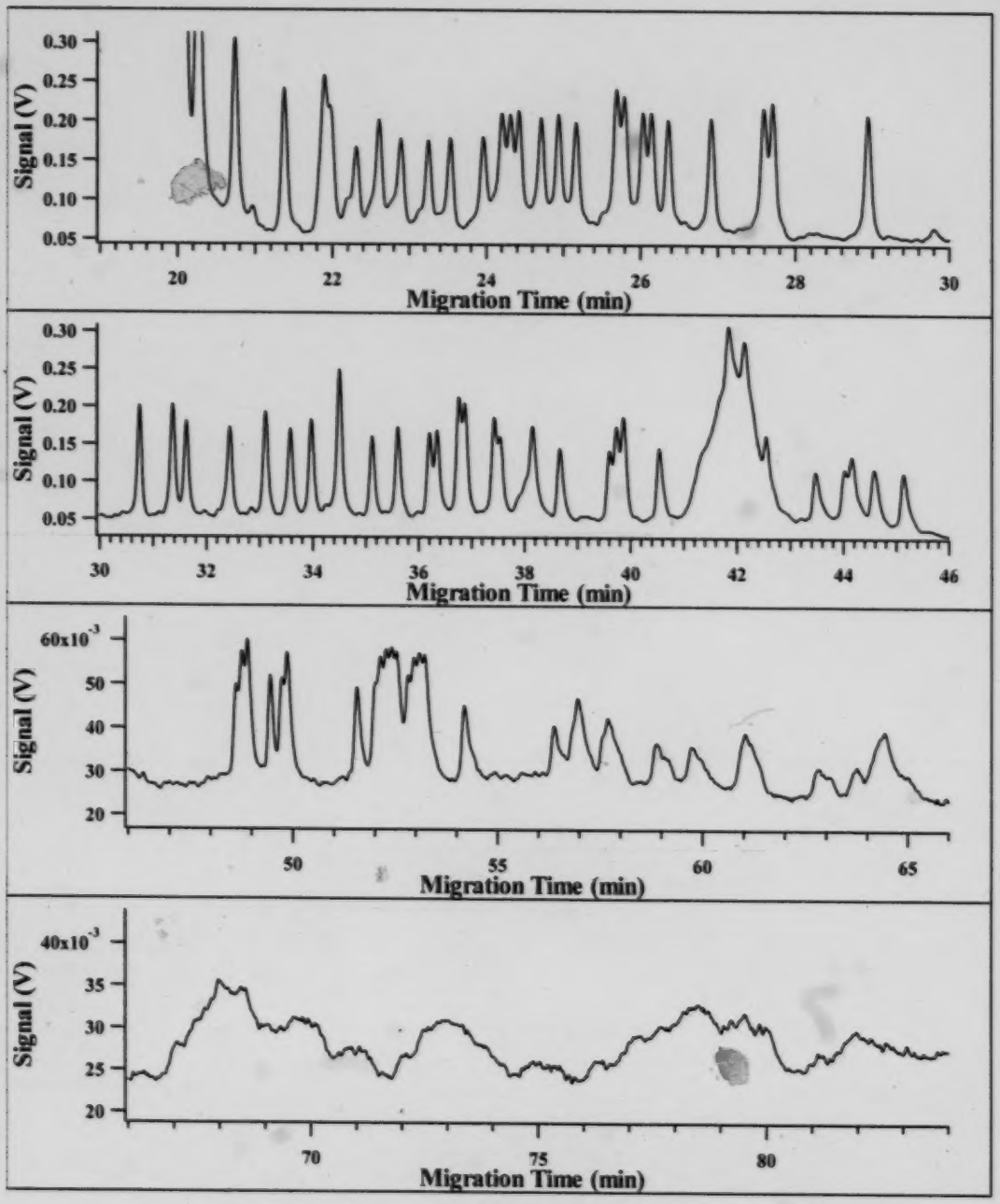

2E. T-termination sequencing reaction. CE parameters: capillary length: 45 cm; capillary coating: 2% HEC (Mw 250,000); sieving: 4% linear polyacrylamide; temperature: 80 °C; run voltage: 100 V / cm.